A chemical oceanographer's view of nitrous oxide in the ocean

Habilitationsschrift
vorgelegt von

Hermann W. Bange

Kiel, März 2006

Hermann W. Bange

Forschungseinheit Chemische Ozeanographie
Forschungsbereich Marine Biogeochemie
IFM-GEOMAR
Leibniz-Institut für Meereswissenschaften an der Universität Kiel

Düsternbrooker Weg 20
24105 Kiel
Tel.: +49-(0)431-600-4204
Fax: +49-(0)431-600-4202
hbange@ifm-geomar.de

"Tatsächlich ist der Fortschritt der Wissenschaften wie ein alter Wüstenpfad übersät mit den Gerippen fallengelassener Theorien, die einstmals ewiges Leben zu besitzen schienen." Arthur Koestler (1905-1983)

"All collecting trips to fairly unknown regions should be made twice; once to make mistakes and once to correct them." from "The log from the Sea of Cortez" by John Steinbeck (1902-1968)

HABILITATION OUTLINE

The two central themes of the publications submitted here in support of my habilitation are:

(A) To decipher the distribution and formation processes of oceanic N_2O and

(B) To quantify the oceanic emissions of N_2O.

During the period of my habilitation (1999-2006, which was delayed by two years due to my move from the Max-Planck-Institut für Chemie, Mainz to the former Institut für Meereskunde, Kiel, now IFM-GEOMAR, Leibniz-Institut für Meereswissenschaften) the following articles have been written:

Theme A: Distribution and formation of oceanic N_2O

1) **Bange, H.W.**, and M.O. Andreae, Nitrous oxide in the deep waters of the world's oceans, *Global Biogeochem. Cycles*, *13* (4), 1127-1135, 1999.

   - Describes the N_2O distribution in deep waters (>2000m). Identification of the deep water mass age/N_2O concentration relationship

2) **Bange, H.W.**, S. Rapsomanikis, and M.O. Andreae, Nitrous oxide cycling in the Arabian Sea, *J. Geophys. Res.*, *106* (C1), 1053-1065, 2001.

   - Presents the N_2O distribution and its formation processes in the Arabian Sea based on measurements during four cruises. Suggestion of a four compartment scheme to explain the N_2O depth profiles in the central Arabian Sea as a result of nitrification and denitrification processes. Suggestion of an alternative microbial formation process via reduction of IO_3^- near the shelf break along the Arabian Peninsula.

3) * Walter, S., I. Peeken, K. Lochte, A. Webb, and **H.W. Bange**, Nitrous oxide measurements during EIFEX, the European Iron Fertilization Experiment in the subpolar South Atlantic Ocean, *Geophys. Res. Lett.*, *32*, L 23613, doi:10.1029/2005GL024619, 2005.

   - Describes N_2O measurements during a Fe fertilization experiment. In contrast to a previous study no increase in the N_2O concentrations during the course of the experiment was found.

4) * Walter, S., **H.W. Bange**, U. Breitenbach, and D.W.R. Wallace, Nitrous oxide in the North Atlantic Ocean, *Global Biogeochem. Cycles*, in preparation, 2006.

- Summarizes the N_2O distribution in the subpolar, subtropical and tropical North Atlantic Ocean. The N_2O distribution is attributed to formation via nitrification in the subtropical and tropical Atlantic, whereas mixing processes largely influence N_2O in the subpolar Atlantic.

5) * Walter, S., U. Breitenbach, **H.W. Bange**, G. Nausch, and D.W.R. Wallace, Nitrous oxide water column distribution during the transition from anoxic to oxic conditions in the Baltic Sea, *Biogeosci.*, submitted, 2006.

- Shows the effect of rapidly changing O_2 concentrations on the formation and consumption of N_2O in a natural laboratory (i.e. the central Baltic Sea). During the ventilation process by North Sea Water, N_2O was produced, but did not reach the atmosphere due the stable stratification of the central Baltic Sea. N_2O production rates and nitrification rates were estimated.

Theme B: N_2O emissions

6) **Bange, H.W.**, M.O. Andreae, S. Lal, C.S. Law, S.W.A. Naqvi, P.K. Patra, T. Rixen, and R.C. Upstill-Goddard, Nitrous oxide emissions from the Arabian Sea: A synthesis, *Atmos. Chem. Phys.*, *1*, 61-71, 2001.

- Computation of high-resolution (1°latitude x 1°longitude) seasonal and annual N_2O concentration fields and subsequent emissions for the Arabian Sea surface layer using a data base of more than 2400 values.

7) **Bange, H.W.**, Air-sea exchange of nitrous oxide and methane in the Arabian Sea: A simple model of the seasonal variability, *Indian J. Mar. Sci.*, *33* (1), 77-83, 2004.

- Presents a one-dimensional coupled ocean/atmosphere box model in order to investigate the seasonal variability of N_2O in the surface layer of the Arabian Sea.

8) * Walter, S., **H.W. Bange**, and D.W.R. Wallace, Nitrous oxide in the surface layer of the tropical North Atlantic Ocean along a west to east transect, *Geophys. Res. Lett.*, *31* (23), L23S07, doi:10.1029/2004GL019937, 2004.

- Reports continuous N_2O surface measurements and the associated N_2O emissions to the atmosphere in the tropical North Atlantic Ocean.

9) **Bange, H.W.**, Nitrous oxide and methane in European coastal waters, *Estuar. Coastal Shelf Sci.*, submitted, 2005.

- Overview about the distribution and formation/consumption pathways of N_2O in the European coastal waters such as estuaries, deltas, lagoons, fjords, continental shelves etc. Provides a comprehensive data base for a first reasonable assessment of N_2O emissions from European coastal areas, which contribute significantly to the global oceanic N_2O emissions.

10) **Bange, H.W.**, New Directions: The importance of the oceanic nitrous oxide emissions, *Atmos. Environ.*, *40* (1), 198-199, 2006.

- Shows that the often-cited global estimate of oceanic N_2O emissions is underestimated. Proposes a considerable upward revision (2x) of the common estimate that has far reaching consequences for the overall budget of atmospheric N_2O.

* these articles are part of the PhD thesis by Sylvia Walter, "N_2O in the Atlantic Ocean and the Baltic Sea", 154 pp., University of Kiel, 2006.

My contribution to the articles listed above can be assessed as follows:

Article no.	Conceptual contribution	Sample and data analysis	Contribution to the written manuscript
Theme A			
1	1	1	1
2	1	1	1
3	2	2	1
4	2	2	2
5	2	3	2
Theme B			
6	1	1	1
7	1	1	1
8	1	2	1
9	1	1	1
10	1	1	1

1 = major contribution; 2 = significant but not major contribution; 3 = small contribution

Further articles have been written during the time of the habilitation. These articles are closely related to the themes of the habilitation, but are not attached:

Bange, H.W., It's not a gas, *Nature*, *408*, 301-302, 2000.

Bange, H.W., Gaseous nitrogen compounds (NO, N_2O, N_2, NH_3) in the ocean, in *Nitrogen in the marine environment*, edited by D.G. Capone, D.A. Bronk, M.R. Mulholland, and E.J. Carpenter, submitted, Academic Press / Elsevier, 2006.

Bange, H.W., S.W.A. Naqvi, and L.A. Codispoti, The nitrogen cycle in the Arabian Sea, *Progr. Oceanogr.*, *65*, 145-158, 2005.

Bange, H.W., T. Rixen, A.M. Johansen, R.L. Siefert, R. Ramesh, V. Ittekkot, M.R. Hoffmann, and M.O. Andreae, A revised nitrogen budget for the Arabian Sea, *Global Biogeochem. Cycles*, *14* (4), 1283-1297, 2000.

Dahlke, S., S. Wolff, L.-A. Meyer-Reil, **H.W. Bange**, R. Ramesh, S. Rapsomanikis, and M.O. Andreae, *Bodden waters (southern Baltic Sea) as a source of methane and nitrous oxide*, in Proceedings in Marine Sciences, Volume 2: Muddy Coast Dynamics and Resource Management, edited by B.W. Flemming, M.T. Delafontaine, and G. Liebezeit, pp. 137-148, Elsevier Science, Amsterdam, 2000.

Gebhardt, S., S. Walter, G. Nausch, and **H.W. Bange**, Hydroxylamine (NH_2OH) in the Baltic Sea, *Biogeosci. Discuss.*, *1*, 709-724, 2004.

Lendt, R., A. Hupe, V. Ittekkot, **H.W. Bange**, M.O. Andreae, H. Thomas, S. Al Habsi, and S. Rapsomanikis, Greenhouse gases in cold water filaments in the Arabian Sea during the Southwest Monsoon, *Naturwissenschaften*, *86* (10), 489-491, 1999.

Naqvi, S.W.A., **H.W. Bange**, S.W. Gibb, C. Goyet, A.D. Hatton, and R.C. Upstill-Goddard, Biogeochemical ocean-atmosphere transfers in the Arabian Sea, *Progr. Oceanogr.*, *65*, 116-144, 2005.

Wallace, D.W.R., and **H.W. Bange**, Introduction to special section: Results of the Meteor 55: Tropical SOLAS expedition, *Geophys. Res. Lett.*, *31*, L23S01, doi:10.1029/2004GL021014, 2004.

1 INTRODUCTION

Nitrous oxide (N_2O, dinitrogen monoxide, commonly called laughing gas) was isolated and characterized for the first time by the English chemist Joseph Pristley in 1772 [*Greenwood and Earnshaw*, 1984]. 166 years later, in 1938, Adel [*Adel*, 1938] discovered that N_2O occurs in the Earth's atmosphere. The physical properties of the colourless gas N_2O (mw 44.01 g mol^{-1}, mp 182.3 K (–90.9°C), bp 184.7 (–88.5°C), asymmetrical linear structure N=N=O), are comparable to the isoelectronic carbon dioxide (CO_2). For example, both gases show similar solubilities and diffusivities in water [*King et al.*, 1995; *Wilhelm et al.*, 1977]. Like CO_2, N_2O is a radiatively active atmospheric trace gas, however, its global warming potential is, on a 100 years time horizon, about 296 – 340 times higher than that of CO_2 [*Jain et al.*, 2000; *Ramaswamy et al.*, 2001]. Formation or decomposition reactions of N_2O in the troposphere are of minor importance resulting in an almost inert behaviour of tropospheric N_2O. The atmospheric lifetime of N_2O is estimated to be about 114 – 120 years [*Prather et al.*, 2001]. Due to its relatively long atmospheric lifetime, N_2O is mixed into the stratosphere where it is photochemically decomposed. Moreover, by reaction with excited oxygen atoms ($O(^1D)$) in the stratosphere, it forms nitric oxide (NO) radicals, which are involved in one of the major catalytic ozone (O_3) reaction cycles [*Crutzen*, 1970]. In sum, atmospheric N_2O is important in controlling both the radiation and the stratospheric O_3 balances of the Earth. Comprehensive reviews of the chemical, physical and climate-related properties of N_2O are given in recent publications such as the current reports of the Intergovernmental Panel on Climate Change (IPCC) [*IPCC*, 2001] and the World Meteorological Organization (WMO) [*WMO*, 2003], the textbook by Warneck [2000] and in a review article by Trogler [1999].

Atmospheric N_2O concentrations, depicted from the Antarctic and Arctic ice cores as well as from Antarctic firn, show relatively uniform tropospheric N_2O mixing ratios in the range from 260 to 275 ppb (ppb, parts per billion = 10^{-9}) during the period from 1000 to 1900 AD and an increase to the present values during the last 100 years [*Khalil et al.*, 2002; *Prather et al.*, 2001; *Sowers*, 2001]. The global mean tropospheric N_2O mole fraction in 2003/2004 was about

318 – 319 ppb associated with a mean interhemispheric gradient of about 0.7 – 0.8 ppb [*Khalil et al.*, 2002; *Prather et al.*, 2001; *Prinn et al.*, 2000]. Time series of monthly mean N_2O atmospheric mole fractions and annual growth rates measured from 1978 to 2004 within the ALE/GAGA/AGAGE program are shown in Figure 1.

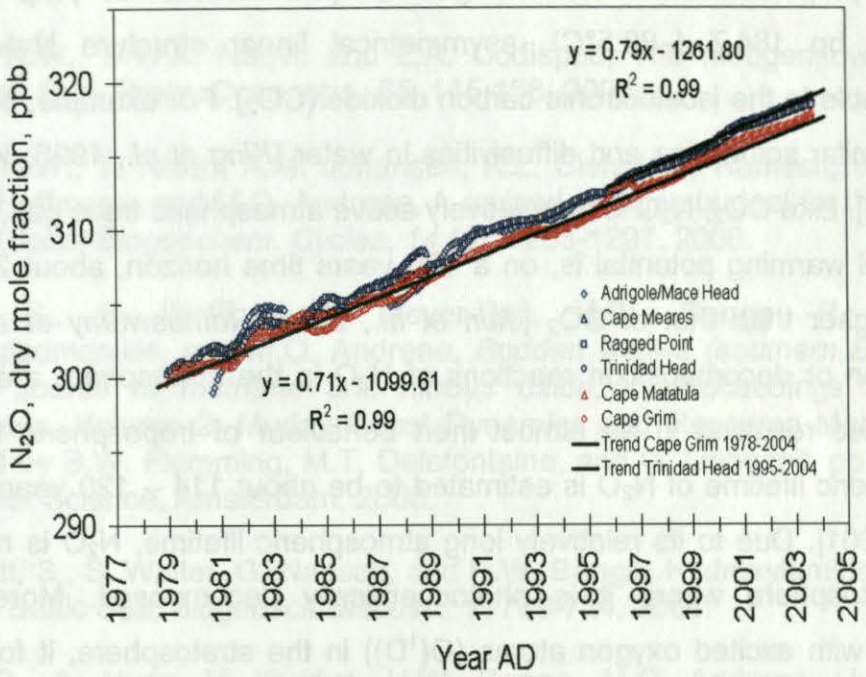

Figure 1: Monthly mean tropospheric N_2O dry mole fractions from the six baseline stations of the ALE/GAGE/AGAGE monitoring program in the northern Hemisphere (Adrigole/Mace Head, Ireland; Cape Meares, Oregon; Ragged Point, Barbados; Trinidad Head, California) and southern hemisphere (Cape Grim, Tasmania; Cape Matatula, American Samoa). The mean annual growth rates are calculated from monthly mean data, which have been smoothed with a 12-point moving average in order to minimize seasonal effects. The actual updated version (2 May 2005) of the ALE/GAGE/AGAGE data set (Prinn et al. [2000]) is available from the anonymous ftp site cdiac.esd.ornl.edu (subdirectory /pub/ale_gage_agage/) at the Carbon Dioxide Information Analysis Center in Oak Ridge, Tennessee, USA.

Higher N_2O values are measured in the northern hemisphere because the majority of the sources of atmospheric N_2O are located the northern hemisphere [*Khalil et al.*, 200; *Prather et al.*, 2001; *Prinn et al.*, 2000]. Due to the lack of significant sink and source reactions, almost no vertical tropospheric N_2O gradient is observed, whereas stratospheric N_2O mixing ratios decrease due to its photochemical decomposition (e.g. down to 120 ppb by 30 km in the mid-latitudes) [*Prather et al.*, 2001]. A summary of the key data of atmospheric N_2O is given in Table 1.

Table 1: Summary of key data of atmospheric N_2O (for references see text).

Mean tropospheric dry mole fraction in 2003/2004	Northern hemisphere[a]: 318.7 ppb Southern hemisphere[b]: 317.7 ppb
Pre-industrial dry mole fraction (before 1900)	260 – 275 ppb
Annual tropospheric growth rate	0.7 – 0.8 ppb $year^{-1}$
Atmospheric life time	114 – 120 years
Global warming potential[c]	296 – 340 x CO_2

[a] Calculated as the mean of the stations Mace Head, Ragged Point and Trinidad Head for the period March 2003 to March 2004 (see also Figure 1). Data were taken from the updated version of the ALE/GAGE/AGAGE data set (released May 2005).
[b] Calculated as the mean of the stations Cape Grim and Point Matatula for the period March 2003 to March 2004 (see also Figure 1). Data were taken from the updated version of the ALE/GAGE/AGAGE data set (released May 2005).
[c] Calculated for a 100 years time horizon.

Major natural sources of atmospheric N_2O are emissions from the oceans and soils. Agricultural soils and a variety of smaller sources such as biomass burning, various industries and cattle farming/feedlots have been identified as directly or indirectly anthropogenic influenced sources of atmospheric N_2O [*Prather et al.*, 2001]. An overview of the major N_2O fluxes is given in Table 2. Since oceanic N_2O emissions are of significant importance for the Earth's climate, deciphering the distribution of oceanic N_2O is crucial to understand the formation pathways of N_2O and to quantify its oceanic emissions to the atmosphere.

Table 2: Compilation of sources and sinks of atmospheric N_2O (in Tg N yr^{-1}) [*Prather et al.*, 2001].

	Range	Mean	
A) Natural sources			
Ocean	1 – 5	3.0	
Atmospheric NH_3 oxidation	0.3 – 1.2	0.6	
Tropical and temperate soils[a]	3.3 – 9.7	6.0	
B) Anthropogenic sources			
Agricultural soils	0.6 – 14.8	4.2	
Biomass burning	0.2 – 1.0	0.5	
Industrial sources[b]	0.7 – 1.8	1.3	
Cattle and feedlots	0.6 – 3.1	2.1	
Sum sources (= A + B)			17.7
C) Sink			
Stratospheric decomposition	9 – 16	12.6	
D) Atmospheric trend (imbalance)	3.1 – 4.7	3.8	
Implied total source (= C + D)			16.4

[a] incl. wet forest, dry savannas, forest, and grasslands.
[b] incl. nylon production, nitric acid production, fossil fuel fired power plants, emissions from automobiles.

2 N_2O DISTRIBUTION IN THE WORLD'S OCEANS

Historical development. The very first study of oceanic N_2O (from the South Pacific Ocean) was published by Craig and Gordon from Scripps Institution of Oceanography (SIO) in La Jolla, California, in 1963 [*Craig and Gordon*, 1963], followed by studies in the North Atlantic Ocean by Junge and Hahn from the Max Planck Institute for Chemistry in Mainz during the late 1960s/early 1970s (see Figure 2) [*Hahn*, 1974; *Hahn*, 1981; *Junge and Hahn*, 1971]. In a retrospective view it is obvious that these early measurements suffered from analytical deficiencies (e.g. calibration problems, sensitivity). In 1976 Yoshinari published his, now "classical", study on N_2O profiles in the North Atlantic Ocean (Sargasso and Caribbean Seas), which turned out to be groundbreaking since it was the first study to report the linear ΔN_2O-O_2 relationship [*Yoshinari*, 1976]. He also introduced ΔN_2O (= $[N_2O]_{measured} - [N_2O]_{equilibrium}$) as a measure of N_2O production and found the linear correlation between ΔN_2O and AOU (apparent

oxygen utilization) [*Yoshinari*, 1976]. It was not until the advent of the electron capture detector (ECD, for an overview see Lovelock [1997]) and the development an appropriate ECD calibration routine when precise and reliable N_2O measurements were made possible [*Cohen*, 1977; *Elkins*, 1980; *Rasmussen et al.*, 1976; *Weiss*, 1981]. The next step towards a better understanding of the oceanic N_2O distribution was the fundamental work on N_2O solubility in seawater by Weiss and Price [1980], which allowed the application of equilibration techniques for high-resolution surveys of surface N_2O concentrations, which are prerequisites for estimates of the N_2O flux across the ocean/atmosphere interface. Up to now the use of an ECD in combination with equilibration or purge-and-trap techniques followed by gas chromatographic separation is state of the art for the determination of dissolved N_2O.

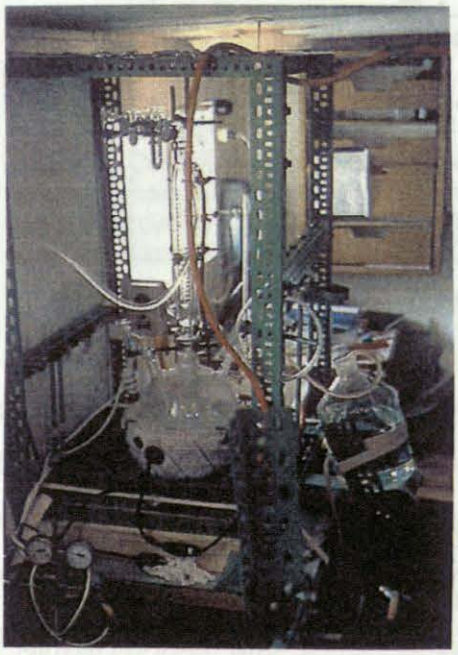

Figure 2: Device for purging and pre-concentration of oceanic N_2O onboard R/V *Meteor* in June 1970 [*Hahn*, 1987].

2.1 Formation and consumption pathways in the ocean

The formation and consumption pathways of oceanic N_2O form integral parts of the nitrogen cycle in the ocean (and its underlying sediments[1]) (Figure 3).

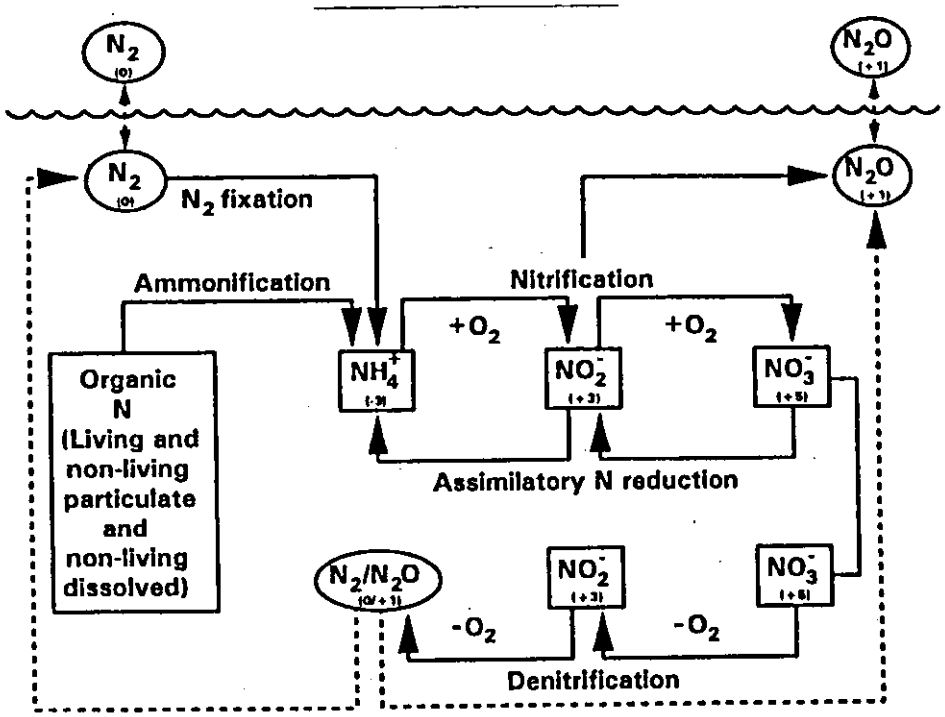

Figure 3: Simplified sketch of the oceanic nitrogen cycle [*Karl et al.*, 2002].

Depth profiles of N_2O show (apart from of a few exceptions found in suboxic and anoxic waters, see below) positive concentration anomalies, expressed as ΔN_2O (= $[N_2O]_{measured} - [N_2O]_{equilibrium}$; $[N_2O]_{equilibrium}$ is a function of water temperature, salinity, atmospheric N_2O dry mole fraction and the ambient air pressure [*Weiss and Price*, 1980]). Positive ΔN_2O values are interpreted as an indicator for in-situ N_2O formation. This caused Yoshinari [1976] to coin the term 'apparent N_2O production' for ΔN_2O. Today's prevailing view is that there are only two microbial processes (i.e. nitrification and denitrification) during which oceanic N_2O is formed either as a by-product or as an intermediate (Figure 4).

[1] Since sediments are not subject of the presented studies, the further discussion will only focus on water column processes.

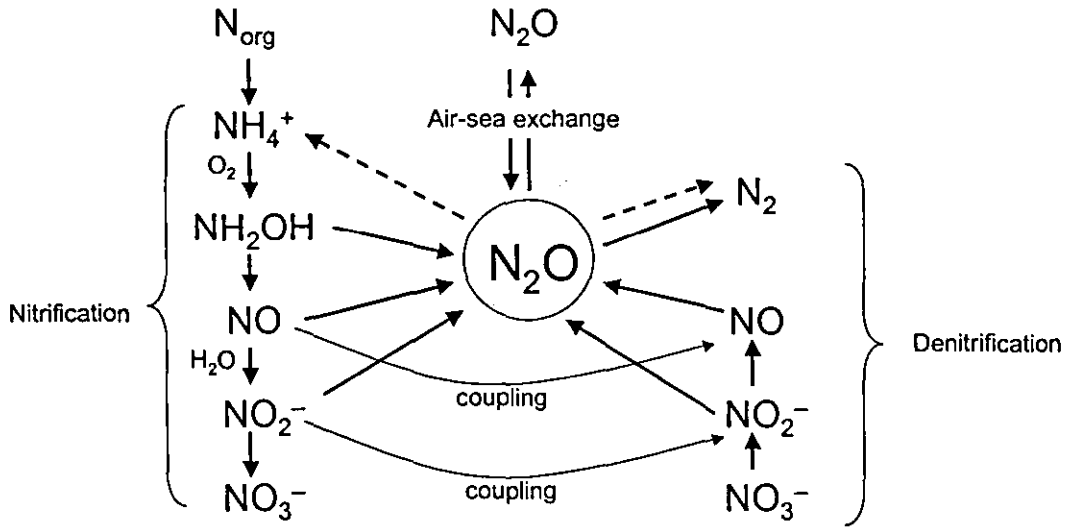

Figure 4: Overview of processes, which influence the N_2O distribution in the ocean. The dashed arrows indicate N_2O reduction during N_2 fixation (see e.g. Yamazaki et al. [1987]). Note that during the oxidation of NH_4^+ oxygen (O_2) is used as oxidizing agent, whereas during the oxidation of NO, water (H_2O) is used (see Ostrom et al. [2000] and references therein).

Nitrification is the oxidation of ammonium (NH_4^+) to nitrate (NO_3^-) via hydroxylamine (NH_2OH), nitric oxide (NO) and nitrite (NO_2^-). Autotrophic nitrification represents the final step of the oceanic remineralisation and is performed in two steps by ammonia-oxidizing bacteria (AOB, e.g. *Nitrosomonas* and *Nitrosospira*) and nitrite-oxidizing bacteria (NOB, e.g. *Nitrobacter* and *Nitrospira*), respectively [*Arp and Stein*, 2003; *Bothe et al.*, 2000; *Kowalchuk and Stephen*, 2001]:

$$NH_4^+ \rightarrow NH_2OH \rightarrow NO \rightarrow NO_2^- \text{ (AOB)}$$
$$NO_2^- \rightarrow NO_3^- \text{ (NOB).}$$

Interestingly, an ammonium-oxidizing archaeon has been isolated recently [*Könneke et al.*, 2005].

During autotrophic nitrification N_2O can be formed by AOB either via the pathways $NH_2OH \rightarrow N_2O$ and $NO \rightarrow N_2O$ [*Arp and Stein*, 2003; *Stein and Yung*, 2003] or via the pathway $NO_2^- \rightarrow NO \rightarrow N_2O$ (the latter is part of the so-called nitrifier-denitrification process) [*Stein and Yung*, 2003; *Wrage et al.*, 2001]. Nitrification is an aerobic process, however, under low-oxygen conditions, N_2O yields are enhanced [*De Bie et al.*, 2002; *Goreau et al.*, 1980] (Figure 5). Alternatively, N_2O can be formed during heterotrophic nitrification (i.e. nitrification linked to aerobic denitrification) via the reaction $NO_2^- \rightarrow NO \rightarrow N_2O$ as well, but, the enzymes involved in the heterotrophic reaction sequence are different from those involved in the autotrophic pathway [see e.g. *Richardson and Watmough*, 1999]. Under oxic conditions, N_2O yields from heterotrophic nitrification are higher than those from autotrophic nitrification. However, the relevance of heterotrophic nitrification for the marine environment is not known yet [*Stein and Yung*, 2003; *Wrage et al.*, 2001]. Additionally, methane oxidising bacteria can also produce N_2O via NH_4^+ oxidation [*Stein and Yung*, 2003; *Sutka et al.*, 2003], however, the relevance of this formation pathway for the marine environment remains to be proven.

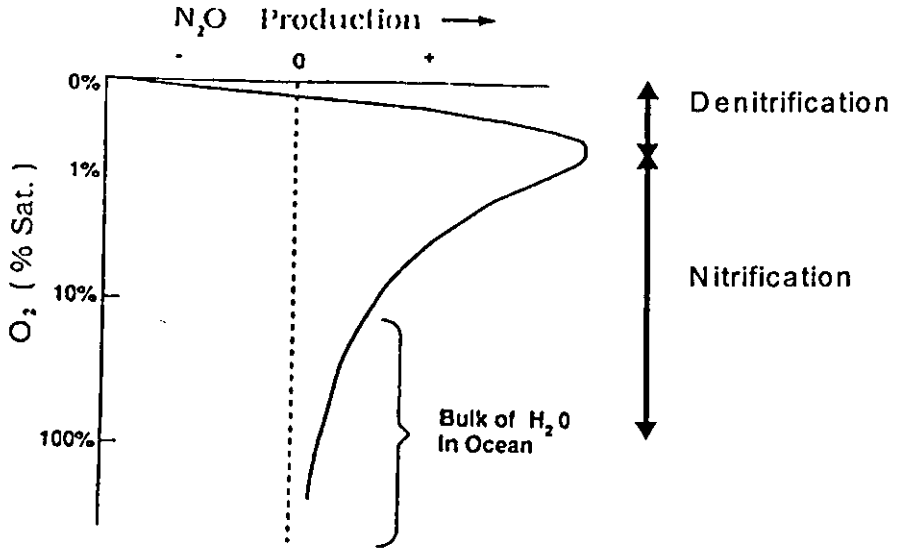

Figure 5: Dependence of N_2O production/consumption on dissolved O_2 concentrations (expressed as % saturation = $100[O_2]_{measured} / [O_2]_{equilibrium}$) [*Codispoti et al.*, 1992].

Denitrification is defined as the respiratory reduction of NO_3^- to dinitrogen (N_2) via NO_2^-, NO and N_2O during organic matter remineralisation. It results in a loss of bioavailable (fixed) nitrogen in the form of gaseous products such as N_2O and N_2:

$$NO_3^- \rightarrow NO_2^- \rightarrow NO \rightarrow N_2O \rightarrow N_2$$

As can be seen from the denitrification reaction sequence N_2O is an intermediate with its concentration at any time determined by the balance between production and consumption (Figure 6). Denitrification is a well-known feature of many different bacteria species in terrestrial and oceanic environments [*Bothe et al.*, 2000; *Tiedje*, 1988; *Zumft*, 1997]. Denitrifiers are usually facultative aerobic bacteria, which can reduce NO_3^- when oxygen becomes limiting. Thus the occurrence of denitrification is favoured under suboxic conditions ($0 < O_2 < 2 - 10$ µmol L^{-1}, *Codispoti et al.*, [2005]; see Figure 5). Denitrification does not occur under anoxic conditions ($O_2 = 0$ µmol L^{-1}, hydrogen sulphide present).

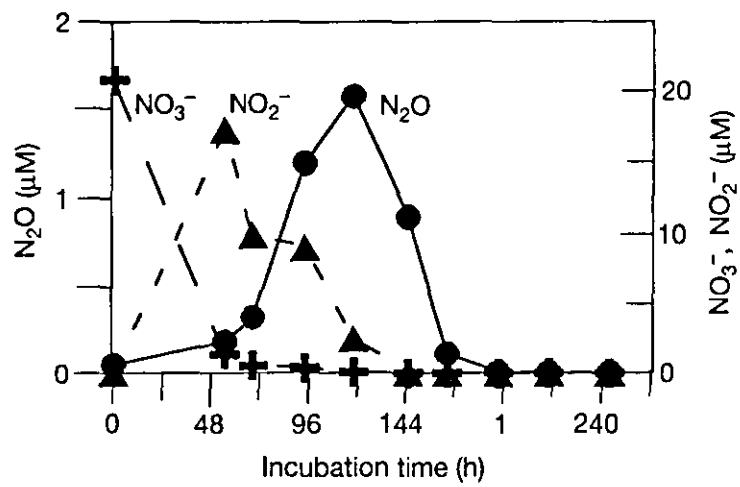

Figure 6: Accumulation and consumption of N_2O during denitrification. The incubation experiment was performed with water from 40 m depth on the southwest continental shelf off India [*Naqvi et al.*, 2000]. Initial O_2 concentration was 15 µmol L^{-1}.

Both, nitrification and denitrification as sources and sinks of oceanic N_2O have been described in the water column, in the sediments and in association with suspended particles (e.g. [*Codispoti et al.*, 2005; *Nevison et*

al., 2003; *Schropp and Schwarz*, 1983; *Seitzinger*, 1990]. N_2O yields from water column nitrification range from 0.01% to 0.42% and from 0.004% to 0.027% in estuarine systems and in the western North Pacific Ocean, respectively [*De Wilde and De Bie*, 2000; *Punshon and Moore*, 2004; *Yoshida et al.*, 1989]. N_2O yields from sedimentary denitrification range from 0.1% to 0.5% with values up to 6% in nutrient-rich regions (see overview in Seitzinger [1998]). The integrated net N_2O formation during denitrification and nitrification in the suboxic portion of the central Arabian Sea was estimated to be about 2% of the nitrogen loss [*Bange et al.*, 2001b].

2.2 Depth profiles

N_2O depth profiles from regions with oxic water masses ($O_2 > 10$ µmol L^{-1}) such as found in the major parts of the Atlantic, Pacific, and Indian Oceans are characterised by a subsurface N_2O maximum which coincides with the minimum of dissolved O_2 and the maximum of NO_3^- [*Butler et al.*, 1989; *Cohen and Gordon*, 1979; *Oudot et al.*, 1990; *Oudot et al.*, 2002] (Figure 7). However, the N_2O subsurface maximum is less pronounced or even absent in the northern (subpolar) North Atlantic Ocean (Figure 7). N_2O concentrations in deep waters below 2000 m show an increasing trend from the deep North Atlantic Ocean to the deep North Pacific Ocean. This trend correlates well with the water age distribution in the ocean and was attributed to nitrification [*Bange and Andreae*, 1999]. N_2O input to deep waters by hydrothermal vent systems seems to be of minor importance [*Bange and Andreae*, 1999; *Lilley et al.*, 1982].

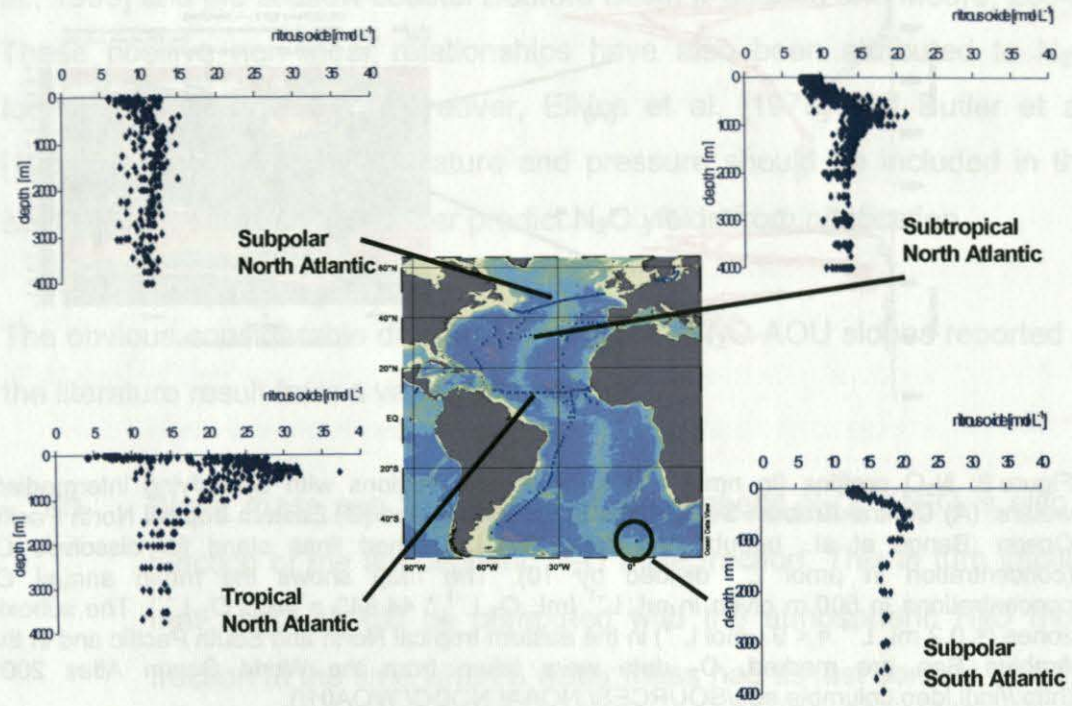

Figure 7: N_2O (in nmol L^{-1}) distribution in the Atlantic Ocean. Data from the North Atlantic Ocean are taken from Walter [2006]. Data from the South Atlantic Ocean are published in Walter et al. [2005].

N_2O profiles from oceanic regions with suboxic zones ($0 < O_2 < 2 - 10$ µmol L^{-1}) such as the Arabian Sea and the eastern tropical North Pacific Ocean, which are sites of intense denitrification, generally show a two-peak structure (Figure 8): N_2O maxima are found at the upper and lower boundaries of the oxygen minimum zone (OMZ), whereas in the core of the suboxic zone, N_2O concentrations are considerably depleted [*Bange et al.*, 2001b; *Cohen and Gordon*, 1978; *Naqvi and Noronha*, 1991]. In anoxic water masses such as found in the central Baltic Sea, the Cariaco Basin, and Saanich Inlet, N_2O concentrations are close to the detection limit [*Brettar and Rheinheimer*, 1991; *Cohen*, 1978; *Hashimoto et al.*, 1983; *Rönner*, 1983].

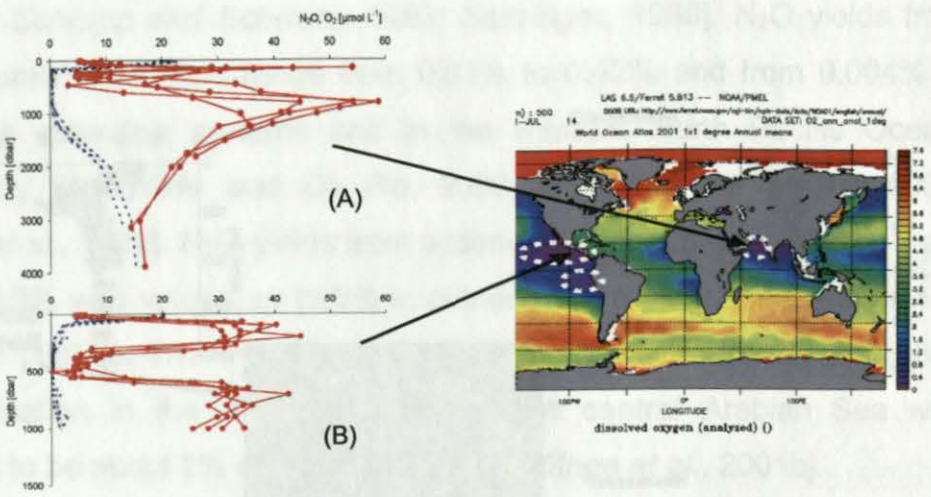

Figure 8: N_2O profiles (in nmol L^{-1}) from oceanic regions with denitrifying intermediate waters: (A) Central Arabian Sea [*Bange et al.*, 2001b] and (B) Eastern tropical North Pacific Ocean (Bange et al., unpublished data, 2004). Dashed lines stand for dissolved O_2 (concentration in µmol L^{-1} divided by 10). The map shows the mean annual O_2 concentrations in 500 m given in mL L^{-1} (mL O_2 L^{-1} * 44.643 = µmol O_2 L^{-1}). The suboxic zones (< 0.2 mL L^{-1} = < 9 µmol L^{-1}) in the eastern tropical North and South Pacific and in the Arabian Sea are marked. O_2 data were taken from the World Ocean Atlas 2001 (http://iridl.ldeo.columbia.edu/SOURCES/.NOAA/.NODC/.WOA01/).

Depth profiles of N_2O (apart from exceptions found in suboxic and anoxic waters, see above) show positive concentration anomalies, expressed as ΔN_2O. Because nitrification is directly linked to organic matter remineralisation, plots of ΔN_2O vs. the apparent oxygen utilization (AOU) or N_2O vs. O_2 have been used to identify prevailing formation and consumption processes of oceanic N_2O. AOU is usually used as a measure of the amount of O_2 consumed during organic matter oxidation in the ocean. Plots of ΔN_2O vs. AOU from the majority of the oceanic regions show clear positive linear relationships, suggesting that nitrification is the main N_2O formation process. This is supported by the fact that in most oxic water columns N_2O is positively correlated with NO_3^-, the final product of nitrification. The slope of the linear ΔN_2O-AOU relationship varies between $3*10^{-5}$ and $3*10^{-4}$ [see overview tables in *Bange and Andreae*, 1999; *Bange et al.*, 2001b; *Nevison et al.*, 1995; *Oudot et al.*, 2002; *Suntharalingam and Sarmiento*, 2000] and can be interpreted as the N_2O yield per O_2 molecule consumed indicating that every 33,000 to 3000 molecules of O_2 utilized, about one molecule of N_2O is produced (see also discussion of the discrepancy below). Beside the well-documented linear relationships, non-linear ΔN_2O-AOU 2nd order

polynomial fits have been reported from the Arabian Sea [*Upstill-Goddard et al.*, 1999] and the shallow coastal Bedford Basin [*Punshon and Moore*, 2004]. These positive non-linear relationships have also been attributed to N_2O formation by nitrification. Moreover, Elkins et al. [1978] and Butler et al. [1989] suggested that temperature and pressure should be included in the ΔN_2O-AOU relationship to better predict N_2O yields from nitrification.

The obvious considerable discrepancies of the ΔN_2O-AOU slopes reported in the literature result from a variety of reasons:

(i) Water mass age and history of atmospheric N_2O: ΔN_2O is also a function of the atmospheric N_2O mole fraction. This in turn implies that ΔN_2O should be computed with the atmospheric N_2O mole fraction at the time when a water mass had its last contact with the atmosphere. Using "historical" N_2O dry mole fractions would shift ΔN_2O to higher values. However, it requires the knowledge of the water mass ages and the associated atmospheric N_2O mole fractions, which are not available in most cases.

(ii) Variability of the N_2O yield: the N_2O yield from nitrification is not necessarily uniform in the ocean since it depends on the abundance and composition of the bacterial community (i.e. the biological diversity). The O_2-dependence of N_2O formation might be varying for different bacteria species. Moreover, Nevison et al. [2003] speculated that the remineralisation of nitrogen-enriched organic material (which can be found in regions with high N_2 fixation activities) might lead to an enhancement of the N_2O yield. However, detailed studies on the N_2O yields from marine nitrifiers are lacking.

(iii) N_2O from denitrification: signals of N_2O produced in suboxic zones during denitrification can be advected to adjacent oxic, nitrifying zones [*Bange et al.*, 2001b]. Moreover, N_2O formation in O_2-depleted microniches such as found in sinking particles, can release additional N_2O [*Schropp and Schwarz*, 1983].

(iv) Applicability of AOU: AOU in deep waters does not represent the true oxygen utilization because surface O_2 concentrations at sites of deep-water mass formation might not be in equilibrium with the atmosphere. This leads to overestimation or underestimation of deep water AOU and raises questions concerning the use of AOU as a measure of respiration [see e.g. *Ito et al.*, 2004]. Moreover, uncertainties in the O_2 solubility equations are most pronounced at low temperatures (<1°C) and high salinities (i.e. in the typical features of deep ocean water masses of the thermohaline circulation) as pointed out by *Garcia and Gordon* [1992].

There are caveats against a straightforward interpretation of the linear ΔN_2O-AOU relationship as an indicator for N_2O formation via nitrification. In other words, a linear ΔN_2O-AOU relationship may not necessarily result from nitrification. Most recently, based on N_2O isotopomer data (see below), Yamagishi et al. [2005] argued that net N_2O formation in the oxygen minimum zone (OMZ) of the western North Pacific Ocean mainly results from denitrification with only a small contribution by nitrification. They showed that this N_2O, when diffusing into deep waters, produces a reasonable linear ΔN_2O-AOU relationship. Moreover, by applying a two end-member mixing model, Nevison et al. [2003] showed that isopycnal mixing of water masses with different preformed N_2O and O_2 concentrations can result in a linear ΔN_2O-AOU relationship, which can mask the "true" biological N_2O production (Figure 9). They state: "[...], we find that the biological N_2O yield per mole O_2 consumed cannot be calculated with great confidence from cross-plot correlation slopes. The essential problem is that the N_2O yield is spatially variable. As a result, strong mixing gradients exist in the data that can overwhelm more subtle N_2O production terms." [*Nevison et al.*, 2003].

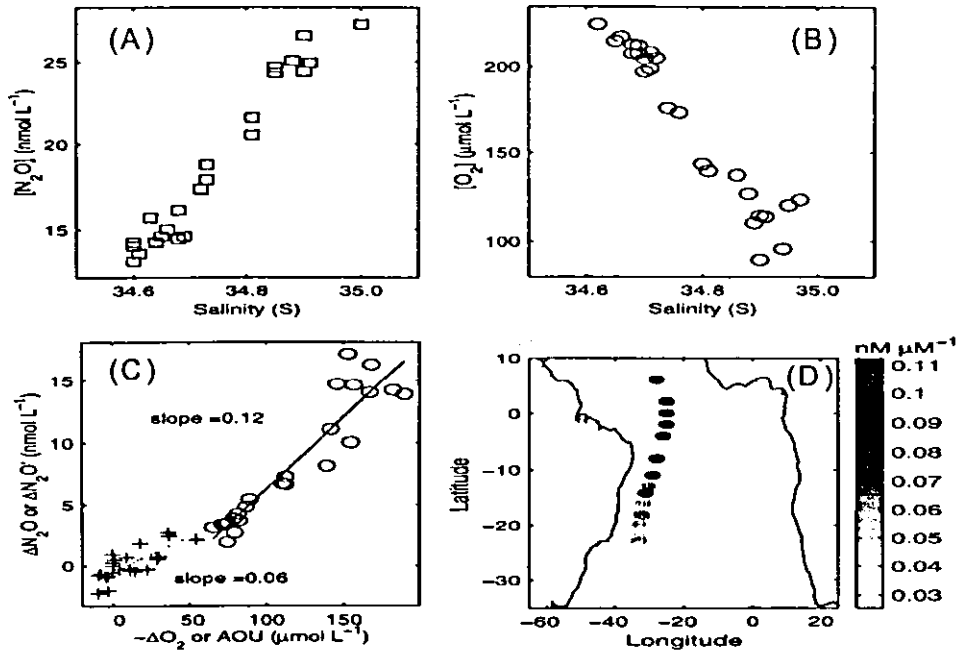

Figure 9: Isopycnal (σ = 26.9) analysis of N_2O and O_2 data from the South Atlantic Ocean [*Nevison et al.*, 2003]. (A): N_2O vs. salinity; (B): O_2 vs. salinity; (C): AOU or $-\Delta O_2$' (Nevison's original axis labelling $-\Delta O_2$ is erroneous) vs. ΔN_2O or ΔN_2O'; (D) ΔN_2O/AOU ratios for the individual stations. $-\Delta N_2O$' = biological source/sink term defined as $[N_2O]_{measured} - [N_2O]_{preformed}$ and $-O_2$' = biological source/sink term defined as $[O_2]_{preformed} - [O_2]_{measured}$. Please note the slope in (C) drops from $0.12*10^{-3}$ to $0.06*10^{-3}$ when plotting $-\Delta N_2O$' vs. $-O_2$'. This indicates that in the case for the South Atlantic Ocean the traditionally used cross plot of ΔN_2O vs. AOU is primarily due to mixing gradients [*Nevison et al.*, 2003].

In view of the above-mentioned uncertainties, the use of a simple ΔN_2O-AOU relationship in model studies of the global oceanic N_2O distribution [*Goldstein et al.*, 2003; *Jin and Gruber*, 2003; *Suntharalingam and Sarmiento*, 2000] might fail to simulate small-scale features of N_2O water column distributions.

A linear relationship between ΔN_2O (N_2O) and AOU (O_2 or NO_3^-) does not exist in suboxic water masses (eastern tropical Pacific Ocean and Arabian Sea, see also Figure 8) and in anoxic water masses (e.g. Baltic Sea, Cariaco Basin) indicating a complex interplay between N_2O formation and consumption during denitrification. The characteristic N_2O double peak structures found in the central Arabian Sea were explained with a coupling of denitrification and nitrification at about 150 m around the upper boundary of the OMZ, followed by N_2O consumption due to denitrification in the core of the OMZ at about 200 – 400 m. The second, broad N_2O peak in about 800 – 1000 m was attributed to nitrification (with a signal of denitrification still visible) [*Bange et al.*, 2001b]. Results from incubation experiments with water

samples from the denitrifying oxygen minimum zone off northern Chile are in line with the observations from the Arabian Sea. Denitrification was found to be the main N_2O formation process but also the main consumption process resulting in a net depletion of N_2O in the core of the suboxic zone [*Castro-González and Fraías*, 2004].

2.3 N_2O in the ocean surface layer

Global maps of N_2O in the upper 10 m of the world's oceans have been computed based on the extensive N_2O data set collected by Weiss et al. [1992] since 1977 (see also Nevison et al. [2004]) with additional data from two campaigns by Butler et al. [1988] and Lobert et al. [1996] (Figure 10). Based on the combined data sets by Weiss et al. [1992] and Butler et al. [1988], Nevison et al. [1995] calculated a global mean N_2O surface saturation of 103.5% (for a definition of the saturation see section 3.1). The global distribution of N_2O surface anomalies (here defined as $\Delta pN_2O = pN_2O_{measured} - pN_2O_{equilibrium}$, positive anomalies indicating a release of N_2O to the atmosphere) is shown in Figure 10. Common features of both maps in Figure 10 are:

(i) Enhanced N_2O anomalies in the equatorial upwelling regions of the eastern Pacific and Atlantic Oceans,

(ii) Enhanced N_2O anomalies along coastal upwelling regions such as along the west coasts of North and Central America, off Peru, off Northwest Africa and the northwestern Indian Ocean (Arabian Sea) and

(iii) N_2O anomalies close to zero (i.e. near equilibrium) in the North and South Atlantic Ocean, the South Indian Ocean and the central gyres of the North and South Pacific Ocean.

Differences in the two maps result mainly from different interpolation methods. Additionally, both maps are biased by insufficient data coverage in some parts of the ocean (e.g. in the Indian and western Pacific Oceans, see Figure 10A). The interpolation methods for filling and smoothing used by

Nevison et al. [1995] seem to be more appropriate for extrapolating data east-west than north-south. This can be clearly seen in the resulting ΔpN_2O distributions in the northern Indian and the eastern tropical North Pacific Oceans (Figure 10B). In contrast to the statistical filling and smoothing method used by Nevison et al. [1995], Suntharalingam and Sarmiento [2000] used a spatially adaptive multi-variate regression analysis with different predictor variables (multi-variate adaptive regression splines, MARS, for details of the model see *Suntharalingam* [1997]). The map shown in Figure 8C is based on a MARS model run with a combination of four predictor variables, namely mixed layer depth, subsurface O_2 minimum concentration, sea surface temperature and wind-driven upwelling rate (listed in the order of significance). The enhanced ΔpN_2O values predicted for the Hudson Bay and off the coast of China are model artefacts [*Suntharalingam*, 1997]. When comparing both maps (Figures 10B and 10C) a significant discrepancy for the Southern Ocean south off Africa is obvious. Nevison et al.'s [1995] map shows enhanced values up to 51 µatm ΔpN_2O, whereas in the map by Suntharalingam and Sarmiento [2000] maximum values up to 20 µatm are shown. It seems that Nevison et al.'s [1995] interpolation method amplifies local distributions, whereas Suntharlingam and Sarmiento's [2000] method tends to smooth the distribution according to the large-scale distributions of the predictor variables.

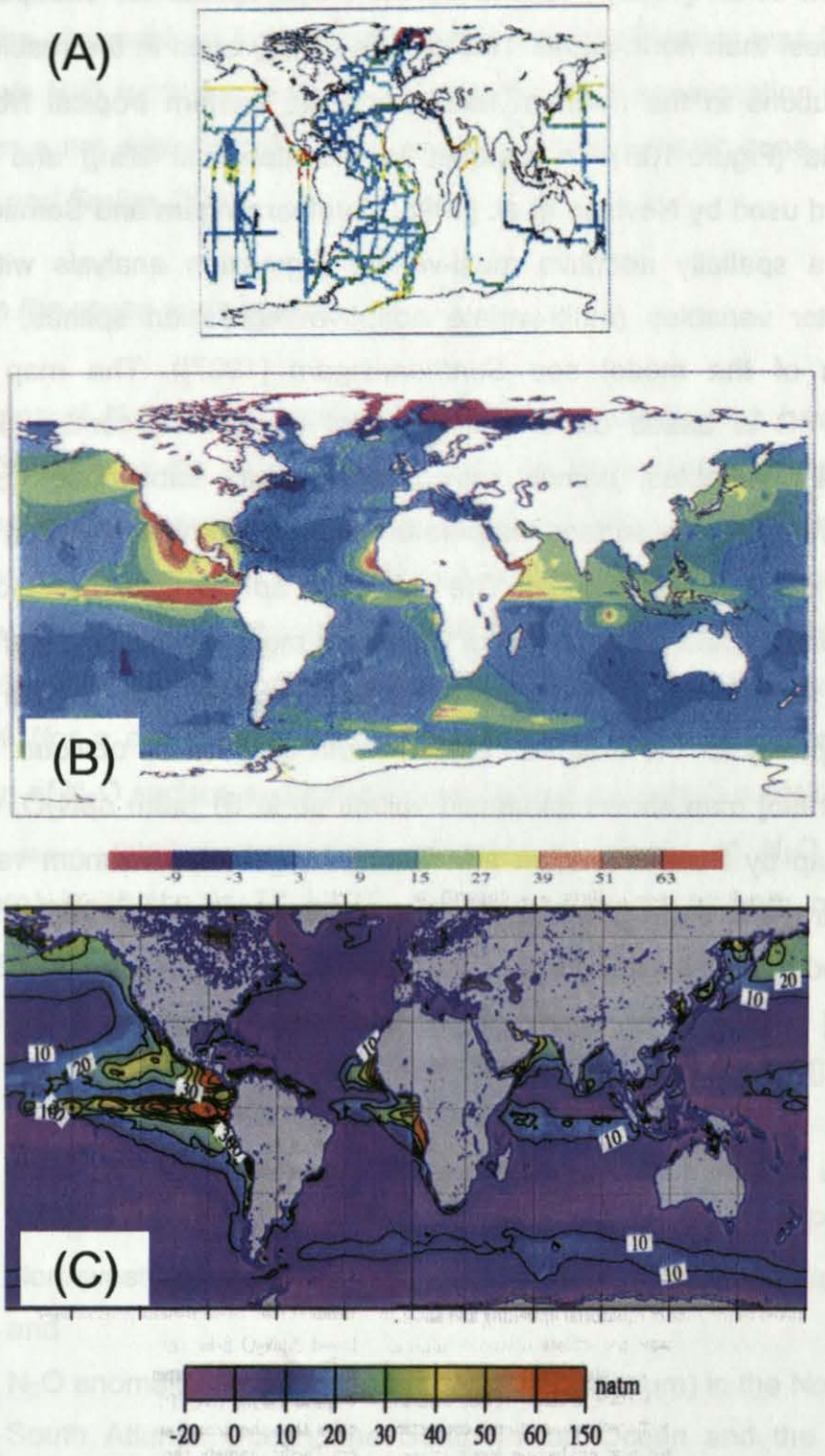

Figure 10: Maps of ΔpN_2O (in natm) in the surface layers of the world's oceans. (A) Distribution of surface ΔpN_2O measurements used to create maps (B) and (C). Colour coding is the same as in (B). (B), map by Nevison et al. [1995] and (C), map by Suntharalingam and Sarmiento [2000]. Please note that the colour coding is non-linear and different for maps (B) and (C).

2.4 N_2O in coastal areas

During the last few years coastal areas such as estuaries, intertidal areas, upwelling regions, and mangrove ecosystems have received increasing attention as sites of intense N_2O formation and release to the atmosphere (see also the sections on eutrophication and N_2O budget). Studies on the biogeochemical cycling of N_2O in coastal regions have been undertaken to a large extent in European and North American coastal regions. A compilation of coastal N_2O measurements worldwide is given in Bange et al. [1996b]. More recently, I [*Bange*, 2005] compiled and reviewed N_2O studies in European coastal regions (Baltic Sea, North Sea, NE Atlantic, Mediterranean Sea, Black Sea). My major conclusions are:

(i) Maximum N_2O saturations are usually observed in estuaries, whereas in open coastal waters N_2O saturations are close to the expected equilibrium saturation indicating a vigorous production of N_2O in estuarine systems. Additionally, N_2O distributions in estuaries show a pronounced seasonal variability.

(ii) It is obvious that sedimentary denitrification and water column nitrification are the major N_2O formation processes. However, the yield of N_2O from both processes strongly depends on the local O_2 concentrations; thus dissolved O_2 is the key factor regulating N_2O production (and its subsequent emissions to the atmosphere).

(iii) In anoxic waters, such as the deep basin of the central Baltic Sea or parts of the shallow Po River delta, N_2O is consumed by water column denitrification.

The conclusions are in line with a recent seasonal study of N_2O in the water column of the Bedford Basin (Northwest Atlantic Ocean), which showed that water column nitrification was the dominant N_2O formation pathway. N_2O consumption was only temporarily observed when dissolved O_2 was considerably depleted (2.5 µmol L^{-1}) shifting the system from oxic to suboxic conditions [*Punshon and Moore*, 2004].

Coastal upwelling. The narrow band of coastal upwelling such as found along the Arabian Peninsula and the coast of Somalia have been identified as "hot spots" for N_2O emissions showing N_2O surface saturations of up to 330% [*Bange et al.*, 2001a; *De Wilde and Helder*, 1997]. The high N_2O saturations result from the upwelling of subsurface water masses where N_2O formation is favoured due to suboxic conditions [*Bange et al.*, 2001b]. N_2O concentrations in coastal upwelling areas are closely correlated with the low seasurface temperatures characteristic for upwelled subsurface water masses (Figure 11). Because the coastal upwelling in the western Arabian Sea is triggered by the seasonal occurring Southwest Monsoon winds, N_2O emissions also show a pronounced seasonality [*Bange et al.*, 2001a].

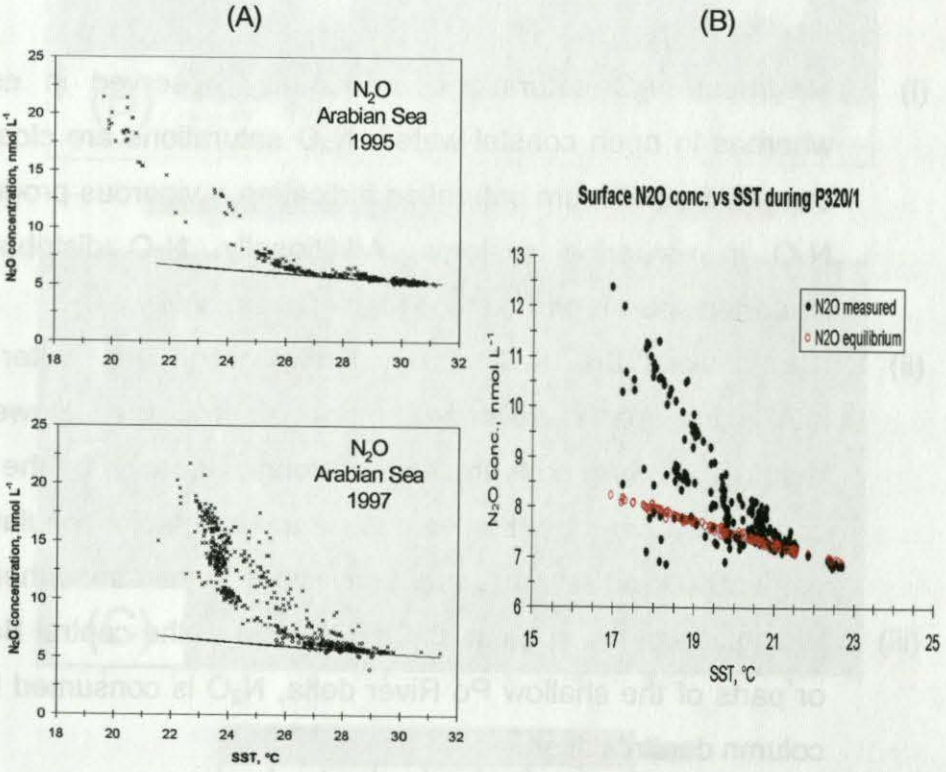

Figure 11: N_2O concentrations in coastal upwelling areas; (A) off the Arabian Peninsula [*Bange et al.*, 1996c; *Bange et al.*, 2000]; the black line represents the corresponding equilibrium concentrations; and (B) off Mauritania (NW Africa) [*Gebhardt and Bange*, 2005, unpublished data]; red circles represent the corresponding equilibrium concentrations.

High precision time series of atmospheric N_2O have been used successfully to quantify N_2O emissions from temporal upwelling events along the coast off California [*Lueker et al.*, 2003] and from the Southern Ocean [*Nevison et al.*,

2005]. This seems to be a promising approach, however, it depends on the existence of high-precision N_2O time series, which are at the moment only available at a few coastal sites [*Prinn et al.*, 2000].

Mangrove forests. The ecosystems of the mangrove forests have a high potential of N_2O formation and release to the atmosphere. N_2O in mangrove sediments from Puerto Rico is mainly produced by nitrification [*Bauza et al.*, 2002] whereas the results of incubation experiments with mangrove soils from the east coast of Australia revealed that denitrification is the main N_2O formation pathway [*Kreuzwieser et al.*, 2003]. The N_2O release from Puerto Rico mangrove sediments was found to be higher than comparable N_2O emissions from intertidal estuarine sediments [*Corredor et al.*, 1999; *Middelburg et al.*, 1995]. Actual results from N_2O measurements at three sites in a mangrove forest on the east coast of central China support this view [*Alongi et al.*, 2005]. However, at these sites a pronounced seasonality was observed showing maximal N_2O emissions in summer, whereas in autumn they were close to zero. A realistic estimate of the contribution of N_2O emissions from mangroves to the global oceanic budget of atmospheric N_2O is not possible at the moment because of the very small number of available measurements.

2.5 Coastal eutrophication and Fe fertilization

Coastal eutrophication (i.e. enhanced nutrient input to the coastal areas) can result in a shift from oxic conditions to anoxic conditions. This is especially important in view of the fact that oceanic N_2O formation strongly depends on dissolved O_2 (Figure 5). Indeed, Naqvi et al. [2000] observed, during an anoxic event along the West coast of India, N_2O concentrations up to 533 nmol L^{-1}. The accumulation of N_2O was mainly attributed to the onset of denitrification at low O_2 concentrations with the assumption that the activity of the N_2O reductase (which catalyses the reduction of N_2O to N_2) was not established [*Firestone and Tiedje*, 1979] because of frequent aeration of the shallow shelf waters (so-called stop-and-go denitrification). A similar scenario was observed in the shallow Bedford Basin [*Punshon and Moore*, 2004].

Based on their results, Naqvi et al. [2000] cautioned that N_2O formation and thus its subsequent release to the atmosphere from shallow hypoxic systems might increase due to the fact that the numbers of oxygen-starved coastal zones is increasing as well [*UNEP*, 2004]. Eutrophication can also significantly stimulate the sedimentary N_2O formation by denitrification, which was demonstrated by Seitzinger and Nixon [1985] in microcosm experiments.

N_2O releases from mangrove ecosystems appear to be very sensitive to eutrophication: N_2O release across the sediment/atmosphere interface was enhanced significantly (up to 2800 times) when NH_4^+ was added to mangrove sediments in Puerto Rico [*Bauza et al.*, 2002; *Muñoz-Hincapié et al.*, 2002]. When NO_3^- was added, the enhancement was less pronounced indicating that N_2O production by nitrification was dominating. Comparable results were obtained at an Australian mangrove site where N_2O emissions increased by a factor of 50 to 100 times when nitrogen (NO_3^- and NH_4^+) was added [*Kreuzwieser et al.*, 2003]. Therefore, it seems realistic to expect that the contribution of mangrove ecosystems to global coastal emissions of N_2O will increase due to increasing nutrient inputs caused by the ongoing industrialization and intensification of agricultural activities in tropical countries.

Fuhrman and Capone [1991] pointed out that stimulating open ocean productivity by iron (Fe) addition [*Martin et al.*, 1991] might result in an enhanced formation of N_2O. Thus, enhanced N_2O formation by Fe addition might counteract the climatic benefits of a drawdown of atmospheric CO_2. Fuhrman and Capone [1991] argued that enhanced productivity would lead to enhanced nitrogen export from the euphotic zone, which in turn would result in additional N_2O formation via enhanced nitrification. The idea of a link between Fe fertilization and enhanced N_2O formation was supported by the study of Law and Ling [2001] who found a small but significant N_2O accumulation in the pycnocline during the Southern Ocean Iron Enrichment Experiment (SOIREE) in the Australasian sector of the Southern Ocean (61°S, 140°E) in February 1999. Recently, Jin and Gruber [2003] predicted the long-term effect of Fe fertilization on oceanic N_2O emissions on a global

scale with a coupled physical-biogeochemical model. Based on their model results they concluded that Fe fertilization-induced N_2O emissions could offset the radiative benefits of the CO_2 drawdown [*Jin and Gruber*, 2003]. However, during EIFEX, the European Iron Fertilization experiment in the subpolar South Atlantic Ocean in February/March 2004, no N_2O accumulation was detected within 33 days [*Walter et al.*, 2005]. It seems that Fe fertilization does not necessarily trigger additional N_2O formation, which might depend on the prevailing environmental conditions (e.g., the fate of the Fe-induced phytoplankton bloom). The link between Fe addition and enhancement of N_2O formation and the subsequent release of N_2O to the atmosphere remains to be proven.

2.6 N_2O isotope studies

Nitrogen (N) has two stable isotopes, ^{14}N and ^{15}N, which contribute 99.63% and 0.37%, respectively, to its composition [*Greenwood and Earnshaw*, 1984]. Oxygen (O) has three stable isotopes, ^{16}O, ^{17}O and ^{18}O, which contribute 99.76%, 0.04% and 0.2%, respectively, to its composition [*Greenwood and Earnshaw*, 1984]. ^{17}O has not been determined in oceanic N_2O yet, thus the following discussion focuses on the isotopic signatures of ^{15}N and ^{18}O. The stable isotopic ratio $^{15}N/^{14}N$ of N_2O is expressed relative to atmospheric N_2 as $\delta^{15}N_{atm}$:

$$\delta^{15}N_{atm}\ (\text{sample})\ [‰] = (((^{15}N/^{14}N)_{sample} / (^{15}N/^{14}N)_{std} - 1)*1000.$$

In the same way, the isotope ratio of $^{16}O/^{18}O$ of N_2O is usually expressed as $\delta^{18}O_{VSMOW}$ relative to Vienna standard mean ocean water (VSMOW). However, in some cases $\delta^{18}O_{atm}$ relative to O_2 in the atmosphere is reported. $\delta^{18}O_{VSMOW}$ can be converted to $\delta^{18}O_{atm}$ with the equation $\delta^{18}O_{atm} = -23.0 + \delta^{18}O_{VSMOW} / 1.0235$ [*Kim and Craig*, 1990]. Mean atmospheric $\delta^{15}N_{atm}$ and $\delta^{18}O_{VSMOW}$ of N_2O in tropospheric air are 6.72 ± 0.12 ‰ and 44.62 ± 0.21 ‰, respectively [*Kaiser et al.*, 2003].

Following the early studies of $\delta^{15}N$ and $\delta^{18}O$ of atmospheric N_2O by Moore [1974], Yoshida and Matsuo [1983] and Wahlen and Yoshinari [1985], measurements of the isotopic composition of oceanic N_2O have become a tool to decipher the various biogeochemical pathways of N_2O in the oceanic environment and to quantify the oceanic contribution to the atmospheric N_2O [*Kim and Craig*, 1993; *Stein and Yung*, 2003]. The isotopic composition of oceanic N_2O is determined by the isotopic signals of biological sources and sinks, its atmospheric imprint, and mixing processes within the ocean. This, in turn, implies that there are characteristic signals of enrichment or depletion (so called fractionation), which can be attributed to different biological processes as well as physical processes such as the gas exchange across the ocean/atmosphere interface.

Laboratory studies. The isotope composition of biologically derived N_2O depends on the isotope composition of the substrates such as NO_3^- (denitrification) and NH_4^+ (nitrification) and the isotopic depletion/enrichment during these processes. An overview of the isotopic depletion/enrichment of N_2O in culture experiments with different strains of denitrifying (*Pseudomonas flourescens*, *Pseudomonas aureofaciens*, *Paracoccus denitrificans*), nitrifier-denitrifying (*Nitrosomonas europaea*) and methane oxidizing bacteria (*Methylococcus capsulatus*) is shown in Figure 12. It is obvious that the range of the resulting nitrogen depletion in N_2O during denitrification and nitrification is similar. The isotope signal of oxygen in N_2O produced during nitrification is introduced by the $\delta^{15}O$ value of dissolved O_2 ($\delta^{15}O$ = 22 – 37 ‰) and H_2O ($\delta^{15}O$ = ~0 ‰) as oxidizing agents (Ostrom et al. [2000], see also Figure 4). The isotopic signal resulting from air-sea exchange is small compared to the biological processes. Therefore, biological N_2O formation should yield a clear isotopic signature in oceanic N_2O. However, the identification of nitrification or denitrification as N_2O producing processes strongly depends on the knowledge of the isotope signatures of the substrates, which can vary temporarily and spatially.

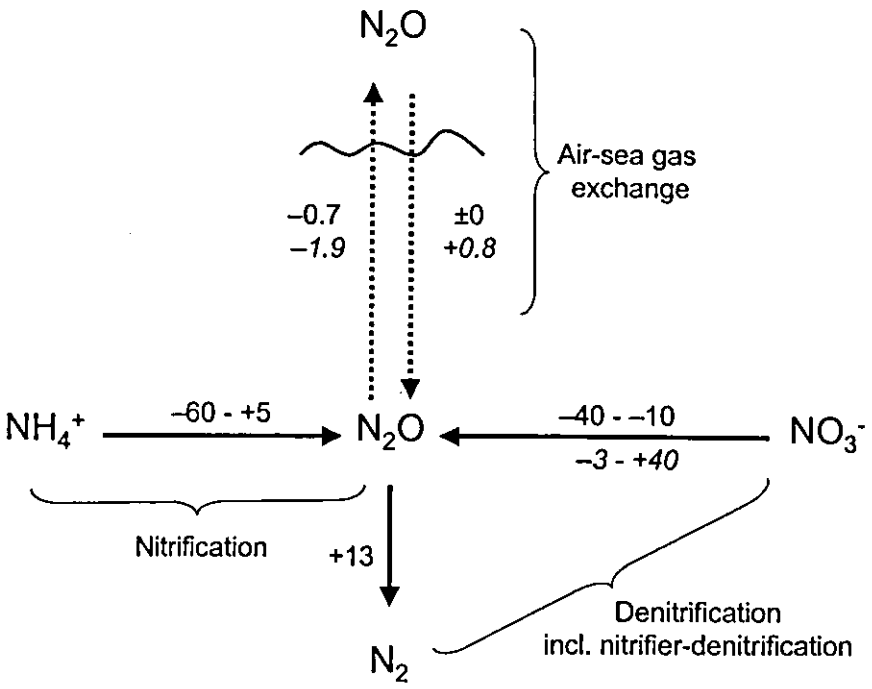

Figure 12: Isotopic depletion/enrichment for nitrogen and oxygen in N_2O relative to the substrates NO_3^- and NH_4^+, and the product N_2. Negative values depict isotopic depletion in N_2O and positive values depict isotopic enrichment in N_2O. Data for oxygen depletion/enrichment in N_2O are given in italics. Biological data were taken from Barford et al. [1999], Casciotti et al. [2002], Sutka et al. [2003], [2004], Toyoda et al. [2005] and Yoshida [1988]. Air-sea gas exchange data are from Inoue and Mook [1994].

An overview of studies of the isotopic signature of oceanic N_2O is given in Table 3. The main results are discussed in detail in the following sections.

Early field studies. The first measurements of $\delta^{15}N$ of dissolved N_2O in the eastern tropical North Pacific Ocean revealed that N_2O in the suboxic zone was enriched in ^{15}N relative to N_2O in the troposphere whereas N_2O in the surface layer was slightly depleted in ^{15}N relative to tropospheric N_2O [*Yoshida et al.*, 1984]. This is in line with the argumentation that N_2O in suboxic waters is consumed during denitrification and that N_2O is formed during nitrification in oxic waters. Surprisingly, Yoshida et al. [1989], found ^{15}N-enriched N_2O in the oxic waters of the upper 2000m of the western North Pacific and concluded that N_2O is mainly produced by denitrification.

Table 3: Overview of the suggested N_2O formation pathways based on isotope measurements of N_2O.

Oceanic region	Measured isotopic parameters of N_2O*	Suggested main formation pathways**	References
Eastern tropical N Pacific	$\delta^{15}N$	- Nit. in oxic waters - Denit. in suboxic waters	Yoshida et al. [1984]
Western N Pacific	$\delta^{15}N$	- Denit. in oxic waters	Yoshida et al. [1989]
N and S Pacific	$\delta^{15}N$, $\delta^{18}O$	- Nit. or coupled nit./denit. in deep waters	Kim and Craig [1990]
Subtrop. N Pacific, stat. ALOHA	$\delta^{15}N$, $\delta^{18}O$, SP_{N2O}	- Nit. via two different pathways	Dore et al. [1998]; Ostrom et al. [2000]; Popp et al. [2002]
Arabian Sea	$\delta^{15}N$, $\delta^{18}o$	- Coupled nit./denit. in oxic waters - Denit. in suboxic waters	Naqvi et al. [1998a]; [1998b]
Eastern tropical N Pacific	$\delta^{15}N$, $\delta^{18}O$	- Coupled nit./denit. in oxic waters - Denit. in suboxic waters	Yoshinari et al. [1997]
Western N Pacific, stat. KNOT	$\delta^{15}N$, $\delta^{18}O$, SP_{N2O}	- Nit.	Toyoda et al. [2002]
Western N Pacific, stat. KNOT	$\delta^{15}N$, $\delta^{18}O$, SP_{N2O}	- Denit. in oxic waters	Yamagishi et. al. [2005]

* SP_{N2O} stands for the site preference, for a definition see the section about isotopomers
** nit. stands for nitrification and denit. stands for denitrification.

Dual isotope signatures. The first N_2O dual isotope ($\delta^{15}N$ and $\delta^{18}O$) measurements from seawater were presented by Kim and Craig [1990]. At three stations in the North and South Pacific Ocean, N_2O was found to be slightly depleted relative to tropospheric N_2O in ^{15}N and ^{18}O down to about 600m, whereas in deep and bottom waters N_2O was found to be enriched in ^{15}N and ^{18}O relative to tropospheric N_2O. The reason for the unexpected enrichment of deep water N_2O is unclear. Kim and Craig [1990] speculated about nitrification with subsequent reduction by denitrification (which might take place in the interior of sinking particles) or, alternatively, N_2O formation during nitrification from a ^{15}N enriched intermediate such as NH_2OH.

With the application of the newly developed continuous-flow isotope-ratio monitoring mass spectrometers, the required seawater sample volume for N_2O dual isotope measurements has been drastically reduced and therefore facilitated the determination of high resolution depth profiles of the N_2O dual isotope signature [*Brand*, 1996; *Yoshinari et al.*, 1997]. Repeated measurements of N_2O depth profiles at the Hawaii ocean time series station ALOHA in the subtropical North Pacific Ocean revealed that $\delta^{15}N$ and $\delta^{18}O$ of N_2O were in equilibrium with tropospheric N_2O at the ocean surface and steadily decreased from the ocean surface to minimum values in about 100-300m at the base of the euphotic zone, followed by an increase to maximum values in 800m. The depletion of both ^{15}N and ^{18}O was attributed to result from nitrification [*Dore et al.*, 1998; *Ostrom et al.*, 2000; *Popp et al.*, 2002]. A more detailed study at ALOHA which included measurements of $\delta^{18}O$ in dissolved O_2 and H_2O, revealed that N_2O might be formed by two different pathways: First, by nitrification via NH_2OH or NO in most depths and, second, by nitrifier-denitrification via reduction of NO_2^- (between 350-500m) [*Ostrom et al.*, 2000]. The situations in the central Arabian Sea and the eastern tropical North Pacific Ocean are complex. N_2O was found to be strongly enriched in both ^{15}N and ^{18}O in the denitrifying oxygen minimum zone, whereas N_2O in the surface layer was depleted in ^{15}N but slightly enriched in ^{18}O compared to tropospheric N_2O [*Naqvi et al.*, 1998a; 1998b; *Yoshinari et al.*, 1997]. N_2O in the core of the oxygen minimum zone was obviously formed by denitrification since the final reduction step to N_2 should result in enriched N_2O. However, the 'light' N_2O found above the OMZ might be explained with a coupled nitrification-denitrification pathway where NO is formed during nitrification which is then reduced to N_2O during denitrification [*Naqvi et al.*, 1998a; *Naqvi et al.*, 1998b; *Yoshinari et al.*, 1997].

<u>*Isotopomers.*</u> As mentioned in the introduction, N_2O is an asymmetrical molecule and therefore it is possible to distinguish so-called isotopomers according to the position of ^{15}N within the N_2O molecule (the corresponding δ notation is given in parenthesis): $^{14}N^{15}NO$ ($\delta^{15}N^{\alpha}$) and $^{15}N^{14}NO$ ($\delta^{15}N^{\beta}$) [*Toyoda and Yoshida*, 1999]. The ^{15}N site preference (SP_{N2O}) in N_2O is given

as $\delta^{15}N^{\alpha} - \delta^{15}N^{\beta}$. The mean tropospheric SP_{N2O} is 18.7 ± 2.2 ‰ [*Yoshida and Toyoda*, 2000]. However, Kaiser et al. [2004] recently reported a mean tropospheric SP_{N2O} of 46.3 ± 1.4 ‰. The reason for the large discrepancy is unknown, but it was speculated that it might result from the use different primary standards [*Kaiser et al.*, 2003, 2004]. Measurements of SP_{N2O} should allow to identify the mechanisms of N_2O formation according to the different microbial pathways [*Sutka et al.*, 2003; *Sutka et al. 2006*; *Toyoda et al.*, 2005]. The SP_{N2O} strongly depends on both the bacterial strains used and the actual formation pathway. For example, *Nitrosomonas europaea* and *Nitrosospira multiformis*, both nitrifier-denitrifiers, can produce N_2O via both NH_2OH oxidation and NO_2^- reduction. Indeed, the SP_{N2O} were different for the NH_2OH oxidation pathway (~33 ‰) and the NO_2^- reduction pathway (~ –0.4 ‰) [*Sutka et al.*, 2003, 2004]. Most recently, based on a study with cultures of AOB, nitrifier-denitrifiers and denitrifiers, Sutka et al. [2006] concluded that the characteristic SP_{N2O} of nitrification and denitrification (incl. nitrifier-denitrification) are generally ~33 ‰ and ~0 ‰, respectively. Thus, isotopomers might be used to distinguish between N_2O produced during oxidation (nitrification) and reduction (denitrification and nitrifier-denitrification) processes, however, it seems that isotopomers cannot be used to reveal subtle differences such as nitrifier-denitrification and denitrification [*Sutka et al.*, 2006]. The range of SP_{N2O} (–0.6 to –0.5 ‰) from the denitrifiers *Pseudomonas chlororaphis* and *Pseudomonas aureofaciens* measured by Sutka et al. [2006] are in contrast to the results by Toyoda et al. [2005] who found a much larger variability for the SP_{N2O} produced by two other denitrifiers which showed SP_{N2O} of 23.3 ± 4.2 ‰ (*Pseudomonas fluorescens*) and –5.1 ± 1.8 ‰ (*Paracoccus denitrificans*) [*Toyoda et al.*, 2005]. However, this discrepancy is in line with the theoretical considerations by Schmidt et al. [2004], who argued that the observed SP_{N2O} and the associated $\delta^{18}O$ signatures during NO reduction to N_2O are reflecting the different types of NO reductases used by the different bacteria.

Up to now, the oceanic distributions of N_2O isotopomers have been determined at station ALOHA in the subtropical North Pacific [*Popp et al.*,

2002], at station KNOT (Kyodo North Pacific Ocean Time series) in the western North Pacific [*Toyoda et al.*, 2002; *Yamagishi et al.*, 2005], and in the eastern tropical North Pacific (ETNP) [*Yamagishi et al.*, 2005]. The SP_{N2O} profile at KNOT showed a steady increase from low values at the ocean surface (12 ‰) to a maximum (up to 36 ‰) in about 250–750m [*Toyoda et al.*, 2002]. A similar SP_{N2O} profile was observed at ALOHA, however, the low SP_{N2O} values were rather uniform in the depth range 0–500m and then increased to about 25 ‰ in 600-900m [*Popp et al.*, 2002]. The shape of the SP_{N2O} profiles at KNOT and ALOHA was explained with N_2O formation during nitrification, but the exact reaction pathway remained unclear [*Popp et al.*, 2002; *Toyoda et al.*, 2002]. In contrast, on the basis of additional isotopomer data from KNOT, Yamagishi et al. [2005] suggested net N_2O formation in the oxygen minimum zone, which is mainly resulting from both formation and consumption during denitrification with only a minor contribution by nitrification.

2.7 The world's oceans – a major source of atmospheric N_2O

The sources and sinks of atmospheric N_2O as reported by the IPCC (Intergovernmental Panel on Climate Change) in 2001 are summarized in Table 2 [*Prather et al.*, 2001]. It suggests a reasonably balanced present-day budget of atmospheric N_2O[2] and an oceanic contribution of about 17% to the overall sources of N_2O and about 31% to the natural sources. Remarkably, the N_2O ocean source in the IPCC report is low compared to other estimates (Figure 13).

[2] At the beginning of the 1990s, a considerable imbalance in the N_2O budget has been suggested, caused by a significant downward revision of N_2O formation during biomass burning and fossil fuel combustion due to sampling artefacts [*Muzio and Kramlich*, 1988]. In current budget estimates the apparently "missing sources" are mainly compensated by higher estimates of natural and anthropogenic-induced N_2O emissions from terrestrial ecosystems.

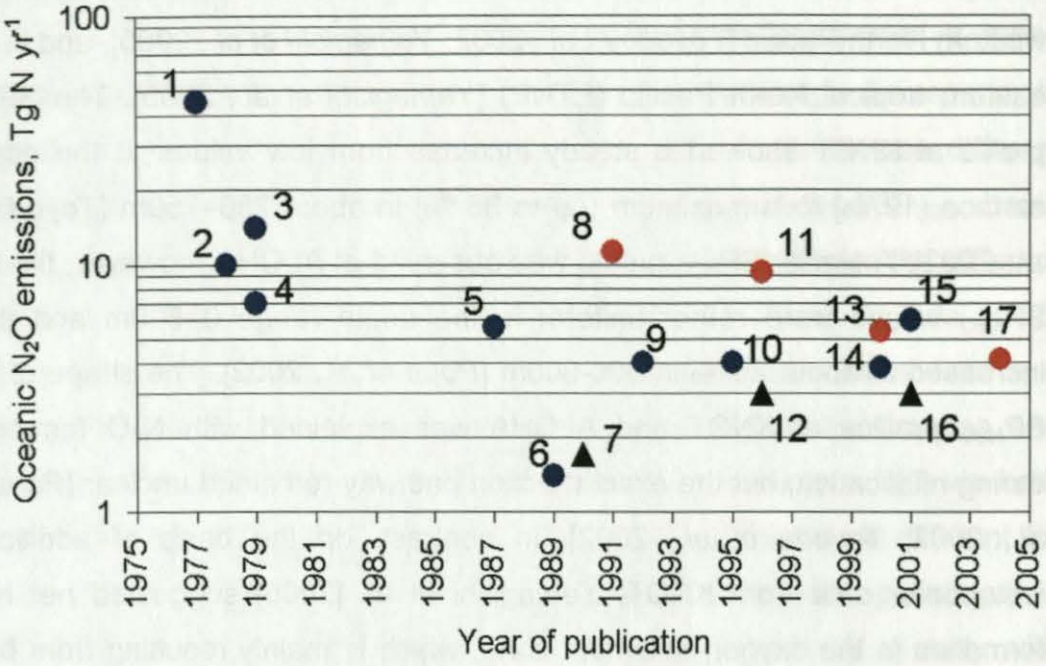

Figure 13: Historical development of global oceanic N_2O emission estimates. Please note the logarithmic y-axis. The red circles mark estimates, which explicitly included coastal emissions. The black triangles mark the IPCC reports. References: 1 [*Hahn and Junge*, 1977]; 2 [*Elkins et al.*, 1978]; 3 [*Singh et al.*, 1979]; 4 [*Cohen and Gordon*, 1979]; 5 [*Cline et al.*, 1987]; 6 [*Butler et al.*, 1989]; 7 [*Watson et al.*, 1990]; 8 [*Capone*, 1991]; 9 [*Najjar*, 1992]; 10 [*Nevison et al.*, 1995]; 11 [*Bange et al.*, 1996b]; 12 [*Denman et al.*, 1996]; 13 [*Seitzinger et al.*, 2000]; 14 [*Suntharalingam and Sarmiento*, 2000]; 15 [*Codispoti et al.*, 2001]; 16 [*Prather et al.*, 2001]; 17 [*Nevison et al.*, 2004].

This might result from the fact that the IPCC estimate does not take into account N_2O emissions from coastal areas such as continental shelves, estuaries and coastal upwelling zones: On the basis of a compilation of N_2O measurements in coastal areas, Bange et al. [1996b] calculated an overall oceanic flux of 7 – 11 Tg N yr^{-1} and concluded that coastal areas such as estuaries, shelf and coastal upwelling areas contribute significantly (approximately 61%, i.e. 4.2 – 6.6 Tg N yr^{-1}) to the global oceanic emissions. This is in line with predictions from the model studies by Capone [1991], Seitzinger and Kroeze [1998], and Nevison et al. [2004] who estimated that coastal areas may contribute from 7 to 49 %, to the overall global oceanic N_2O emissions (Table 4). Beside different methodological approaches (empirical models vs. extrapolation of measurements) the considerable range of uncertainty is introduced by the fact that the applied classification of coastal areas is not uniform. For example, the overall areal contributions

range from 3.3% [*Nevison et al.*, 2004] up to 18.6% [*Bange et al.*, 1996b] (Table 4).

Table 4: Comparison of coastal N_2O flux estimates (modified from Nevison et al. [2004]).

Study	Area, km^2	% of total ocean area[a]	N_2O flux, Tg N yr^{-1}	% of total ocean N_2O Flux[b]
Capone [1991]				
Coastal upwelling	$3.6\ 10^7$	10	4.7	42
Nearshore / estuaries	$5\ 10^6$	1.4	0.74	6.5
Sum	*$4.1\ 10^7$*	*11.4*	*5.4*	*48.5*
Bange et al. [1996b]				
Coastal upwelling	$8.8\ 10^5$	0.2	0.3	3
Coastal waters / marginal seas	$6.5\ 10^7$	18	2.7	25
Estuaries	$1.4\ 10^6$	0.4	3.6	33
Sum	*$6.7\ 10^7$*	*18.6*	*6.6*	*61*
Seitzinger and Kroeze [1998][c]				
Continental shelves	not given	?	0.63	15
Estuaries	$1.4\ 10^6$	0.4	0.21	5
Sum	*?*	*?*	*0.84*	*20*
Nevison et al. [2004]				
Coastal upwelling	$1.75\ 10^6$	0.5	0.2	5
Continental shelf (<200m)	$1.0\ 10^7$	2.8	0.08	2
Sum	*$1.2\ 10^7$*	*3.3*	*0.28*	*7*

[a] compared to a total ocean area of $361\ 10^6$ km^2 [*Menard and Smith*, 1966].
[b] Seitzinger et al. [2000] and Nevison et al. [2004] assumed a total ocean source of 4 Tg N yr^{-1}. Bange et al. [1996b] assumed a 7.4 Tg N yr^{-1} source and Capone [1991] assumed an 11.25 Tg N yr^{-1} source.
[c] see also Seitzinger et al. [2000].

The results of the global N_2O coastal emissions estimates mentioned above are supported by two recently published regional studies: Naqvi et al. [2000] measured the N_2O distribution in the coastal area along the West coast of India and concluded that N_2O emissions were considerably enhanced (up to 0.25 Tg N yr^{-1}) due to a temporarily occurring shift of the ecosystem from oxic to anoxic conditions. Thus, the N_2O emissions from the Indian coast alone might account for about 8% of the IPCC's global estimate given in Table 2. A comparable result was published in a recent study about N_2O measurements in European coastal waters. On the basis of a comprehensive compilation of N_2O measurements, I (*Bange*, [2005]) estimated that N_2O emissions from the continental shelf seas and estuaries of Europe range

from 0.15 to 0.4 Tg N yr^{-1} (with a mean of 0.31 Tg N yr^{-1}). Thus, European coastal waters may contribute up to 13% to the IPCC's global N_2O emission estimate of 3 Tg N yr^{-1} (Table 2).

Despite the inherent considerable uncertainties of the oceanic N_2O flux estimates (i.e. spatial and temporal biases of the measurements, classification of coastal areas, different air-sea gas exchange approaches) it is reasonable to conclude that the oceanic source as given in the N_2O budget of the IPCC (Table 2) most likely is an underestimation. Averaging the source estimates published since 1978 (Figure 13, excluding the obviously unrealistic estimate by Hahn and Junge [1977]), yields a mean oceanic N_2O source of 6.6 ± 3.6 Tg N yr^{-1} (mean ± sd, n = 13) or 5.6 Tg N yr^{-1} (median) with a range from 1.4 (min) to 14 (max) Tg N yr^{-1}. An upward revision will shift the $(T/O)_{N2O}$ ratio (T stands for natural soil emissions and O stands for the oceanic emissions) from 2 to 1 which is in reasonable agreement with the suggestion of a constant $(T/O)_{N2O}$ ratio of 1.3 ± 0.2 during the last 33,000 years as depicted from the dual isotope signature of N_2O in an Antarctic ice core paleo record [*Sowers et al.*, 2003].

Thus, I recommend, that the oceanic N_2O source estimate should be revised (at least doubled) in the forthcoming IPCC report which has significant implications for the overall atmospheric N_2O budget: Recalculating[3] the overall mean atmospheric N_2O sources (natural and anthropogenic), based on the IPCC 2001 values, yields a median of 19 Tg N yr^{-1} (range from 13 to 29 Tg N yr^{-1}, at 90% confidence interval). Introducing a revised oceanic N_2O source of 7 ± 4 Tg N yr^{-1} yields a median of 24 Tg N^{-1} (range 16 – 34 Tg N yr^{-1}, 90% confidence interval) (Figure 14).

[3] Calculations where performed with the statistical method for "estimating uncertainties in total global budgets of atmopheric trace gases" developed by Khalil [1992]. The program code, version 1993, was provided by M.A.K. Khalil, Andarz Company, Portland, Oregon, USA.

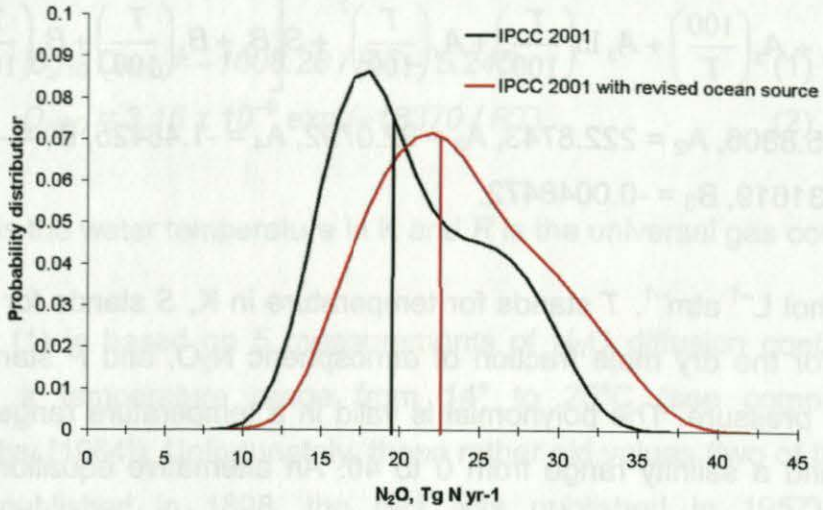

Figure 14: The probability distribution functions [*Khalil*, 1992] for atmospheric N_2O sources. The black line was calculated with the values listed in the IPCC 2001 report [*Prather et al.*, 2001] and the red line is based on the calculation with a revised oceanic N_2O source.

A comparison with the sum of the N_2O sink and the atmospheric trend (16 Tg N yr^{-1}, range 12 – 21 Tg N yr^{-1}, taken from Table 2) reveals that the N_2O budget might not be balanced, especially in view of the fact that an ocean source of 7 Tg N yr^{-1} has to be considered as a conservative estimate. This indicates that either the N_2O sink is underestimated or that one of the N_2O sources might be overestimated (mostly likely candidate is N_2O emissions from agricultural soils as indicated by the large range of uncertainty of its emission estimate).

3 EQUATIONS TO DESCRIBE THE PHYSICAL PROPERTIES OF OCEANIC N_2O

3.1 N_2O solubility in seawater

The Bunsen solubility of N_2O (C_w in mol L^{-1}) in seawater in equilibrium with moist air at P = 1 atm is usually calculated with the polynomial given by Weiss and Price [1980]:

$$C_w = Fx^{'}P \text{ and}$$

$$\ln F = A_1 + A_2\left(\frac{100}{T}\right) + A_3 \ln\left(\frac{T}{100}\right) + A_4\left(\frac{T}{100}\right)^2 + S\left[B_1 + B_2\left(\frac{T}{100}\right) + B_3\left(\frac{T}{100}\right)^2\right] \text{ with}$$

A_1 = -165.8806, A_2 = 222.8743, A_3 = 92.0792, A_4 = -1.48425, B_1 = -0.056235, B_2 = 0.031619, B_3 = -0.0048472.

F is in mol L^{-1} atm^{-1}. T stands for temperature in K, S stands for salinity, x' stands for the dry mole fraction of atmospheric N_2O, and P stands for the ambient pressure. The polynomial is valid in a temperature range from 0 to 40 °C and a salinity range from 0 to 40. An alternative equation for C_w in gravimetric units (mol kg^{-1}) can be found as well in Weiss and Price [1980]. C_w at T = 25°C, S = 35, x' = 318 ppb and P = 1 atm is 6.38 nmol L^{-1}. It doubles to about 12.42 nmol L^{-1} when the temperature is set to 5°C.

N_2O saturations (*sat*) in % (i.e., 100% = equilibrium) are calculated as

$$sat = 100\ C_w / C_a,$$

where C_w is the (measured) N_2O in-situ concentration (see below) and C_a is the (calculated) equilibrium concentration of dissolved N_2O based on the N_2O atmospheric dry mole fraction. For calculating C_a in the ocean mixed layer, actual ambient air mole fractions were taken from the AGAGE (Advanced Global Atmospheric Gases Experiment, see Prinn et al. [2000]) data set, which is available from the anonymous ftp site cdiac.esd.ornl.edu (subdirectory /pub/ale_gage_agage/agage/gc-md/monthly) at the Carbon Dioxide Information Analysis Center in Oak Ridge, Tennessee.

3.2 N_2O diffusion in water

The N_2O diffusion coefficients (D_{N2O} in m^2 s^{-1}) are calculated with equation (1) derived from the data given in Broecker and Peng [1974] and, alternatively, with the equation (2) derived from a compilation of measurements [*Rhee*, 2000]:

$$\log_{10} D_{N2O} = -1008.28 / RT - 5.245 \quad (1)$$

$$D_{N2O} = 3.16 \times 10^{-6} \exp(-18370 / RT), \quad (2)$$

where T is the water temperature in K and R is the universal gas constant.

Equation (1) is based on 5 measurements of N_2O diffusion coefficients in water in a temperature range from 14° to 25°C (see compilation by Himmelblau [1964]). Unfortunately, these rather old values (two of them were already published in 1898, the rest was published in 1957) show a considerable scatter, indicating an uncertainty of up to 20% for values calculated with equation (1) [*Broecker and Peng*, 1974]. Equation (2) is based on a compilation of 49 measurements of N_2O diffusion coefficients in water in the temperature range from 14° to 95°C (see Rhee [2000]), thus providing a more reasonable fit for the N_2O diffusion with a considerable reduced uncertainty of less than 10% [*Rhee*, 2000]. A correction for N_2O diffusion in seawater is usually not applied since the effect of seawater on the diffusion of dissolved gases is variable [*King et al.*, 1995] and, to my knowledge, no measurements of the N_2O diffusion in seawater have been published.

3.3 Air-sea exchange approaches

The air–sea exchange flux density (F) of N_2O is parameterised as

$$F = k_w(u) (C_w - C_a),$$

where k_w is the gas transfer coefficient as a function of wind speed (u in 10m height), C_w is the N_2O seawater concentration, and C_a is the equilibrium N_2O concentration in seawater. C_a is calculated using the equation of Weiss and Price [1980] (see above). The measured wind speeds is normalized to 10 m height by using the relationship of Garratt [1977]. To calculate k_w, I used the tri-linear k_w–u relationship of Liss and Merlivat [1986] (LM86), the quadratic k_w–u relationship of Wanninkhof [1992] (W92), and the combined linear and

quadratic k_w–u relationship from Nightingale et al. [2000] (N00). Equations of the LM86, W92, and N00 approaches are given below. k_w was adjusted by multiplying with $(Sc/600)^{-n}$ (n = 2/3 for wind speeds <3.6 m s^{-1} and n = 1/2 for wind speeds >3.6 m s^{-1}) for LM86, $(Sc/660)^{-0.5}$ for W92, and $(Sc/600)^{-0.5}$ for N00, where Sc is the Schmidt number for N_2O:

$$Sc = \nu D_{N2O}^{-1}$$

Sc was calculated using empirical equations for the kinematic viscosity of seawater (ν) [*Siedler and Peters*, 1986] and the diffusion coefficient of N_2O in water (D_{N2O}, equation given above).

The approach of Liss and Merlivat [1986] (LM86) consists of three equations for the calculation of k_w (in m s^{-1}):

$$k_w = 4.72\ 10^{-7}\ u_{10} \qquad (u_{10} \leq 3.6\ m\ s^{-1})$$
$$k_w = 7.92\ 10^{-6}\ u_{10} - 2.68\ 10^{-5} \qquad (3.6\ m\ s^{-1} < u_{10} \leq 13\ m\ s^{-1})$$
$$k_w = 1.64\ 10^{-5}\ u_{10} - 1.40\ 10^{-4} \qquad (u_{10} > 13\ m\ s^{-1}).$$

The LM86 relationship is based on data obtained from a lake study and a laboratory study at high wind speeds. The approach of Liss and Merlivat [1986] is usually applied with both short-term and long-term wind speeds. Wanninkhof [1992] (W92) proposed the following relationship for the calculation of k_w (in m s^{-1}) with climatological wind speed data:

$$k_w = 1.08\ 10^{-6}\ \overline{u}_{10}^{\,2}.$$

This approach is only valid when using long-term averaged (climatological) wind speeds. When using in-situ wind speeds the following equation is recommended [*Wanninkhof*, 1992]:

$$k_w = 8.61\ 10^{-7}\ u_{10}^{\,2}.$$

The k_w–u relationship of Nightingale et al. [2000] (N00) is given by (k_w in m s^{-1}):

$$k_w = 9.25\ 10^{-7}\ u_{10} + 6.17\ 10^{-7}\ u_{10}^2.$$

The N00 relationship shows a dependence on wind speeds intermediate between those of Liss and Merlivat [1986] and Wanninkhof [1992]. Moreover, the N00 relationship is in reasonable agreement with estimates of k_w based on globally averaged wind speeds.

4 METHODS

This section contains short descriptions of the two main sampling methods applied. In general, N_2O was separated with a gas chromatographic method and detected with an electron capture detector. Further details of the analytical method are described in Bange et al. [1996a] and Bange et al. [2001b]. For calibration we used standard gas mixtures of N_2O in synthetic air, which have been calibrated against the NOAA (National Oceanic and Atmospheric Administration, Boulder, Co.) or SIO (Scripps Institution of Oceanography, La Jolla, Ca.) standard scale. Further details can be found in the attached publications.

Depth profiles. Triplicate water samples from various depths were taken from a water bottle sampling rosette, equipped with a CTD-sensor. The analytical method applied is a modification of the method described by Bange et al. [2001b]: Bubble free samples were taken immediately following oxygen sampling in 24 mL glass vials, sealed directly with butyl rubber stoppers and crimped with aluminium caps. To prevent microbial activity, samples were poisoned with 500 µL of saturated or moderately concentrated aqueous mercury chloride ($HgCl_2$) solutions [*Walter*, 2006]. Samples were either analysed onboard or stored in the dark and, if possible, cooled until analysis in our home laboratory. In a time series experiment Walter [2006] found that N_2O concentrations in samples treated as described above did not change

significantly over 10 months. N_2O water concentrations (C_w) were calculated as follows:

$$C_w\left[molL^{-1}\right] = \frac{Fx'PV_{wp} + \frac{x'P}{RT}V_{hs}}{V_{wp}}$$

where F stands for the Bunsen solubility in mol L^{-1} atm^{-1} (see above), x' is the dry gas mole fraction of N_2O in the headspace in ppb, P is the atmospheric pressure in atm (set to 1 atm), V_{wp} and V_{hs} stand for the volumes of the water (14 mL) and headspace (10 mL), respectively. R is the gas constant (8.2054 10^{-2} L atm mol^{-1} K^{-1}) and T in K is the temperature during equilibration. The standard deviation of the N_2O concentration (C_w) was approximated with (C_{wmax} – C_{wmin}) / 1.91, where C_{wmin} and C_{wmax} stand for the minimal and maximal N_2O concentrations of the triplicate samples, respectively. The factor 1.91 is derived from the statistical method by David [1951].

Continuous sampling for ocean surface surveys. Seawater was pumped continuously from a depth of about 4-5 m by a submersible water pump installed in the moon pools of the ships into a shower-type equilibrator developed by R.F. Weiss (Scripps Institution of Oceanography, La Jolla, Ca.). N_2O concentrations (C, in mol L^{-1}) were calculated by applying the solubility equation of Weiss and Price [1980] (see above). Time series of seawater temperature (SST), salinity, and atmospheric pressure were obtained from the ship's records. Differences between the seawater temperature at the seawater intake and the continuously recorded water temperature in the equilibrator were corrected as follows:

$$C_w = C\, F(T_{eq}) / F(SST)$$

with $F(SST)$ and $F(T_{eq})$ representing the N_2O solubility at seawater temperature and water temperature inside the equilibrator at the time of the measurement, respectively.

5 OUTLOOK

Despite the fact that our knowledge about the oceanic distribution, the formation pathways and the oceanic emission of N_2O has considerably increased during the last four decades we are far from being able to sketch a comprehensive picture. Various open questions and technical challenges remain to be solved in the future:

- Measurements of the N_2O diffusivity in seawater are needed. This will help to reduce the uncertainty in emission estimates.

- Reliable, high-precision N_2O sensors for the use at ocean time series stations or ships of opportunity should be developed in order to expand the spatial and temporal coverage of oceanic N_2O measurements. For example, time series measurements with an array of moored N_2O sensors along the West coast of South America might help to monitor the upwelling variability during El Niño/La Niña events.

- We still have only a rudimentary idea about N_2O cycling in coastal areas. We need to know more about the seasonality, the major formation and consumption pathways and the driving forces of these processes. In this context, the ongoing dramatic increase in the frequency of oxygen-starved zones seems to be of central importance [*UNEP*, 2004]. Ongoing eutrophication in various parts of the world (e.g. in SE Asia) might lead to enhanced N_2O emissions from coastal areas.

- During the last years the oceanic anaerobic ammonium oxidation (anammox, $NO_2^- + NH_4^+ \rightarrow N_2$) has received increasing attention as an additional, previously overlooked, significant loss process of fixed nitrogen [*Dalsgaard et al.*, 2005; *Devol*, 2003; *Hulth et al.*, 2005; *Ward*, 2003]. Recently, anammox has been found in suboxic zones of the Benguela upwelling [*Kuypers et al.*, 2005] and at the oxic/anoxic interface of the Black Sea [*Kuypers et al.*, 2003]. Based on the results

from the Benguela upwelling, Kuypers et al. [2005] concluded that the resulting N_2 is exclusively formed by anammox and not, as commonly thought, by denitrification. They suggested that denitrifiers only supply the NO_2^- for the anammox bacteria, which then convert the NO_2^- to N_2. This suggestion is especially interesting in view of the observed N_2O double peak profiles in the suboxic zones of the Arabian Sea and the eastern tropical North Pacific (see Figure 8). Up to now there are no hints of N_2O being an intermediate or a by-product of anammox [Hulth et al., 2005; *Ward*, 2003]. Assuming that anammox is the dominating nitrogen loss process in suboxic zones, and further assuming that N_2O is not involved in anammox then the question arises what causes the strong N_2O depletion in the core of the suboxic zones? The N_2O depletion is usually attributed to N_2O reduction to N_2 via denitrification, which was confirmed by recent incubation experiments [*Castro-González and Fraías*, 2004]. Thus, there is a need for studies about the role of anammox for the oceanic N_2O distribution in suboxic zones.

- Isotope measurements of N_2O have been introduced as a promising tool to decipher the formation pathways of oceanic N_2O. However, it turned out that isotopic measurements in some cases are difficult to explain (e.g. in the Arabian Sea, see Table 3) and that they even can lead to contradicting results. For example, from the interpretation of the N_2O isotope measurements at station KNOT in the western North Pacific Ocean it is not clear whether nitrification or denitrification is the main N_2O formation pathway (see Table 3). We need to learn more about the N_2O forming pathways and the resulting N_2O isotope signatures of the different types of N_2O producing organisms. The recently isolated NH_4^+ oxidizing archaeon [*Könneke et al.*, 2005] raises the question whether we have overlooked N_2O forming organisms other than bacteria. N_2O isotope studies might help to identify unknown N_2O formation pathways. Moreover, there is an obvious discrepancy in the measured mean tropospheric SP_{N2O} (19 ‰ vs. 43 ‰, Kaiser et al. [2004]), which is not resolved yet. Thus, there seems to be an urgent need for interlaboratory calibration of the N_2O isotope methods

- Tropospheric N_2O has an oxygen isotope anomaly $\Delta^{17}O$ of 0.9 ± 0.1 ‰ [*Kaiser et al.*, 2003]. This anomaly mainly results from N_2O formation by non-mass-dependent isotope fractionations by various chemical reactions in atmosphere, during industrial processes and during biomass burning [*Kaiser and Röckmann*, 2005]. Moreover, it was speculated that N_2O from microbial processes may account for about 37% of the observed $\Delta^{17}O$ of atmospheric N_2O [*Kaiser and Röckmann*, 2005]. This is line with the suggestion by Michalski et al. [2003] who proposed that the oxygen isotope anomaly of aerosol NO_3^- ($\Delta^{17}O$ = 20 – 30.8 ‰) should lead to an oxygen isotope anomaly of oceanic N_2O in those regions where NO_3^- aerosols are deposited to the ocean and denitrification takes place. However, $\Delta^{17}O$ measurements of N_2O from the oceanic environments are needed to verify the hypothesis by Kaiser and Röckmann [2005] and Michalski et al. [2003].

- Apart from the classical denitrification pathway, alternative pathways for N_2O formation in suboxic zones have been suggested which should be tested with laboratory experiments and field measurements:

  (i) The possible decomposition of organic matter via oxidation by IO_3^- to yield N_2O might be written as follows:

$$81.3\ IO_3^- + (CH_2O)_{106}(NH_3)_{16}H_3PO_4 \rightarrow$$
$$81.3\ I^- + 106\ CO_2 + 8\ N_2O + 130\ H_2O + H_3PO_4.$$

  I calculated for the reaction given above a $\Delta G°$ = –2712 kJ per mole glucose, which is comparable with $\Delta G°$ values given for the oxidation of organic matter by IO_3^- yielding NH_3 (–2605 kJ mol^{-1}), HNO_3 (–2804 kJ mol^{-1}), or N_2 (–3047 kJ mol^{-1}). I proposed that the decomposition of organic carbon via the IO_3^-/I^- mechanism might contribute to the N_2O and N_2 accumulation in suboxic zones of the western Arabian Sea (for details of the calculation and discussion see Bange et al., (2001b]).

(ii) Beside microbial N_2O formation chemical formation via the following reactions can be postulated:

$$2\ NH_4^+ + 4\ MnO_2 + 6\ H^+ \rightarrow N_2O + 4\ Mn^{2+} + 7\ H_2O \quad (A)$$

$$2\ NO_3^- + 4\ Mn^{2+} + 3\ H_2O \rightarrow N_2O + 4\ MnO_2 + 6\ H^+ \quad (B)$$

The latter reaction is part of the so-called chemodenitrification where NO_3^- is reduced by Mn^{2+} to N_2, which is known to occur in sediments. In order to estimate the thermodynamical feasibility the half-reactions (C)-(E) have to be taken into account:

$$N_2O + 8\ e^- + 10\ H^+ \rightarrow 2\ NH_4^+ + H_2O \quad (C)$$

$$2\ NO_3^- + 8\ e^- + 10\ H^+ \rightarrow N_2O + 5\ H_2O \quad (D)$$

$$MnO_2 + 2\ e^- + 4\ H^+ \rightarrow Mn^{2+} + 2\ H_2O \quad (E)$$

The resulting pε and Δpε values as a function of the pH are given in Table 5.

Table 5: pε for reactions (C), (D) and (E) and resulting Δpε for reactions (A) and (B).

PH	Pε (C)	pε (D)	pε (E)	Δpε (E) – (C) ($NH_4^+ + MnO_2 \rightarrow N_2O$)	Δpε (D) – (E) ($NO_3^- + Mn^{2+} \rightarrow N_2O$)
0	10.94	18.85	20.84	9.90	-1.99
7	2.19	10.10	6.84	4.65	3.26
8	**0.94**	**8.85**	**4.84**	**3.90**	**4.01**
14	-6.56	1.35	-7.16	-0.60	8.51

pε (≡ $-\log e^-$ = pε° + log [{ox}/{red}]) gives the electron activity at equilibrium and measures the relative tendency of a solution to accept or transfer electrons [Stumm and Morgan, 1996]. pε were calculated for 25°C. Standard redox potentials (E°) were taken from Greenwood and Earnshaw [1984] and converted to pε° by pε° = E°/(0.05916 V) [Stumm and Morgan, 1996].

Since Δpε (= Δlog K = $-\Delta G/2.3nRT$) for reactions (A) and (B) are positive at the mean oceanic pH (= 8) we can conclude that reactions (A) and (B) are thermodynamically favourable. N_2O and Mn measurements in the central Arabian Sea are shown Figure 15. It

seems reasonable to speculate that the reduction of NO_3^- by Mn^{2+} (reaction B) might take place at the upper and lower boundaries of the suboxic zone.

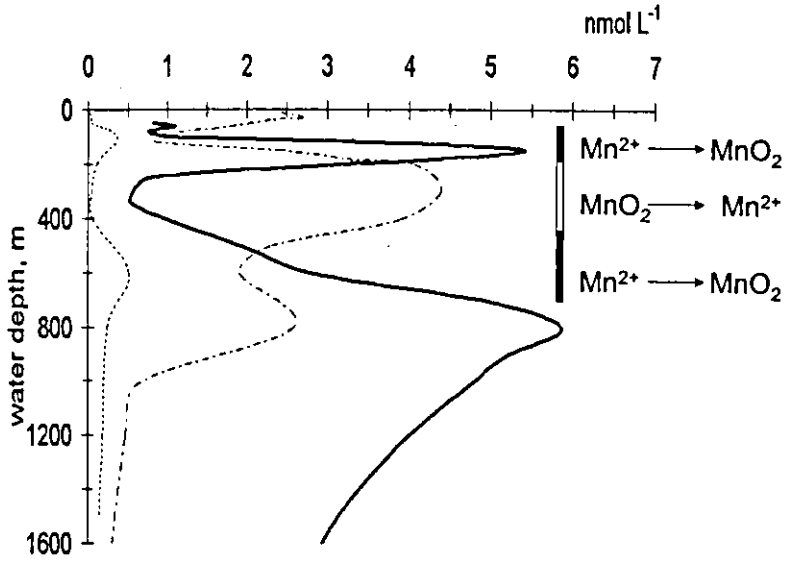

Figure 15: N_2O (solid line, concentration divided by 10), dissolved Mn^{2+} (dash-dotted line) and particulate MnO_2 (dashed line) in the central Arabian Sea. Possible redox cycling of Mn^{2+}/MnO_2 in the suboxic zone is indicated. Data are from Bange et al. [2001] (N_2O) and Saager et al. [1989] (MnO_2). Dissolved Mn^{2+} are unpublished data from U. Schüßler and W. Balzer, University of Bremen. Please note that the data were taken by different working groups at different locations and time, thus the data presented reveal only a schematic picture.

➢ We need to know more about the role of the marine nitrogen cycle and N_2O for possible feedback mechanisms within the Earth system. Oceanic O_2 distribution is likely to be altered in the near future due to the impending global change. Any variations of the oceanic O_2 concentrations, in turn, will lead to a change in the amount of N_2O produced via nitrification or denitrification (see Figure 5). At the moment we cannot assess the consequences for the future oceanic N_2O release to the atmosphere, but we can have a clue to the future from the past: Suthhof et al. [2001] showed that the temporal variations of the denitrification signal of the suboxic zones of both the Arabian Sea and the eastern tropical North Pacific during the last 17,000 years is paralleled by the reconstructed atmospheric N_2O from a Greenland ice core record (Figure 16). This implies that variations in the amount of the

water column denitrification might led to changes in the magnitude of N_2O formation and its subsequent release to the atmosphere. However, any change of the atmospheric N_2O concentrations will also influence the Earth's climate. A possible ocean/atmosphere feedback scenario mediated by N_2O emissions from the Arabian Sea was presented by Bange et al. [2005] (Figure 17). I suggest that the processes outlined in Figure 17 are worthy of inclusion in models that seek to produce realistic scenarios of climate change.

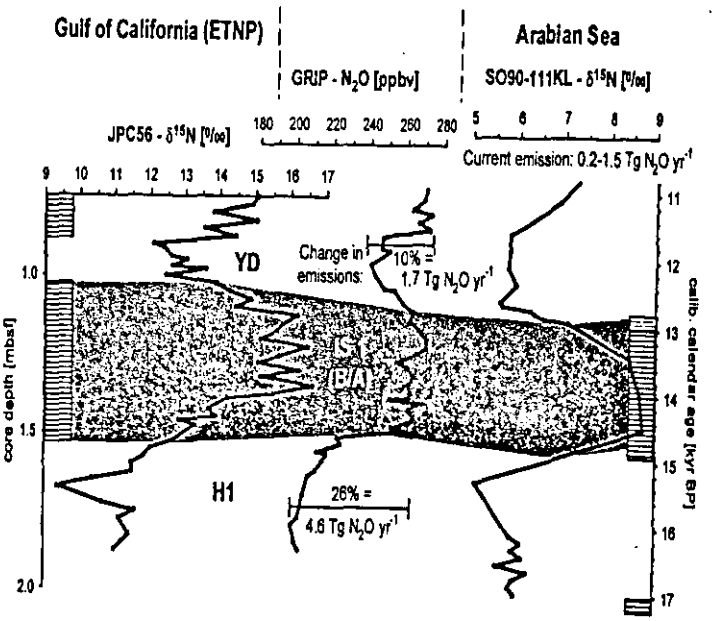

Figure 16: $\delta^{15}N$ profiles from sediment cores in the eastern tropical North Pacific (ETNP) and Arabian Sea compared to reconstructed atmospheric N_2O data from the GRIP (Greenland Ice Core Project) ice core. YD stands for Younger Dryas, IS1 stands for Interstadial 1, H stands for Heinrich event 1, B/A stands for Bølling/Allerød event. Figure was taken from Suthhof et al. [2001].

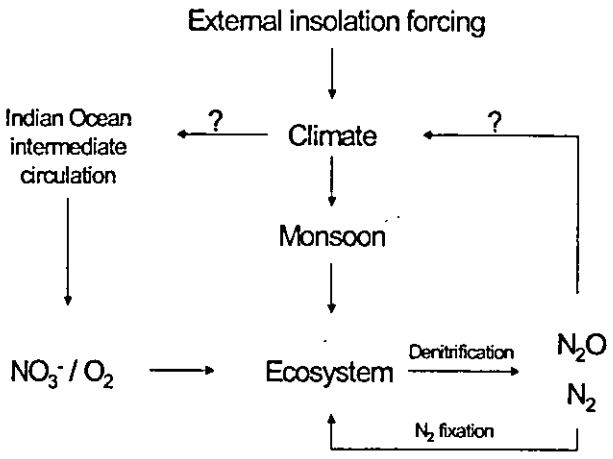

Figure 17: Possible climate/Arabian Sea feedback scenario. The questions marks point to yet to be quantified interactions. Following the concept for the forcing mechanisms of the Indian Ocean Monsoon Regime presented by Clemens et al. [1991], the external insolation forcing via variations in the Earth's orbit results in an internal climate response with variations in the strength of the Arabian Sea Southwest Monsoon. In turn, variations of the Southwest Monsoon strength lead to variations in nutrient supply to the surface layer by coastal upwelling. Additionally, a change in the climate may also influence the intermediate circulation of the Indian Ocean leading to changes in the supply of NO_3^- and O_2 to the Arabian Sea. These processes then feed back to the global climate system. They do this by modulating the N_2O source term and by impacting the oceanic biological pump's ability to sequester atmospheric CO_2 via denitrification's impact on NO_3^- one of the limiting nutrients for phytoplankton. When NO_3^- becomes limiting N_2-fixation might increase.

6 Acknowledgements

I am very grateful to Doug Wallace for providing the excellent working conditions to write my habilitation and for his continuing support during that time. The support and expertise provided by the members of the FB2 – Marine Biogeochemie has been central to making this work a success. The many measurement campaigns would not have been successful without the help of the chief scientists, the captains and the crews of R/V *Meteor*, R/V *Sonne*, and R/V *Gauss*. The cooperation and help of the many colleagues at sea is greatly appreciated. Moreover, I acknowledge the support by the workshop, administration, and library of IFM-GEOMAR. Thanks also to the technicians, namely G. Petrick, and other support staff at IFM-GEOMAR.

I especially thank Sylvia Walter for her enthusiasm for N_2O during the last 4 years, the many stimulating discussions and her never-ending patience with me when discussing biological issues! Many thanks go to the students who helped us with the measurements during the cruises and in the laboratory; especially, I would like to thank Imke Goertz und Uli Breitenbach. Last but not the least, particular thanks go to Ute Weidinger for her continuing moral support.

Thank you to all who have taken interest in my work and to those who have provided inspiration through many discussions. For his help in my understanding of the marine nitrogen cycle I must specifically thank Wajih Naqvi.

My work at the IFM-GEOMAR (Kiel) and at the Max-Planck-Institut für Chemie (Mainz) has been funded by the Bundesministerium für Bildung und Forschung (grants within the framework of the German JGOFS-Arabian Sea Study, 1995 – 2000), the Deutsche Forschungsgemeinschaft (various grants since 2001), and, the Forschungsbereich 2 – Marine Biogeochemie of IFM-GEOMAR.

Finally, I must thank my family and friends, who provide grounding in the real world, which often seems far removed from life as a scientist.

7 REFERENCES

Adel, A., Further detail in the rock-salt prismatic solar spectrum, *Astrophys. J.*, *88*, 186-188, 1938.

Alongi, D.M., J. Pfitzner, L.A. Trott, F. Tirendi, P. Dixon, and D.W. Klumpp, Rapid sediment accumulation and microbial mineralization in forests of the mangrove *Kandelia candel* in the Jiulongjiang estuary, China, *Estuarine Coastal Shelf Sci.*, *63*, 605-618, 2005.

Arp, D.J., and L.Y. Stein, Metabolism of inorganic N compounds by ammonia-oxidizing bacteria, *Critical Rev. Biochem. Molecular Biol.*, *38*, 471-495, 2003.

Bange, H.W., Nitrous oxide and methane in European coastal waters, *Estuar. Coastal Shelf Sci., submitted*, 2005.

Bange, H.W., and M.O. Andreae, Nitrous oxide in the deep waters of the world's oceans, *Global Biogeochem. Cycles*, *13* (4), 1127-1135, 1999.

Bange, H.W., M.O. Andreae, S. Lal, C.S. Law, S.W.A. Naqvi, P.K. Patra, T. Rixen, and R.C. Upstill-Goddard, Nitrous oxide emissions from the Arabian Sea: A synthesis, *Atmos. Chem. Phys.*, *1*, 61-71, 2001a.

Bange, H.W., S.W.A. Naqvi, and L.A. Codispoti, The nitrogen cycle in the Arabian Sea, *Progr. Oceanogr.*, *65*, 145-158, 2005.

Bange, H.W., S. Rapsomanikis, and M.O. Andreae, The Aegean Sea as a source of atmospheric nitrous oxide and methane, *Mar. Chem.*, *53* (1-2), 41-49, 1996a.

Bange, H.W., S. Rapsomanikis, and M.O. Andreae, Nitrous oxide in coastal waters, *Global Biogeochem. Cycles*, *10* (1), 197-207, 1996b.

Bange, H.W., S. Rapsomanikis, and M.O. Andreae, Nitrous oxide emissions from the Arabian Sea, *Geophys. Res. Lett.*, *23* (22), 3175-3178, 1996c.

Bange, H.W., S. Rapsomanikis, and M.O. Andreae, Nitrous oxide cycling in the Arabian Sea, *J. Geophys. Res.*, *106* (C1), 1053-1065, 2001b.

Bange, H.W., T. Rixen, A.M. Johansen, R.L. Siefert, R. Ramesh, V. Ittekkot, M.R. Hoffmann, and M.O. Andreae, A revised nitrogen budget for the Arabian Sea, *Global Biogeochem. Cycles*, *14* (4), 1283-1297, 2000.

Barford, C.C., J.P. Montoya, M.A. Altabet, and R. Mitchell, Steady-state nitrogen isotope effects of N_2 and N_2O production in *Paracoccus denitrificans*, *Appl. Environ. Microbiol.*, *65* (3), 989-994, 1999.

Bauza, J.F., J.M. Morell, and J.E. Corredor, Biogeochemistry of nitrous oxide production in Red Mangrove (*Rhizophora mangle*) forest sediments, *Estuarine Coastal Shelf Sci.*, *55*, 697-704, 2002.

Bothe, H., G. Jost, M. Schloter, B.B. Ward, and K.-P. Witzel, Molecular analysis of ammonia oxidation and denitrification in natural environments, *FEMS Microbiol. Rev.*, *24*, 673-690, 2000.

Brand, W.A., High precision isotope ratio monitoring techniques in mass spectrometry, *J. Mass Spectrom.*, *31*, 225-235, 1996.

Brettar, I., and G. Rheinheimer, Denitrification in the central Baltic: Evidence for H_2S oxidation as motor of denitrification at the oxic-anoxic interface, *Mar. Ecol. Prog. Ser.*, *77*, 157-169, 1991.

Broecker, W.S., and T.-H. Peng, Gas exchange rates between air and sea, *Tellus*, *26*, 21-35, 1974.

Butler, J.H., J.W. Elkins, C.M. Brunson, K.B. Egan, T.M. Thompson, T.J. Conway, and B.D. Hall, Trace gases in and over the West Pacific and East Indian Oceans during the El Niño-Southern Oscillation event of 1987, Air Resources Laboratory, Silver Spring, MD, USA, 1988.

Butler, J.H., J.W. Elkins, T.M. Thompson, and K.B. Egan, Tropospheric and dissolved N_2O of the west Pacific and east Indian Oceans during the El Nino Southern Oscillation Event of 1987, *J. Geophys. Res.*, *94* (D12), 14,865-14,877, 1989.

Capone, D.G., Aspects of the marine nitrogen cycle with relevance to the dynamics of nitrous oxide and nitric oxide, in *Microbial production and consumption of greenhouse gases*, edited by J.E. Rogers, and W.E. Whitman, pp. 255-275, Am. Soc. Microbiol., Washington, 1991.

Casciotti, K.L., D.M. Sigman, M. Galanter Hastings, J.K. Böhlke, and A. Hilkert, Measurements of the oxygen isotopic composition of nitrate in seawater and freshwater using the denitrifier method, *Anal. Chem.*, *74*, 4905-4912, 2002.

Castro-González, M., and L. Fraías, N_2O cycling at the core of the oxygen minimum zone off northern Chile, *Mar. Ecol. Progr. Ser.*, *280*, 1-11, 2004.

Clemens, S., W. Prell, D. Murray, G. Shimmield, and G. Weedon, Forcing mechanisms of the Indian Ocean monsoon, *Nature*, *353*, 720-725, 1991.

Cline, J.D., D.P. Wisegarver, and K. Kelly-Hansen, Nitrous oxide and vertical mixing in the equatorial Pacific during the 1982-1983 El Niño, *Deep-Sea Res.*, *34*, 857-873, 1987.

Codispoti, L.A., J.A. Brandes, J.P. Christensen, A.H. Devol, S.W.A. Naqvi, H.W. Paerl, and T. Yoshinari, The oceanic fixed nitrogen and nitrous oxide budgets: Moving targets as we enter the anthropocene?, *Scientia Marina*, *65* (Suppl. 2), 85-105, 2001.

Codispoti, L.A., J.W. Elkins, T. Yoshinari, G.E. Friederich, C.M. Sakamoto, and T.T. Packard, On the nitrous oxide flux from productive regions that contain low oxygen waters, in *Oceanography of the Indian Ocean*, edited by B.N. Desai, pp. 271-284, A.A. Balkema, Rotterdam, 1992.

Codispoti, L.A., T. Yoshinari, and A.H. Devol, Suboxic respiration in the oceanic water column, in *Respiration in aquatic ecosystems*, edited by P.A. Del Giorgio, and P.J.I.B. Williams, pp. 225-247, Oxford University Press, Oxford, 2005.

Cohen, Y., Shipboard measurement of dissolved nitrous oxide in seawater by electron capture gas chromatography, *Anal. Chem.*, *49* (8), 1238-1240, 1977.

Cohen, Y., Consumption of dissolved nitrous oxide in an anoxic basin, Saanich Inlet, British Columbia, *Nature*, *272*, 235-237, 1978.

Cohen, Y., and L.I. Gordon, Nitrous oxide in the oxygen minimum of the eastern tropical North Pacific: Evidence for its consumption during denitrification and possible mechanisms for its production, *Deep-Sea Res.*, *25*, 509-524, 1978.

Cohen, Y., and L.I. Gordon, Nitrous oxide production in the ocean, *J. Geophys. Res.*, *84* (C1), 347-353, 1979.

Corredor, J.E., J.M. Morell, and J. Bauzá, Atmospheric nitrous oxide fluxes from mangrove sediments, *Mar. Pollut. Bull.*, *38* (6), 473-478, 1999.

Craig, H., and L.I. Gordon, Nitrous oxide in the ocean and the marine atmosphere, *Geochim. Cosmochim. Acta*, *27*, 949-955, 1963.

Crutzen, P.J., The influence of nitrogen oxides on the atmospheric ozone content, *Q. J. R. Meteorol. Soc.*, *96*, 320-325, 1970.

Dalsgaard, T., B. Thamdrup, and D.E. Canfield, Anaerobic ammonium oxidation (anammox) in the marine environment, *Res. Microbiol.*, *156* (4), 457-464, 2005.

David, H.A., Further applications of range to analysis of variance, *Biometrika*, *38*, 393-409, 1951.

De Bie, M.J.M., J.J. Middelburg, M. Starink, and H.J. Laanbroek, Factors controlling nitrous oxide at the microbial community and estuarine scale, *Mar. Ecol. Progr. Ser.*, *240*, 1-9, 2002.

Devol, A.H., Solution to a marine mystery, *Nature*, *422*, 575-576, 2003.

De Wilde, H.J.P., and M.J.M. De Bie, Nitrous oxide in the Schelde estuary: Production by nitrification and emission to the atmosphere, *Mar. Chem.*, *69*, 203-216, 2000.

De Wilde, H.P.J., and W. Helder, Nitrous oxide in the Somali Basin: The role of upwelling, *Deep-Sea Res. II*, *44* (6-7), 1319-1340, 1997.

Denman, K., E. Hofmann, and H. Marchant, Marine biotic responses to environmental change and feedbacks to climate, in *Climate Change 1995, The Science of Climate Change, Contribution of Working Group I to the second Assessment Report of the Intergovernmental Panel on Climate Change*, edited by J.T. Houghton, L.G. Meira Filho, B.A. Callander, N. Harris, A. Kattenberg, and K. Maskell, pp. 483-516, Cambridge University Press, Cambridge, UK, 1996.

Dore, J.E., B.N. Popp, D.M. Karl, and F.J. Sansone, A large source of atmospheric nitrous oxide from subtropical North Pacific surface waters, *Nature*, *396*, 63-66, 1998.

Elkins, J.W., Determination of dissolved nitrous oxide in aquatic systems by gas chromatography using electron capture detection and multi phase equilibration, *Anal. Chem.*, *52*, 263-267, 1980.

Elkins, J.W., S.C. Wofsy, M.B. McElroy, C.E. Kolb, and W.A. Kaplan, Aquatic sources and sinks for nitrous oxide, *Nature*, *275*, 602-606, 1978.

Firestone, M.K., and J.M. Tiedje, Temporal change in nitrous oxide and dinitrogen from denitrification following onset of anaerobiosis, *Appl. Environ. Microbiol.*, *38*, 673-679, 1979.

Fuhrman, J.A., and D.G. Capone, Possible biogeochemical consequences of ocean fertilization, *Limnol. Oceanogr.*, *36* (8), 1951-1959, 1991.

Garcia, H.E., and L.I. Gordon, Oxygen solubility in seawater: Better fitting equations, *Limnol. Oceanogr.*, *37* (6), 1307-1312, 1992.

Garratt, J.R., Review of the drag coefficients over oceans and continents, *Mo. Weath. Rev.*, *105*, 915-929, 1977.

Goldstein, B., F. Joos, and T.F. Stocker, A modeling study of oceanic nitrous oxide during the Younger Dryas cold period, *Geophys. Res. Lett.*, *30* (2), doi:10.1029/2002GL016418, 2003.

Goreau, T.J., W.A. Kaplan, S.C. Wofsy, M.B. McElroy, F.W. Valois, and S.W. Watson, Production of NO_2^- and N_2O by nitrifying bacteria at reduced concentrations of oxygen, *Appl. Environ. Microbiol.*, *40* (3), 526-532, 1980.

Greenwood, N.N., and A. Earnshaw, *Chemistry of the elements*, Pergamon Press, Oxford, 1984.

Hahn, J., The North Atlantic Ocean as a source of atmospheric N_2O, *Tellus*, *26*, 160-168, 1974.

Hahn, J., Nitrous oxide in the oceans, in *Denitrification, nitrification and atmospheric nitrous oxide*, edited by C.C. Delwiche, pp. 191-277, John Wiley & Sons, Inc., New York, 1981.

Hahn, J., in: *Atmosphärische Spurenstoffe*, edited by R. Jaenicke, page 429, VCH, Weinheim, 1987.

Hahn, J., and C. Junge, Atmospheric nitrous oxide: A critical review, *Z. Naturforsch.*, *32a*, 190-214, 1977.

Hashimoto, L.K., W.A. Kaplan, S.C. Wofsy, and M.B. McElroy, Transformation of fixed nitrogen and N_2O in the Cariaco Trench, *Deep-Sea Res.*, *30* (6A), 575-590, 1983.

Himmelblau, D.M., Diffusion of dissolved gases in liquids, *Chem. Rev.*, *64*, 527-550, 1964.

Hulth, S., R.C. Aller, D.E. Canfield, T. Dalsgaard, P. Engström, F. Gilbert, K. Sundbäck, and B. Thamdrup, Nitrogen removal in marine environments: Recent findings and future research challenges, *Mar. Chem.*, *94*, 125-145, 2005.

Inoue, H., and W.G. Mook, Equilibrium and kinetic nitrogen and oxygen isotope fractionations between dissolved and gaseous N_2O, *Chem. Geology*, *113*, 135-148, 1994.

IPCC, *Climate Change 2001: The scientific basis. Contribution of working group I to the third assessment report of the Intergovernmental Panel on Climate Change*, 881 pp., Cambridge University Press, Cambridge (UK) and New York (USA), 2001.

Ito, T., M.J. Follows, and E.A. Boyle, Is AOU a good measure of respiration in the oceans?, *Geophys. Res. Lett.*, *31*, L17305, doi:10.1029/2004GL020900, 2004.

Jain, A.K., B.P. Briegleb, K. Minschwaner, and D.J. Wuebbles, Radiative forcing and global warming potentials of 39 greenhouse gases, *J. Geophys. Res.*, *105* (D16), 20,773-20,790, 2000.

Jin, X., and N. Gruber, Offsetting the radiative benefit of ocean iron fertilization by enhancing N_2O emissions, *Geophys. Res. Lett.*, *30* (24), 2249, doi:10.1029/2003GL018458, 2003.

Junge, C., and J. Hahn, N_2O measurements in the North Atlantic, *J. Geophys. Res.*, *76*, 8143-8146, 1971.

Kaiser, J., S. Park, K.A. Boering, C.A.M. Brenninkmeijer, A. Hilkert, and T. Röckmann, Mass spectrometric method for the absolute calibration of the intramolecular nitrogen isotope distribution in nitrous oxide, *Anal. Bioanal. Chem.*, *378*, 256-269, 2004.

Kaiser, J., and T. Röckmann, Absence of isotope exchange in the reaction of $N_2O + O(^1D)$ and the global $\Delta^{17}O$ budget of N_2O, *Geophys. Res. Lett.*, *32*, L15808, doi:10.1029/2005GL023199, 2005.

Kaiser, J., T. Röckmann, and C.A.M. Brenninkmeijer, Complete and accurate mass spectrometric isotope analysis of tropospheric nitrous oxide, *J. Geophys. Res.*, *108* (D15), 4476, doi:10.1029/2003JD003613, 2003.

Karl, D., A. Michaels, B. Bergman, D. Capone, E. Carpenter, R. Letelier, F. Lipschultz, H. Paerl, D. Sigman, and L. Stal, Dinitrogen fixation in the world's oceans, *Biogeochem.*, *57/58*, 47-98, 2002.

Khalil, M.A.K., A statistical method for estimating uncertainties in the global budget of atmospheric trace gases, *J. Environ. Sci. Health*, *A27* (3), 755-770, 1992.

Khalil, M.A.K., R.A. Rasmussen, and M.J. Shearer, Atmospheric nitrous oxide: Patters of global change during recent decades and centuries, *Chemosphere*, *47*, 807-821, 2002.

Kim, K.-R., and H. Craig, Two-isotope characterization of N_2O in the Pacific Ocean and constraints on its origin in deep water, *Nature*, *347*, 58-61, 1990.

Kim, K.-R., and H. Craig, Nitrogen-15 and oxygen-18 characteristics of nitrous oxide: A global perspective, *Science*, *262*, 1855-1857, 1993.

King, D.B., W.J. De Bryun, M. Zheng, and E.S. Saltzman, Uncertainties in the molecular diffusion coefficient of gases in water for the estimation of air-sea exchange, in *Air-water gas transfer*, edited by B. Jähne, and E.C. Monahan, pp. 13-22, AEON Verlag & Studio, Hanau, Germany, 1995.

Könneke, M., A.E. Bernhard, J. De la Torre, C.B. Walker, J.B. Waterbury, and D.A. Stahl, Isolation of an autotrophic ammonia oxidizing marine archaeon, *Nature*, *437*, 543-546, 2005.

Kowalchuk, G.A., and J.R. Stephen, Ammonia-oxidizing bacteria: A model for molecular microbial ecology, *Ann. Rev. Microbiol.*, *55*, 485-529, 2001.

Kreuzwieser, J., J. Buchholz, and H. Rennenberg, Emission of methane and nitrous oxide by Australian mangrove ecosystems, *Plant Biol.*, *5*, 423-431, 2003.

Kuypers, M.M.M., G. Lavik, D. Woebken, M. Schmid, B.M. Fuchs, R. Amann, B.B. Jørgensen, and M.S.M. Jetten, Massive nitrogen loss from Benguela upwelling system through anaerobic ammonium oxidation, *Proc. Natl. Acad. Sci.*, *102* (18), 6478-6483, 2005.

Kuypers, M.M.M., A.O. Sliekers, G. Lavik, M. Schmid, B.B. Jørgensen, J.G. Kuenen, J.S.S. Damsté, M. Strous, and M.S.M. Jetten, Anaerobic ammonium oxidation by anammox bacteria in the Black Sea, *Nature*, *422*, 608-611, 2003.

Law, C.S., and R.D. Ling, Nitrous oxide flux and response to increased iron availability in the Antarctic Circumpolar Current,, *Deep-Sea Res. II, 48*, 2509-2527, 2001.

Lilley, M.D., M.A. de Angelis, and L.I. Gordon, CH_4, H_2, CO, N_2O in submarine hydrothermal vent waters, *Nature, 300*, 48-50, 1982.

Liss, P.S., and L. Merlivat, Air-sea exchange rates: introduction and synthesis, in *The Role of Air-Sea Exchange in Geochemical Cycling*, edited by P. Buat-Ménard, pp. 113-127, D. Reidel Publishing Company, Dordrecht, 1986.

Lobert, J.M., J.H. Butler, L.S. Geller, S.A. Yvon, S.A. Montzka, R.C. Myers, A.D. Clarke, and J.W. Elkins, BLAST 94: Bromine latitudinal air/sea transect 1994: report on oceanic measurements of methyl bromide and other compounds, National Oceanic and Atmospheric Administration, Silver Spring, MD, 1996.

Lovelock, J.E., Midwife to the greens: The electron capture detector, *Microbiologia SEM, 13*, 11-22, 1997.

Lueker, T.J., S.J. Walker, M.K. Vollmer, R.F. Keeling, C. Nevison, R.F. Weiss, and H.E. Garcia, Coastal upwelling air-sea fluxes revealed in atmospheric observations of O_2/N_2, CO_2 and N_2O, *Geophys. Res. Lett., 30* (6), 1292, doi: 10.1029/2002GL016615, 2003.

Martin, J.H., R.M. Gordon, and S.E. Fitzwater, The case for iron, *Limnol. Oceanogr., 36* (8), 1793-1802, 1991.

Menard, H.W., and S.M. Smith, Hypsometry of the ocean basin provinces, *J. Geophys. Res., 71* (18), 4305-4325, 1966.

Michalski, G., Z. Scott, M. Kabiling, and M.H. Thiemens, First measurements and modeling of $\Delta^{17}O$ in atmospheric nitrate, *Geophys. Res. Lett., 30* (16), 1870, doi:10.1029/2003GL017015, 2003.

Middelburg, J.J., G. Klaver, J. Nieuwenhuize, R.M. Markusse, T. Vlug, and F.J.W.A. van der Nat, Nitrous oxide emissions from estuarine intertidal sediments, *Hydrobiologia, 311*, 43-55, 1995.

Moore, H., Isotopic measurements of atmospheric nitrogen compounds, *Tellus, 26* (1-2), 169-174, 1974.

Muñoz-Hincapié, M., J.M. Morell, and J.E. Corredor, Increase of nitrous oxide flux to the atmosphere upon nitrogen addition to red mangrove sediments, *Mar. Poll. Bull., 44*, 992-996, 2002.

Muzio, L.J., and J.C. Kramlich, An artifact in the measurement of N_2O from combustion sources, *Geophys. Res. Lett., 15* (12), 1369-1372, 1988.

Najjar, R.G., Marine biogeochemistry, in *Climate System Modeling*, edited by K.E. Trenberth, pp. 241-280, Cambridge University Press, Cambridge, 1992.

Naqvi, S.W.A., D.A. Jayakumar, P.V. Narveka, H. Naik, V.V.S.S. Sarma, W. D'Souza, S. Joseph, and M.D. George, Increased marine production of N_2O due to intensifying anoxia on the Indian continental shelf, *Nature, 408*, 346-349, 2000.

Naqvi, S.W.A., and R.J. Noronha, Nitrous oxide in the Arabian Sea, *Deep-Sea Res., 38*, 871-890, 1991.

Naqvi, S.W.A., T. Yoshinari, J.A. Brandes, A.H. Devol, D.A. Jayakumar, P.V. Narvekar, M.A. Altabet, and L.A. Codispoti, Nitrogen isotopic studies in the suboxic Arabian Sea, *Proc. Indian Acad. Sci. (Earth Planet. Sci.), 107* (4), 367-378, 1998a.

Naqvi, S.W.A., T. Yoshinari, D.A. Jayakumar, M.A. Altabet, P.V. Narvekar, A.H. Devol, J.A. Brandes, and L.A. Codispoti, Budgetary and biogeochemical implications of N_2O isotope signatures in the Arabian Sea, *Nature, 394*, 462-464, 1998b.

Nevison, C., J.H. Butler, and J.W. Elkins, Global distribution of N_2O and ΔN_2O-AOU yield in the subsurface ocean, *Global Biogeochem. Cycles, 17* (4), 1119, doi:10.1029/2003GB002068, 2003.

Nevison, C., T. Lueker, and R.F. Weiss, Quantifying the nitrous oxide source from coastal upwelling, *Global Biogeochem. Cycles*, *18*, GB1018, doi:10.1029/2003GB002110, 2004.

Nevison, C.D., R.F. Keeling, R.F. Weiss, B.N. Popp, X. Jin, P.J. Fraser, L.W. Porter, and P.G. Hess, Southern Ocean ventilation inferred from seasonal cycles of atmospherioc N_2O and O_2/N_2 at Cape Grim, Tasmania, *Tellus*, *57B*, 218-229, 2005.

Nevison, C.D., R.F. Weiss, and D.J. Erickson III, Global oceanic emissions of nitrous oxide, *J. Geophys. Res.*, *100* (C8), 15,809-15,820, 1995.

Nightingale, P., G. Malin, C.S. Law, A.J. Watson, P.S. Liss, M.I. Liddicoat, J. Boutin, and R.C. Upstill-Goddard, In situ evaluation of air-sea gas exchange parameterizations using novel conservative and volatile tracers, *Global Biogeochem. Cycles*, *14* (1), 373-387, 2000.

Ostrom, N.E., M.E. Russ, B. Popp, T.M. Rust, and D.M. Karl, Mechanisms of nitrous oxide production in the subtropical North Pacific based on determinations of the isotopic abundances of nitrous oxide and di-nitrogen, *Chemosphere: Global Change Science*, *2* (3-4), 281-290, 2000.

Oudot, C., C. Andrie, and Y. Montel, Nitrous oxide production in the tropical Atlantic Ocean, *Deep-Sea Res.*, *37*, 183-202, 1990.

Oudot, C., P. Jean-Baptiste, E. Fourré, C. Mormiche, M. Guevel, J.-F. Ternon, and P. Le Corre, Transatlantic equatorial distribution of nitrous oxide and methane, *Deep-Sea Res. I*, *49*, 1175-1193, 2002.

Popp, B.N., M.B. Westley, S. Toyoda, T. Miwa, J.E. Dore, N. Yoshida, T.M. Rust, F.J. Sansone, M.E. Russ, N. Ostrom, and P.H. Ostrom, Nitrogen and oxygen isotopomeric constraints on the origins and sea-to air flux of N_2O in the oligotrophic subtropical North Pacific gyre, *Global Biogeochem. Cycles*, *1064, doi 10.1029/2001GB001806*, 2002.

Prather, M., D. Ehhalt, F. Dentener, R. Derwent, E. Dlugokencky, E. Holland, I. Isaksen, J. Katima, V. Kirchhoff, P. Matson, P. Midgley, and M. Wang, Atmospheric chemistry and greenhouse gases, in *Climate Change 2001: The Scientific Basis. Contribution of Working Group I to the Third Assessment Report of the Intergovernmental Panel on Climate Change*, edited by J.T. Houghton, Y. Ding, D.J. Griggs, M. Noguer, P.J. Van der Linden, X. Dai, K. Maskell, and C.A. Johnson, pp. 239-287, Cambridge University Press, Cambridge, UK, 2001.

Prinn, R.G., R.F. Weiss, P.J. Fraser, P.G. Simmonds, D.M. Cunnold, F.N. Alyea, S.O. O'Doherty, P. Salameh, B.R. Miller, J. Huang, R.H.J. Wang, D.E. Hartley, C. Harth, L.P. Steele, G. Sturrock, P.M. Midgley, and A. McCulloch, A history of chemically and radiatively important gases in air deduced from ALE/GAGE/AGAGE, *J. Geophys. Res.*, *105* (D14), 17,751-17,792, 2000.

Punshon, S., and R.M. Moore, Nitrous oxide production and consumption in a eutrophic coastal embayment, *Mar. Chem.*, *91*, 37-51, 2004.

Ramaswamy, V., O. Boucher, J. Haigh, D. Hauglustaine, J. Haywood, G. Myhre, T. Nakajima, G.Y. Shi, and S. Solomon, Radiative forcing of climate change, in *Climate Change 2001: The Scientific Basis. Contribution of Working Group I to the Third Assessment Report of the Intergovernmental Panel on Climate Change*, edited by J.T. Houghton, Y. Ding, D.J. Griggs, M. Noguer, P.J. Van der Linden, X. Dai, K. Maskell, and C.A. Johnson, pp. 349-416, Cambridge University Press, Cambridge, UK, 2001.

Rasmussen, R.A., J. Krasnec, and D. Pierotti, N_2O analysis in the atmosphere via electron capture-gas chromatography, *Geophys. Res. Let.*, *3* (10), 615-618, 1976.

Rhee, T.S., The process of air-water gas exchange and its application, PhD thesis, Texas A&M University, College Station, 2000.

Richardson, D.J., and N.J. Watmough, Inorganic nitrogen metabolism in bacteria, *Current Opinion in Chemical Biology*, *3*, 207-219, 1999.

Rönner, U., Distribution, production and consumption of nitrous oxide in the Baltic Sea, *Geochim. Cosmochim. Acta*, *47*, 2179-2188, 1983.

Saager, P.M., H.J.W. de Baar, and P.H. Burkill, Manganese and iron in the Indian Ocean waters, *Geochim. Cosmochim. Acta*, *53*, 2259-2267, 1989.

Schmidt, H.L., R.A. Werner, N. Yoshida, and R. Well, Is the isotopic composition of nitrous oxide an indicator for its origin from nitrification or denitrification? A theoretical approach fromm referred data and microbiological and enzyme kinetic aspects, *Rapid Communication Mass Spectrometry*, *18* (18), 2036-2040, 2004.

Schropp, S.J., and J.R. Schwarz, Nitrous oxide production by denitrifying microorganisms from the eastern tropical Pacific and the Caribbean Sea, *Geomicrobiol. J.*, *3* (1), 17-31, 1983.

Seitzinger, S.P., Denitrification in aquatic sediments, in *Denitrification in Soil and Sediment*, edited by N.P. Revsbech, and J. Sörensen, pp. 301-321, Plenum Press, New York, 1990.

Seitzinger, S.P., and C. Kroeze, Global distribution of nitrous oxide production and N inputs in freshwater and coastal marine ecosystems, *Global Biogeochem. Cycles*, *12* (1), 93-113, 1998.

Seitzinger, S.P., C. Kroeze, and R.V. Styles, Global distribution of N_2O emissions from aquatic systems: Natural emissions and anthropogenic effects, *Chemosphere: Global Change Sci.*, *2*, 267-279, 2000.

Seitzinger, S.P., and S.W. Nixon, Eutrophication and the rate of denitrification and N_2O production in coastal marine sediments, *Limnol. Oceanogr.*, *30* (6), 1332-1339, 1985.

Siedler, G., and H. Peters, Properties of sea water, in *Oceanography*, Landolt-Börnstein New Ser., Group V, vol. 3a, edited by J. Sündermann, pp. 233–264, Springer Verlag, New York, 1986.

Singh, H.B., L.J. Salas, and H. Shigeishi, The distribution of nitrous oxide (N_2O) in the global atmosphere and the Pacific Ocean, *Tellus*, *31*, 313-320, 1979.

Sowers, T., The N_2O record spanning the penultimate deglaciation from the Vostok ice core, *J. Geophys. Res.*, *106* (D23), 31,903-31,914, 2001.

Sowers, T., R.B. Alley, and J. Jubenville, Ice core records of tropospheric N_2O covering the last 106,000 years, *Science*, *301*, 945-948, 2003.

Stein, L.Y., and Y.L. Yung, Production, isotopic composition, and atmospheric fate of biologically produced nitrous oxide, *Ann. Rev. Earth Planet. Sci.*, *31*, 329-356, 2003.

Stumm, W., and J.J. Morgan, *Aquatic Chemistry*, 1022 pp., John Wiley & Sons, Inc., New York, 1996.

Suntharalingam, P., Modeling the global oceanic nitrous oxide distribution, Ph.D. thesis, Princeton University, Princeton, 1997.

Suntharalingam, P., and J.L. Sarmiento, Factors governing the oceanic nitrous oxide distribution: Simulations with an ocean general circulation model, *Global Biogeochem. Cycles*, *14* (1), 429-454, 2000.

Suthhof, A., V. Ittekkot, and B. Gaye-Haake, Millennial-oscillation of denitrification intensity in the Arabian Sea during the late Quaternary and its potential influence on atmospheric N_2O and global climate, *Global Biogeochem. Cycles*, *15* (3), 637-649, 2001.

Sutka, R.L., N.E. Ostrom, P.H. Ostrom, H. Gandhi, and J.A. Breznak, Nitrogen isotopomer site preference of N_2O produced by *Nitrosomas europaea* and *Methylococcus capsulatus* Bath, *Rapid Commun. Mass Spectrom.*, *17* (7), 738-745, 2003.

Sutka, R.L., N.E. Ostrom, P.H. Ostrom, H. Gandhi, and J.A. Breznak, Erratum: Nitrogen istotopomer site preference of N_2O produced by *Nitrosomas europaea* and *Methylococcus capsulatus* Bath, *Rapid Communications Mass Spectrometry*, *18*, 1411-1412, 2004.

Sutka, R.L., N.E. Ostrom, P.H. Ostrom, J.A. Breznak, H. Gandhi, A.J. Pitt, and F. Li, Distinguishing nitrous oxide production from nitrification and denitrification on the basis of isotopomere abundances, *Appl. Environ. Microbiol.*, *72* (1), 638-644, 2006.

Tiedje, J.M., Ecology of denitrification and dissimilatory nitrate reduction to ammonium, in *Biology of anaerobic microorganisms*, edited by A.J.B. Zehnder, pp. 179-244, Wiley & Sons, New York, 1988.

Toyoda, S., H. Mutobe, H. Yamagishi, N. Yoshida, and Y. Tanji, Fractionation of N_2O isotopomers during production by denitrifier, *Soil Biol. Biochem.*, *37*, 1535-1545, 2005.

Toyoda, S., and N. Yoshida, Determination of nitrogen isotopomers of nitrous oxide on a modified isotope ratio mass spectrometer, *Anal. Chem.*, *71* (20), 4711-4718, 1999.

Toyoda, S., N. Yoshida, T. Miwa, Y. Matsui, H. Yamagishi, U. Tsunogai, Y. Nojiri, and N. Tsurushima, Production mechanism and global budget of N_2O inferred from its isotopomers in the western North Pacific, *Geophys. Res. Lett.*, *29* (3), 10.1029/2001GL014311, 2002.

Trogler, W.C., Physical properties and mechanisms of formation of nitrous oxide, *Coordination Chem. Rev.*, *187*, 303-327, 1999.

UNEP (United Nations Environmental Program), Global Environment Outlook Year Book 2003, pp. 76, UNEP, Nairobi, Kenya, 2004.

Upstill-Goddard, R.C., J. Barnes, and N.J.P. Owens, Nitrous oxide and methane during the 1994 SW monsoon in the Arabian Sea/northwestern Indian Ocean, *J. Geophys. Res.*, *104* (C12), 30,067-30,084, 1999.

Wahlen, M., and T. Yoshinari, Oxygen isotope ratios in N_2O from different environments, *Nature*, *313*, 780-782, 1985.

Walter, S., N_2O in the Atlantic Ocean and the Baltic Sea, Ph.D. thesis, 154 pp., University of Kiel, Kiel, 2006.

Walter, S., I. Peeken, K. Lochte, A. Webb, and H.W. Bange, Nitrous oxide measurements during EIFEX, the European Iron Fertilization Experiment in the subpolar South Atlantic Ocean, *Geophys. Res. Lett.*, *32*, L23613, doi:10.1029/2005GL024619, 2005.

Wanninkhof, R., Relationship between wind speed and gas exchange over the ocean, *J. Geophys. Res.*, *97* (C5), 7373-7382, 1992.

Ward, B.B., Significance of anaerobic ammonium oxidation in the ocean, *Trends Microbiol.*, *11* (9), 408-410, 2003.

Warneck, P., *Chemistry of the natural atmosphere*, 927 pp., Academic Press, San Diego, CA, 2000.

Watson, R.T., H. Rohde, H. Oeschger, and U. Siegenthaler, Greenhouse gases and aerosols, in *Climate Change, The IPCC scientific Assessment*, edited by J.T. Houghton, G.J. Jenkins, and J.J. Ephraums, pp. 1-40, Cambridge University Press, Cambridge, UK, 1990.

Weiss, R.F., Determination of carbon dioxide and methane by dual catalyst flame ionization chromatography and nitrous oxide by electron capture chromatography, *J. Chromatogr. Sci.*, *19*, 611-616, 1981.

Weiss, R.F., and B.A. Price, Nitrous oxide solubility in water and seawater, *Mar. Chem.*, *8*, 347-359, 1980.

Weiss, R.F., F.A. Van Woy, and P.K. Salameh, Surface water and atmospheric carbon dioxide and nitrous oxide observations by shipboard automated gas chromatography: Results from expeditions between 1977 and 1990, Carbon Dioxide Information Analysis Center, Oak Ridge National Laboratory, Oak Ridge, Tennessee, USA, 1992.

Wilhelm, E., R. Battino, and R.J. Wilcock, Low-pressure solubility of gases in liquid water, *Chem. Rev.*, *77* (2), 219-262, 1977.

WMO (World Meteorological Organization), Scientific assessment of ozone depletion: 2002, pp. 498, WMO, Geneva, 2003.

Wrage, N., G.L. Velthof, M.L. Van Beusichem, and O. Oenema, Role of nitrifier denitrification in the production of nitrous oxide, *Soil Biol. Biochem.*, *33*, 1723-1732, 2001.

Yamagishi, H., N. Yoshida, S. Toyoda, B.N. Popp, M.B. Westley, and S. Watanabe, Contributions of denitrification and mixing on the distribution of nitrous oxide in the North Pacific, *Gephys. Res. Lett.*, *32*, L04603, doi:10.1029/2004GL021458, 2005.

Yamazaki, T., N. Yoshida, E. Wada, and S. Matsuo, N_2O reduction by *Azotobacter vinelandii* with emphasis on kinetic nitrogen isotope effects, *Plant Cell Physiol.*, *28* (2), 263-271, 1987.

Yoshida, N., ^{15}N-depleted N_2O as a product of nitrification, *Nature*, *335*, 528-529, 1988.

Yoshida, N., A. Hattori, T. Saino, S. Matsuo, and E. Wada, $^{15}N/^{14}N$ ratio of dissolved N_2O in the eastern tropical Pacific Ocean, *Nature*, *307*, 442-444, 1984.

Yoshida, N., and S. Matsuo, Nitrogen isotope ratio of atmospheric N_2O as a key to the global cycle of N_2O, *Geochem. J.*, *17*, 231-239, 1983.

Yoshida, N., H. Morimoto, M. Hirano, I. Koike, S. Matsuo, E. Wada, T. Saino, and A. Hattori, Nitrification rates and ^{15}N abundances of N_2O and NO_3^- in the western North Pacific, *Nature*, *342*, 895-897, 1989.

Yoshida, N., and S. Toyoda, Constraining the atmospheric N_2O budget from intramolecular site preference in N_2O isotopomers, *Nature*, *405*, 330-334, 2000.

Yoshinari, T., Nitrous oxide in the sea, *Mar. Chem.*, *4*, 189-202, 1976.

Yoshinari, T., M.A. Altabet, S.W.A. Naqvi, L. Codispoti, A. Jayakumar, M. Kuhland, and A. Devol, Nitrogen and oxygen isotopic composition of N_2O from suboxic waters of the eastern tropical North Pacific and the Arabian Sea - Measurements by continuous-flow isotope-ratio monitoring, *Mar. Chem.*, *56* (3-4), 253-264, 1997.

Zumft, W.G., Cell biology and molecular basis of denitrification, *Microbiol. Molecul. Biol. Rev.*, *61* (4), 533-616, 1997.

ATTACHMENTS

Theme A: Distribution and formation of oceanic N_2O

1) **Bange, H.W.**, and M.O. Andreae, Nitrous oxide in the deep waters of the world's oceans, *Global Biogeochem. Cycles*, *13* (4), 1127-1135, 1999.

2) **Bange, H.W.**, S. Rapsomanikis, and M.O. Andreae, Nitrous oxide cycling in the Arabian Sea, *J. Geophys. Res.*, *106* (C1), 1053-1065, 2001.

3) Walter, S., I. Peeken, K. Lochte, A. Webb, and **H.W. Bange**, Nitrous oxide measurements during EIFEX, the European Iron Fertilization Experiment in the subpolar South Atlantic Ocean, *Geophys. Res. Lett.*, *32*, L 23613, doi:10.1029/2005GL024619, 2005.

4) Walter, S., **H.W. Bange**, U. Breitenbach, and D.W.R. Wallace, Nitrous oxide in the North Atlantic Ocean, *Global Biogeochem. Cycles*, in preparation, 2006.

5) Walter, S., U. Breitenbach, **H.W. Bange**, G. Nausch, and D.W.R. Wallace, Nitrous oxide water column distribution during the transition from anoxic to oxic conditions in the Baltic Sea, *Biogeosci.*, submitted, 2006.

Theme B: N_2O emissions

6) **Bange, H.W.**, M.O. Andreae, S. Lal, C.S. Law, S.W.A. Naqvi, P.K. Patra, T. Rixen, and R.C. Upstill-Goddard, Nitrous oxide emissions from the Arabian Sea: A synthesis, *Atmos. Chem. Phys.*, *1*, 61-71, 2001.

7) **Bange, H.W.**, Air-sea exchange of nitrous oxide and methane in the Arabian Sea: A simple model of the seasonal variability, *Indian J. Mar. Sci.*, *33* (1), 77-83, 2004.

8) Walter, S., **H.W. Bange**, and D.W.R. Wallace, Nitrous oxide in the surface layer of the tropical North Atlantic Ocean along a west to east transect, *Geophys. Res. Lett.*, *31* (23), L23S07, doi:10.1029/2004GL019937, 2004.

9) **Bange, H.W.**, Nitrous oxide and methane in European coastal waters, *Estuar. Coastal Shelf Sci.*, submitted, 2005.

10) **Bange, H.W.**, New Directions: The importance of the oceanic nitrous oxide emissions, *Atmos. Environ.*, *40* (1), 198-199, 2006.

GLOBAL BIOGEOCHEMICAL CYCLES, VOL. 13, NO 4, PAGES 1127-1135, DECEMBER 1999

Nitrous oxide in the deep waters of the world's oceans

Hermann W. Bange and Meinrat O. Andreae

Biogeochemistry Department, Max Planck Institute for Chemistry, Mainz, Germany

Abstract. We present a compilation and analysis of N_2O data from the deep-water zone of the oceans below 2000 m. The N_2O values show an increasing trend from low concentrations in the North Atlantic Ocean to high concentrations in the North Pacific Ocean, indicating an accumulation of N_2O in deep waters with time. We conclude that the observed N_2O accumulation is mainly caused by nitrification in the global deep-water circulation system (i.e., the "conveyor belt"). Hydrothermal and sedimentary N_2O fluxes are negligible. We estimate the annual N_2O deep-water production to be 0.3 ± 0.1 Tg. Despite the fact that the deep sea below 2000 m represents about 95% of the total ocean volume, it contributes only about 3–16% to the global open-ocean N_2O production. A rough estimate of the oceanic N_2O budget suggests that the loss to the atmosphere is not balanced by the deep-sea nitrification and pelagic denitrification. Therefore an additional source of 3.8 Tg N_2O yr^{-1} attributed to nitrification in the upper water column (0–2000 m) might exist. With a simple model we estimated the effect of changes in the North Atlantic Deep Water (NADW) formation for deep-water N_2O. The upper water N_2O budget is not significantly influenced by variations in the N_2O deep-water formation. However, the predicted decrease in the NADW formation rate in the near future might lead to an additional source of atmospheric N_2O in the range of about 0.02–0.4 Tg yr^{-1}. This (anthropogenically induced) source is small, and it will be difficult to detect its signal against the natural variations in the annual growth rates of tropospheric N_2O.

1. Introduction

Nitrous oxide (N_2O) is an atmospheric trace gas which significantly influences, directly and indirectly, Earth's climate. In the troposphere it acts as a greenhouse gas, and in the stratosphere it is the major source for NO radicals, which are involved in one of the main ozone reaction cycles [*Prather et al.*, 1996].

Recently published source estimates indicate that the world's oceans play a major, but not dominant, role in the global budget of atmospheric N_2O [*Bouwman et al.*, 1995; *Khalil and Rasmussen*, 1992; *Prather et al.*, 1996]. Most of the world's ocean surface layer is near gas-exchange equilibrium with the atmosphere [*Nevison et al.*, 1995], whereas a subsurface N_2O accumulation is generally associated with the oxygen minimum, indicating that nitrification ($NH_4^+ \rightarrow NO_2^- \rightarrow NO_3^-$) is responsible for N_2O production [*Butler et al.*, 1989; *Cohen and Gordon*, 1979; *Yoshinari*, 1976]. In intermediate layers with extreme oxygen depletion (i.e., suboxic conditions), as found in the Arabian Sea and the eastern tropical Pacific Ocean, N_2O is also produced in considerable amounts by denitrification ($NO_3^- \rightarrow NO_2^- \rightarrow N_2O \rightarrow N_2$) [*Codispoti and Christensen*, 1995]. Recent dual-isotope measurements of $\delta^{15}N$ and $\delta^{18}O$ brought some new insights. *Dore et al.* [1998] suggested that nitrification is the dominant N_2O production pathway in surface waters of the subtropical Pacific Ocean. Additionally, *Naqvi et al.* [1998] speculated about a coupling of nitrification and denitrification in the surface layer of the Arabian Sea. Measurements of N_2O in deep waters are sparse, and the mechanism of the N_2O production in deep waters is still under debate [*Kim and Craig*, 1990; *Yoshida et al.*, 1989].

Here we present a compilation of N_2O measurements from water depths below 2000 m in order to evaluate the global distribution of N_2O in deep waters of the world's oceans. On the basis of this data set, an estimate of the magnitude of N_2O deep-water production and a discussion about its role for the global N_2O budget are presented. With a simple model we evaluate the implications of possible changes in the North Atlantic Deep Water (NADW) formation for the global N_2O budget.

2. Data Compilation

In Table 1 we present an overview of N_2O data from deep waters below 2000 m. The boundary of 2000 m was chosen to gain a most representative data set for N_2O in the deep waters. Three points led to our choice:

1. In order to investigate the N_2O distribution in the deep waters, we have to exclude the effects of the thermocline circulation, which could reach down to about 1000–1500 m [*Broecker and Peng*, 1982].

2. As mentioned in section 1, N_2O is mainly produced in the oxygen minimum zone (OMZ), whose lower boundary is found down to about 1200 m in the world's oceans [*Broecker and Peng*, 1982]. Since N_2O is produced in considerable amounts in the OMZ, there is usually a decreasing N_2O gradient toward deep-water layers. A check of the available data sets for N_2O gradients revealed that the choice of 2000 m minimizes a possible bias due to N_2O gradients at the top of the deep-water layer (see also discussion of diapycnal mixing in section 4).

Paper number 1999GB900082
0886-6236/99/1999GB900082$12.00

Table 1. Compilation of N_2O Data in Deep Waters Below 2000 m.

Latitude, °N or °S[a]	Longitude, °W[a] or °E	Date	Depth interval, m	Mean N_2O, nmol L^{-1}	SD[b] nmol L^{-1}	Minimum, nmol L^{-1}	Maximum, nmol L^{-1}	Samples	Calculated[c] (C) or Estimated[c] (E)	Reference
					North Atlantic					
65	−1.5	Aug. 1976	2100–2500	11.0	2.6	7.4	14.7	8	C	*Hahne* [1977]
64	0	Aug. 1976	2000–2800	12.2	1.4	10.0	15.6	13	C	*Hahne* [1977]
39.1	−62.4	May, July 1972	2000–5000	16	0.5	15	16	7	E	*Yoshinari* [1976]
35.9	−63.7	June 1972	2000–5000	15	0.7	14	16	14	E	*Yoshinari* [1976]
					South Atlantic					
−36	−45.1	Oct. 1994	2000–5000	16	1	14	17	8	E	*Butler et al.* [1995]
					North Indian					
24.3	58.2	Sept. 1986	2000–2700	25.3		24.0	26.6	2	C	*Law and Owens* [1990][d]
23.7	59.1	Sept. 1986	2000–2750	17.4	4.7	12.5	21.9	3	C	*Law and Owens* [1990][d]
22.7	60.7	Sept. 1986	2000–3000	23.5	4.4	20.1	28.5	3	C	*Law and Owens*, [1990][d]
21.8	64	April–May 1994	2000–2750	27	5.5	22	33	3	E	*Lal et al.* [1996]
21.3	63.3	Sept. 1986	2000–3000	20.7	4.1	16.6	24.7	3	C	*Law and Owens* [1990][d]
20	65.8	May 1997	2000–3150	18.8		14.4	23.2	2	C	Bange et al., submitted manuscript [1999]
19	67	Sept. 1986	2000–3200	15.3	2.2	13.0	17.5	3	C	*Law and Owens* [1990][d]
19	64	April–May 1994	2000–3000	26	6.1	20	33	3	E	*Lal et al.* [1996]
18	69	Dec. 1988	2000–3000	25	1.1	24	26	3	E	*Naqvi and Noronha* [1991]
18	58	Aug. 1995	2600–3200	16.5	1.8	14.8	18.3	3	C	Bange et al., submitted manuscript [1999]
17.5	59.1	July 1997	2000–3600	20.8	4.0	16.4	24.2	3	C	Bange et al., submitted manuscript [1999]
17.2	59.8	July 1995	2900–3900	16.5	1.0	16.0	17.5	3	C	Bange et al., submitted manuscript [1999]
16.3	61.4	Aug. 1995	2000–3900	17.2	3.7	12.2	24.8	10	C	Bange et al., submitted manuscript [1999]
16.2	60.3	May 1997	2500–4100	16.7	3.5	12.9	21.7	4	C	Bange et al., submitted manuscript [1999]
16	62	July 1997	2000–3950	18.5	3.4	14.4	22.4	4	C	*Law and Owens* [1990][d]
16	62	July 1995	2500–3900	17.9	1.0	16.3	18.8	5	C	*Law and Owens* [1990][d]
15.6	68.6	May 1997	3000–3900	18.3	3.1	16.1	21.8	3	C	Bange et al., submitted manuscript [1999]
14.5	65	July 1995	2000–4000	12.3	5.1	8.1	21.0	5	C	Bange et al., submitted manuscript [1999]
14.5	64.6	May 1997	2000–4000	18.3	1.9	15.7	20.4	5	C	Bange et al., submitted manuscript [1999]
14.4	66.9	Sept. 1986	2500–3900	22.4	2.3	19.3	23.5	4	C	Bange et al., submitted manuscript [1999]
12	67	Sept. 1986	2250–4200	13.5	1.5	11.2	14.4	4	C	Bange et al., submitted manuscript [1999]
11	64	May–July 1994	2000–3000	24	5.4	20	30	3	E	*Lal et al.* [1996]
10.1	64.7	May 1997	2000–4050	16.2	1.3	15.5	18.0	5	C	Bange et al., submitted manuscript [1999]
10	65	July 1995	2250–4400	15.7	2.2	12.7	19.6	7	C	Bange et al., submitted manuscript [1999]
8	67	Sept. 1986	2000–4500	11	1.3	9.1	11.8	4	C	*Law and Owens* [1990][d]
6	65	July 1995	2050–4400	20.4	1.7	18.2	22.4	6	C	Bange et al., submitted manuscript [1999]
4	67	Sept. 1986	2000–3050	10.3		7.5	13.0	2	C	*Law and Owens* [1990][d]
3	65	July 1995	2000–2800	19.1	2.3	16.5	21.5	5	C	Bange et al., submitted manuscript [1999]
					South Indian					
-27.63	90	June 1987	2000–3000	22.0		20.5	23.4	2	C	*Butler et al.* [1988]

Table 1.

Latitude, °N or °S[a]	Longitude, °W[a] or °E	Date	Depth interval, m	Mean N_2O, nmol L^{-1}	SD[b], nmol L^{-1}	Minimum, nmol L^{-1}	Maximum, nmol L^{-1}	Samples	Calculated (C)[c] or Estimated (E)[c]	Reference
					North Pacific					
48.4	155.6	May 1987	2500–3100	28.6		25.9	31.3	2	C	*Butler et al.* [1988]
48	156.0	May 1987	3900–5900	22.2	0.8	21.7	23.1	3	C	*Butler et al.* [1988]
47.7	156.3	May 1987	2000–4600	21.6	4.0	16.1	25.6	4	C	*Butler et al.* [1988]
47.5	156.5	May 1987	2000–3900	22.6		21.6	23.6	2	C	*Butler et al.* [1988]
47.1	157.0	May 1987	2500–4600	24.6	1.4	23.6	26.2	3	C	*Butler et al.* [1988]
46.8	157.1	May 1987	2500–4900	22.0	1.5	20.4	24.1	4	C	*Butler et al.* [1988]
46.8	−126.8	July 1977	2000–2500	25		24	26	2	E	*Cohen and Gordon* [1979]
46.6	157.3	May 1987	2950–4500	23.2	1.2	21.8	24.1	3	C	*Butler et al.* [1988]
46.4	157.5	May 1987	2950–4900	22.4	1.0	21.6	23.5	3	C	*Butler et al.* [1988]
46.2	157.7	May 1987	2500–4900	23.1	1.8	21.6	25.0	3	C	*Butler et al.* [1988]
46.0	157.9	May 1987	2500–5100	21.1	2.7	18.9	24.8	4	C	*Butler et al.* [1988]
45.8	158.1	May 1987	2500–5000	20.8	3.0	18.7	25.2	4	C	*Butler et al.* [1988]
45.5	158.4	May 1987	2950–3900	22.5		20.9	24.0	2	C	*Butler et al.* [1988]
45.2	160.3	Aug.–Sept.1983	2000–4800	24	3.8	19	30	11	E	*Yoshida et al.* [1989]
28.1	152.9	Aug.–Sept.1983	2500–4000	26	3.4	22	29	3	E	*Yoshida et al.* [1989]
22.4	170.1	Oct.–Dec. 1993	2000–5000	22.5	4.0	19	28	4	E	*Usui et al.* [1998]
22.8	−158.1	Oct.–Dec. 1993	2000–5000	22	3.0	20	26.5	4	E	*Usui et al.* [1998]
22.8	−148.0	Sept.–Oct. 1996	2000–3000	25.5		23	28	2	E	*Dore et al.* [1998]
22.6	−107.7	Dec. 1993	2250–2500	25	1.1	24	26	3	E	*Yoshinari et al.* [1997]
15.1	−105.9	Jan. 1977	2000–2750	18		17	19	2	E	*Cohen and Gordon* [1979]
10.8	−111.9	Jan. 1977	2000–2500	18		16	19	2	E	*Cohen and Gordon* [1979]
0.1	−159	Oct.–Dec. 1993	2500–5000	20	1.4	18	20	3	E	*Usui et al.* [1998]

[a] West longitudes and south latitudes are given as negative values.
[b] SD stands for standard deviation.
[c] Calculated (C) indicates that the values are based on data listed in reports. Estimated (E) indicates that the values are estimated from figures in the given reference.
[d] Original data set provided by C. S. Law.

Table 2. Overview of the data used in Figures 1 and 2.

	N_2O,[a] nmol L^{-1}	Age of Deep Water at 3000 m,[b] years
North Atlantic Ocean	13.6 ± 2.3 (4)	153 ± 66 (6)
South Atlantic Ocean	16 (1)	465 (1)
North Indian Ocean	18.7 ± 4.4 (28)	1227 ± 43 (5)
South Indian Ocean	22.0 (1)	1250 (1)
North Pacific Ocean	22.7 ± 2.5 (22)	1759 ± 176 (19)

Data are given as mean ± standard deviation. The number of profiles used for averaging is given in parentheses.
[a] Based on the data compilation in Table 1.
[b] Based on the data set by *Broecker et al.* [1988].

3. The choice of a 3000-m boundary would reduce the available data considerably, making an interpretation more difficult.

Unfortunately, only a few data are available as data reports, and thus we had to include data extracted from figures which are associated with an enhanced error for the extracted data. In order to keep the data uncertainties as small as possible, we generally did not consider N_2O data presented as contour plots, and we considered only depth profiles with more than one point below 2000 m. N_2O concentrations are usually given in nmol L^{-1} or ng L^{-1}. References reporting saturation values (in %) or excess N_2O (i.e., ΔN_2O in nmol L^{-1}), which require a correction introducing further uncertainties, were therefore not considered. Unfortunately, there are no data from the South Pacific and the Southern Oceans which match our criteria, and only a single profile was found for both the South Atlantic and the south Indian Oceans (Table 1). The very early N_2O measurements from the South Pacific Ocean reported by *Craig and Gordon* [1963] and from the North Atlantic Ocean reported by *Junge et al.* [1971] appear to be biased by analytical problems and thus are not included in Table 1. Despite our rigorous selection criteria, we were able to tabulate mean N_2O values from 56 depth profiles, providing for the first time an overview of the N_2O distribution in deep waters of the world's ocean.

3. Results

The N_2O data listed in Table 1 vary between 7 and 33 nmol L^{-1}. Surprisingly, the range for the data from the north Indian Ocean, which exclusively consists of data from the Arabian Sea, is exceptionally high. The reason for this variability is unknown (but see also section 4). From the mean values of each profile we calculated overall mean N_2O concentrations for the major ocean basins (Table 2). The highest mean N_2O value (22.7 ± 2.5 nmol L^{-1}) was found for the north Pacific Ocean, whereas the lowest mean N_2O value (13.6 ± 2.3 nmol L^{-1}) was found for the North Atlantic Ocean (Figure 1). Because the deep waters of the North Atlantic, north Indian, and North Pacific Oceans represent the major starting and turning points of the global deep-water circulation system (i.e., the so-called conveyor belt system), we might argue that the observed N_2O differences are caused by an accumulation on the two flow paths from the deep North Atlantic to the deep North Pacific Oceans and from the Weddell Sea to the north Indian Ocean [*Broecker*, 1991; *Schmitz*, 1995; *You*, 1999]. To test this hypothesis, we considered the mean age of the deep waters at 3000-m depth in each ocean basin (Table 2) [*Broecker et al.*, 1988]. We found a good correlation between the mean ages of the deep waters and the mean N_2O concentrations, indicating that N_2O in the deep waters is accumulating with time (Figure 2). The slope of the linear regression (5.7 ± 1.0 nmol m^{-3} yr^{-1}) in Figure 2 can be set equal to an annual N_2O accumulation rate. With the volume of about 1.15×10^{18} m^3 for the depth range from 2000 to 6000 m [*Menard and Smith*, 1966] we estimate an annual N_2O accumulation of 0.29 ± 0.05 Tg yr^{-1}.

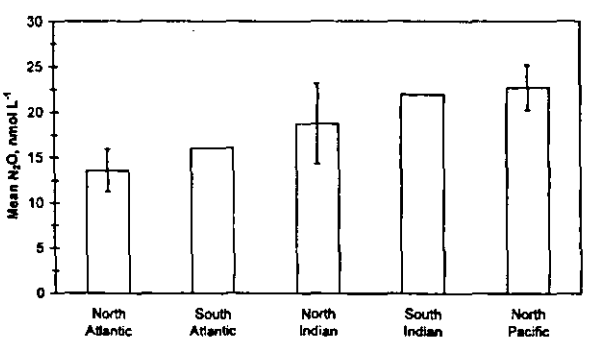

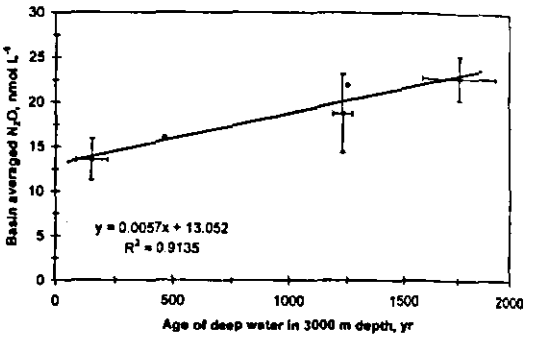

Figure 2. Basin-averaged N_2O concentrations in deep waters below 2000 m versus basin-averaged ages of the deep waters in 3000 m.

4. Discussion

What causes the observed N_2O accumulation? There are several possibilities:

First, mixing of waters with different N_2O concentrations may play a role. Transport of N_2O into the deep waters is mainly driven by diapycnal diffusivity along N_2O concentration gradients at the upper boundary of the deep-water layer (i.e., 2000 m). The diapycnal flux F_d of N_2O can be parameterized as

$$F_d = -K\, dN_2O / dz = -K\, [(N_2O)_h - (N_2O)_z] / (h - z),$$

where K is the diapycnal eddy diffusivity, dN_2O/dz is the concentration gradient, $(N_2O)_h$ stands for the N_2O concentration in depth h (above 2000 m), and $(N_2O)_z$ stands for the concentration in depth z (below 2000 m). Mean N_2O concentration gradients are listed in Table 3. N_2O gradients in the North Atlantic Ocean are close to zero, whereas the steepest N_2O

Table 3. Overview of the Calculated N_2O Concentration Gradients Across 2000 m.

Ocean Basin	Mean dN_2O/dz, µmol m^{-4}	SD,[a] µmol m^{-4}	Profiles	Data Set Used[b]
North Atlantic				
	0.001		1	*Hahne* [1977]
	> –0.001[c]		4	*Yoshinari* [1976]
South Atlantic				
	–0.010[c]		1	*Butler et al.* [1995]
North Indian				
	–0.011	0.009	19	Bange et al., submitted manuscript [1999]
	–0.013	0.010	9	*Law and Owens* [1990]
South Indian				
	–0.007	0.003	4	*Butler et al.* [1988]
North Pacific				
	–0.009	0.002	12	*Butler et al.* [1988]
Mean	–0.007			

Negative gradients indicate that $(N_2O)_h$ (i.e., above 2000 m) is greater than $(N_2O)_z$ (i.e., below 2000 m).
[a] SD stands for standard deviation.
[b] See also Table 1.
[c] Estimated from figure in the given reference.

gradients were observed for the north Indian Ocean (i.e., the Arabian Sea). The Arabian Sea appears to be the site of pronounced cross-isopycnal and dianeutral mixing processes [*Brandes et al.*, 1998; *You*, 1999]. Mixing effects in connection with very high N_2O values (up to 110 nmol L^{-1}) as found in the oxygen minimum zone (150–1200 m) of the Arabian Sea [*Law and Owens*, 1990] might be the reason for the observed wide range of N_2O concentrations of the Arabian Sea data listed in Table 1. With a mean N_2O gradient (dN_2O/dz) of about –0.01 µmol m^{-4}, a mean diapycnal diffusivity K for deep water of 0.1 x 10^{-4} m^2 s^{-1} [*Polzin et al.*, 1997], and an ocean area of 290 x 10^{12} m^2 (i.e., the ocean area with water depths deeper than 2000 m [*Menard and Smith*, 1966]), we estimate a diapycnal flux of about 0.04 Tg N_2O yr^{-1}. This is about 13% of the N_2O accumulation in the deep waters, indicating a small contribution by vertical transport of N_2O.

Second, N_2O may be emitted into deep waters through hydrothermal vents. The few measurements of N_2O concentrations in the hydrothermal vent waters of the Galapagos spreading center (0.8°N, 86.0°W) range from about 10 nmol L^{-1} to about 110 nmol L^{-1} [*Lilley et al.*, 1982]. The observed good linear correlations of the N_2O vent concentrations with silica showed either positive or negative slopes. Thus *Lilley et al.* [1982] speculated that N_2O might be consumed or produced in hydrothermal vents depending on the local redox potential. With the recent estimate of the global hydrothermal input of 0.15 ± 0.11 Tmol Si yr^{-1} [*Tréguer et al.*, 1995] and the observed N_2O to Si molar ratios of –0.034 x 10^{-3} and 0.178 x 10^{-3} [*Lilley et al.*, 1982], we estimate the global N_2O input by hydrothermal vents to range from –0.0002 to 0.001 Tg N_2O yr^{-1}. Thus we conclude that the contribution of hydrothermal systems to the deep-water accumulation of 0.3 Tg N_2O yr^{-1} is negligible.

Third, N_2O is produced in sediments by denitrification and/or nitrification and can be subsequently released into the water column above [*Seitzinger*, 1990, *Usui et al.*, 1998]. Unfortunately, only a few N_2O fluxes from deep-sea sediments of the equatorial Pacific and the subtropical North Pacific have been reported [*Usui et al.*, 1998]. On the basis of the flux data by *Usui et al.* [1998] (which range from 0.17 to 0.23 nmol N m^{-2} h^{-1}) and by applying a deep ocean area of 290 x 10^{12} m^2 (i.e., the ocean area with water depths deeper than 2000 m [*Menard and Smith*, 1966]), we extrapolate an annual N_2O release of 0.010 to 0.013 Tg. The sedimentary flux represents about 3–4% of the N_2O deep-water accumulation of 0.3 Tg N_2O yr^{-1} indicating that the N_2O flux across the sediment–water column interface in the deep sea is of minor importance.

Fourth, N_2O could be produced in situ in the deep water. In most studies of oceanic N_2O a positive linear correlation between excess N_2O (ΔN_2O = N_2O(observed) – N_2O(saturated)) and the apparent oxygen utilization (AOU = O_2(saturated) – O_2(observed)) was observed. This led to the prevailing view that during decomposition of organic material in the ocean, nitrification is the main source for oceanic N_2O [*Butler et al.*, 1989; *Cohen and Gordon*, 1979; *Yoshinari*, 1976]. Since most studies on oceanic N_2O focus on the upper water column, only a few ΔN_2O–AOU relationships including deep-water data are available [*Butler et al.*, 1989; *Cohen and Gordon*, 1979; *Law and Owens*, 1990; *Naqvi and Noronha*, 1991; H. W. Bange et al., Nitrous oxide cycling in the Arabian Sea, submitted to *Journal of Geophysical Research*, 1999 (hereinafter referred to as Bange et al., submitted manuscript)]. The good correlations of the ΔN_2O–AOU relationships found for the Pacific Ocean (Table 4) indicate that N_2O in deep waters of the Pacific Ocean is produced by nitrification. Nitrification in the Arabian Sea deep waters seems to be biased by another process as indicated by the low correlation coefficient [Bange et al., submitted manuscript, 1999]. We speculate that down-mixing of water affected by denitrification might be the reason for the observed low correlation [Bange et al., submitted manuscript, 1999] (see also above discussion about diapycnal mixing).

The unexpected finding of the considerable ^{15}N enrichment in deep-water N_2O caused a controversy about the prevailing production mechanism in deep waters. *Yoshida et al.* [1989] proposed that denitrification in particulate organic matter is the major process, whereas *Kim and Craig* [1990] argued that N_2O is produced by nitrification, which might be associated with a

Table 4. ΔN_2O–AOU Relationships Which Include Deep-Water Data.

Ocean Area	Slope (ΔN_2O/AOU)	Intercept	R^2 / Samples	Depth Range, m	Reference
Eastern tropical North Pacific	0.152 ± 0.013	−31.33	0.916 / 14	700–3000[b]	*Cohen and Gordon* [1979]
Northeastern Pacific	0.218 ± 0.026	−46.25	0.976 / 5	1000–2500[b]	*Cohen and Gordon* [1979]
Western Pacific, eastern Indian	0.125+0.00993 t[a]	−13.5	not given	0–5900	*Butler et al.* [1989]
Arabian Sea	0.1066+0.00455 t[a]	3.20	not given	0–3500[b]	*Naqvi and Noronha* [1991]
Arabian Sea	AOU<197: 0.033	5.5	significant at the	0–3500	*Law and Owens* [1990]
	AOU>197: 0.31	−49.4	1% level		
Arabian Sea	0.0910	−15.0	0.14 / 46	2000–4500	Bange et al., submitted manuscript [1999]
	0.0672	−11.0	0.25 / 15		
	0.3363	−68.4	0.55 / 5		

AOU, apparent oxygen utilization. ΔN_2O is given in nmol L^{-1}, and AOU is given in µmol L^{-1}.
[a] t stands for temperature in °C.
[b] Without data affected by denitrification.

subsequent consumption by denitrification in the interior of organic particulates. In a recent study on nitrate respiration in aggregates in the bottom waters of the northeast Pacific Ocean, *Wolgast et al.* [1998] found that denitrification could occur in microzones of the aggregates. The observations by *Wolgast et al.* [1998] suggest strongly that (strictly anaerobic) denitrification can occur in (well-oxygenated) deep-sea environments, implying that denitrification could be potentially involved in N_2O production or consumption in deep waters. However, no N_2O formation rates were measured by *Wolgast et al.* [1998]; therefore the question of whether nitrification or denitrification is the main N_2O formation process in deep waters requires further experimental efforts.

On the basis of the above discussion, we conclude that N_2O accumulation in the deep ocean is resulting mainly from nitrification processes; however, denitrification cannot be excluded definitely. There also might be a small contribution by down mixing of N_2O from upper layers. Hydrothermal and sedimentary N_2O sources are most probably negligible.

In Table 5 we present an overview of the current open-ocean N_2O budget. The deep-water nitrification is about 12–16% of the global oceanic N_2O produced by pelagic denitrification and about 3–16% of the N_2O loss from the open ocean to the atmosphere (Table 5). Obviously, the sum of the N_2O produced in the deep-water and pelagic denitrification zones does not balance the N_2O loss to the atmosphere, implying an unrealistically high loss of oceanic N_2O. Assuming steady state for the oceanic N_2O cycle, we can speculate that the missing N_2O source of about 3.8 Tg yr^{-1} is attributable to production by pelagic nitrification in the upper water column (above 2000 m). This sums up to an overall oceanic nitrification of 4.1 Tg N_2O yr^{-1} (i.e., deep-water plus upper water nitrification). Considering the considerable uncertainties of the fluxes listed, we conclude that our estimate is only slightly higher than the recent estimate of 2.4 Tg N_2O yr^{-1} produced by nitrification in the open ocean [*Capone*, 1996]. In *Capone*'s [1996] estimate, pelagic denitrification (6.7 Tg N_2O yr^{-1}) is the dominating open-ocean N_2O source. In contrast, we conclude that nitrification could be the dominating source for N_2O in the open ocean. This is in line with the results of *Dore et al.* [1998], who suggested that nitrification as the dominant N_2O production pathway could explain the observed isotopic signature of N_2O in the troposphere.

Table 5. Global Budget for Oceanic N_2O in the Open Ocean.

	Average Tg N_2O yr^{-1}	Range Tg N_2O yr^{-1}	Reference
Sources			
Deep-water nitrification	0.3 ± 0.1		this paper
Net production via pelagic denitrification[a]	2.2	1.9–2.5	
Sink			
Loss to atmosphere	6.3	1.9–10.7	*Nevison et al.* [1995]
ΣSources - Sink	−3.8		

[a] Estimated on the basis of the global pelagic denitrification of 60–80 Tg N yr^{-1} [*Codispoti and Christensen*, 1985; *Gruber and Sarmiento*, 1997], assuming that 2% is transformed to N_2O as observed in the Arabian Sea [Bange et al., submitted manuscript, 1999; *Mantoura et al.*, 1993].

5. Model

Besides the observed N_2O deep-sea accumulation, another question arises: what are the consequences of possible climatically induced changes in the pattern of the deep-sea circulation (i.e., the "conveyor belt" system)?

With a simple box model we estimated the time variation of the N_2O concentration in deep water (below 2000 m) in the period 1903–2065 A.D.:

$$dC_{N2O}/dt = (\beta\, x'\, V_{NADW}) + S - C_{deep}\, V_{upw}$$

where x' is the atmospheric N_2O dry mole fraction in ppb, V_{NADW} is the volume flow of the NADW formation in 10^6 m^3 s^{-1}, β is the solubility function for N_2O in seawater, S stands for the observed N_2O accumulation in deep waters, V_{upw} is the deep-water upwelling flow (which is equal to V_{NADW}), and C_{deep} is the mean N_2O deep-water concentration.

5.1. Input Parameters

The deep-water N_2O accumulation S was set to 0.3 Tg N_2O yr^{-1}. The 1903 start value for x' was set to 278.8 ppb N_2O [*Battle et al.*, 1996] and 18×10^6 m^3 s^{-1} for the North Atlantic Overturning [*Sarmiento et al.*, 1998]. Annual decrease rates of

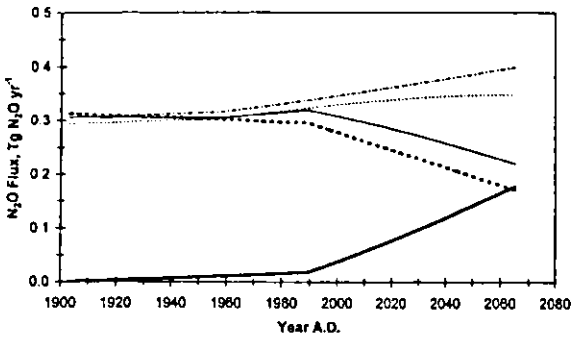

Figure 3. Model results of the temporal development of the N_2O fluxes in the deep sea: the dashed-dotted line represents $F_{control}$, the thin solid line represents F_{NADW}, the thick solid line represents ΔF, the thin dashed line represents N_2O accumulation in the deep sea, and the thick dashed line stands for F_{upw}.

0.01×10^6 m^3 s^{-1} (1903–1990) and 0.1×10^6 m^3 s^{-1} (1990–2065) for the North Atlantic Overturning were adapted from *Sarmiento et al.* [1998]. In a control run the overturning was set to a constant value of 18×10^6 m^3 s^{-1}. Annual tropospheric N_2O growth rates were set to 0.6% yr^{-1} (1903–1958) and 0.22% yr^{-1} (1959–1990) [*Battle et al.*, 1996]. The annual N_2O growth rate for the period 1990–2065 was modified to include an N_2O feedback effect due to changes in the uptake N_2O by NADW formation. We did not account for interhemispheric differences resulting from the fact that the annual growth rates were derived from South Pole snowpack and NADW formation takes place in the Northern Hemisphere. However, since the annual growth rates for both the Southern and Northern Hemispheres seem to be in phase for the period considered, the small interhemispheric difference of about 1–1.5 ppb N_2O [*Weiss*, 1994] is negligible. Dissolved N_2O concentrations were calculated with the solubility equation given by *Weiss and Price* [1980], assuming that the N_2O concentration in the North Atlantic is always equal to the equilibrium concentration (neglecting seasonal variations of N_2O in the North Atlantic surface water). This assumption appears to be reasonable since N_2O surface concentrations from the North Atlantic Ocean are mainly driven by the seasonality of the sea surface temperature (SST), implying a mean annual N_2O concentration equal to the equilibrium value [*Nevison et al.*, 1995]. Moreover, we did not account for long-term trends of the SST and sea surface salinity (SSS) of the North Atlantic surface waters (in the model they are fixed at 2°C and 35‰, respectively), because sensitivity studies of our model indicated that temporal changes in SST and SSS result in negligible changes of the annual N_2O fluxes.

5.2. Results

The resulting fluxes are presented in Figure 3. The model results are given as N_2O fluxes such as $F_{control}$ (i.e., constant North Atlantic Deep Water formation), F_{NADW} (i.e., temporal modulated formation of NADW), F_{upw} (i.e., the N_2O flux out of the deep-sea into the intermediate layers), and ΔF (i.e., $F_{control} - F_{NADW}$). ΔF is a measure for the amount of N_2O which is not "buried" in the deep sea, representing an indirect source for atmospheric N_2O. F_{upw} shows a maximum of 0.31 Tg N_2O yr^{-1} at the beginning of the century and, consequently, decreases when the NADW formation is reduced. Assuming that the N_2O production in the upper water layer at the beginning of the century was about the same as today (3.8 Tg N_2O yr^{-1} for nitrification and 2.2 Tg N_2O yr^{-1} for denitrification; see Table 5), we estimate that N_2O upwelled into the upper water layers contributes less than 5% to the N_2O sources in the upper water column. Thus the N_2O surface distribution and, consequently, the N_2O air–sea exchange are not significantly influenced by variations in the deep-water formation of N_2O.

The results for ΔF show a slight increase from 1903 until 1990 correlating with the variations in the deep-water formation. The change in the annual atmospheric N_2O growth rate in 1959 results in an increase of F_{NADW}, which does not yield a decrease of the rate of ΔF. From 1990 on, the accelerated slowing of the North Atlantic Overturning results in an accelerated increase of ΔF (Figure 3). The mean ΔF was calculated to be 0.017 Tg N_2O yr^{-1} for 1990. This shows that the indirect N_2O source by reduced NADW formation represents only about 0.4% of the annual N_2O growth rate of about 5.6 Tg in 1990. An arbitrarily introduced, complete shutdown of the North Atlantic Overturning (which is theoretically predicted to take place at a flow rate of approximately 10×10^6 m^3 s^{-1} [*Rahmstorf*, 1998], a threshold value which will be reached in the year 2065, according to the model by *Sarmiento et al.* [1998]) will result in a maximal atmospheric N_2O source of 0.40 Tg yr^{-1}. This is about 5.8% of the modeled annual N_2O growth rate of 6.9 Tg for the year 2065.

Our simple estimate does not include changes of the deep-water formation in the Southern Ocean (e.g., in the Weddell Sea). A recent estimate yielded a flow rate of about 15×10^6 m^3 s^{-1}, indicating that deep-water formation in the Southern Ocean is of the same magnitude as the North Atlantic Overturning [*Broecker et al.*, 1998]. Thus we conclude that the N_2O fluxes presented in Figure 3 are conservative and could increase when including temporal changes in the deep-water formation in the Southern Ocean.

6. Conclusions

Despite the fact that the deep-water zone of the world's oceans represents about 95% of the total ocean volume, it contributes only about 3–16% (i.e., 0.3 Tg N_2O yr^{-1}) to the global open-ocean N_2O production. This emphasizes the role of the upper ocean for the cycling of oceanic N_2O.

A rough estimate of the oceanic budget N_2O suggested that the loss to the atmosphere could be balanced only by an additional source of 3.8 Tg N_2O yr^{-1} attributed to nitrification in upper waters (0–2000 m).

The predicted decrease in the NADW formation rate in the near future will lead to an additional source of atmospheric N_2O in the range of about 0.02–0.4 Tg yr^{-1}, amplifying the annual N_2O growth rate, which in turn increases possible climatic changes via an enhanced greenhouse warming effect and thus might lead again to changes in the NADW formation. However, the signal of this (anthropogenically induced) feedback mechanism is small and will be very difficult to detect against the natural variations in the annual growth rates of tropospheric N_2O.

Acknowledgments. We especially thank C.S. Law for digging out his N_2O data from the 1986 Arabian Sea expedition. We thank C. Strametz for help with the manuscript. Our data from the Arabian Sea were measured as part of the German JGOFS–Arabian Sea Process Study

funded by the German Bundesministerium für Bildung, Wissenschaft, Forschung und Technologie through grants 03F0137A, 03F0183G, and 03F0241C and by the Max Planck Society.

References

Battle, M., et al., Atmospheric gas concentrations over the past century measured in air from firn at the South Pole, *Nature, 383*, 231–235, 1996.

Bouwman, A.F., K.W. Van der Hoek, and J.G.J. Olivier, Uncertainties in the global source distribution of nitrous oxide, *J. Geophys. Res., 100*, 2785–2800, 1995.

Brandes, J.A., A.H. Devol, T. Yoshinari, D.A. Jayakumar, and S.W.A. Naqvi, Isotopic composition of nitrate in the central Arabian Sea and eastern tropical North Pacific: A tracer for mixing and nitrogen cycles, *Limnol. Oceanogr., 43*, 1680–1689, 1998.

Broecker, W.S., and T.-H. Peng, *Tracers in the Sea*, 690 pp., Eldigio, Palisades, N.Y., 1982.

Broecker, W.S., The great ocean conveyor, *Oceanography, 4*, 79–89, 1991.

Broecker, W.S., M. Andree, G. Bonani, W. Wolfli, H. Oeschger, M. Klas, A. Mix, and W. Curry, Preliminary estimates for the radiocarbon age of deep water in the glacial ocean, *Paleoceanography, 3*, 659–669, 1988.

Broecker, W.S., et al., How much deep water is formed in the Southern Ocean?, *J. Geophys. Res., 103*, 15,833–15,843, 1998.

Butler, J.H., J.W. Elkins, C.M. Brunson, K.B. Egan, T.M. Thompson, T.J. Conway, and B.D. Hall, Trace gases in and over the west Pacific and east Indian Oceans during the El Niño–Southern Oscillation event of 1987, NOAA Data Report ERL ARL–16, Air Resour. Lab., Silver Spring, M.D., 1988.

Butler, J.H., J.W. Elkins, T.M. Thompson, and K.B. Egan, Tropospheric and dissolved N_2O of the west Pacific and east Indian Oceans during the El Niño Southern Oscillation Event of 1987, *J. Geophys. Res., 94*, 14,865–14,877, 1989.

Butler, J.H., J.M. Lobert, S.A. Yvon, and L.S. Geller, The distribution and cycling of halogenated trace gases, in *Reports on Polar Research No. 168 – The expedition ANTARKTIS XII of RV "Polarstern" in 1994/95: Reports of legs ANT XII/1 and 2*, edited by G. Kattner and D.K. Fütterer, pp. 33–40, Alfred Wegener Inst. for Polar and Mar. Res., Bremerhaven, Germany, 1995.

Capone, D.G., A biologically constrained estimate of oceanic N_2O flux, *Mitt. Int. Ver. Limnol., 25*, 105–113, 1996.

Codispoti, L.A., and J.P. Christensen, Nitrification, denitrification and nitrous oxide cycling in the eastern tropical South Pacific, *Mar. Chem., 16*, 277–300, 1985.

Cohen, Y., and L.I. Gordon, Nitrous oxide production in the ocean, *J. Geophys. Res., 84*, 347–353, 1979.

Craig, H., and L.I. Gordon, Nitrous oxide in the ocean and the marine atmosphere, *Geochim. Cosmochim. Acta, 27*, 949–955, 1963.

Dore, J.E., B.N. Popp, D.M. Karl, and F.J. Sansone, A large source of atmospheric nitrous oxide from subtropical North Pacific surface waters, *Nature, 396*, 63–66, 1998.

Gruber, N., and J.L. Sarmiento, Global patterns of marine nitrogen fixation and denitrification, *Global Biogeochem. Cycles, 11*, 235–266, 1997.

Hahne, A., Messungen atmosphärischer Spurengase im Meerwasser, *Ber. der Kernforschungsanlage Jülich 1444*, 58 pp., Kernforschungsanlage Jülich GmbH - Institut für Chemie, Jülich, Germany, 1977.

Junge, C., B. Bockholt, K. Schütz, and R. Beck, N_2O Measurements in air and seawater over the Atlantic, *Meteor Forschungsergeb. B, 6*, 1–11, 1971.

Khalil, M.A.K., and R.A. Rasmussen, The global sources of nitrous oxide, *J. Geophys. Res., 97*, 14,651–14,660, 1992.

Kim, K.-R., and H. Craig, Two-isotope characterization of N_2O in the Pacific Ocean and constraints on its origin in deep water, *Nature, 347*, 58–61, 1990.

Lal, S., P.K. Patra, S. Venkataramani, and M.M. Sarin, Distribution of nitrous oxide and methane in the Arabian Sea, *Curr. Sci., 71*, 894–899, 1996.

Law, C.S., and N.J.P. Owens, Significant flux of atmospheric nitrous oxide from the northwest Indian Ocean, *Nature, 346*, 826–828, 1990.

Lilley, M.D., M.A. de Angelis, and L.I. Gordon, CH_4, H_2, CO, N_2O in submarine hydrothermal vent waters, *Nature, 300*, 48–50, 1982.

Mantoura, R.F.C., C.S. Law, N.J.P. Owens, P.H. Burkill, E.M.S. Woodward, R.J.M. Howland, and C.A. Llewellyn, Nitrogen biogeochemical cycling in the northwestern Indian Ocean, *Deep Sea Res., Part II, 40*, 651–671, 1993.

Menard, H.W., and S.M. Smith, Hypsometry of the ocean basin provinces, *J. Geophys. Res., 71*, 4305–4325, 1966.

Naqvi, S.W.A., and R.J. Noronha, Nitrous oxide in the Arabian Sea, *Deep Sea Res., Part A, 38*, 871–890, 1991.

Naqvi, S.W.A., T. Yoshinari, D.A. Jayakumar, M.A.A. Altabet, P.V. Narvekar, A.H. Devol, J.A. Brandes, and L.A. Codispoti, Budgetary and biogeochemical implications of N_2O isotope signatures in the Arabian Sea, *Nature, 394*, 462–464, 1998.

Nevison, C.D., R.F. Weiss, and D.J. Erickson III, Global oceanic emissions of nitrous oxide, *J. Geophys. Res., 100*, 15,809–15,820, 1995.

Polzin, K.L., J.M. Toole, J.R. Ledwell, and R.W. Schmitt, Spatial variability of turbulent mixing in the abyssal ocean, *Science, 276*, 93–96, 1997.

Prather, M., R. Derwent, D. Ehhalt, P. Fraser, E. Sanhueza, and X. Zhou, Other trace gases and atmospheric chemistry, in *Climate Change 1995, The Science of Climate Change, Contribution of Working Group I to the Second Assessment of the Intergovernmental Panel on Climate Change*, edited by J.T. Houghton et al., pp. 86–103, Cambridge Univ. Press, New York, 1996.

Rahmstorf, S., Decadal variability of the thermohaline ocean circulation, in *Beyond El Niño: Decadal Variability in the Climate System*, edited by A. Navarra, in press, Springer-Verlag, New York, 1998.

Sarmiento, J.L., T.M.C. Hughes, R.J. Stouffer, and S. Manabe, Simulated response of the ocean carbon cycle to anthropogenic climate warming, *Nature, 393*, 245–249, 1998.

Schmitz, W.J., Jr., On the interbasin-scale thermohaline circulation, *Rev. Geophys., 33*, 151–173, 1995.

Seitzinger, S.P., Denitrification in aquatic sediments, in *Denitrification in Soil and Sediment*, edited by N.P. Revsbech and J. Sörensen, pp. 301–321, Plenum, New York, 1990.

Tréguer, P., D.M. Nelson, A.J. Van Bennekom, D.J. DeMaster, A. Leynaert, and B. Quéguiner, The silica balance in the world ocean: A reestimate, *Science, 268*, 375–379, 1995.

Usui, T., I. Koike, and N. Ogura, Vertical profiles of nitrous oxide and dissolved oxygen in marine sediments, *Mar. Chem., 59*, 253–270, 1998.

Weiss, R.F., Changing global concentrations of atmospheric nitrous oxide, in *International Symposium on Global Cycles of Atmospheric Greenhouse Gases*, pp. 78–80, Tohoku Univ., Sendai, Japan, 1994.

Weiss, R.F., and B.A. Price, Nitrous oxide solubility in water and seawater, *Mar. Chem., 8*, 347–359, 1980.

Wolgast, D.M., A.F. Carlucci, and J.E. Bauer, Nitrate respiration associated with detrital aggregates in aerobic bottom waters of the abyssal NE Pacific, *Deep Sea Res., Part II, 45*, 881–892, 1998.

Yoshida, N., H. Morimoto, M. Hirano, I. Koike, S. Matsuo, E. Wada, T. Saino, and A. Hattori, Nitrification rates and ^{15}N abundances of N_2O and NO_3^- in the western North Pacific, *Nature, 342*, 895–897, 1989.

Yoshinari, T., Nitrous oxide in the sea, *Mar. Chem.*, *4*, 189–202, 1976.

Yoshinari, T., M.A. Altabet, S.W.A. Naqvi, L. Codispoti, A. Jayakumar, M. Kuhland, and A. Devol, Nitrogen and oxygen isotopic composition of N_2O from suboxic waters of the eastern tropical North Pacific and the Arabian Sea – Measurements by continuous-flow isotope-ratio monitoring, *Mar. Chem.*, *56*, 253–264, 1997.

You, Y., Dianeutral mixing, transformation and transport of deep water of the Indian Ocean, *Deep Sea Res., Part I*, *46*, 109–148, 1999.

M.O. Andreae and H.W. Bange, Biogeochemistry Department, Max Planck Institute for Chemistry, P.O. Box 3060, D-55020 Mainz, Germany. (bange@mpch-mainz.mpg.de)

(Received May 24, 1999; revised August 31, 1999; accepted September 8, 1999.)

JOURNAL OF GEOPHYSICAL RESEARCH, VOL. 106, NO. C1, PAGES 1053–1065, JANUARY 15, 2001

Nitrous oxide cycling in the Arabian Sea

Hermann W. Bange, Spyridon Rapsomanikis,[1] and Meinrat O. Andreae

Biogeochemistry Department, Max Planck Institute for Chemistry, Mainz, Germany

Abstract. Depth profiles of dissolved nitrous oxide (N_2O) were measured in the central and western Arabian Sea during four cruises in May and July–August 1995 and May–July 1997 as part of the German contribution to the Arabian Sea Process Study of the Joint Global Ocean Flux Study. The vertical distribution of N_2O in the water column on a transect along 65°E showed a characteristic double-peak structure, indicating production of N_2O associated with steep oxygen gradients at the top and bottom of the oxygen minimum zone. We propose a general scheme consisting of four ocean compartments to explain the N_2O cycling as a result of nitrification and denitrification processes in the water column of the Arabian Sea. We observed a seasonal N_2O accumulation at 600–800 m near the shelf break in the western Arabian Sea. We propose that, in the western Arabian Sea, N_2O might also be formed during bacterial oxidation of organic matter by the reduction of IO_3^- to I^-, indicating that the biogeochemical cycling of N_2O in the Arabian Sea during the SW monsoon might be more complex than previously thought. A compilation of sources and sinks of N_2O in the Arabian Sea suggested that the N_2O budget is reasonably balanced.

1. Introduction

Nitrous oxide (N_2O) is an atmospheric trace gas that significantly influences, directly and indirectly, Earth's climate. In the troposphere it acts as a greenhouse gas and in the stratosphere it is the major source for NO radicals, which are involved in one of the main ozone reaction cycles [*Prather et al.*, 1996].

Recently published source estimates indicate that the world's oceans play a major, but not dominant, role in the global budget of atmospheric N_2O [*Bouwman et al.*, 1995; *Khalil and Rasmussen*, 1992]. Most of the world's ocean surface layer is near gas-exchange equilibrium with the atmosphere [*Nevison et al.*, 1995], whereas a subsurface N_2O accumulation is generally associated with the oxygen (O_2) minimum [e.g., *Butler et al.*, 1989; *Cohen and Gordon*, 1979; *Naqvi et al.*, 1994; *Oudot et al.*, 1990]. Significant N_2O depletion was observed in water masses showing intense denitrification, that is, anoxic basins [*Cohen*, 1978; *Elkins et al.*, 1978; *Hashimoto et al.*, 1983; *Rönner*, 1983] and oxygen depleted (suboxic) water bodies (for an overview see, *Codispoti et al.* [1992]). In most studies of oceanic N_2O, a positive linear correlation between excess N_2O (ΔN_2O = N_2O(observed) − N_2O(saturated)) and the apparent oxygen utilization (AOU = O_2(saturated) − O_2(observed)) was observed. This led to the prevailing view that during decomposition of organic material in the ocean, nitrification ($NH_4^+ \rightarrow NO_2^- \rightarrow NO_3^-$) is the main source for oceanic N_2O [*Butler et al.*, 1989; *Cohen and Gordon*, 1979; *Elkins et al.*, 1978; *Oudot et al.*, 1990; *Yoshinari*, 1976]. Based on recent dual-isotope measurements, *Dore et al.* [1998] suggested that N_2O production via nitrification at the interface of the euphotic–aphotic zone plays an important role in the global tropospheric N_2O budget. However, from isotope measurements of the $\delta^{15}N$ and $\delta^{18}O$ values of N_2O in deep water, it is still under debate whether nitrification or denitrification ($NO_3^- \rightarrow NO_2^- \rightarrow N_2O \rightarrow N_2$) is the dominant production pathway in deep water [*Kim and Craig*, 1990; *Yoshida et al.*, 1989]. At the boundaries of oxygen-depleted water bodies, both nitrification and denitrification or a coupling of both processes may produce N_2O [*Codispoti and Christensen*, 1985; *Law and Owens*, 1990; *Naqvi and Noronha*, 1991; *Naqvi et al.*, 1998; *Upstill-Goddard et al.*, 1999]. Here we present our measurements of nitrous oxide in the water column of the central and western Arabian Sea during the intermonsoon and southwest (SW) monsoon periods in 1995 and 1997.

2. Study Area and Sampling Locations

The northwestern part of the Indian Ocean is defined as the Arabian Sea (Figure 1). It is surrounded by the African and Asian continents to the west, north, and east. The southern boundary is usually set at the equator. The Arabian Sea experiences extremes in atmospheric forcing that lead to the greatest seasonal variability observed in any ocean basin. During the SW monsoon (late May to September), the strongest sustained wind stress is in the highly sheared Findlater Jet. The axis of the Findlater Jet extends generally from northern Somalia to northwestern India. During the SW monsoon, coastal upwelling is driven by Ekman divergence of surface water off shore owing to the influence of winds parallel to the coast. The region of coastal upwelling exists up to 400 km off the Arabian Peninsula. Downwelling occurs on the southeastern side of the Findlater Jet, driving subduction of surface waters into the thermocline and promoting deepening of the mixed layer.

The Arabian Sea contains diverse biogeochemical features such as eutrophic, oligotrophic, and low-oxygen environments. The latter lies between 150 and 1000 m depth and represents the thickest oxygen minimum zone (OMZ) found in the world's oceans today. The OMZ of the Arabian Sea is the site of intense denitrification processes and thus plays a major role in the global nitrogen cycle. For further details about the oceanographic and

[1] Now at Laboratory of Atmospheric Pollution Science and Technology, Environmental Engineering Department, Demokritos University of Thrace, Xanthi, Greece.

Paper number 1999JC000284
0148-0227/01/1999JC000284$09.00

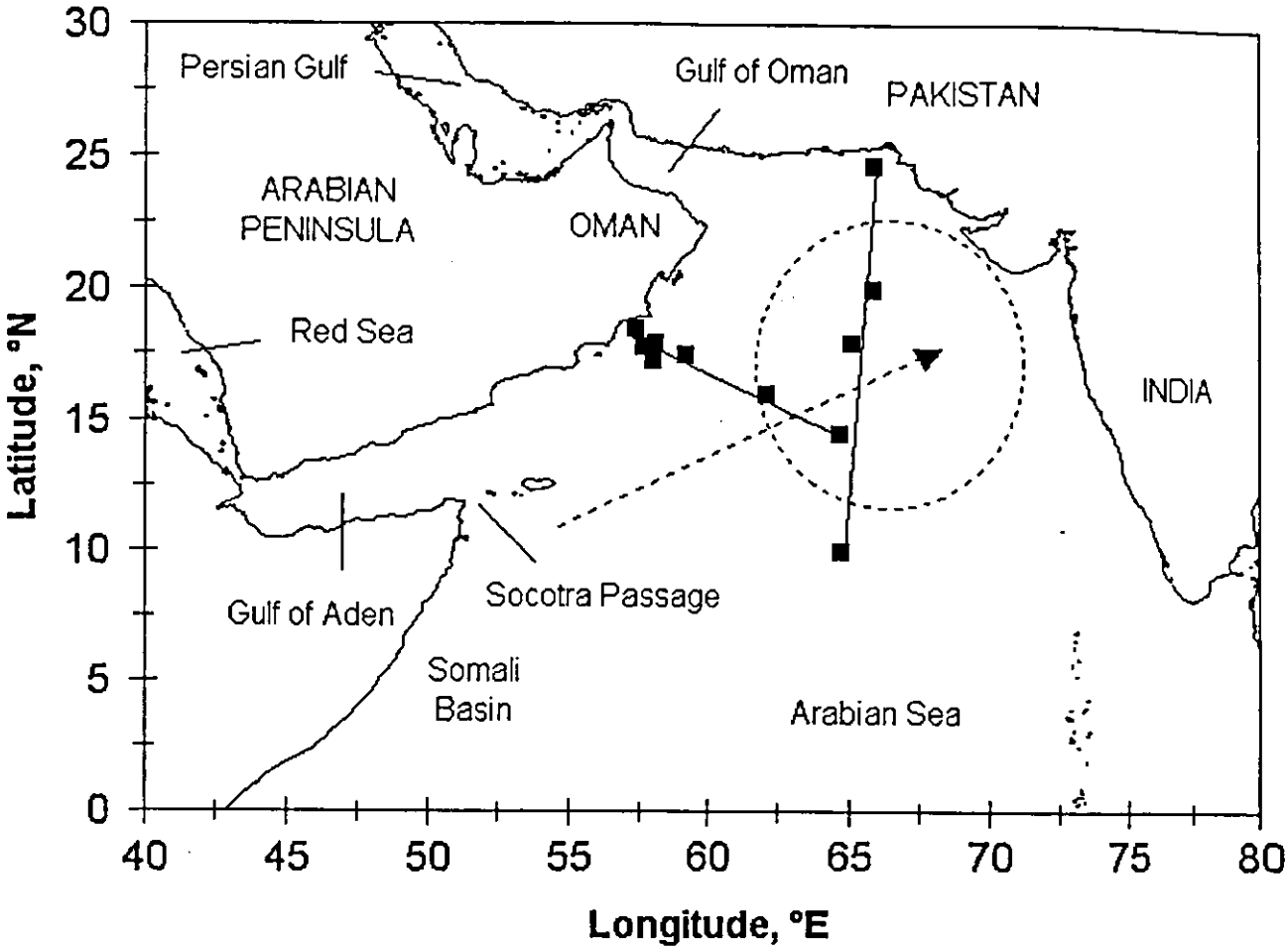

Figure 1. Map of the Arabian Sea with locations of selected stations where N_2O measurements were performed during the German JGOFS – Arabian Sea Process Study in 1995 and 1997 (for further details see Table 1). The two straight lines indicate the NS and NWSE transects as described in the text. The dashed arrow indicates the axis of the Findlater Jet. The dashed circle indicates the approximate distribution of the core of the denitrification zone as indicated by the secondary nitrite maximum ($NO_2^- > 1$ μmol L^{-1}) [*Naqvi*, 1994].

biogeochemical aspects of the Arabian Sea, the reader is referred to literature compilations presenting results from ongoing international research programs such as the Joint Global Ocean Flux Study (JGOFS) – Arabian Sea Process Study [*Burkill*, 1999; *Burkill et al.*, 1993; *Desai*, 1992; *Gage et al.*, 2000; *Ittekkot and Nair*, 1993; *Krishnaswami and Nair*, 1996; *Lal*, 1994; *Smith*, 1999, 1998; *Van Weering et al.*, 1997]. A comprehensive overview of the historical, geological, hydrographic, chemical, and biological aspects of the Arabian Sea in the context of the Indian Ocean is given in a recently published book by *Rao and Griffiths* [1998].

The four cruise legs discussed here were part of the German JGOFS – Arabian Sea Process Study and took place on the German research vessels *Meteor* (M) and *Sonne* (SO) in May 1995 (leg M32/3), July–August 1995 (leg M32/5), May–June 1997 (leg SO119), and June–July 1997 (leg SO120). Legs M32/3, M32/5, and SO119 covered mainly the central Arabian Sea, whereas leg SO120 focused on the coastal upwelling area off the Arabian Peninsula (Figure 1).

3. Method

Duplicate water samples from various depths were drawn into 100-mL glass flasks from bottles mounted on a rosette water sampler. Flasks with two outlets closed by Teflon valves and one outlet sealed with a silicone rubber septum for headspace sampling (Thermolite®, Restek GmbH, Germany) were used. The flasks were rinsed twice with at least two flask volumes of seawater prior to bubble-free filling with the seawater sample. Then 50 mL of the sample was replaced with helium and the remaining water phase was poisoned with saturated $HgCl_2$ solution (0.2 mL) [*Elkins*, 1980; *Yoshinari*, 1976]. Samples were stored at constant room temperature and allowed to equilibrate for at least 2 hours prior to chromatographic analysis. All samples were analyzed within 12 hours after collection. Prior to analysis, the samples were stirred with a magnetic stirrer for 5 min. A 10-mL subsample of the headspace was drawn with a gas-tight glass syringe from the flask and used to purge a thermostated (40°C), 2-mL sample loop connected to a 10-port gas stream selecting valve. Then the valve was switched and the sample was injected with the carrier gas onto the column. N_2O was determined using a gas chromatograph (Model 5890 Series II, Hewlett–Packard, California) equipped with an electron capture detector (ECD). The ECD (Model 19233, Hewlett–Packard, California) was held at a temperature of 350°C. The analysis was carried out at 190°C using a stainless steel column (1.83 m length, 3.2 mm OD, 2.2 mm ID) packed with washed molecular sieve 5A (mesh 80/100, Alltech GmbH, Germany). A mixture of Ar/CH_4

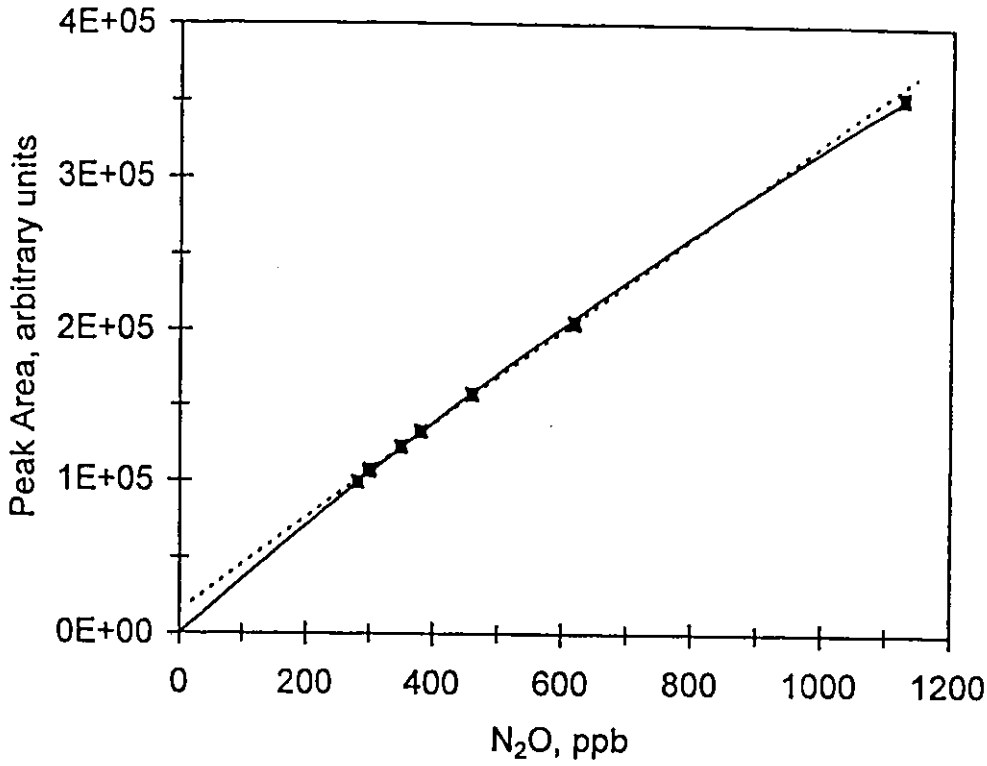

Figure 2. Characteristic response curve of the electron capture detector used in this study. We measured eight calibration gas mixtures: 299.0 ± 0.2, 300.5 ± 0.1, 349.6 ± 0.2, 380.5 ± 0.3 (all calibrated against the SIO-1993 standard scale (R. F. Weiss, personal communication, 1996), and 281, 460, 618, and 1125 ppb N_2O in synthetic air (± 2%; Deuste Steininger GmbH, Mühlhausen, Germany). The dashed line represents a linear fit through the points at 300.5 and 349.6 ppb N_2O (correlation coefficient r^2 = 0.9977, number of samples n = 19). The solid line indicates a quadratic fit ($y = -0.0458x^2 + 364.72x$, $r^2 = 0.9996$, number of samples $n = 47$). Read 4E+05 as 4×10^5.

(95%/5%) was used as the carrier gas at a flow rate of 45 mL min^{-1}. On a molecular sieve 5A column, CO_2 elutes after N_2O; the peaks are well separated under the conditions applied [*McAllister and Southerland*, 1971]. The use of the Ar/CH_4 mixture as carrier gas enhances the ECD sensitivity for N_2O and, additionally, avoids possible interferences from residual effects in the ECD owing to high CO_2 concentrations [*Butler and Elkins*, 1991].

Mixtures of N_2O in synthetic air were used to obtain two-point calibration curves. These mixtures contained 300.5 ± 0.1 and 349.6 ± 0.2 ppb N_2O, separately. These are gravimetrically prepared gas mixtures and were calibrated in the laboratory of R. F. Weiss (Scripps Institution of Oceanography (SIO), California), against the SIO-1993 standard scale (R. F.Weiss, personal communication, 1996). To account for the nonlinear ECD response [*Butler and Elkins*, 1991], we applied a quadratic regression ($y = ax^2 + bx$) for all values <300 ppb and a linear regression for values >300 ppb. Thus N_2O values in the range from 350 to 1050 ppb, which is above the range covered by the calibration gases, may be overestimated by as much as 2% owing to the linear regression applied (Figure 2). Concentrations of dissolved N_2O were calculated as follows:

$$[N_2O]_{dissolved} = [N_2O]_{water\ sample} + [N_2O]_{headspace}$$

$$= x'\beta(T, S)P + x'P/(RT)$$

and $x' = x/(P - p_{H2O})$, where x' is the N_2O dry mole fraction, β is the solubility function [*Weiss and Price*, 1980], T is the temperature of the sample at the time of the analysis, S is the salinity, P is the atmospheric pressure at the time of the analysis, R is the gas constant, x is the measured N_2O wet mole fraction in the headspace, and p_{H2O} is the water vapor pressure according to *Weiss and Price* [1980].

To check our method for systematic errors (e.g., efficiency of equilibration), we cross checked the values obtained by the method described above with the data from a well-established automated equilibration system for underway N_2O measurements in the surface layer. This system was run on board during the same cruises in 1995 and 1997 [*Bange et al.*, 1996, 2000]. The comparison shows a good agreement between both data sets (Figure 3), indicating that systematic errors are mainly introduced by the manual handling of the discrete samples. In order to calculate the theoretical overall analytical precision of our measurements, we assumed typical values and error ranges of 1±0.05 atm, 25±1°C, 35±0.1‰, and 100±10ppb for the pressure, equilibration temperature, salinity, and wet mole fraction, respectively. Computation of the error propagation gave an overall measurement error (i.e., $\Delta[N_2O]_{dissolved}$) of ±0.78 nmol L^{-1}. This results in a relative error ($\Delta[N_2O]_{dissolved}/[N_2O]_{dissolved}$) of ±12.4%. The computation of $\Delta[N_2O]_{dissolved}$ is most sensitive to errors in pressure, whereas errors of the equilibration temperature and salinity are less important. For example, an error of ±0.05 atm for the pressure results in an error of ±7.2%, whereas an error of ±1°C results in an error of ±1% for $\Delta[N_2O]_{dissolved}$. The precision of the measurements estimated from four replicate samples with an average concentration of 35.2 nmol L^{-1} was 7.7 %. This is in reasonable agreement with the theoretical overall error estimate given above.

Each N_2O depth profile is a composite of two casts covering different depth ranges collected at the same station within 24

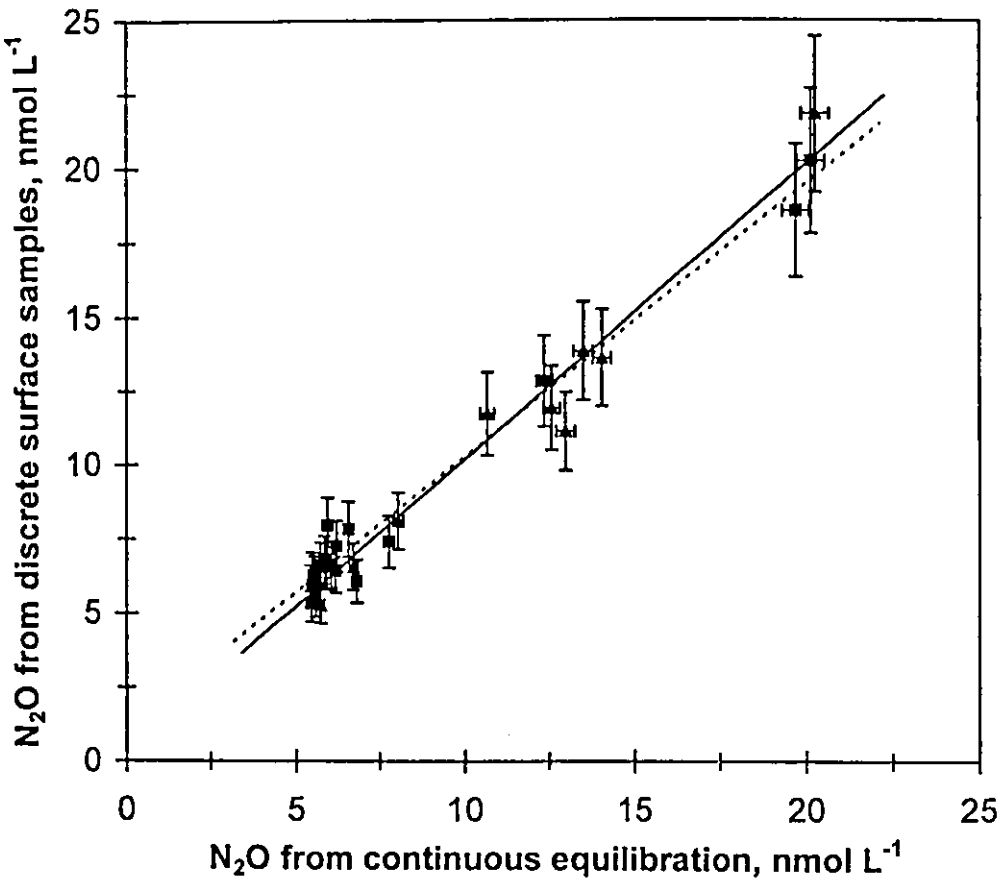

Figure 3. Comparison of N_2O surface concentrations measured by the discrete sampling method as described in the text (water depths 5–20 m) and a continuous equilibration system (pumping from 7 m water depth) [*Bange at al.*, 1996]. Solid squares represent data from M32/3 and M32/3. The dashed line is the linear regression for the data set from M32/3 and M32/5 ($y = 0.924x + 1.08$, $r^2 = 0.98$, $n = 12$). Solid triangles represent data from SO119 and SO120. The solid line is the linear regression for the data set from SO119 and SO120 ($y = 0.997x + 0.26$, $r^2 = 0.97$, $n = 16$).

hours. Equilibrium concentrations of dissolved N_2O and O_2 were calculated with the equations of *Weiss and Price* [1980] and *Weiss* [1970], respectively. We used an atmospheric N_2O dry mole fraction of 309 ppb [*Bange et al.*, 1996] and 311 ppb (H. W. Bange et al., unpublished data, 2000) for the calculation of the N_2O equilibrium concentrations in 1995 and 1997, respectively. Potential seawater temperatures were calculated with the equations listed in *Siedler and Peters* [1986]. Salinity, in situ water temperature, and nutrient data were taken from data compilations of measurements performed simultaneously to the water sampling (F. Pollehne et al., unpublished data, 1996; B. Zeitzschel et al., unpublished data, 1996, 1998; V. Ittekkot et al., unpublished data, 1998). All data presented are available from the German JGOFS Data Management Office (http://www.ifm.uni-kiel.de/pl/dataman/dmpag1.html).

4. Results and Discussion

Some selected stations (Table 1) were grouped into a north–south (NS) transect from 24.7°N to 10°N along 65°E during the intermonsoon period and into a northwest–southeast (NWSE) transect from 18.5°N, 56.5°E to 14.5°N, 65°E during the SW monsoon. (These transects are partly identical with the U.S. JGOFS standard cruise track in the Arabian Sea [*Smith*, 1998].) Depth profiles of the dissolved N_2O and O_2 along the NS and NWSE transects are shown in Figures 4 and 5, respectively.

4.1. NS Transect

The shapes of the N_2O profiles from the NS transect from the shelf break off Pakistan (24.7°N) to the central Arabian Sea (14.5°N) are clearly associated with the extremely low O_2 concentrations ($0 < O_2 < 20$ μmol L^{-1} or expressed in volumetric units $0 < O_2 < 0.25$ mL L^{-1}) in the OMZ in the Arabian Sea (Figures 4b–4d). These profiles have a characteristic double-peak structure. In the upper water column a marked increase in the N_2O concentrations from 5–6 nmol L^{-1} in the surface layer to about 25–55 nmol L^{-1} at 150 m depth forms the first sharp N_2O peak. This peak is followed by a pronounced depletion of dissolved N_2O at about 200–500 m water depth; even undersaturations with concentrations lower than 5 nmol L^{-1} were observed. This depletion of dissolved N_2O is most pronounced between 20° and 18°N (Figures 4c–4d). N_2O concentrations increase again up to 60 nmol L^{-1} at about 800 m to form the second N_2O peak (Figures 4c–4e), followed by a decrease with depth to values of 15 nmol L^{-1} in the deep and bottom waters. The profiles south of 10°N, which are outside the zone of extreme O_2 depletion in the OMZ as indicated by comparably higher O_2 concentrations (Figure 4f), generally showed a

Table 1. List of the Selected Stations Where N_2O Measurements Were Performed During the German JGOFS – Arabian Sea Process Study in 1995 and 1997[a]

Station	Position	Date	Cruise
	NS Transect		
EPT	27.7°N, 65.8°N	May 1997	SO119
NAST	20.0°N, 65.8°E	May 1997	SO119
D1[b]	18.0°N, 65.0°E	May 1995	M32/3
CAST	14.5°N, 65.0°E	May 1997	SO119
SAST/D2	10.0°N, 65.0°E	May 1997	SO119
	NWSE Transect		
CAST	14.5°N, 65.0°E	July 1995	M32/5
T2	16.0°N, 62.0°E	July 1997	SO120
T3	17.5°N, 59.1°E	July 1997	SO120
T4	18.1°N, 58.0°E	August 1995	M32/5
T5	17.3°N, 57.9°E	July 1997	SO120
T6	17.8°N, 57.6°E	July 1997	SO120
Shelf	18.5°N, 56.5°E	June 1997	SO120

[a] See also Figure 1.
[b] Measurements restricted for the depth range 0–2000 m. The profile is a composite of four casts from various depth ranges.

completely different shape of the profile. An accumulation of N_2O from the surface (up to 37 nmol L^{-1} between 500 and 1000 m) is followed by a decrease with depth (15 nmol L^{-1} in the deep and bottom waters) (Figure 4f).

Previous measurements of the depth distribution of N_2O in the Arabian Sea were performed in the central and western regions by *Law and Owens* [1990] (September–October 1986) and *Upstill-Goddard et al.* [1999], and in the central and eastern regions by *Naqvi and Noronha* [1991] (December 1988), *Lal et al.* [1996], and *Patra et al.* [1999] (April–May 1994, February–March 1995, July–August 1995). There is good agreement between the shapes of previously reported N_2O profiles and those presented in Figure 4. Both *Lal et al.* [1996] and *Naqvi and Noronha* [1991] also describe almost identical double-peak structures for stations in the northern central Arabian Sea (compare Figures 4b and 4c). However, there might be slight trends for the reported concentrations. Our maximum concentration along the NS transect was 58 nmol L^{-1} for the second N_2O peak at 18°N, 65°E (Figure 4d), whereas *Naqvi and Noronha* [1991] and *Patra et al.* [1999] observed concentrations up to 80 nmol L^{-1} for the second N_2O peak at 21.8°N, 64.6°E and 18°N, 67°E. *Law and Owens'* [1990] maximum N_2O concentration along their NS transect along 67°E was 59 nmol L^{-1} at 14.5°N, 66.9°E. Undersaturations in the core of the OMZ (compare Figures 3c and 3d) were also observed by *Law and Owens* [1990] and *Naqvi and Noronha* [1991] but not by *Patra et al.* [1999].

Comparison of the results from the various studies suggests that the distribution of N_2O in the central Arabian Sea is only partly known. Differences in the observed N_2O concentrations might result from the different spatial data coverage and/or temporal (i.e., seasonal and interannual) variability in the Arabian Sea (see also the discussion of the ΔN_2O–AOU relationships below). Profiles of N_2O typically show an accumulation in the OMZ of oceanic subsurface layers, most probably owing to nitrification [*Dore et al.*, 1998]. However, when extreme O_2 gradients at the boundaries of the OMZ exist, conditions become ideal for enhanced N_2O production by nitrification at low O_2 concentrations as well as for N_2O production by denitrification. Thus the first N_2O peak observed at approximately 150 m in the central Arabian Sea might result from a coupling of both [*Naqvi et al.*, 1998; *Naqvi and Noronha*, 1991]. Recent dual-isotope measurements indicate that denitrification might be the major production pathway for the second N_2O peak at the lower boundary of the OMZ in approximately 800–1000 m depth [*Naqvi et al.*, 1998]. The pronounced N_2O depletion in the core of the OMZ results from N_2O reduction to N_2 during intense denitrification at extremely low O_2 concentrations [*Naqvi and Noronha*, 1991]. Thus we conclude that the N_2O profiles at the NS transect reflect typical vertical distributions within (>10°N, Figures 4b–4e) and outside (<10°N, Figure 4f) the denitrification zone. Our results are in agreement with previously published ideas about the dominating N_2O production and consumption processes in the central Arabian Sea.

4.2. NWSE Transect

The distribution of dissolved N_2O on the NWSE transect appears to be more complex. The shape of the profile from station CAST (Figure 5b) indicates the characteristic double-peak shape for profiles from the northern part of the NS transect. Going further northwest to station T2 at 16°N, 62°E (Figure 5c), the typical upper N_2O peak at about 150–200 m was only weakly developed. However, following the transect further to the coast, the double-peak structure was again visible at stations T3, T4, and T5 (Figures 5d–5f). The N_2O profile at the shelf break off Oman (Figure 5g) is similar to the one observed at the shelf break off Pakistan (Figure 5f); however, the concentrations are higher at the coast off Oman. The highest concentrations (up to 64 nmol L^{-1}) during the German JGOFS cruises were observed at 700 m depth at station T4 (18°N, 58°E) (Figure 5e). Over the shelf with water depths of about 80 m, dissolved N_2O accumulates from 20 nmol L^{-1} in the surface layer to 40 nmol L^{-1} in the bottom layer (Figure 5h). The results of *Law and Owens* [1990] and *Upstill-Goddard et al.* [1999] also showed high N_2O concentrations (up to ΔN_2O of 104 nmol L^{-1} [*Law and Owens*, 1990]) in the western Arabian Sea, which are as high as those from the central Arabian Sea. Recently published N_2O profiles by *Upstill-Goddard et al.* [1999] from a similar NWSE transect, which was located north of the German JGOFS transect, are in general agreement with ours.

The temporal development of the distributions of N_2O and O_2 on the NWSE transect during three cruises in July–August 1995, May 1997 and June–July 1997 is shown in Plate 1. Using data from two different years may introduce a bias owing to a possible interannual variability; however, since we will focus on a qualitative rather than a quantitative interpretation our approach might be reasonable. The O_2 depleted layer (<20 μmol L^{-1}) extends to the shelf of the Arabian Peninsula, showing only a modest temporal variation (Plates 1d–1f). In contrast, the N_2O concentrations show a considerable seasonal signal (Plates 1a–1c). While during May 1997 (Plate 1a), an N_2O plume originating from the central Arabian Sea is visible, the situation during the early stage of the SW Monsoon (June–July 1997, Plate 1b) and during the fully developed SW Monsoon (July–August 1995, Plate 1c) is completely different. During the SW Monsoon the development of a strong local source of N_2O near the shelf break at 700 m depth (corresponding to a potential density (σ_θ) of 27.3) is obvious. Either an in situ source (e.g., denitrification) or a seasonally occurring boundary current transporting N_2O-enriched water might be the reason for the observed enhanced N_2O concentrations:

1. Water mass analysis indicated that Red Sea water with a

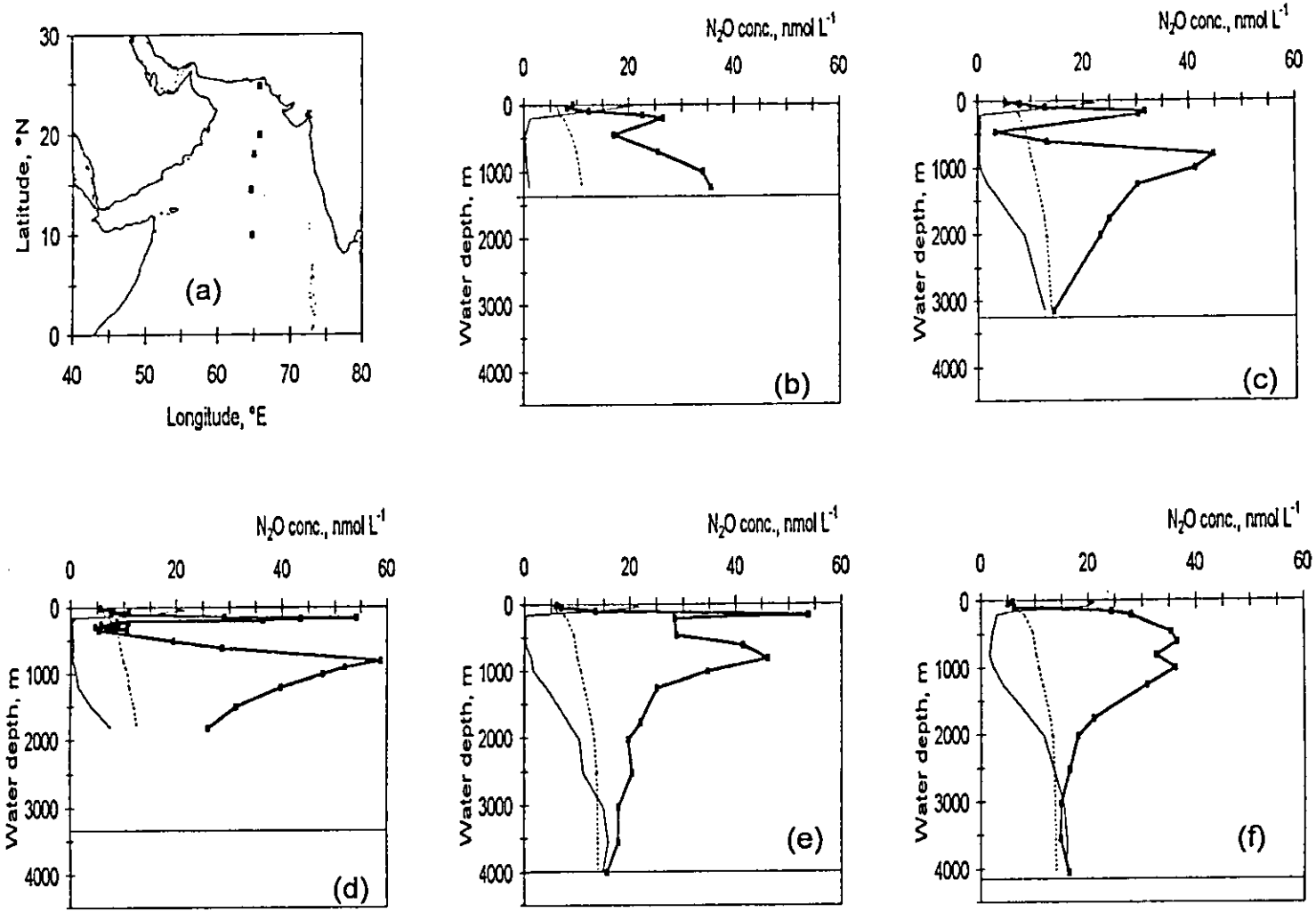

Figure 4. Concentrations of N_2O (in nmol L^{-1}) and O_2 (in 10^{-1} μmol L^{-1}) along the NS transect along 65°E (thick line, dissolved N_2O; dashed line, calculated equilibrium N_2O; thin line, O_2 concentration ; the horizontal line indicates sea bottom). (a) Map with station locations, (b) EPT, (c) NAST, (d) D1, (e) CAST, and (f) SAST. For an overview of the station positions and dates of measurements, see Table 1.

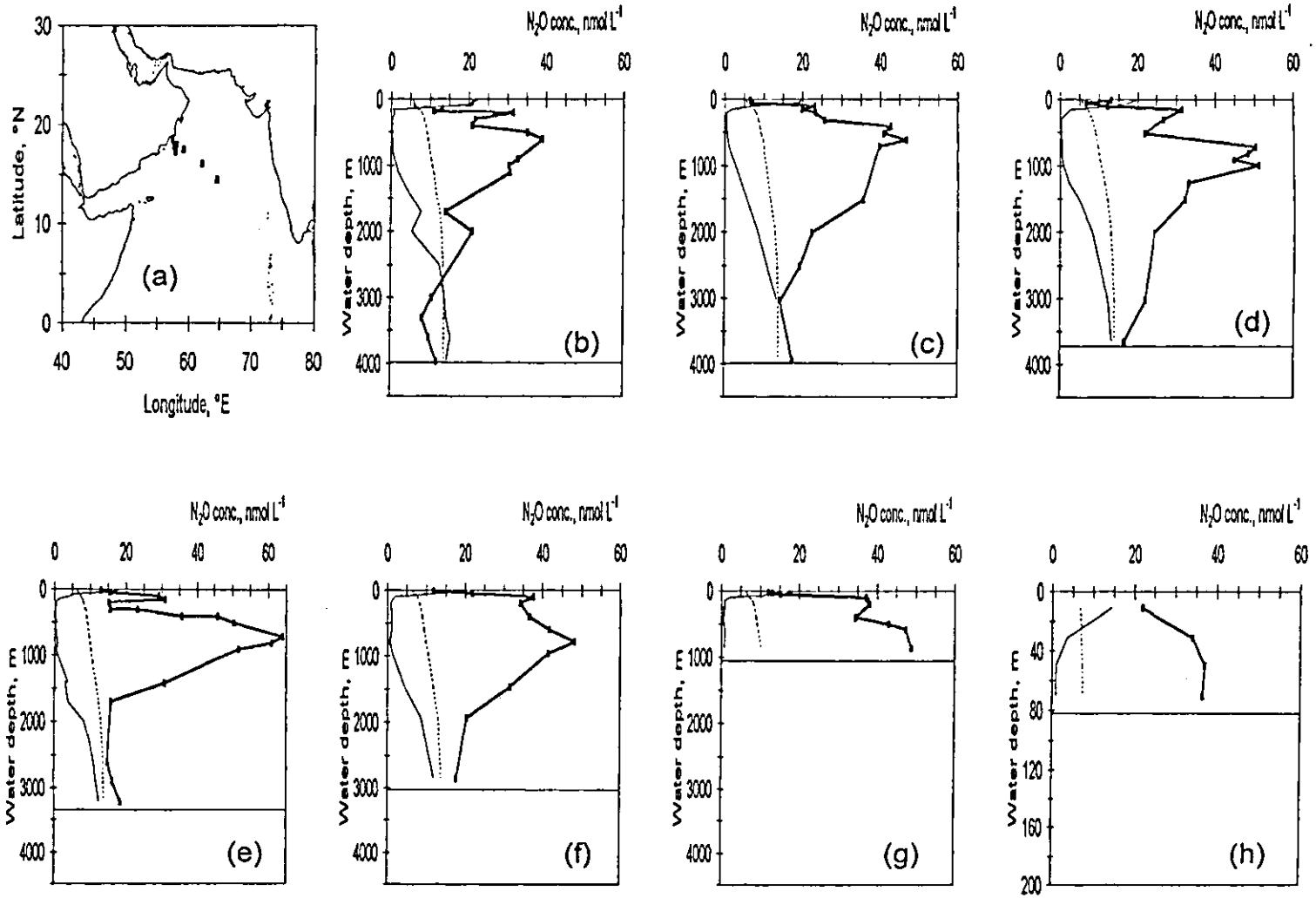

Figure 5. Concentrations of N_2O (in nmol L^{-1}) and O_2 (in 10^{-1} μmol L^{-1}) along the NWSE transect (thick line, dissolved N_2O; dashed line, calculated equilibrium N_2O; thin line, O_2 concentration; horizontal line indicates sea bottom). (a) Map with station locations, (b) CAST, (c) T2, (d) T3, (e) T4, (f) T5, (g) T6, and (h) shelf. For an overview of the station positions and dates of measurements, see Table 1.

core σ_θ of 27.2 at 600–700 m was not detectable, probably because its inflow to the Arabian Sea is usually blocked during the SW Monsoon [*Morrison et al.*, 1998; *Shenoi et al.*, 1993]. Instead, we can speculate that an inflow of N_2O-enriched water from the Somali Basin [*De Wilde and Helder*, 1997] through the Socotra Passage might occur [*Schott et al.*, 1997; *You*, 1997].

2. The O_2 concentrations in the OMZ on the NWSE transect were depleted in O_2, comparable to those in the central Arabian Sea and favoring conditions for denitrification. However, the OMZ of the western Arabian Sea is not characterized by the permanent secondary nitrite (NO_2^-) maximum [*Morrison et al.*, 1998], which is often used as an indicator for the occurrence of denitrification [*Naqvi*, 1991].

Interestingly, *Farrenkopf et al.* [1997] found extremely high subsurface maxima of iodide (I^-) near the Arabian Peninsula (around 17°N, 57°E) at 600–800 m depth (σ_θ = 27.3–27.5). They concluded that, within the OMZ, organic matter decomposition via bacterial reduction of iodate (IO_3^-) to I^- could be as important as denitrification. A possible decomposition of organic matter via oxidation by IO_3^- to yield N_2O might be written as follows:

$$81.3\ IO_3^- + (CH_2O)_{106}(NH_3)_{16}H_3PO_4$$

$$\rightarrow 81.3\ I^- + 106\ CO_2 + 8\ N_2O + 130\ H_2O + H_3PO_4.$$

Following the concept of *Froelich et al.* [1979] ($\Delta G°$ data were taken from *Stumm and Morgan* [1996]), we calculated for the reaction given above a $\Delta G° = -2712$ kJ per mole glucose, which is comparable with $\Delta G°$ values given for the oxidation of organic matter by IO_3^- yielding NH_3 (–2605 kJ mol^{-1}), HNO_3 (–2804 kJ mol^{-1}), or N_2 (–3047 kJ mol^{-1}) [*Farrenkopf et al.*, 1997]. Despite the fact that the I^- data from *Farrenkopf et al.* [1997] are from the transition from the SW monsoon to the intermonsoon (October 1992) and might be therefore not representative for the peak of SW monsoon (July–August), we speculate that the observed enhanced N_2O concentrations might be coupled to a bacterially mediated IO_3^-/I^- cycle. The mean decomposition of particulate organic matter between 505 and 809 m water depth at U.S. JGOFS station S2 (18.1°N, 58°E) measured during the spring intermonsoon and SW monsoon 1995 was about 1.5 μmol C m^3 d^{-1} [*Lee et al.*, 1998]. Converting this with the molar ratio of N_2O to organic carbon of 8/106 (see equation above) yields a theoretical N_2O production of 0.113 μmol m^3 d^{-1}. From our measurements we estimated an accumulation of N_2O between 500 and 800 m of about 20 nmol L^{-1} from May to August (Plates 1a–1c). Assuming that this accumulation is representative for the time interval of the organic flux measurements (204 days), we estimated the N_2O production to be about 0.098 μmol m^3 d^{-1}. Thus the observed N_2O accumulation is slightly lower than the theoretically predicted N_2O production, indicating that the decomposition of organic carbon via the IO_3^-/I^- mechanism might contribute to the N_2O production. However, it is very unlikely that almost all organic carbon is converted to N_2O. More likely a mixture of N_2O and more energetically favored products (e.g., N_2) will occur. We conclude that there is not yet a satisfactory explanation for the local source of N_2O at the shelf break in the western Arabian Sea; neither an inflow event nor enhanced N_2O production via denitrification or other mechanisms have been substantiated.

4.3. ΔN_2O–AOU Relationship

As mentioned in the introduction, a positive correlation between ΔN_2O and AOU, indicating N_2O formation via

Table 2. ΔN_2O–AOU ($\Delta N_2O = m\text{AOU} + n\text{AOU}^2 + b$) Relationships for the Arabian Sea[a]

Arabian Sea Region	Date	*m*, *n*	*b*	r^2 / Number of Samples	Remarks	References
Central/west	Sept.–Oct. 1986	0.033, 0	5.5	(both significant at the 1% level)	AOU <197	*Law and Owens* [1990]
		0.310, 0	–49.4		AOU >197	
Central/east	Dec. 1988	(0.1066 + 0.00455 *t*), 0	3.2	not given	O_2 > 0.25 mL L^{-1}, *t* is temperature in °C	*Naqvi and Noronha* [1991]
Somali Basin, Gulf of Aden	July–Aug. 1992	0.172, 0	–1.26	0.92 / 51	intermediate waters <2000 m	*De Wilde and Helder* [1997]
Central/east	April–May 1994	0.1482, 0	1.03	0.71 / 31	water depths <1000 m and 0<AOU<200	*Patra et al.* [1999]
	Feb.–March 1995	0.1553, 0	3.05	0.65 / 59		
	July–Aug. 1995	0.1464, 0	1.17	0.90 / 30		
Central/west	Aug.–Oct. 1994	0.049[b], 0.0004	0.83	not given	water depth <500 m	*Upstill-Goddard et al.* [1999]
		–1.58, 0.0043	151.3		water depth >500 m	
	Nov.–Dec. 1994	0.007[b], 0.0006	0.25		only valid above OMZ	
Central/west	May 1995	0.1256, 0	1.31	0.81 / 16	water depth <150 m	this study
	July–Aug. 1995	0.0935, 0	2.12	0.73 / 41		
	May 1997	0.0799, 0	2.71	0.66 / 33		
	June–July 1997	0.1056, 0	1.84	0.86 / 45		
Central/west	May 1995	0.0952, 0	2.00	0.70 / 46	water depth <2000 m and O_2>0.25 mL L^{-1}	this study
	July–Aug. 1995	0.0609, 0	1.61	0.48 / 39		
	May 1997	0.0700, 0	2.55	0.63 / 63		
	June–July 1997	0.0865, 0	3.27	0.70 / 51		
Central/west	July–Aug. 1995	0.0910, 0	–15.0	0.14 / 46	water depth >2000 m	this study
	May 1997	0.0672, 0	–11.0	0.25 / 15		
	June–July 1997	0.3363, 0	–68.4	0.55 / 5		

[a] ΔN_2O in nmol L^{-1} and AOU in μmol L^{-1}. *r* stands for correlation coefficient.
[b] Original values (–0.049, –0.007) were reported erroneously (R. C. Upstill-Goddard, personal communication, 2000).

Table 3. Rates of N_2O Production in the OMZ ($O_2 < 0.25$ mL L^{-1}) of the Central Arabian Sea

	Integrated ΔN_2O,[a] Tg N_2O	Range of N_2O Production Using 1- / 10-Year Ventilation Time,[b] Tg N_2O yr^{-1}
May 1995	2.5	2.5 / 0.25
July–Aug. 1995	1.9 ± 0.5	1.9 / 0.19
May 1997	1.6 ± 0.3	1.6 / 0.16
June–July 1997	2.4 ± 0.5	2.4 / 0.24
Average	2.1	2.1 / 0.21

[a] Calculated as mean vertical integrated ΔN_2O times area of the OMZ affected by denitrification (1.95×10^{12} m^2, [*Naqvi*, 1991]).
[b] One-year ventilation time according to *Naqvi and Shailaja* [1993]; 10-year ventilation time according to *Olson et al.* [1993].

nitrification, is found in a variety of oceanic environments. An overview of previously published ΔN_2O–AOU relationships for the Arabian Sea together with those calculated on the basis of our N_2O data is presented in Table 2. In a recent study, *Upstill-Goddard et al.* [1999] showed that a second-order polynomial gave the best statistical fit to their data from the western and central Arabian Sea. We found considerable differences between the various ΔN_2O–AOU relationships. Even for data from the same year and season (e.g., July–August 1995, Table 2), the values differ considerably and could be explained only by a different spatial data coverage. Seasonal or interannual trends might be obscured in the data for various reasons, such as the difference in the yield of N_2O production owing to the composition and the amount of organic matter to be oxidized or to an additional N_2O source, e.g., assimilatory nitrate reduction [*Elkins et al.*, 1978]. Assimilatory nitrate reduction ($NO_3^- \rightarrow NO_2^- \rightarrow NH_4^+$) was proposed by some authors as a possible source of N_2O in nitrate-enriched waters, e.g., in upwelling regions; however, this hypothesis has never been proved [*Oudot et al.*, 1990; *Pierotti and Rasmussen*, 1980]. Most ΔN_2O–AOU relationships for the Arabian Sea are based on data sets excluding data affected by denitrification in the OMZ (i.e., $O_2 < 0.25$ mL L^{-1}). This indicates a shift in the pathways of N_2O production from nitrification to denitrification in the OMZ of the central Arabian Sea, which can not be represented by the common ΔN_2O–AOU relationship. The situation is even more complicated because N_2O can also be consumed during denitrification, leading to low N_2O values in the core of the OMZ in the central Arabian Sea. Despite the fact that the ΔN_2O–AOU relationships for deep water (>2000 m) are statistically not significant, they all show similar positive trends comparable to those observed for the upper ocean (Table 2). Thus we can speculate that nitrification is still the main pathway for N_2O production, but it might be balanced by subsequent N_2O reduction via denitrification as proposed by *Kim and Craig* [1990].

4.4. N_2O Budget for the Arabian Sea

To obtain knowledge of the N_2O production in the Arabian Sea, we estimated N_2O production for the OMZ affected by denitrification ($O_2 < 0.25$ mL L^{-1}) (Table 3). For this purpose we calculated the N_2O column abundances, defined as the vertically integrated profile of ΔN_2O. With the mean ΔN_2O calculated for each leg, it is possible to estimate the net N_2O production within the OMZ, assuming an area for the denitrification of 1.95×10^{12} m^2 [*Naqvi*, 1991] and a ventilation time of 1–10 years [*Naqvi and Shailaja*, 1993; *Olson et al.*, 1993]. The applied OMZ area affected by denitrification is 30% higher than the revised value of 1.37×10^{12} m^2 recently proposed by *Naqvi* [1991]. However, using a larger area appears more appropriate to account for the area distribution of the N_2O production processes (see discussion of the NWSE transect above). Moreover, the considerable range in the OMZ ventilation times (1–11 years) reported in the literature (for a discussion see *Naqvi* [1994]) introduces a more significant uncertainty.

Annual N_2O production in the OMZ was previously calculated to be 0.4 Tg by *Mantoura et al.* [1993] on the basis of the 1986 data set of *Law and Owens* [1990]. However, *Mantoura et al.* [1993] used a 10-year ventilation time; thus their value can be considered as a lower limit. Applying a ventilation time of 1 year scales their value up to 4 Tg N_2O yr^{-1}. A comparison with our results (0.2–2 Tg N_2O yr^{-1}, Table 3) reveals that the results are in reasonable agreement, despite possible biases due to seasonal and interannual variabilities. We calculated a mean N_2O production in the OMZ of 1.1 Tg yr^{-1} (i.e., 0.7 Tg N yr^{-1}) which represents about 2% of the mean pelagic denitrification of about 33 Tg N yr^{-1} [*Bange et al.*, 2000].

Table 4. N_2O Budget for the Arabian Sea North of 6°N

	Mean, Tg N_2O yr^{-1}	Range, Tg N_2O yr^{-1}	References
	Sources		
Net N_2O production in the OMZ	1.7	0.2–2	this study, Table 3
		0.4–4[a]	*Mantoura et al.* [1993]
N_2O input by Red Sea and Persian Gulf	0.03[b]	0–0.06[c]	
N_2O input across 6°N	0.1	0–0.2[c]	this study, Figure 6
	Sinks		
Loss to the atmosphere	0.4	0.2–0.6	*Bange et al.* [2000]
Loss in eastern margin sediments	1.3	not given	*Naqvi and Noronha* [1991]
Sources – sinks	0.13		

[a] Original value of 0.25 Tg N yr^{-1} (0.4 Tg N_2O yr^{-1}) scaled to an OMZ ventilation time of 3 years.
[b] *Rhein et al.* [1997] estimated inflows of 0.3×10^6 m^3 s^{-1} for Red Sea ($\sigma_\theta = 27.2$) and 0.18×10^6 m^3 s^{-1} for the Persian Gulf ($\sigma_\theta = 26.6$) waters. Associated N_2O concentrations were 60 nmol L^{-1}, estimated from *De Wilde and Helder*'s [1997] station 276-04 (400–700 m) in the Gulf of Aden in August 1992, and 21 nmol L^{-1} calculated from *Law and Owens*' [1990] northernmost station (station 11, 24.8°N, 57.2°E, September 1986) in the Gulf of Oman.
[c] We assumed an error of ±100% owing to the implicit considerable uncertainties of our estimate.

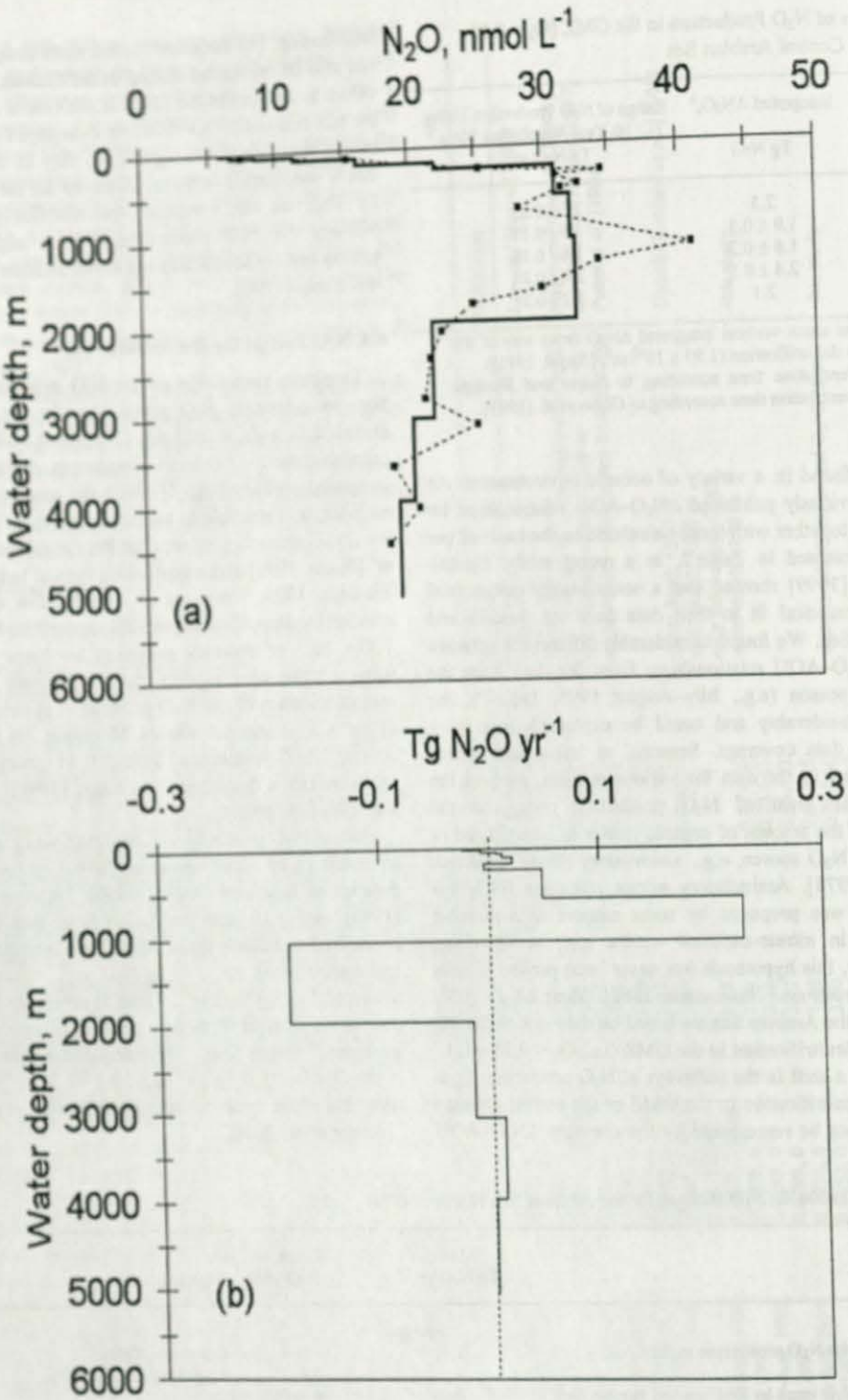

Figure 6. N_2O flux into and out of the Arabian Sea along 6°N: (a) N_2O concentrations (dashed line, N_2O profile at 6°N, 65°E in July 1995 during cruise M32/5; solid line, calculated standard level mean N_2O profile). (b) Resulting mean annual N_2O flux for the layers of the GCM (negative values represent outflows and positive values represent inflows into the Arabian Sea across 6°N).

An overall N_2O budget for the Arabian Sea based on the data presented here and found in the literature is presented in Table 4. In order to obtain consistent N_2O flux estimates we adopted the approach used by *Bange et al.* [2000] for a revision of the nitrogen fluxes of the Arabian Sea. The southern boundary of the Arabian Sea was set to 6°N spanning a line from the Somali coast to the southern tip of Sri Lanka (for details see *Bange et al.* [2000]).

In order to assess the mean annual N_2O exchange across the southern boundary of the Arabian Sea at 6°N, monthly values for

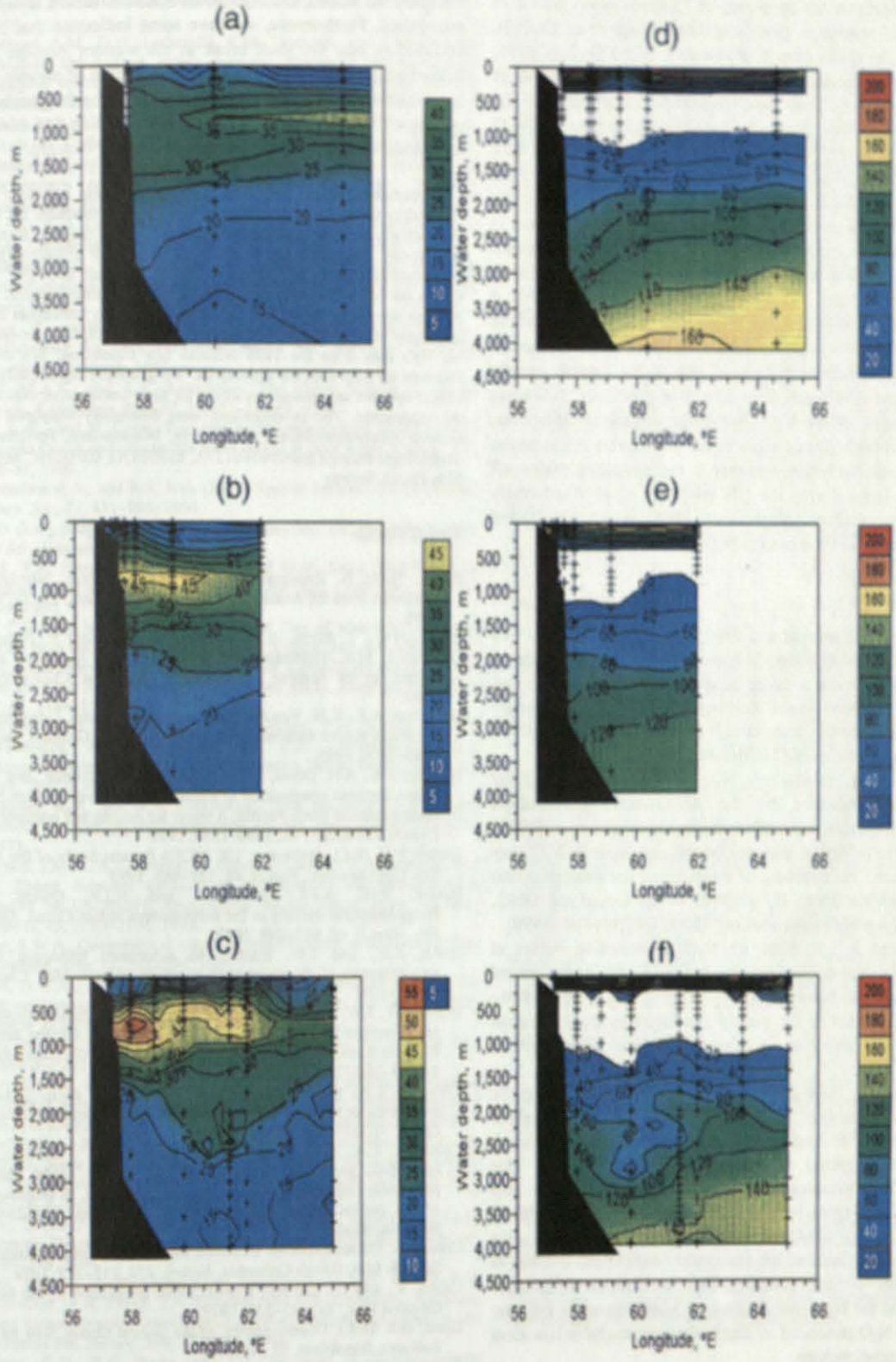

Plate 1. Concentrations of N_2O (in nmol L^{-1}) and O_2 (in μmol L^{-1}) along the NWSE transect in the western Arabian Sea. (left), N_2O: (a) May 1997, (b) June–July 1997, and (c) July–August 1995. (right), O_2 (white areas indicate concentrations below 20 μmol L^{-1}): (d) May 1997, (e) June–July 1997, and (f) July–August 1995.

the water transport across 6°N were extracted from a general circulation model (GCM) consisting of 13 depth layers with a 1° x 1° horizontal resolution (for details see *Bange et al.* [2000]). N_2O values were taken from a profile at 6°N, 65°E (July 1995, M32/5). The N_2O concentrations were scaled to the grid points of the GCM (Figure 6a). Then we calculated for each grid point the mean annual N_2O flux. Summing the fluxes yields the net N_2O fluxes for each layer (Figure 6b). The resulting overall net flux sums up to an annual input into the Arabian Sea of about 0.1 Tg N_2O. The major sink for N_2O in the Arabian Sea is its consumption in eastern margin sediments and the major source is the N_2O production in the OMZ. Inputs by Red Sea and Persian Gulf waters as well as advective input from the south appear to play only a minor role. The budget from the data in Table 4 seems to be reasonably balanced. However, the magnitude of the sedimentary N_2O loss is under debate. As discussed by *Naqvi et al.* [1992], the observed N_2O gradients at the eastern margin sediments could also result from advective processes, indicating an overestimation of the N_2O sink in the sediments. Moreover, our estimate of the N_2O emissions to the atmosphere might be too low since recent N_2O measurements in the upwelling region off southwestern India during the SW monsoon showed extremely high N_2O concentrations [*Naqvi et al.*, 1998], which may lead to an upward revision of the current N_2O emission estimates.

5. Conclusions

A compilation of sources and sinks of N_2O in the Arabian Sea suggested that the N_2O budget is reasonably balanced. In view of our results, we propose a rough scheme of N_2O production and consumption pathways in the Arabian Sea. Our scheme consists of four compartments that could explain the characteristic double-peak structure of N_2O in the Arabian Sea:

Compartment 1, 0–150 m: N_2O is mainly produced by nitrification as indicated by the ΔN_2O–AOU relationships (Table 2). However, isotope data measured by *Naqvi et al.* [1998] revealed that nitrification may not be the only source. N_2O may also be produced via coupling of nitrification and denitrification associated with the steep O_2 gradient at the top of the OMZ, forming the sharp N_2O peak at about 150 m [*Naqvi et al.*, 1998].

Compartment 2, 150–1000 m: N_2O consumption occurs at 300–500 m (i.e., the denitrifying core of the OMZ) of the central Arabian Sea. At the lower boundary of the OMZ at about 800–1000 m, N_2O seems to be mainly produced by denitrification when the O_2 concentrations are increasing again [*Naqvi et al.*, 1998].

Compartment 3, 1000–2000 m: In the central Arabian Sea the denitrification signal (i.e., $\delta^{15}N$ of NO_3^-) is assumed to be mixed down to a depth of at least 1500 m owing to ventilation processes such as cross-isopycnal mixing [*Brandes et al.*, 1998]. This implies that N_2O produced at the bottom of the OMZ is also mixed down by cross-isopycnal mixing, forming the broad second N_2O peak. ΔN_2O–AOU relationships (excluding data affected by denitrification) are reasonably valid from 0–2000 m (Table 2) Thus we can conclude that nitrification contributes significantly to the N_2O production throughout the water column; however, the N_2O produced by denitrification results in less clear ΔN_2O–AOU relationships.

Compartment 4, below 2000 m: No statistically significant ΔN_2O–AOU relationship was found. N_2O produced by nitrification may be reduced subsequently by denitrification [*Kim and Craig*, 1990].

This scheme may also be valid for the western Arabian Sea; however, owing to the seasonal variability of the complex hydrographic situation (e.g., coastal upwelling, inflow of marginal sea water), the N_2O double-peak structure is not well-established. Furthermore, we have some indication that N_2O at 600–800 m near the shelf break in the western Arabian Sea is formed via a different process such as oxidation of organic matter by reduction of IO_3^- to I^-, indicating that the biogeochemical cycling of N_2O in the central and western Arabian Sea during the SW Monsoon is more complex than previously thought.

Acknowledgments. We thank G. Schebeske and our glass blower B. Beickler for their invaluable assistance. We acknowledge the help of many other colleagues and the officers and crews of the R/V *Meteor* and R/V *Sonne*. Thanks are due to the chief scientists F. Pollehne (M32/3), B. Zeitzschel (M32/5 and SO120), and V. Ittekkot (SO119). Special thanks are due to the team of the R/V *Sonne* scientific-technical service for their support on board. We are indebted to many colleagues for their generosity in sharing data. We especially thank C. S. Law for providing his N_2O data from the 1986 Arabian Sea expedition. We thank C. Strametz for help with the manuscript. We gratefully acknowledge J. M. Lobert and two anonymous reviewers for their constructive criticisms of the manuscript. The investigations were financially supported by the German Bundesministerium für Bildung, Wissenschaft, Forschung und Technologie through grants 03F0137A, 03F0183G, 03F0241C and by the Max Planck Society.

References

Bange, H.W., S. Rapsomanikis, and M.O. Andreae, Nitrous oxide emissions from the Arabian Sea, *Geophys. Res. Lett.*, *23*, 3175–3178, 1996.

Bange, H.W., T. Rixen, A.M. Johansen, R.L. Siefert, R. Ramesh, V. Ittekkot, M.R. Hoffmann, and M.O. Andreae, A revised nitrogen budget for the Arabian Sea, *Global Biogeochem. Cycles*, in press, 2000.

Bouwman, A.F., K.W. Van der Hoek, and J.G.J. Olivier, Uncertainties in the global source distribution of nitrous oxide, *J. Geophys. Res.*, *100*, 2785–2800, 1995.

Brandes, J.A., A.H. Devol, T. Yoshinari, D.A. Jayakumar, and S.W.A. Naqvi, Isotopic composition of nitrate in the central Arabian Sea and eastern tropical North Pacific: A tracer for mixing and nitrogen cycles, *Limnol. Oceanogr.*, *43*, 1680–1689, 1998.

Burkill, P.H. (Ed.), Arabesque, UK JGOFS Process Study of the Arabian Sea, *Deep Sea Res., Part II*, *46*, 529–863, 1999.

Burkill, P.H., R.F.C. Mantoura, and N.J.P. Owens (Eds.), Biogeochemical cycling in the northwestern Indian Ocean, *Deep Sea Res., Part II*, *40*, 643–849, 1993.

Butler, J.H., and J.W. Elkins, An automated technique for the measurements of dissolved N_2O in natural waters, *Mar. Chem.*, *34*, 47–61, 1991.

Butler, J.H., J.W. Elkins, T.M. Thompson, and K.B. Egan, Tropospheric and dissolved N_2O of the West Pacific and Indian Oceans during the El Niño Southern Oscillation event of 1987, *J. Geophys. Res.*, *94*, 14,865–14,877, 1989.

Codispoti, L.A., and J.P. Christensen, Nitrification, denitrification and nitrous oxide cycling in the Eastern Tropical South Pacific, *Mar. Chem.*, *16*, 277–300, 1985.

Codispoti, L.A., J.W. Elkins, T. Yoshinari, G.E. Friederich, C.M. Sakamoto, and T.T. Packard, On the nitrous oxide flux from productive regions that contain low oxygen waters, in *Oceanography of the Indian Ocean*, edited by B.N. Desai, pp. 271–284, A.A. Balkema, Brookfield, Vt., 1992.

Cohen, Y., Consumption of dissolved nitrous oxide in an anoxic basin, Saanich Inlet, British Columbia, *Nature*, *272*, 235–237, 1978.

Cohen, Y., and L.I. Gordon, Nitrous oxide production in the ocean, *J. Geophys. Res.*, *84*, 347–353, 1979.

Desai, B.N. (Ed.), *Oceanography of the Indian Ocean*, 780 pp., A.A. Balkema, Brookfield, Vt., 1992.

De Wilde, H.P.J., and W. Helder, Nitrous oxide in the Somali Basin: The role of upwelling, *Deep Sea Res., Part II*, *44*, 1319–1340, 1997.

Dore, J.E., B.N. Popp, D.M. Karl, and F.J. Sansone, A large source of atmospheric nitrous oxide from subtropical North Pacific surface waters, *Nature*, *396*, 63–66, 1998.

Elkins, J.W., Determination of dissolved nitrous oxide in aquatic systems by gas chromatography using electron capture detection and multi phase equilibration, *Anal. Chem.*, *52*, 263–267, 1980.

Elkins, J.W., S.C. Wofsy, M.B. McElroy, C.E. Kolb, and W.A. Kaplan, Aquatic sources and sinks for nitrous oxide, *Nature, 275*, 602–606, 1978.

Farrenkopf, A.M., G.W. Luther III, V.W. Truesdale, and C.H. Van der Weijden, Sub-surface iodide maxima: Evidence for biologically catalyzed redox cycling in the Arabian Sea OMZ during the SW monsoon, *Deep Sea Res., Part II, 44*, 1391–1409, 1997.

Froelich, P.N., G.P. Klinkhammer, M.L. Bender, N.A. Luedtke, G.R. Heath, D. Cullen, P. Dauphin, D. Hammond, B. Hartman, and V. Maynard, Early oxidation of organic matter in pelagic sediments of the eastern equatorial Atlantic: Suboxic diagenesis, *Geochim. Cosmochim. Acta, 43*, 1075–1090, 1979.

Gage, J.D., L.A. Levin, and G.A. Wolff (Eds.), Benthic processes in the deep Arabian Sea, *Deep Sea Res., Part II, 47*, 1–375, 2000.

Hashimoto, L.K., W.A. Kaplan, S.C. Wofsy, and M.B. McElroy, Transformation of fixed nitrogen and N_2O in the Cariaco Trench, *Deep Sea Res., Ser. A, 30*, 575–590, 1983.

Ittekkot, V., and R.R. Nair (Eds.), *Monsoon Biogeochemistry*, 200 pp., Selbstverlag des Geol.-Paläontologischen Inst. der Univ. Hamburg, Hamburg, Germany, 1993.

Khalil, M.A.K., and R.A. Rasmussen, The global sources of nitrous oxide, *J. Geophys. Res., 97*, 14,651–14,660, 1992.

Kim, K.-R., and H. Craig, Two-isotope characterization of N_2O in the Pacific Ocean and constraints on its origin in deep water, *Nature, 347*, 58–61, 1990.

Krishnaswami, S., and R.R. Nair (Eds.), Special Section: JGOFS (India), *Curr. Sci., 71*, 831–905, 1996.

Lal, D. (Ed.), *Biogeochemistry of the Arabian Sea*, 250 pp., Indian Acad. of Sci., Bangalore, 1994.

Lal, S., P.K. Patra, S. Venkataramani, and M.M. Sarin, Distribution of nitrous oxide and methane in the Arabian Sea, *Curr. Sci., 71*, 894–899, 1996.

Law, C.S., and N.J.P. Owens, Significant flux of atmospheric nitrous oxide from the northwest Indian Ocean, *Nature, 346*, 826–828, 1990.

Lee, C., et al., Particle organic carbon fluxes: Compilation of results from the 1995 US JGOFS Arabian Sea Process Study, *Deep Sea Res., Part II, 45*, 2489–2501, 1998.

Mantoura, R.F.C., C.S. Law, N.J.P. Owens, P.H. Burkill, E.M.S. Woodward, R.J.M. Howland, and C.A. Llewellyn, Nitrogen biogeochemical cycling in the northwestern Indian Ocean, *Deep Sea Res., Part II, 40*, 651–671, 1993.

McAllister, W.A., and W.V. Southerland, New use for a 0.5-nanometer molecular sieve gas chromatography column, *Anal. Chem., 43*, 1536, 1971.

Morrison, J.M., L.A. Codispoti, S. Gaurin, B. Jones, V. Manghnani, and Z. Zheng, Seasonal variation of hydrographic and nutrient fields during the US JGOFS Arabian Sea Process Study, *Deep Sea Res., Part II, 45*, 2053–2101, 1998.

Naqvi, S.W.A., Geographical extent of denitrification in the Arabian Sea, *Oceanol. Acta, 14*, 281–290, 1991.

Naqvi, S.W.A., Denitrification processes in the Arabian Sea, in *The Biogeochemistry of the Arabian Sea*, edited by D. Lal, pp. 181–202, Indian Acad. of Sci., Bangalore, 1994.

Naqvi, S.W.A., and R.J. Noronha, Nitrous oxide in the Arabian Sea, *Deep Sea Res., 38*, 871–890, 1991.

Naqvi, S.W.A., and M.S. Shailaja, Activity of the respiratory electron transport system and respiration rates within the oxygen minimum layer of the Arabian Sea, *Deep Sea Res., Part II, 40*, 687–695, 1993.

Naqvi, S.W.A., R.J. Noronha, M.S. Shailaja, K. Somasundar, and R. Sen Gupta, Some aspects of the nitrogen cycling in the Arabian Sea, in *Oceanography of the Indian Ocean*, edited by B.N. Desai, pp. 285–311, A.A. Balkema, Brookfield, Vt., 1992.

Naqvi, S.W.A., D.A. Jayakumar, M. Nair, M.D. Kumar, and M.D. George, Nitrous oxide in the western Bay of Bengal, *Mar. Chem., 47*, 269–278, 1994.

Naqvi, S.W.A., T. Yoshinari, D.A. Jayakumar, M.A.A. Altabet, P.V. Narvekar, A.H. Devol, J.A. Brandes, and L.A. Codispoti, Budgetary and biogeochemical implications of N_2O isotope signatures in the Arabian Sea, *Nature, 394*, 462–464, 1998.

Nevison, C.D., R.F. Weiss, and D.J. Erickson III, Global oceanic emissions of nitrous oxide, *J. Geophys. Res., 100*, 15,809–15,820, 1995.

Olson, D.B., G.L. Hitchcock, R.A. Fine, and B.A. Warren, Maintenance of the low-oxygen layer in the central Arabian Sea, *Deep Sea Res., Part II, 40*, 673–685, 1993.

Oudot, C., C. Andrie, and Y. Montel, Nitrous oxide production in the tropical Atlantic Ocean, *Deep Sea Res., 37*, 183–202, 1990.

Patra, P.K., S. Lal, S. Venkataramani, S.N. De Sousa, V.V.S.S. Sarma, and S. Sardesai, Seasonal and spatial variability in N_2O distribution in the Arabian Sea, *Deep Sea Res., Part I, 46*, 529–543, 1999.

Pierotti, D., and R.A. Rasmussen, Nitrous oxide measurements in the eastern tropical Pacific Ocean, *Tellus, 32*, 56–72, 1980.

Prather, M., R. Derwent, D. Ehhalt, P. Fraser, E. Sanhueza, and X. Zhou, Other trace gases and atmospheric chemistry, in *Climate Change 1995, The Science of Climate Change, Contribution of Working Group I to the Second Assessment of the Intergovernmental Panel on Climate Change*, edited by J.T. Houghton et al., pp. 86–103, Cambridge Univ. Press, New York, 1996.

Rao, T.S.S., and R.C. Griffiths, *Understanding the Indian Ocean; Perspectives on oceanography*, 187 pp., United Nations Educ., Sci. and Cult. Org. (UNESCO), Paris, 1998.

Rhein, M., L. Stramma, and O. Plähn, Tracer signals of the intermediate layer of the Arabian Sea, *Geophys. Res. Lett., 24*, 2561–2564, 1997.

Rönner, U., Distribution, production and consumption of nitrous oxide in the Baltic Sea, *Geochim. Cosmochim. Acta, 47*, 2179–2188, 1983.

Schott, F.A., J. Fischer, U. Garternicht, and D. Quadfasel, Summer monsoon response of the northern Somali Current, 1995, *Geophys. Res. Lett., 24*, 2565-2568, 1997.

Shenoi, S.S.C., S.R. Shetye, A.D. Gouveia, and G.S. Michael, Salinity extrema in the Arabian Sea, in *Monsoon Biogeochemistry*, edited by V. Ittekkot and R.R. Nair, pp. 37–49, Selbstverlag des Geol.-Paläontologischen Inst. der Univ. Hamburg, Hamburg, Germany, 1993.

Siedler, G., and H. Peters, Properties of sea water, in *Landolt–Börnstein, Oceanography, New Ser., Group V*, vol. 3a, edited by J. Sündermann, pp. 233–264, Springer Verlag, New York, 1986.

Smith, S.L. (Ed.), The 1994-1996 Arabian Sea expedition: Oceanic response to monsoonal forcing, Part 1, *Deep Sea Res., Part II, 45*, 1905–2501, 1998.

Smith, S.L. (Ed.), The 1994-1996 Arabian Sea expedition: Oceanic response to monsoonal forcing, Part 2, *Deep Sea Res., Part II, 46*, 1531–1964, 1999.

Stumm, W., and J.J. Morgan, *Aquatic Chemistry*, 1022 pp., John Wiley, New York, 1996.

Upstill-Goddard, R.C., J. Barnes, and N.J.P. Owens, Nitrous oxide and methane during the 1994 SW monsoon in the Arabian Sea/northwestern Indian Ocean, *J. Geophys. Res., 104*, 30,067–30,084, 1999.

Van Weering, T.C.E., W. Helder, and P. Schalk (Eds.), Netherlands Indian Ocean Program 1992–1993: First results, *Deep Sea Res., Part II, 44*, 1177–1480, 1997.

Weiss, R.F., The solubility of nitrogen, oxygen and argon in water and seawater, *Deep Sea Res., 17*, 721–735, 1970.

Weiss, R.F., and B.A. Price, Nitrous oxide solubility in water and seawater, *Mar. Chem., 8*, 347–359, 1980.

Yoshida, N., H. Morimoto, M. Hirano, I. Koike, S. Matsuo, E. Wada, T. Saino, and A. Hattori, Nitrification rates and ^{15}N abundances of N_2O and NO_3^- in the western North Pacific, *Nature, 342*, 895–897, 1989.

Yoshinari, T., Nitrous oxide in the sea, *Mar. Chem., 4*, 189–202, 1976.

You, Y., Seasonal variations of thermocline circulation and ventilation in the Indian Ocean, *J. Geophys. Res., 102*, 10,391–10,422, 1997.

M. O. Andreae and H. W. Bange, Biogeochemistry Department, Max Planck Institute for Chemistry, P.O. Box 3060, D-55020 Mainz, Germany. (bange@mpch-mainz.mpg.de)

S. Rapsomanikis, Laboratory of Atmospheric Pollution Science and Technology, Environmental Engineering Department, Demokritos University of Thrace, GR-67100 Xanthi, Greece.

(Received May 19, 1999; revised August 1, 2000;
accepted August 23, 2000.)

Nitrous oxide measurements during EIFEX, the European Iron Fertilization Experiment in the subpolar South Atlantic Ocean

Sylvia Walter,[1] Ilka Peeken,[1] Karin Lochte,[1] Adrian Webb,[2] and Hermann W. Bange[1]

Received 12 September 2005; revised 4 November 2005; accepted 10 November 2005; published 15 December 2005.

[1] We measured the vertical water column distribution of nitrous oxide (N_2O) during the European Iron Fertilization Experiment (EIFEX) in the subpolar South Atlantic Ocean during February/March 2004 (R/V *Polarstern* cruise ANT XXI/3). Despite a huge build-up and sedimentation of a phytoplankton bloom, a comparison of the N_2O concentrations within the fertilized patch with concentrations measured outside the fertilized patch revealed no N_2O accumulation within 33 days. This is in contrast to a previous study in the Southern Ocean, where enhanced N_2O accumulation occurred in the pycnocline. Thus, we conclude that Fe fertilization does not necessarily trigger additional N_2O formation and we caution that a predicted radiative offset due to a Fe-induced additional release of oceanic N_2O might be overestimated. Rapid sedimentation events during EIFEX might have hindered the build-up of N_2O and suggest, that not only the production of phytoplankton biomass but also its pathway in the water column needs to be considered if N_2O radiative offset is modeled. **Citation:** Walter, S., I. Peeken, K. Lochte, A. Webb, and H. W. Bange (2005), Nitrous oxide measurements during EIFEX, the European Iron Fertilization Experiment in the subpolar South Atlantic Ocean, *Geophys. Res. Lett.*, *32*, L23613, doi:10.1029/2005GL024619.

1. Introduction

[2] Inspired by the iron (Fe) limitation hypothesis [*Martin et al.*, 1991], several Fe fertilization experiments have been performed in high nutrient-low chlorophyll (HNLC) regions such as the Southern Ocean, and the subarctic and equatorial Pacific Ocean [see, e.g., *Boyd*, 2004, 2002]. *Fuhrman and Capone* [1991] pointed out that stimulating ocean productivity by Fe addition might result in an enhanced formation of nitrous oxide (N_2O). This point is especially important in view of the fact that N_2O is an atmospheric trace gas with a high global warming potential [*Jain et al.*, 2000]. Thus, enhanced N_2O formation by Fe addition might counteract the climatic benefits of a drawdown of atmospheric carbon dioxide (CO_2).

[3] *Fuhrman and Capone* [1991] argued that enhanced productivity will lead to an enhanced nitrogen export from the euphotic zone, which in turn would result in additional N_2O formation via enhanced nitrification ($NH_4^+ \rightarrow NH_2OH \rightarrow NO_2^- \rightarrow NO_3^-$). N_2O formed via nitrification is thought to be dominating in the oxic part of the world's oceans [see, e.g., *Nevison et al.*, 2003]. The idea of a link between Fe fertilization and enhanced N_2O formation was supported by the study of *Law and Ling* [2001], who found a small but significant N_2O accumulation in the pycnocline during the Southern Ocean Iron Enrichment Experiment (SOIREE) in the Australasian sector of the Southern Ocean (61°S, 140°E) in February 1999. Recently, *Jin and Gruber* [2003] predicted the long-term effect of Fe fertilization on oceanic N_2O emissions on a global scale with a coupled physical-biogeochemical model. Based on their model results they concluded that Fe fertilization-induced N_2O emissions could offset the radiative benefits of the CO_2 drawdown [*Jin and Gruber*, 2003].

[4] Here we present our measurements of N_2O during the European Iron Fertilization Experiment (EIFEX; R/V *Polarstern* cruise ANT XXI/3) in the subpolar South Atlantic Ocean from 9 February to 21 March 2004 [*Smetacek and cruise participants*, 2005].

2. The EIFEX Setting

[5] A mesoscale cyclonic eddy, embedded in a meander of the Antarctic Polar Front, was identified as suitable for the EIFEX study [*Strass et al.*, 2005]. The eddy was centered at 49.4°S 2.25°E and extended over an area of 60 × 100 km. First fertilization was performed on 12–13 February by releasing 6000 kg iron sulfate ($FeSO_4$) into the mixed layer over an area of 150 km^2. Since iron concentrations had been decreasing (P. Croot, personal communication, 2004), fertilization was repeated on 26–27 February by releasing 7000 kg $FeSO_4$ over an area of 400 km^2. All sampled stations were located inside the eddy; the stations within fertilized waters will be called in-stations and those from unfertilized waters out-stations (Table 1). Inside and outside the fertilized patch was determined by photosynthetic activity (Fv/Fm) performed by Fast-Repetition-Rate-Fluorescence (FastTracka, Chelsea, UK) [*Röttgers et al.*, 2005]. Fv/Fm is known to be a very sensitive parameter, which increases immediately after iron fertilization.

[6] The hydrographic settings of the sampling stations were not uniform: The in-stations' hydrographic properties did not show any variability. However, the out-station 514 showed, in comparison with the in-stations, enhanced potential water temperatures in the density (σ_t) range from 27.25 to 27.7 kg m^{-3} (corresponding to a approximate depth range from 200 to 400 m). The hydrographic properties of the out-stations 546 and 587 were almost identical to the in-stations. This implies that station 514 is not a representative out-station and was therefore excluded

[1]Forschungsbereich Marine Biogeochemie, Leibniz-Institut für Meereswissenschaften at University of Kiel (IFM-GEOMAR), Kiel, Germany.
[2]Department of Oceanography, University of Cape Town, Rondebosch, South Africa.

0094-8276/05/2005GL024619$05.00

Table 1. N_2O Measurements During EIFEX[a]

Station Number	Latitude,°S	Longitude,°E	Date	Days After First/ Second Fertilization	Patch Class.	N_2O ML Conc.,[b] nmol L^{-1}	N_2O ML Sat.,[b] %
513	49.59	2.05	28 Feb 04	16/2	In	13.3 ± 0.1 (5)	102 ± 1 (5)
514	49.31	2.34	29 Feb 04	17/3	Out	13.5 ± 0.3 (3)	104 ± 2 (3)
544	49.36	1.87	07 Mar 04	24/10	In	13.8 ± 0.5 (3)	106 ± 4 (3)
546	49.47	2.09	10 Mar 04	27/13	Out	13.1 (2)	102 (2)
570	49.43	2.05	14 Mar 04	31/17	In	13.1 ± 0.3 (5)	102 ± 3 (5)
580	49.12	2.38	16 Mar 04	33/19	In	12.5 ± 0.2 (3)	97 ± 1 (3)
586	49.50	2.10	18 Mar 04	35/21	Out	13.1 ± 0.5 (4)	102 ± 4 (4)

[a]Class. stands for classification and indicates whether a profile was inside or outside of the fertilized patch. ML stands for mixed layer; here defined as the depth where the temperature differs from the surface temperature by more than 0.5°C. Conc. and Sat. stand for concentration and saturation, respectively.

[b]Given as average ± standard deviation. Number of depths used for averaging is given in parentheses.

from the comparison (see also discussion of N_2O data below).

3. Methods

[7] Triplicate water samples from various depths were taken from a 24 x 12 L-bottle rosette, equipped with a CTD-sensor. The analytical method applied is a modification of the method described by *Bange et al.* [2001]: Bubble free samples were taken immediately following oxygen (O_2) sampling in 24 mL glass vials, sealed directly with butyl rubber stoppers and crimped with aluminium caps. To prevent microbial activity, samples were poisoned with 500 µL of a saturated aqueous mercury chloride ($HgCl_2$) solution. The samples were stored in the dark at 4 °C until analysis in our home laboratory from June to August 2004. In a time series experiment we found that N_2O concentrations in samples treated as described above did not change significantly over 10 months (S. Walter, Nitrous oxide in the Atlantic Ocean, Ph.D. thesis, in preparation, University of Kiel, 2005). N_2O water concentrations (C_w) were calculated as follows:

$$C_w[\text{nmol L}^{-1}] = \left(\beta x' P V_{wp} + \frac{x' P}{RT} V_{hs}\right) / V_{wp}$$

where β stands for the Bunsen solubility in nmol L^{-1} atm^{-1} [*Weiss and Price*, 1980], x′ is the dry gas mole fraction of N_2O in the headspace in ppb, P is the atmospheric pressure in atm (set to1 atm), V_{wp} and V_{hs} stand for the volumes of the water (14 mL) and headspace phases (10 mL), respectively. R is the gas constant (8.2054 10^{-2} L atm mol^{-1} K^{-1}) and T is the temperature during equilibration.

[8] For calibration we used standard gas mixtures with 311.8 ± 0.2 ppb and 346.5 ± 0.2 ppb N_2O in synthetic air (DEUSTE Steininger GmbH, Mühlhausen, Germany). The standard mixtures have been calibrated against the NOAA (National Oceanic and Atmospheric Administration, Boulder, Colorado) standard scale in the laboratories of the Air Chemistry Division of the Max Planck Institute for Chemistry, Mainz, Germany). The standard deviation of the N_2O concentration (C_w) was approximated with (C_{wmax} − C_{wmin})/1.91, where C_{wmin} and C_{wmax} stand for the minimal and maximal N_2O concentrations of the triplicate samples, respectively. The factor 1.91 is derived from the statistical method by *David* [1951]. The overall mean analytical error was ±2.7% (±0.5 nmol L^{-1}).

[9] N_2O saturations (*sat*) in% (i.e., 100% = equilibrium) were calculated as $sat = 100\ C_w/C_a$, where C_a is the equilibrium concentration of dissolved N_2O based on the N_2O atmospheric dry mole fraction, water temperature, and salinity [*Weiss and Price*, 1980]. For calculating C_a in the mixed layer an ambient air mole fraction of 317.8 ppb was applied, which is the average of the monthly mean N_2O dry mole fractions measured at the AGAGE (Advanced Global Atmospheric Gases Experiment [see *Prinn et al.*, 2000]) baseline monitoring station Cape Grim (Tasmania) during February and March 2004. AGAGE data are available from the anonymous ftp site cdiac.esd.ornl.edu (subdirectory/pub/ale_gage_agage/agage/gc-md/monthly) at the Carbon Dioxide Information Analysis Center in Oak Ridge, Tennessee.

[10] Dissolved O_2, nitrate, and CTD data were provided by the participating working groups. Further details can be found in the cruise report by *Smetacek and cruise participants* [2005].

4. Results and Discussion

[11] An overview of the N_2O measurements during EIFEX is given in Table 1 and in Figure 1. Mixed layer N_2O saturations were comparable to surface saturations (~103%) from the same region measured during the Ajax cruise leg 2 in Jan-Feb 1984 [*Weiss et al.*, 1992]. Moreover, the overall mean N_2O deep water (>2000 m) concentration of 17.5 ± 0.2 nmol L^{-1} is in good agreement with the N_2O deep water-water age relationship by *Bange and Andreae* [1999]. Both, the observed surface saturation and deep-water concentration support the view that the N_2O samples were not affected by the time lag between sampling and measurements.

[12] In agreement with the results from SOIREE [*Law and Ling*, 2001], we did not observe a difference in N_2O mixed layer saturations between in-stations and out-stations (Table 1), which implies that N_2O emissions were not significantly different either.

[13] The N_2O profiles showed a pronounced maximum between 500 and 750 m which was associated with the O_2 minimum and the nitrate maximum (Figure 1) indicating that nitrification was the main N_2O formation process. Our N_2O concentrations are comparable to N_2O measurements from the South Atlantic and Southern Oceans [*Butler et al.*, 1995; *Law and Ling*, 2001; *Rees et al.*, 1997].

[14] Following the approach by *Law and Ling* [2001], we fitted a polynomial to the N_2O-σ_t data of stations 546 and 587 (Figure 2). Out-station 514 was excluded because it

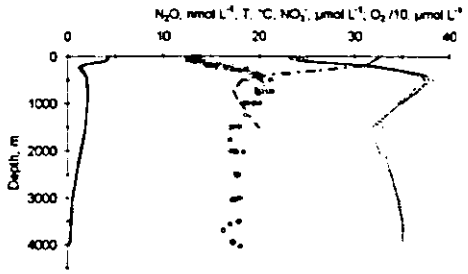

Figure 1. N_2O (open circles), water temperature (solid lines), NO_3^- (dashed lines), and O_2 (dashed dotted line) at the EIFEX stations listed in Table 1. O_2 data are only available for station 570 in the depth range from 0–1500 m. Please note that O_2 is given in μmol L^{-1} divided by 10.

obviously was not representative as indicated by the data in Figure 2 (see also section EIFEX setting). A comparison of the N_2O concentrations of the in-stations with the polynomial fit based on the out stations revealed no significant differences (Figure 2). A third-order polynomial fit to the in-stations ($-52.766x^3 + 4320.7x^2 - 117{,}915x + 1{,}072{,}529$, $r^2 = 0.95$, $n = 67$, standard error of predicted $N_2O = \pm 0.63$ nmol L^{-1}) was almost identical to the out-stations' fit ($-48.474x^3 + 3967.8x^2 - 108{,}241x + 984{,}148$, $r^2 = 0.96$, $n = 30$, standard error of predicted $N_2O = \pm 0.56$ nmol L^{-1}). Thus, we conclude that no significant changes in the N_2O concentrations occurred during EIFEX.

[15] Our conclusion is in contrast to the observation by *Law and Ling* [2001]. They found an accumulation of N_2O up to 0.9–1 nmol L^{-1} in the pycnocline (60–80 m water depth) within 13 days during SOIREE. Adapting a N_2O accumulation rate of 0.08 nmol L^{-1} d^{-1}(=1 nmol L^{-1}/13 days), an increase of 2.6 nmol L^{-1} (=0.08 nmol L^{-1} × 33 days) would have been expected for a N_2O accumulation in the pycnocline in 100–200 m during EIFEX. This was not the case (Figure 2). It is possible that N_2O accumulation in the pycnocline was not detected because of insufficient analytical precision and/or coarse sampling of the depths profiles: A possible N_2O accumulation must have been low (<0.5 nmol L^{-1} over the duration of the experiment as implied by our mean analytical error) or must have taken place in a narrow depth range of less than 40 m (i.e., the mean depth spacing of sampling from the surface to the pycnocline in about 200 m). Moreover, in contrast to EIFEX, Fe addition during SOIREE was performed four times within a week over a much smaller area (50 km^2 [*Law and Ling*, 2001]). Therefore, the observed N_2O accumulation in the pycnocline during SOIREE may have been a fast short-term response to the intensive short-term Fe fertilization. Because we started N_2O sampling 16 days after the first Fe addition (i.e., 2 days after the second Fe addition) we might have missed this short-term signal during EIFEX.

[16] During EIFEX chlorophyll *a* (chl *a*) standing stocks increased 3 fold until day 26, but remarkably decreased thereafter [*Peeken et al.*, 2005]. The main beneficiaries of the iron fertilization were diatoms in all size classes (L. Hoffmann et al., Different reactions of Southern Ocean phytoplankton size classes to iron fertilisation, submitted to *Limnology and Oceanography*, 2005). Toward the end of the experiment, the diatom marker fucoxanthin and chl *a* could be followed down the water column to 4000 m and a low ratio of phaeopigments to chl *a* indicated the export of fresh material most likely originating from the iron fertilized patch [*Peeken et al.*, 2005]. An explanation for the absence of an increase of N_2O in the deep (e.g., in the O_2 minimum zone) might be the very rapid export of the fresh phytoplankton material to the deep ocean during EIFEX [*Peeken et al.*, 2005], which started about 23 days after the second Fe addition. Thus, we can argue that the rapid export of organic material during EIFEX might have been too rapid for the nitrifying bacteria in the deep ocean to adapt to and, thus, an additional build-up of N_2O in the deep could not take place. Nitrifying bacteria, especially ammonium-oxidizing bacteria (AOB), are known for lag phases up to several weeks after periods of low metabolic activities [*Schmidt et al.*, 1999].

[17] The responsible process for the N_2O accumulation during SOIREE [*Law and Ling*, 2001] and the proposed further increase of N_2O in prolonged iron fertilization experiments could not be identified. Thus, a possible link between N_2O accumulation and Fe fertilization remains to be not a simple cause-and-effect mechanisms and the

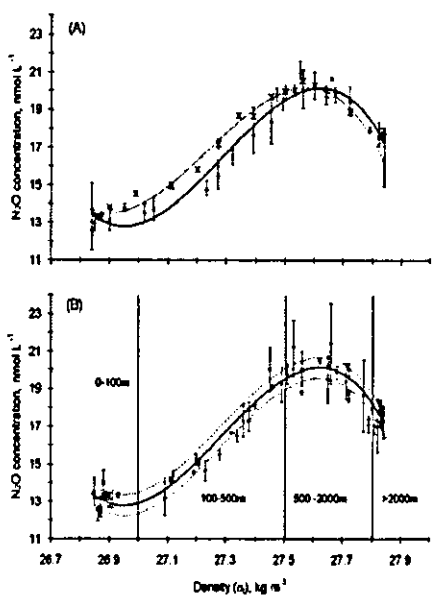

Figure 2. N_2O concentrations vs. density (σ_t) during EIFEX. (a) Out-stations: Triangles stand for stations 546 and 587 and crosses stand for station 514. The bold solid line represents a third-order polynomial fit based on stations 546 and 587 (see text for statistical details). The thin solid line represents a third-order polynomial fit based on station 514. (b) In-stations: 513, 544, 570, and 580 (symbols) compared with the polynomial fit based on out-stations 546 and 587 (bold line, see Figure 2a). The dashed lines indicate the standard error of the predicted N_2O. Depths intervals are indicated.

magnitude of a possible radiative offset still needs to be proven.

5. Conclusions

[18] We did not observe a N_2O accumulation during the in situ iron fertilization experiment EIFEX in the subpolar South Atlantic Ocean in February/March 2004. This is in contrast to previous measurement by *Law and Ling* [2001] in the Australasian sector of the Southern Ocean. We conclude that Fe fertilization does not necessarily trigger additional N_2O formation, which might depend on differences of the environmental conditions (e.g., the fate of the Fe-induced phytoplankton bloom). We caution, therefore, that predictions of a radiative offset caused by a Fe-induced additional release of oceanic N_2O [*Jin and Gruber*, 2003; *Law and Ling*, 2001] might be overestimated. In order to solve this problem further long-term experiments with particular emphasis on sedimentation processes are necessary to prove a link between Fe addition and enhancement of N_2O formation and the subsequent release of N_2O to the atmosphere.

[19] **Acknowledgments.** We thank Katrin Bluhm, Linn Hoffmann, and Dieter Wolf-Gladrow for their help during sampling. We are grateful to B. Cisewski, H. Leach, H. Prandke, and V. Strass ("the CTD group") for making the CTD data available for us. We acknowledge the help of the chief scientist Victor Smetacek, the ANT XXI/3 participants and the officers and crew of R/V *Polarstern* for conducting a successful experiment. We especially thank R. Hoffmann for the calibration of our standards. Two anonymous reviewers provided valuable comments. The investigations were financially supported by the IFM-GEOMAR Forschungsbereich Marine Biogeochemie.

References

Bange, H. W., and M. O. Andreae (1999), Nitrous oxide in the deep waters of the world's oceans, *Global Biogeochem. Cycles*, *13*, 1127–1135.

Bange, H. W., S. Rapsomanikis, and M. O. Andreae (2001), Nitrous oxide cycling in the Arabian Sea, *J. Geophys. Res.*, *106*, 1053–1065.

Boyd, P. W. (2002), The role of iron in the biogeochemistry of the Southern Ocean and equatorial Pacific: A comparison of in situ iron enrichments, *Deep Sea Res., Part II*, *49*, 1803–1821.

Boyd, P. (2004), Ironing out algal issues in the Southern Ocean, *Science*, *304*, 396–397.

Butler, J. H., J. M. Lobert, S. A. Yvon, and L. S. Geller (1995), The distribution and cycling of halogenated trace gases, *Ber. Polarforsch.*, *168*, 27–40.

David, H. A. (1951), Further applications of range to analysis of variance, *Biometrika*, *38*, 393–409.

Fuhrman, J. A., and D. G. Capone (1991), Possible biogeochemical consequences of ocean fertilization, *Limnol. Oceanogr.*, *36*(8), 1951–1959.

Jain, A. K., B. P. Briegleb, K. Minschwaner, and D. J. Wuebbles (2000), Radiative forcing and global warming potentials of 39 greenhouse gases, *J. Geophys. Res.*, *105*, 20,773–20,790.

Jin, X., and N. Gruber (2003), Offsetting the radiative benefit of ocean iron fertilization by enhancing N_2O emissions, *Geophys. Res. Lett.*, *30*(24), 2249, doi:10.1029/2003GL018458.

Law, C. S., and R. D. Ling (2001), Nitrous oxide flux and response to increased iron availability in the Antarctic Circumpolar Current, *Deep Sea Res., Part II*, *48*, 2509–2527.

Martin, J. H., R. M. Gordon, and S. E. Fitzwater (1991), The case for iron, *Limnol. Oceanogr.*, *36*, 1793–1802.

Nevison, C., J. H. Butler, and J. W. Elkins (2003), Global distribution of N_2O and ΔN_2O-AOU yield in the subsurface ocean, *Global Biogeochem. Cycles*, *17*(4), 1119, doi:10.1029/2003GB002068.

Peeken, I., L. Hoffmann, P. Assmy, U. Bathmann, B. Cisewski, H. Leach, K. Lochte, O. Sachs, E. Sauter, and V. Strass (2005), Export of fresh algal material during the Southern Ocean iron fertilisation experiment, EIFEX (abstract), paper presented at Summer Meeting 2005, Am. Soc. of Limnol. and Oceanogr., Santiago de Compostela, Spain.

Prinn, R. G., et al. (2000), A history of chemically and radiatively important gases in air deduced from ALE/GAGE/AGAGE, *J. Geophys. Res.*, *105*, 17,751–17,792.

Rees, A. P., N. J. P. Owens, and R. C. Upstill-Goddard (1997), Nitrous oxide in the Bellingshausen Sea and Drake Passage, *J. Geophys. Res.*, *102*, 3383–3391.

Röttgers, R., F. Colijn, and M. Dibbern (2005), Algal physiology and biooptics, *Ber. Polarforsch. Meeresforsch.*, *500*, 82–88.

Schmidt, I., T. Gries, and T. Willuweit (1999), Nitrification—Fundamentals of the metabolism and problems at the use of ammonia oxidizers (in German with English abstract), *Acta Hydrochim. Hydrobiol.*, *27*, 121–135.

Smetacek, V., and cruise participants (2005), The expedition ANT XXI/3 of R/V *Polarstern*, *Ber. Polarforsch. Meeresforsch.*, *500*, 1–134.

Strass, V., B. Cisewski, S. Gonzalez, H. Leach, K.-D. Loquay, H. Prandke, H. Rohr, and M. Thomas (2005), The physical setting of the European Iron Fertilisation Experiment 'EIFEX' in the Southern Ocean, *Ber. Polarforsch. Meeresforsch.*, *500*, 15–46.

Weiss, R. F., and B. A. Price (1980), Nitrous oxide solubility in water and seawater, *Mar. Chem.*, *8*, 347–359.

Weiss, R. F., F. A. Van Woy, and P. K. Salameh (1992), Surface water and atmospheric carbon dioxide and nitrous oxide observations by shipboard automated gas chromatography: Results from expeditions between 1977 and 1990, report, Carbon Dioxide Inf. Anal. Cent., Oak Ridge Natl. Lab., Oak Ridge, Tenn.

H. W. Bange, K. Lochte, I. Peeken, and S. Walter, Forschungsbereich Marine Biogeochemie, Leibniz-Institut für Meereswissenschaften at University of Kiel (IFM-GEOMAR), Düstembrooker Weg 20, 24105 Kiel, Germany. (hbange@ifm-geomar.de)

A. Webb, Department of Oceanography, University of Cape Town, Private Bag X3, Rondebosch 7701, South Africa.

Nitrous oxide in the North Atlantic Ocean

Sylvia Walter, Hermann W. Bange, Ulrich Breitenbach, Douglas W.R. Wallace

Forschungsbereich Marine Biogeochemie
IFM-GEOMAR
Düsternbrooker Weg 20
24105 Kiel, Germany

ms in preparation for *Global Biogeochem. Cycles*

Version 8 February 2006

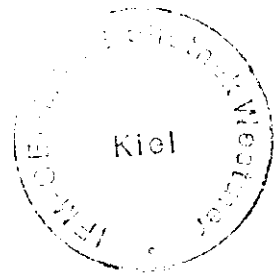

Abstract

In order to investigate the role of the North Atlantic Ocean as a source of atmospheric nitrous oxide and to decipher the major formation pathways of nitrous oxide, measurements of dissolved nitrous oxide were made during three cruises in the tropical, subtropical and subpolar North Atlantic in Oct./Nov. 2002, Mar./Apr. 2004, and May 2002, respectively. Nitrous oxide was close to equilibrium or slightly supersaturated in the surface layers suggesting that the North Atlantic acts as a weak source of nitrous oxide to the atmosphere. Depth profiles showed supersaturation throughout the water column with a distinct increasing trend from the subpolar to the tropical region. Lowest nitrous oxide concentrations, near equilibrium and with an average of 11.0 ± 1.7 nmol L^{-1}, were found in the subpolar North Atlantic where the profiles showed no clear maxima. Highest values up to 37.3 nmol L^{-1} occurred in the tropical North Atlantic with clear maxima at approximately 400 m. A positive correlation of nitrous oxide with nitrate, as well as excess nitrous oxide with AOU, was only observed in the subtropical and tropical regions. Therefore, we conclude that the formation of nitrous oxide occurs in the tropical region rather than in the subpolar region of the North Atlantic and suggest nitrification is the dominant formation pathway in the subtropical and tropical regions.

1. Introduction

Nitrous oxide (N_2O) is an important atmospheric trace gas due to its influence on the Earth's climate. In the troposphere N_2O acts as a greenhouse gas whereas in the stratosphere it is involved in the depletion of ozone by providing NO-radicals [*Prather et al.*, 2001]. Since the beginning of the industrial revolution the global mean tropospheric N_2O mole fraction has risen rapidly from 270 ppb up to 314 ppb in 1998 [*Prather et al.*, 2001]. About 24 % of the natural sources of atmospheric N_2O are contributed by the oceans [*Prather et al.*, 2001; *Seitzinger et al.*, 2000]. Nitrous oxide is an important component of the oceanic nitrogen cycle, mainly formed by the microbial processes of nitrification and denitrification [*Codispoti et al.*, 2001; *Goreau et al.*, 1980]: Nitrification is an aerobic two-step process in which ammonium is oxidized to nitrate ($NH_4^+ \rightarrow NH_2OH \rightarrow NO_2^- \rightarrow NO_3^-$) by two different groups of bacteria. In this process nitrous oxide is assumed to be a by-product, however until now the exact pathway for N_2O production remains unclear. In suboxic habitats nitrate can be reduced by denitrification to molecular nitrogen ($NO_3^- \rightarrow NO_2^- \rightarrow NO \rightarrow N_2O \rightarrow N_2$), here nitrous oxide is an intermediate product. Especially at oxic/suboxic boundaries N_2O is produced by coupled nitrification and denitrification, due to the transfer of common intermediates [*Yoshinari et al.*, 1997]. Another possibility is aerobic denitrification, whereby under fully aerobic conditions organisms convert ammonia into nitrogen gas without the intermediary accumulation of nitrite [*Robertson et al.*, 1988]. All processes depend on oxygen concentrations, as well as the availability of substrates such as ammonium and nitrate. Many organisms are able to switch between different pathways depending on environmental conditions, and also the yield of N_2O during a process depends on environmental conditions [*Goreau et al.*, 1980; *Poth and Focht*, 1985; *Richardson*, 2000]. Positive correlations of N_2O with apparent oxygen utilization (AOU) or nitrate are interpreted as production of nitrous oxide by nitrification [*Yoshinari*, 1976; *Cohen and Gordon*, 1978; *Yoshida et al.*, 1989]. However, up to now the dominant production pathway for N_2O on the global scale and the contribution of different pathways still remains unclear [*Codispoti et al.*, 2001; *Popp et al.*, 2002].

Information on the vertical N_2O distribution in the North Atlantic is sparse, only a few profiles are available. The first vertical profiles for the North Atlantic were published by *Junge and Hahn* [1971] and *Yoshinari* [1976], additional data were collected by *Butler et*

al. [1995], and recently data from a transect at 7°30′ N were reported by *Oudot et al.* [2002]. In this paper we present a comprehensive set of 73 vertical profiles of nitrous oxide from three trans-Atlantic cruises, covering the subpolar North Atlantic, the subtropical and the tropical North Atlantic. Based on these new data, we examine the regional differences of the N_2O distribution and its formation pathways.

2. Study area

2.1 Research cruises

Samples from the three cruises were collected over the period from May 2002 to April 2004 (see Fig. 1).

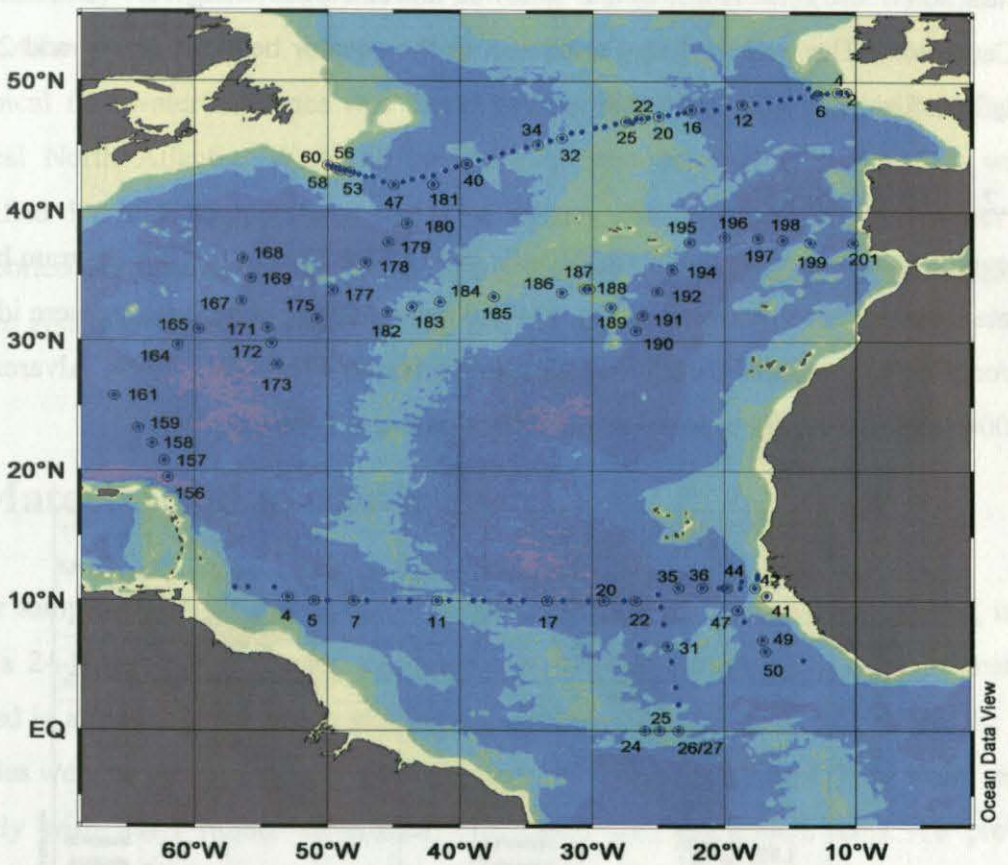

Fig. 1: Cruise tracks for `Gauss 384-1′ (subpolar North Atlantic, May 16th to June 14th 2002), `Meteor 60-5′ (subtropical North Atlantic, March 9th to April 14th 2004) and `Meteor 55′ (tropical North Atlantic, October 13th to November 16th 2002). Numbers are given for stations where N_2O profiles were measured.

The first cruise (May / June 2002), started in Hamburg, Germany with the German research vessel `Gauss´. The cruise track followed the WOCE-A2 transect to Halifax, Canada. Depth profiles of N_2O were measured at 16 stations. The WOCE-A2 transect is located between 42 °N and 49 °N.

The subtropical North Atlantic was investigated during March / April 2004 onboard the research vessel `Meteor`. The cruise started in Fort de France, Martinique (French Antilles) in the western part of the Atlantic and ended in Lisbon (Portugal). Samples were taken at 37 stations. Most stations were co-located with stations where samples were taken during the Transient Tracers in the Ocean Program (TTO) in 1982.

The tropical North Atlantic samples were taken during the M55-SOLAS cruise [*Wallace and Bange*, 2004] in October/November 2002, again with the German research vessel `Meteor`. This cruise started in the western tropical North Atlantic in Willemstad, Curaçao (Netherlands Antilles) and followed a cruise track along 10 – 11 °N to Douala (Cameroon). The track included a transect to the equator between 26 °W and 23.5 °W. N_2O profiles were taken at 20 stations.

2.2 Hydrography

Several water masses in the North Atlantic can be identified in the T-S-diagram based on data from the three cruises (see Fig. 2). The main Atlantic water masses were identified according to commonly used classification schemes [Tomczak, 1999; Alvarez et al., 2004; Aiken et al., 2000; Joyce et al., 2001; Poole and Tomczak, 1999].

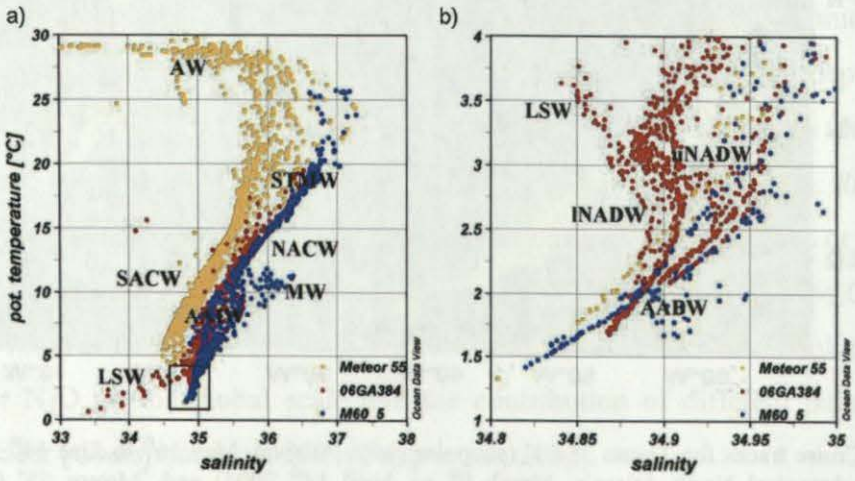

Fig. 2: T-S-diagram of the North Atlantic; 2a) T-S-diagram with data from all three cruises; 2b) T-S-diagram in Fig. 2a framed by box.; AW: Amazon Water; STMW: Subtropical Mode Water; MW: Mediterranean Water; SACW: South Atlantic Central Water; NACW: North Atlantic Central Water; ;AAIW: Antarctic Intermediate Water, AABW: Antarctic Bottom Water; lNADW: lower North Atlantic Deep Water; uNADW: upper North Atlantic Deep Water; LSW: Labrador Sea Water

The WOCE A2 transect (Gauss 384-1 cruise), is located at the boundary region between the subpolar gyre [*Gordon*, 1986] and the subtropical gyre [*Krauss*, 1996]. This region is highly variable, characterized by the exchange of upper-ocean water between the gyres mainly via the North Atlantic Current, and the Labrador Current. One of the most important water masses here is the Labrador Sea Water (LSW). These water masses provide the major part of the North Atlantic Intermediate Water in combination with the outflow of Mediterranean Sea Water (MW), which is detected in the eastern basin of the subtropical Atlantic Ocean near the Strait of Gibraltar [*Richardson et al.*, 2000] and the Antarctic Intermediate Water (AAIW) from the south [*Lorbacher*, 2000]. Additional water masses of the southern hemisphere that penetrate into the North Atlantic are the South Atlantic Central Water (SACW) and the Antarctic Bottom Water (AABW). SACW flows northwards, and mixes with the North Atlantic Central Water (NACW) at approximately 15 °N in the western and 20 °N in the eastern basin [*Poole and Tomczak*, 1999; *Aiken et al.*, 2000].

A typical freshwater influence was found during the Meteor 55 cruise in the western tropical North Atlantic. Water of the Amazon was detected in the surface water, identified by high temperatures and low salinity. These plumes of freshwater are transported northwards by the North Brazil Current and eastwards by the equatorial current system [*Fratantoni and Glickson*, 2002].

3. Material and methods

Water samples for N_2O analysis were collected in triplicate from various depths, taken with a 24-Niskin-bottle rosette, equipped with a CTD-sensor. The analytical method applied is a modification of the method described by [*Bange et al.*, 2001]. Bubble free samples were taken immediately following oxygen sampling in 24 mL glass vials, sealed directly with butyl rubber stoppers and crimped with aluminium caps. To prevent microbial activity, samples were poisoned with 500 µL of 2 mM mercury chloride solution. Then 10 mL of sample was replaced with a helium headspace for each vial, and the samples were allowed to equilibrate for at least two hours at room temperature (temperature was recorded continuously). A 9 mL subsample from the headspace was used to flush a 2 mL sample loop after passing through a moisture trap (filled with

Sicapent®, Merck Germany). Gaschromatographic separation was performed at 190 °C on a packed molecular sieve column (6ft x 1/8"SS, 5A, mesh 80/100, Alltech GmbH, Germany). The N_2O was detected with an electron capture detector. A mixture of argon with 5 % by volume methane was used as carrier gas with a flow of 21 mL min^{-1}. For the two-point calibration procedure we used standard gas mixtures with 311.8 ± 0.2 ppb and 346.5 ± 0.2 ppb N_2O in synthetic air (Deuste Steininger GmbH, Mühlhausen Germany). The standard mixtures have been calibrated against the NOAA (National Oceanic and Atmospheric Administration, Boulder, Co.) standard scale in the laboratories of the Air Chemistry Division of the Max Planck Institute for Chemistry, Mainz, Germany.

Calculations

N_2O water concentrations (C_{N2O}) were calculated as follows:

$$C_{N2O}\left[\text{nmol L}^{-1}\right] = \left(\beta \times P\, V_{wp} + \frac{x\,P}{R\,T} V_{hs}\right) / V_{wp} \qquad (1)$$

where β stands for the Bunsen solubility in nmol L^{-1} atm^{-1} [*Weiss and Price*, 1980], x is the dry gas mole fraction of N_2O in the headspace in ppb, P is the atmospheric pressure in atm, V_{wp} and V_{hs} stand for the volumes of the water and headspace phases, respectively. R is the gas constant (8.2054 10^{-2} L atm mol^{-1} K^{-1}) and T is the temperature during equilibration. The salinity was measured by the CTD-Sensor during water sample collection. The overall relative mean analytical error was estimated to be ± 1.8 %.

The excess N_2O (ΔN_2O) was calculated as the difference between the calculated N_2O equilibrium concentration and the measured concentration of N_2O as follows

$$\Delta N_2O\ [\text{nmol L}^{-1}] = N_2O\ (\text{observed}) - N_2O\ (\text{equilibrium}). \qquad (2)$$

To calculate the N_2O equilibrium concentration we used three different atmospheric mole fractions. Between the mixed layer and the atmosphere, N_2O exchanges in about three weeks [*Najjar*, 1992], thus we calculated ΔN_2O in the mixed layer using the actual atmospheric N_2O value of 318 ppb measured during the 'Meteor 55' cruise [*Walter et al.*, 2004]. Below the thermocline, exchange with the atmosphere is unlikely, thus, calculated N_2O equilibrium concentrations depend on the atmospheric N_2O mole fraction at the time of deep-water formation. However, the exact atmospheric mole fraction of N_2O

during deep-water formation is unknown because of uncertainty in age determination of water masses. Generally, tropical Atlantic deep waters below 2000 m seem to be older than 200 years [*Broecker and Peng*, 2000]. Therefore for depths > 2000 m ΔN_2O was calculated with the tropospheric preindustrial value of 270 ppb [*Flückiger et al.*, 1999]. An average of the actual and the preindustrial atmospheric value (i.e., 294 ppb) was used for the depth range between the upper thermocline and 2000 m. The thermocline was defined as the depth where the temperature differs from the surface temperature by more than 0.5 °C [*Tomczak and Godfrey*, 2001]. For the subtropical and subpolar region we calculated ΔN_2O with these same mole fractions, although the age of water masses is different to the tropical Atlantic and therefore some values may be underestimated, whereas others may be overestimated. The resulting uncertainties of ΔN_2O are about 10-15 %; however, our conclusions are not significantly affected by this uncertainty. The equilibrium values of dissolved oxygen (O_2) were calculated with the equation given by [*Weiss*, 1970].

The apparent oxygen utilization (AOU) was calculated as followed:

$$AOU\ [\mu mol\ L^{-1}] = O_2\ (equilibrium) - O_2\ (observed). \quad (3)$$

4. Results

4.1 Distribution of nitrous oxide in the North Atlantic

4.1.1 N_2O distribution along isopycnal levels

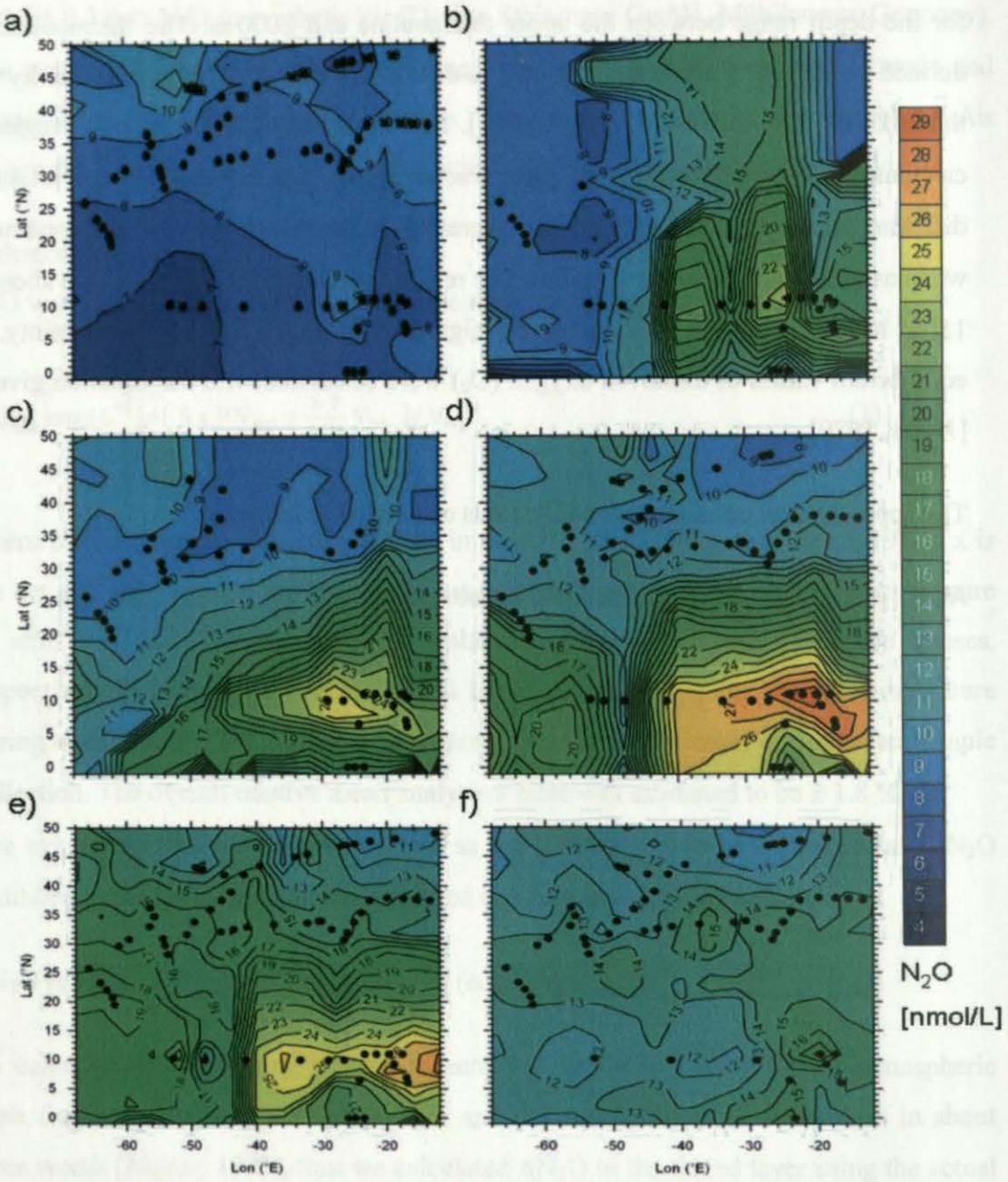

Fig. 3: Distribution of N_2O in the North Atlantic along isopycnal levels. Dots indicate stations with available data for the isopycnal levels. 3a) surface – thermocline; 3b) thermocline – 26.0; 3c) 26.1 – 26.5; 3d) 26.6 – 27.0; 3e) 27.1 – 27.5; 3f) 27.6 – 27.93

In the surface layer of the North Atlantic (Fig. 3a) N_2O concentrations were relatively uniform with 8.5 ± 1.2 nmol L^{-1}. In the region of the Labrador Current N_2O

concentrations were enhanced with an average of 11.6 ± 0.9 nmol L^{-1}. During the 'Meteor 55' cruise, a plume of Amazon Water had been identified in the western basin of the tropical North Atlantic [*Körtzinger*, 2003]. In contrast to [*Oudot et al.*, 2002], who reported enhanced values in the plume of the Amazon River, we found no influence on N_2O concentrations [*Walter et al.*, 2004].

Below the thermocline, N_2O concentrations were variable with respect to depths and regions. We found highest concentrations in the eastern basin of the tropical North Atlantic throughout the water column, with maximum concentrations on σ_θ surfaces between 26.3 and 27.1 (Fig. 3b-e). At the Midatlantic Ridge, located at approximately 40 °W, a distinct boundary between the western and eastern Atlantic basins was observed (Fig. 3d-e). In the eastern subtropical North Atlantic, at approximately 1000 m (σ_θ 27.6-27.7), a tongue of outflow water from the Mediterranean Sea was detected by higher values of salinity and temperature [*Richardson et al.*, 2000]. However, we found no apparent influence of the Mediterranean water on N_2O concentrations.

Like the surface layer, deep waters (Fig. 3f) showed nearly uniform N_2O concentrations, though with higher values of 13.3 ± 1.6 nmol L^{-1}. However, a weak but distinct trend of decreasing concentrations from the tropics (13.1 ± 1.3 nmol L^{-1}) to the subpolar North Atlantic (11.1 ± 1.4 nmol L^{-1}) could be observed.

4.1.2 Vertical N_2O distribution

The vertical distribution of N_2O showed characteristically different profiles in different regions of the North Atlantic (Fig. 4a-c), and between the western and eastern basins of these regions (Fig. 5a-c).

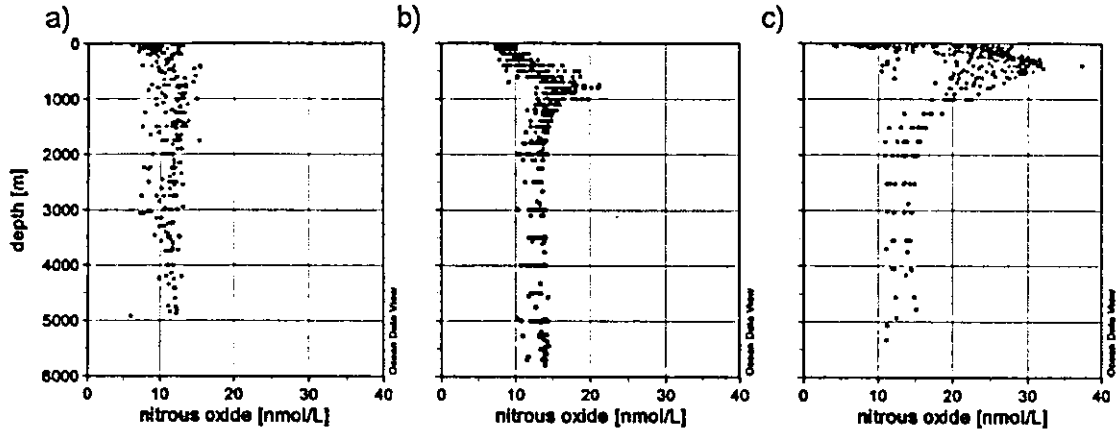

Fig. 4: N_2O concentration in the North Atlantic plotted against depth. 4a) subpolar, 4b) subtropical, 4c) tropical North Atlantic

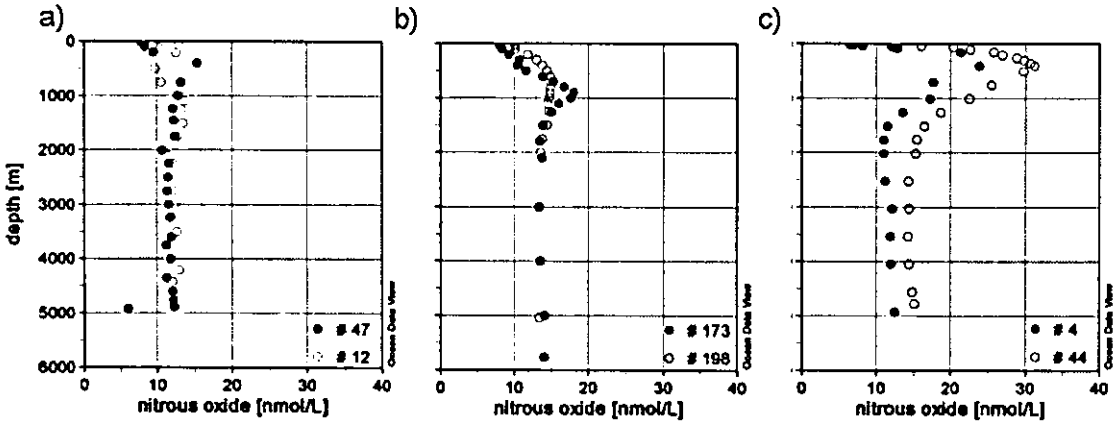

Fig. 5: Selected vertical N_2O profiles in the western basin (filled symbols) and the eastern basin (open symbols) in the North Atlantic. Stations were indicated by numbers. 5a) subpolar, 5b) subtropical, 5c) tropical North Atlantic

In the subpolar North Atlantic (Fig. 4a) vertical gradients of nitrous oxide were weak over the complete cruise track, with no clear or only a very weakly pronounced sub-surface maximum. N_2O concentrations were near equilibrium (11.0 ± 1.3 nmol L^{-1}) throughout the water column, with average concentrations of 8.6 ± 1.4 nmol L^{-1} in the surface layer (σ_θ 25.3-27.0) and 11.3 ± 1.5 nmol L^{-1} below the thermocline down to the bottom (σ_θ 26.2-27.7). No differences between the western and the eastern basin were found (Fig. 5a).

In contrast, N_2O distributions and profiles in both the subtropical and tropical North Atlantic showed strong variations with water depth (Fig. 4b-c, Fig. 5b-c). In both regions, the profiles generally had one distinct maximum. In the surface layer (σ_θ 19.3-26.8) concentrations were uniform, increasing below the thermocline up to a maximum and decreasing down to approximately 2000 m (σ_θ 22.1-27.8). Below 2000 m (σ_θ 27.8-27.9) N_2O concentrations were nearly constant with depth in both basins.

In the subtropical North Atlantic (Fig. 4b) N_2O surface concentrations were 8.7 ± 0.7 nmol L^{-1}, comparable to those in the subpolar North Atlantic. Maximum values were found at depths between 600 to 1000 m (σ_θ 26.7 – 27.7); values ranged from 14.0 in the eastern basin (#195) to 21.3 nmol L^{-1} in the western basin (#156). Below 2000 m ($\sigma_\theta > 27.8$), concentrations were nearly constant at 13.1 ± 0.9 nmol L^{-1}. Profiles in the western subtropical North Atlantic showed distinct maxima, while in the eastern basin no clear maximum was expressed (Fig. 5b). From the western to the eastern basin maximum concentrations decreased slightly from 17.7 ± 1.4 nmol L^{-1} to 15.1 ± 0.7 nmol L^{-1}. East of the Midatlantic Ridge maxima were not clearly expressed and were broader. Additionally, maximum ΔN_2O values were lower in the eastern (5.5 ± 0.6 nmol L^{-1}) than in the western basin (7.9 ± 1.3 nmol L^{-1}).

In the tropical North Atlantic (Fig. 4c) surface concentrations, with an average of 7.4 ± 1.1 nmol L^{-1}, were slightly lower than in the subtropical and subpolar North Atlantic. In contrast to the subtropical North Atlantic, maxima of N_2O concentrations were found at shallower depths of approximately 400m (σ_θ 26.8 – 27.1). The maximum values were higher in general, and ranged from 23.8 nmol L^{-1} in the western basin (#4) to 32.1 nmol L^{-1} in the eastern basin (#47). At station #36, located in the Guinea Dome area [*Siedler et al.*, 1992; *Snowden and Molinari*, 2003], we observed the highest N_2O values of about 37.3 nmol L^{-1} at 400 m (σ_θ 27.0) (Fig. 4c). At the equatorial stations the N_2O maxima were found at shallower water depths (240 m to 280 m, σ_θ 26.6 – 27.0). Maximum values ranged from 22.3 nmol L^{-1} (#26) to 24.9 nmol L^{-1} (#24). Below 2000 m ($\sigma_\theta > 27.8$) concentrations in the tropical North Atlantic were similar to those in the subtropics with an average of 13.2 ± 1.3 nmol L^{-1}. In both basins of the tropical North Atlantic profiles looked similar with sharp and clear maxima, however, concentrations throughout the water column increased from west to east (Fig. 5c). Below 2000 m ($\sigma_\theta > 27.8$) N_2O concentrations were about 2 nmol L^{-1} higher in the eastern than in the

western basin, whereas the difference of the maximum values was even higher (approximately 8 nmol L^{-1}).

N_2O profiles of the subtropical and tropical North Atlantic are in good agreement, both in absolute concentrations and shape of profiles, with those measured during the Bromine Latitudinal Air/Sea Transect II (BLAST II) cruise in Oct./Nov. 1994 [*Butler et al.*, 1995] http://www.cmdl.noaa.gov/hats/ocean/blast2/blastii.html. Below 1500 m in the North Atlantic as far as 20 °S, the mean N_2O concentration observed by Butler et al. was about 13.5 ± 1.0 nmol L^{-1} (n = 18) which is in good agreement with our measurements (12.6 ± 1.5 nmol L^{-1}, n = 449).

4.2 Comparison of nitrous oxide with other parameters

Parameters most relevant for comparison with nitrous oxide are those assumed to be directly in connection with production pathways of N_2O, like oxygen or the apparent oxygen utilization (AOU), and nitrate. In general, we found ΔN_2O positively correlated with AOU and nitrate (Fig. 6). However, in view of differences between the basins, these correlations might not be sufficient and need higher resolution. Therefore data were divided as shown in Figure 7.

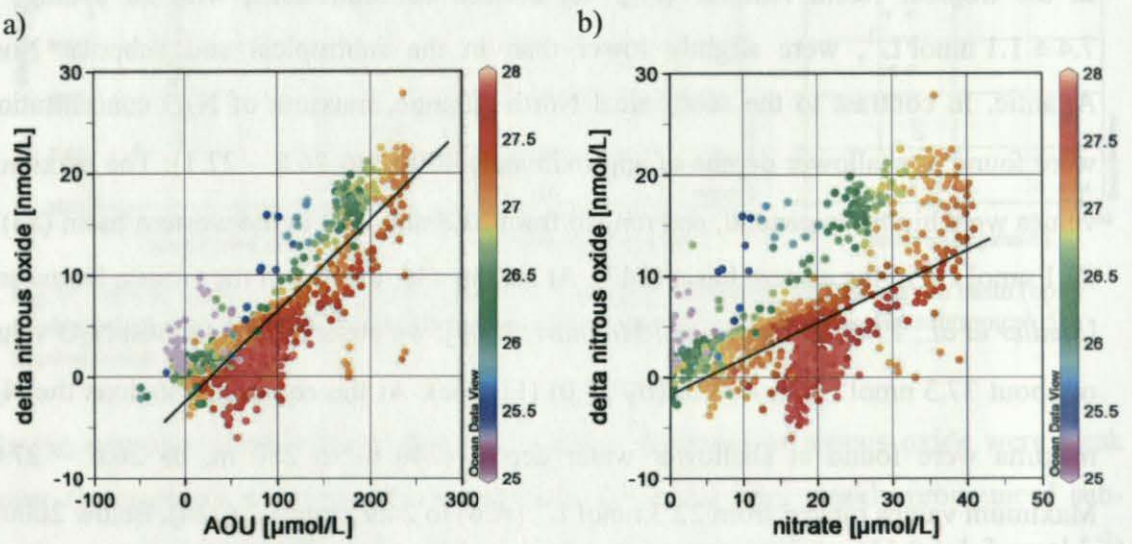

Fig. 6: ΔN_2O in comparison with AOU (6a) and nitrate (6b) for the North Atlantic, sigma σ_θ is colour coded in kg m^{-3}.
$y(\Delta N_2O) = 0.089x(AOU) - 3.245$ $R^2 = 0.71$
$y(\Delta N_2O) = 0.331x(NO_3^-) - 1.263$ $R^2 = 0.32$

In Fig. 7a-f correlations between the excess of N_2O (ΔN_2O) with AOU (Fig. 7a-c) and with NO_3^- (Fig. 7d-f) are divided for all data of the respective regions.

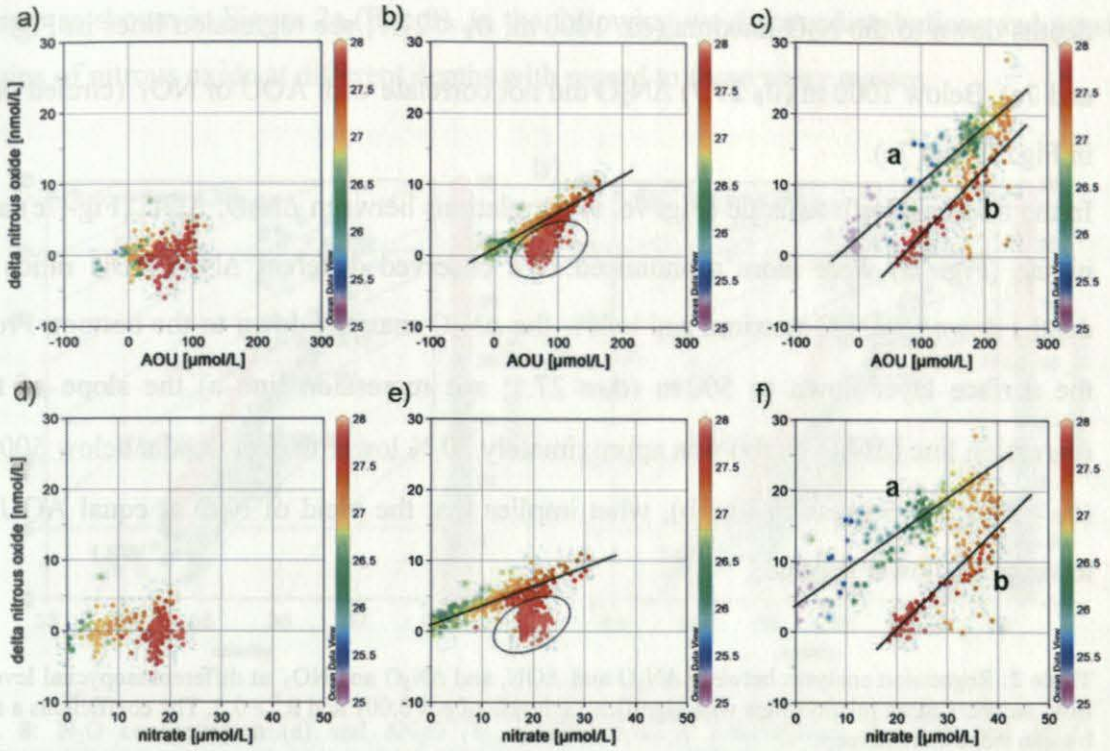

Fig. 7: ΔN_2O in comparison with AOU (7a-c) and nitrate (7d-f), sigma σ_θ is colour coded in kg m^{-3}.
7a and 7d) subpolar North Atlantic
7b and 7e) subtropical North Atlantic;
y (ΔN_2O) = 0.0473x (AOU) + 1.1409, R^2 = 0.86 for σ_θ < 27.7 (~ <1000m);
y (ΔN_2O) = 0.2497x (NO_3^-) + 1.1776, R^2 = 0.80 for σ_θ < 27.7 (~ <1000m);
circled data represent σ_θ > 27.7(~ >1000m)
7c and 7f) tropical North Atlantic;
line a: y (ΔN_2O) = 0.0785x (AOU) + 2.4381, R^2 = 0.87 for σ_θ < 27.1 (~ <500m);
line b: y (ΔN_2O) = 0.0942x (AOU) – 6.6675, R^2 = 0.81 for σ_θ > 27.1 (~ >500m);
line a: y (ΔN_2O) = -0.4848x (NO_3^-) + 3.1756, R^2 = 0.79 for σ < 27.1 (~ <500m);
line b: y (ΔN_2O) = 0.7379x (NO_3^-) – 14.665 R^2 = 0.79 for σ > 27.1 (~ >500m)

Since a multiple regression analysis turned out to be not applicable due to the co-linearity between the independent variables nitrate and AOU, we applied simple regression analysis for the isopycnal levels below the thermocline (see Tab. 2). Above the thermocline in the surface layer no correlations were found.

In the subpolar North Atlantic (Fig. 7a, d) ΔN_2O is low, with values near zero. There were no significant correlations found with AOU (Fig. 7a) or nitrate (Fig. 7d; see Tab. 2).

In the subtropical North Atlantic (Fig. 7b, e) ΔN_2O was also low with values ranging from 0 to 10 nmol L^{-1}. In contrast to the subpolar North Atlantic we found significant correlations between ΔN_2O, AOU (Fig. 7b) and nitrate (Fig. 7e; see Tab. 2), especially at depths down to the N_2O maxima (ca. 1000 m; $\sigma_\theta < 27.7$; see regression lines in Fig. 7b and 7e). Below 1000 m (σ_θ 27.7) ΔN_2O did not correlate with AOU or NO_3^- (circled data in Fig. 7b and 7e).

In the tropical North Atlantic (Fig. 7c, f) correlations between ΔN_2O, AOU (Fig. 7c) and nitrate (Fig. 7f) were more pronounced. We observed different ΔN_2O/AOU ratios at depths down to ΔN_2O maxima and below the ΔN_2O maxima down to the bottom. From the surface layer down to 500 m ($\sigma_\theta < 27.1$; see regression line a) the slope of the regression line (ΔN_2O/AOU) was approximately 20 % lower than at depths below 500 m ($\sigma_\theta > 27.1$; see regression line b), what implies that the yield of N_2O at equal AOU is lower at shallower depths.

Table 2: Regression analyses between ΔN_2O and AOU, and ΔN_2O and NO_3^- at different isopycnal levels. Bold numbers mean relationships with significance levels of $p < 0.001$ and $R^2 > 0.5$. The coefficients a and b mean slope and intercept.

			ΔN_2O / AOU			**ΔN_2O / NO_3^-**		
region	**sigma**	**n**	**a**	**b**	**R^2**	**a**	**b**	**R^2**
subpolar	thermocline - 26.0	-	-	-	-	-	-	-
	26.1 - 26.5	-	-	-	-	-	-	-
	26.6 - 27.0	13	0.045	-0.209	0.21	0.205	-0.882	0.09
	27.1 - 27.5	49	0.028	-0.452	0.23	0.159	-1.087	0.14
	27.6 - 27.9	179	0.022	-1.714	0.07	0.164	-3.240	0.03
subtropical	thermocline - 26.0	-	-	-	-	-	-	-
	26.1 - 26.5	45	**0.038**	**1.307**	**0.58**	**0.297**	**1.337**	**0.51**
	26.6 - 27.0	106	**0.065**	**0.397**	**0.75**	**0.390**	**0.186**	**0.68**
	27.1 - 27.5	121	**0.055**	**0.426**	**0.67**	**0.312**	**-0.052**	**0.60**
	27.6 - 27.9	355	0.069	-3.083	0.38	-0.126	4.579	0.02
tropical	thermocline - 26.0	34	**0.080**	**3.783**	**0.72**	**0.599**	**4.681**	**0.61**
	26.1 - 26.5	39	**0.099**	**-1.421**	**0.83**	**0.777**	**-3.212**	**0.81**
	26.6 - 27.0	98	0.107	-3.112	0.49	0.376	6.068	0.20
	27.1 - 27.5	63	0.114	-10.638	0.43	1.289	-35.05	0.42
	27.6 - 27.9	69	**0.075**	**-4.853**	**0.67**	**0.619**	**-11.83**	**0.66**

5. Discussion

Based on our results, we were able to assign measured N_2O concentrations to the water masses as shown in Figure 2a (Fig. 8). In the following we discuss distributions and possible origins of nitrous oxide at different depths with regard to these water masses.

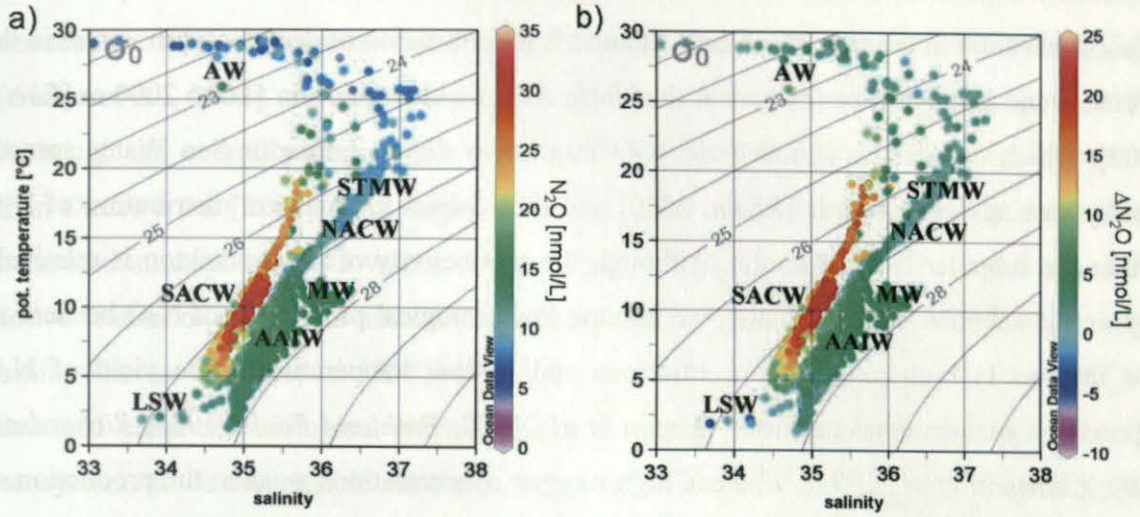

Fig. 8: N_2O concentration (a) and ΔN_2O (b) distributed in a T-S-diagram, the N_2O and ΔN_2O concentrations are colour coded in nmol L^{-1}. AW: Amazon Water; STMW: Subtropical Mode Water; MW: Mediterranean Water; SACW: South Atlantic Central Water; NACW: North Atlantic Central Water; AAIW: Antarctic Intermediate Water; LSW: Labrador Sea Water

5.1 N_2O in the surface layer of the North Atlantic

In the surface layer of the North Atlantic the distribution of N_2O was relatively uniform, with concentrations near equilibrium. This is in line with the assumption that denitrification and nitrification as sources of nitrous oxide in the surface layer seem to be negligible due to the high oxygen concentrations and light inhibition of nitrification [*Horrigan et al.*, 1981]. Thus, correlations between ΔN_2O, AOU and nitrate were nonexistent. Accordingly, we suggest that the N_2O distribution in the surface layer is most likely driven by solubility and mixing effects. This is also applicable for the enhanced N_2O concentrations found in the Labrador Current. The ΔN_2O concentrations, which are corrected for temperature, showed no enhanced values in this region. Thus, higher N_2O concentrations in the Labrador Current are likely caused by the solubility effect as well. In the warmer surface layer of the tropical North Atlantic ΔN_2O values were up to 4 nmol L^{-1}, indicating the tropical North Atlantic acts as a weak source for atmospheric N_2O [*Walter et al.*, 2004].

5.2 N_2O below the surface layer down to 2000 m

Variations of N_2O vertical profiles reflected effects of water mass ventilation and sub-surface N_2O production history. In the subpolar North Atlantic we assume that the hydrographic setting (such as convection processes during deep water formation and vertical mixing) is responsible for the observed concentrations and distributions of N_2O and ΔN_2O. The most important feature in the subpolar North Atlantic is the formation of deep water in winter in the Labrador and Irminger Seas as part of the North Atlantic circulation in 500 to 2000 m [*Rhein*, 2000], which carries the atmospheric N_2O imprint to depth. Labrador Sea Water spreads rapidly east- and southwards [*Rhein*, 2000] and thus causes the uniform distribution of N_2O within the subpolar North Atlantic. Although the productivity of phytoplankton is relatively high in the subpolar North Atlantic, we assume low biological production of N_2O because of two factors: 1) high oxygen concentrations and 2) low temperatures. The yield of N_2O depends on oxygen concentration [*Goreau et al.*, 1980; *Poth and Focht*, 1985; *Richardson*, 2000; *Codispoti et al.*, 1992], whereas high oxygen concentrations weaken the production of N_2O. Furthermore the low temperatures of the North Atlantic might have been crucial as well. The temperature dependence of both nitrification rates and enzyme activities is controversially discussed [*Berounsky and Nixon*, 1990; *Vouve et al.*, 2000; *Barnard et al.*, 2005; *Herbert*, 1999; *Rheinheimer*, 1964; *Hansen et al.*, 1981; *Rysgaard et al.*, 1996], however growth rates and biological production of bacteria clearly depend on the prevailing temperatures [*Bock and Wagner*, 2001; *Hoppe et al.*, 2002]. Thus, N_2O production might not be limited directly by temperature but indirectly by the limited abundance of N_2O producing bacteria.

In the subtropical North Atlantic concentrations of N_2O and ΔN_2O were distinctly higher compared to the subpolar North Atlantic. Profiles differed clearly between the western and eastern basin. N_2O profiles in the western basin showed clearly expressed N_2O maxima between 600 to 1000 m. This pattern was not observable east of the Midatlantic Ridge where N_2O and ΔN_2O concentrations were lower than in the western basin, and no peak maxima were observed. Hydrographic processes likely explain the shape of profiles, especially the advection of Labrador Sea Water (LSW) into the eastern basin. LSW with low N_2O concentrations is transported either along the eastern continental slope of America or across the Charlie-Gibbs-Fracture-Zone [*Bower et al.*, 2002]. It flows into the eastern subtropical basin at 500-2000 m [*Rhein*, 2000; *Alvarez et al.*, 2004], and spreads north- and southwards [*Bower et al.*, 2002; *Rhein*, 2000]. In the western basin N_2O concentrations and profiles are in agreement with profiles published by [*Yoshinari*, 1976], who also found maximum values in

water masses with lower oxygen concentrations. These were identified as Antarctic Intermediate Water (AAIW), which flows northwards. We assume the AAIW transports N_2O from the south to the subpolar North Atlantic. At depths shallower than 1000 m ($\sigma_\theta < 27.7$) ΔN_2O was significantly correlated with oxygen utilization and nitrate concentrations (Fig. 7b, 7e; Tab. 2), indicating nitrification has contributed to measured N_2O concentrations.

In the tropical North Atlantic the N_2O profiles and the observed trend along the West-East transect are in overall agreement with recently published data from a transect along 7.5 °N [*Oudot et al.*, 2002] and a previous study in the Guinea Dome area [*Oudot et al.*, 1990]. Although the overall pattern is the same, we observed generally lower N_2O concentrations than *Oudot et al.* [2002]. This might be a result of a calibration disagreement, supported by measured atmospheric N_2O values of 316 ppb in 1993. For example, we found a peak N_2O concentration of up to 37.3 nmol L^{-1} in South Atlantic Central Water (SACW) of the eastern basin, whereas *Oudot et al.* [2002] reported values of up to 60 nmol kg^{-1}. *Oudot et al.* [2002] assumed enhanced biological activity and remineralization of organic matter in upwelling ecosystems to be responsible for these higher values in the east. However, upwelling in this area is a temporary event [*Voituriez et al.*, 1982; *Siedler et al.*, 1992], and during our cruise no upwelling was observed.

Despite the fact that upwelling might have a long-term large-scale effect, we suppose additional reasons for the higher N_2O concentrations in the eastern basin. The productivity in the eastern basin is fueled not only by coastal upwelling [*Signorini et al.*, 1999] but also by dust deposition off the West African coast [*Mills et al.*, 2004]. Moreover, nutrient input by major tropical rivers such as the Senegal, Gambia and Niger [*Perry et al.*, 1996] contribute to enhanced production off the West African coast, indicated by enhanced chlorophyll a concentrations (for the 2002 seasonal cycle of chlorophyll a see monthly data set of Sea-viewing Wide Field-of-view Sensor (SeaWiFS): http://earthobservatory.nasa.gov/Observatory/Datasets/chlor.seawifs.html.

Enhanced productivity leads to a high export production [*Antia et al.*, 2001]. Subsequently lowered O_2 concentrations in the eastern intermediate layers due to the demineralization of organic matter support the production of N_2O. Therefore, enhanced N_2O concentrations in the eastern basin at this time of year (Oct./Nov. 2002) might be a residual signal of past high production episode [*Signorini et al.*, 1999].

Upwelling events, indicated by lower sea surface temperatures, were only found at the equator. Surface N_2O concentration and sea surface temperature were positively correlated

[*Walter et al.*, 2004], and the comparably shallow N_2O maxima along the equator were caused by upwelling.

Due to the occurrence of linear relationships between ΔN_2O and AOU and between N_2O and nitrate we conclude that nitrification might be the major pathway of N_2O formation in the tropical Atlantic Ocean [*Yoshida et al.*, 1989]. Like N_2O, ΔN_2O showed an increasing trend from West to East indicating that nitrification is more pronounced in the eastern than the western basin of the tropical Atlantic.

5.3 N_2O in deep waters > 2000 m ($\sigma_\theta > 27.8$)

Because the deep ocean contains high nitrate concentrations, nitrification was assumed to be responsible for N_2O production [*Zehr and Ward*, 2002; *Bange and Andreae*, 1999]. Due to the low ΔN_2O in deep waters and insufficient correlations with nitrate and AOU, we assume N_2O at these depths probably originates from deep water formation and mixing processes of southern and northern hemisphere water masses. N_2O profiles from a cruise into the Antarctic circumpolar current (2 °E / 49.5 °) [Walter et al., in press] and BLAST II data east of Patagonia reveal distinctly higher N_2O concentrations in the deep waters of the southern hemisphere, with values of approximately 17 nmol L^{-1}. Northwards transport within Antarctic Bottom Water could lead to enhanced N_2O concentrations in the deep water of the North Atlantic by mixing and diffusion process.

6. Conclusions

N_2O concentrations in the North Atlantic showed characteristic variations in the vertical and horizontal distributions. In general, distribution of N_2O can be explained by a combination of biological and hydrographic reasons. The main conclusions of the present study are

- Production of N_2O by nitrification occurs mainly in the tropical North Atlantic, especially in the eastern basin. Maximum values were found in the Antarctic Intermediate Water (AAIW) in the western basin, and in the South Atlantic Central Water (SACW) in the eastern basin.
- Vertical N_2O distribution and shape of profiles in the subtropical North Atlantic originate from production by nitrification and advection of AAIW from the south into the western subtropical North Atlantic, respectively advection of LSW from the north in the eastern subtropical North Atlantic.

- In the subpolar North Atlantic mainly mixing processes may control the distribution of N_2O, particularly the deep water formation in the Labrador Sea. Production seems to be negligible.
- Tropical and subtropical regions showed supersaturation throughout the water column, thus the tropical and subtropical North Atlantic act as a source of atmospheric N_2O.
- Outflow water of the Amazon or the Mediterranean Sea does not affect the N_2O concentration.

Acknowledgements

We thank the captains and crews of FS Meteor and FS Gauss for their help during sampling. We especially thank Peter Fritsche, Hans Peter Hansen, Frank Malien and Jens Schafstall for nutrient and oxygen measurements and CTD handling during the Meteor cruises. Thanks to Klaus Peter Koltermann and his colleagues of the Bundesamt für Seeschifffahrt und Hydrographie in Hamburg for the opportunity to participate on the cruise 'Gauss 384-1'. Thanks to R. Hoffmann (Max Planck Institute for Chemistry, Mainz, Germany) for calibration of our standard gas mixtures. This study was financially supported by the Deutsche Forschungsgemeinschaft (DFG) by grants no WA1434/1, WA1434/3, and WA 1434/5.

References

Aiken, J., N. Rees, S. Hooker, P. Holligan, A. Bale, D. Robins, G. Moore, R. Harris, and D. Pilgrim, The Atlantic Meridional Transect: overview and synthesis of data, *Progress in Oceanography, 45* (3-4), 257-312, 2000.

Alvarez, M., F.F. Perez, H. Bryden, and A.F. Rios, Physical and biogeochemical transports structure in the North Atlantic subpolar gyre, *Journal of Geophysical Research-Oceans, 109* (C3), 2004.

Antia, A.N., W. Koeve, G. Fischer, T. Blanz, D. Schulz-Bull, J. Scholten, S. Neuer, K. Kremling, J. Kuss, R. Peinert, D. Hebbeln, U. Bathmann, M. Conte, U. Fehner, and B. Zeitzschel, Basin-wide particulate carbon flux in the Atlantic Ocean: Regional export patterns and potential for atmospheric CO_2 sequestration, *Global Biogeochemical Cycles, 15* (4), 845-862, 2001.

Bange, H.W., and M.O. Andreae, Nitrous oxide in the deep waters of the world's oceans, *Global Biogeochemical Cycles, 13* (4), 1127-1135, 1999.

Bange, H.W., S. Rapsomanikis, and M.O. Andreae, Nitrous oxide cycling in the Arabian Sea, *Journal of Geophysical Research-Oceans, 106* (C1), 1053-1065, 2001.

Barnard, R., P.W. Leadley, and B.A. Hungate, Global change, nitrification, and denitrification: A review, *Global Biogeochemical Cycles, 19* (1), doi: 10.1029/2004GB002282, 2005.

Berounsky, V.M., and S.W. Nixon, Temperature and the annual cycle of nitrification in waters of Narragansett Bay, *Limnology and Oceanography, 35* (7), 1610-1617, 1990.

Bock, E., and M. Wagner, Oxidation of inorganic nitrogen compounds as an energy source, in *The Prokaryotes: An Evolving Electronic Resource for the Microbiological Community*, 3rd edition, release 3.7, Springer Verlag, New York, 2001 http://141.150.157.117:8080/prokPUB/index.htm

Bower, A.S., B. Le Cann, T. Rossby, W. Zenk, J. Gould, K. Speer, P.L. Richardson, M.D. Prater, and H.M. Zhang, Directly measured mid-depth circulation in the northeastern North Atlantic Ocean, *Nature, 419* (6907), 603-607, 2002.

Broecker, W.S., and T.-H. Peng, Comparison of ^{39}Ar and ^{14}C ages for waters in the deep ocean, *Nuclear Instruments and Methods in Physics Research B, 172*, 473-478, 2000.

Butler, J.H., J.M. Lobert, S.A. Yvon, and L.S. Geller, The distribution and cycling of halogenated trace gases, in *Reports on Polar Research No. 168 - The expedition ANTARKTIS XII of RV "Polarstern" in 1994/95: Reports of legs ANT XII/1 and 2*, edited by G. Kattner, and D.K. Fütterer, pp. 33-40, Alfred Wegener Institute for Polar and Marine Research, Bremerhaven, 1995.

Codispoti, L.A., J.A. Brandes, J.P. Christensen, A.H. Devol, S.W.A. Naqvi, H.W. Paerl, and T. Yoshinari, The oceanic fixed nitrogen and nitrous oxide budgets: Moving targets as we enter the anthropocene?, *Scientia Marina, 65* (Suppl. 2), 85-105, 2001.

Codispoti, L.A., J.W. Elkins, T. Yoshinari, G.E. Friederich, C.M. Sakamoto, and T.T. Packard, *On the nitrous oxide flux from productive regions that contain low oxygen waters*, 271-284 pp., Oxford and IBH, New Delhi (India), 1992.

Cohen, Y., and L.I. Gordon, Nitrous oxide in the oxygen minimum of the eastern tropical North Pacific: evidence for its consumption during denitrification and possible mechanisms for its production, *Deep-Sea Research, 25* (6), 509-524, 1978.

Flückiger, J., A. Dallenbach, T. Blunier, B. Stauffer, T.F. Stocker, D. Raynaud, and J.M. Barnola, Variations in atmospheric N_2O concentration during abrupt climatic changes, *Science, 285* (5425), 227-230, 1999.

Fratantoni, D.M., and D.A. Glickson, North Brazil current ring generation and evolution observed with SeaWiFS, *Journal of Physical Oceanography, 32* (3), 1058-1074, 2002.

Gordon, A.L., Interocean exchange of thermohaline water, *Journal of Geophysical Research, 91*, 5037-5047, 1986.

Goreau, T.J., W.A. Kaplan, S.C. Wofsy, M.B. McElroy, F.W. Valois, and S.W. Watson, Production of NO_2^- and N_2O by nitrifying bacteria at reduced concentrations of oxygen, *Applied and Environmental Microbiology, 40* (3), 526-532, 1980.

Hansen, J.I., T.H. Blackburn, and K. Henriksen, Seasonal distribution of nitrifying bacteria and rates of nitrification in coastal marine sediments, *Microbial Ecology, 7* (4), 297-304, 1981.

Herbert, R.A., Nitrogen cycling in coastal marine ecosystems, *FEMS Microbiology Reviews, 23*, 563-590, 1999.

Hoppe, H.G., K. Gocke, R. Koppe, and C. Begler, Bacterial growth and primary production along a north-south transect of the Atlantic Ocean, *Nature, 416* (6877), 168-171, 2002.

Horrigan, S.G., A.F. Carlucci, and P.M. Williams, Light inhibition of nitrification in sea-surface films, *Journal of Marine Research, 39* (3), 557-565, 1981.

Joyce, T.M., A. Hernandez-Guerra, and W.M. Smethie, Zonal circulation in the NW Atlantic and Caribbean from a meridional World Ocean Circulation Experiment hydrographic section at 66°W, *Journal of Geophysical Research-Oceans, 106* (C10), 22095-22113, 2001.

Junge, C., and J. Hahn, N_2O measurements in the North Atlantic, *Journal of Geophysical Research, 76* (33), 8143-8146, 1971.

Körtzinger, A., A significant CO_2 sink in the tropical Atlantic Ocean associated with the Amazon River plume, *Geophysical Research Letters, 30* (24), 2287, doi: 10.1029/2003GL018841, 2003.

Krauss, W., Comments on the development of our knowledge of the general circulation of the North Atlantic Ocean, *The Warmwatersphere of the North Atlantic Ocean,* W. Krauss (ed.), pp 1-31, Gebrüder Borntraeger, Berlin-Stuttgart, 1996.

Lorbacher, K., Niederfrequente Variabilität meridionaler Transporte in der Divergenzzone des nordatlantischen Subtropen- und Subpolarwirbels - Der WOCE-Schnitt A2, *Bericht des Bundesamtes für Seeschifffahrt und Hydrographie, 22,* 156, 2000.

Mills, M.M., C. Ridame, M. Davey, J. La Roche, and R.J. Geider, Iron and phosphorus co-limit nitrogen fixation in the eastern North Atlantic, *Nature, 429,* 292-294, 2004.

Najjar, R.G., Marine biogeochemistry, in *Climate System Modeling*, edited by K.E. Trenberth, pp. 241-280, Cambridge University Press, Cambridge, 1992.

Oudot, C., C. Andrie, and Y. Montel, Nitrous oxide production in the tropical Atlantic Ocean, *Deep-Sea Research Part* I, *37* (2), 183-202, 1990.

Oudot, C., P. Jean-Baptiste, E. Fourre, C. Mormiche, M. Guevel, J.-F. Ternon, and P. Le Corre, Transatlantic equatorial distribution of nitrous oxide and methane, *Deep-Sea Research Part* I, *49,* 1175-1193, 2002.

Perry, G.D., P.B. Duffy, and N.L. Miller, An extended data set of river discharges for validation of general circulation models, *Journal of Geophysical Research, 101* (D16), 21,339-21,349, 1996.

Poole, R., and M. Tomczak, Optimum multiparameter analysis of the water mass structure in the Atlantic Ocean thermocline, *Deep-Sea Research Part I-Oceanographic Research Papers, 46* (11), 1895-1921, 1999.

Popp, B.N., M.B. Westley, S. Toyoda, T. Miwa, J.E. Dore, N. Yoshida, T.M. Rust, F.J. Sansone, M.E. Russ, N.E. Ostrom, and P.H. Ostrom, Nitrogen and oxygen isotopomeric constraints on the origins and sea-to-air flux of N_2O in the oligotrophic subtropical North Pacific gyre, *Global Biogeochemical Cycles, 16* (4), doi: 10.1029/2001GB001806, 2002.

Poth, M., and D.D. Focht, ^{15}N kinetic analysis of N_2O production by *Nitrosomonas europaea* - an examination of nitrifier denitrification, *Applied and Environmental Microbiology, 49* (5), 1134-1141, 1985.

Prather, M., D. Ehhalt, F. Dentener, R. Derwent, E. Dlugokencky, E. Holland, I. Isaksen, J. Katima, V. Kirchhoff, P. Matson, P. Midgley, and M. Wang, Atmospheric chemistry and greenhouse gases, in *Climate Change 2001: The Scientific Basis. Contribution of Working Group I to the Third Assessment Report of the Intergovernmental Panel on Climate Change*, edited by J.T. Houghton, Y. Ding, D.J. Griggs, M. Noguer, P.J. Van der Linden, X. Dai, K. Maskell, and C.A. Johnson, pp. 239-287, Cambridge University Press, Cambridge, UK, 2001.

Rhein, M., Oceanography - Drifters reveal deep circulation, *Nature, 407* (6800), 30-31, 2000.

Rheinheimer, G., Untersuchungen über den Einfluß der Temperatur auf die Nitrifikation im Elbe-Aestuar, *Archiv für Mikrobiologie, 49,* 283-290, 1964.

Richardson, D.J., Bacterial respiration: a flexible process for a changing environment, *Microbiology, 146,* 551-571, 2000.

Richardson, P.L., A.S. Bower, and W. Zenk, A census of Meddies tracked by floats, *Progress in Oceanography, 45* (2), 209-250, 2000.

Robertson, L.A., E.W.J. van Niel, R.A.M. Torremans, and J.G. Kuenen, Simultaneous nitrification and denitrification in aerobic chemostat cultures of *Thiosphaera pantotropha, Applied and Environmental Microbiology, 54* (11), 2812-2818, 1988.

Rysgaard, S., K. Finster, and H. Dahlgaard, Primary production, nutrient dynamics and mineralisation in a northeastern Greenland fjord during the summer thaw, *Polar Biology, 16* (7), 497-506, 1996.

Seitzinger, S.P., C. Kroeze, and R.V. Styles, Global distribution of N_2O emissions from aquatic systems: Natural emissions and anthropogenic effects, *Chemosphere: Global Science Change, 2* (3), 267-279, 2000.

Siedler, G., N. Zangenberg, and R. Onken, Seasonal changes in the tropical Atlantic circulation - Observation and simulation of the Guinea Dome, *Journal of Geophysical Research-Oceans*, *97* (C1), 703-715, 1992.

Signorini, S.R., R.G. Murtugudde, C.R. McClain, J.R. Christian, J. Picaut, and A.J. Busalacchi, Biological and physical signatures in the tropical and subtropical Atlantic, *Journal of Geophysical Research-Oceans*, *104* (C8), 18367-18382, 1999.

Snowden, D.P., and R.L. Molinari, Subtropical cells in the Atlantic Ocean: An observational summary, in *Interhemispheric Water Exchange in the Atlantic Ocean*, edited by G.J. Goni, and P. Malanotte-Rizzoli, pp. 287-312, Elsevier, New York, 2003.

Tomczak, M., Some historical, theoretical and applied aspects of qualitative water mass analysis, *Journal of Marine Research*, *57*, 275-303, 1999.

Tomczak, M., and J.S. Godfrey, *Regional Oceanography: An Introduction*, 2001. http://www.es.flinders.edu.au/~mattom/regoc/pdfversion.html

Voituriez, B., A. Herbland, and R. Leborgne, Equatorial upwelling in the eastern Atlantic during FGGE, *Oceanologica Acta*, *5* (3), 301-314, 1982.

Vouve, F., G. Guiraud, C. Marol, M. Girard, P. Richard, and M.J.C. Laima, NH_4^+ turnover in intertidal sediments of Marennes-Oleron Bay (France): effect of sediment temperature, *Oceanologica Acta*, *23* (5), 575-584, 2000.

Wallace, D.W.R., and H.W. Bange, Introduction to special section: Results of the *Meteor* 55: Tropical SOLAS Expedition, *Geophysical Research Letters*, *31* (L23S01), 1-4, 2004.

Walter, S., H.W. Bange, and D.W.R. Wallace, Nitrous oxide in the surface layer of the tropical North Atlantic Ocean along a west to east transect, *Geophysical Research Letters*, *31* (23), 2004.

Walter, S., I. Peeken, K. Lochte, A. Webb, and H.W. Bange, Nitrous oxide measurements during EIFEX, the European Iron Fertilization Experiment in the subpolar South Atlantic Ocean, *Geophys. Res. Lett.*, *32*, L 23613, doi:10.1029/2005GL024619, 2005.

Weiss, R.F., The solubility of nitrogen, oxygen and argon in water and seawater, *Deep-Sea Research*, *17*, 721-735, 1970.

Weiss, R.F., and B.A. Price, Nitrous oxide solubility in water and seawater, *Marine Chemistry*, *8*, 347-359, 1980.

Yoshida, N., H. Morimoto, M. Hirano, I. Koike, S. Matsuo, E. Wada, T. Saino, and A. Hattori, Nitrification rates and ^{15}N abundances of N_2O and NO_3^- in the western North Pacific, *Nature*, *342*, 895-897, 1989.

Yoshinari, T., Nitrous oxide in the sea, *Marine Chemistry*, *4*, 189-202, 1976.

Yoshinari, T., M.A. Altabet, S.W.A. Naqvi, L. Codispoti, A. Jayakumar, M. Kuhland, and A. Devol, Nitrogen and oxygen isotopic composition of N_2O from suboxic waters of the eastern tropical North Pacific and the Arabian Sea - Measurement by continuous-flow isotope-ratio monitoring, *Marine Chemistry*, *56* (3-4), 253-264, 1997.

Zehr, J.P., and B.B. Ward, Nitrogen cycling in the ocean: New perspectives on processes and paradigms, *Applied and Environmental Microbiology*, *68* (3), 1015-1024, 2002.

Nitrous oxide water column distribution during the transition from anoxic to oxic conditions in the Baltic Sea

S. Walter[1]*, U. Breitenbach[1], H.W. Bange[1], G. Nausch[2], D.W.R. Wallace[1]

[1]Forschungsbereich Marine Biogeochemie
IFM-GEOMAR, Leibniz-Institut für Meereswissenschaften
Düsternbrooker Weg 20
24105 Kiel, Germany

[2]Leibniz-Institut für Ostseeforschung
Warnemünde, Germany

* corresponding author:
ph. +49-431-600 1538
fax: +49-431-600 4202
e-mail: swalter@ifm-geomar.de

ms version 10 Februar 2006

submitted *Biogeosciences*

Abstract

In January 2003, a major inflow of cold and oxygen-rich North Sea Water in the Baltic Sea terminated an ongoing stagnation period in parts of the central Baltic Sea. In order to investigate the role of North Sea Water inflow to the Baltic Sea with regard to the production of nitrous oxide (N_2O), we measured dissolved and atmospheric N_2O at 26 stations in the southern and central Baltic Sea in October 2003.

At the time of our cruise, water renewal had proceeded to the eastern Gotland Basin, whereas the western Gotland Basin was still unaffected by the inflow. The deep water renewal was detectable in the distributions of temperature, salinity, and oxygen concentrations as well as in the distribution of the N_2O concentrations: Shallow stations in the Kiel Bight and Pomeranian Bight were well-ventilated with uniform N_2O concentrations near equilibrium throughout the water column. In contrast, stations in the deep basins, such as the Bornholm and the Gotland Deep, showed a clear stratification with deep water affected by North Sea Water. Inflowing North Sea Water led to changed environmental conditions, especially enhanced oxygen (O_2) or declining hydrogen sulfide (H_2S) concentrations, thus, affecting the conditions for the production of N_2O. Pattern of N_2O profiles and correlations with parameters like oxygen and nitrate differed between the basins. The dominant production pathway seems to be nitrification rather than denitrification.

No indications for advection of N_2O by North Sea Water were found. A rough budget revealed a significant surplus of in situ produced N_2O after the inflow. However, due to the permanent halocline, it can be assumed that the formed N_2O does not reach the atmosphere. Hydrographic aspects therefore are decisive factors determining the final release of produced N_2O to the atmosphere.

1. Introduction

1.1 Nitrous oxide

Nitrous oxide (N_2O) is an important atmospheric trace gas which influences, directly and indirectly, the Earth's climate: In the troposphere, it acts as a greenhouse gas with a relatively long atmospheric lifetime of 114 years (Prather et al., 2001). In the stratosphere it is the major source for nitric oxide radicals, which are involved in one of the main ozone reaction cycles (WMO, 2003).

N_2O is mainly formed during microbial processes such as nitrification and denitrification. Nitrification is an aerobic two-step process in which ammonium is oxidized to nitrate. In this process, in which typically two groups of bacteria are involved, N_2O is assumed to be a by-product, the exact metabolism however is still under discussion (Ostrom et al., 2000). In suboxic habitats, nitrate can be reduced by denitrification to molecular nitrogen, with N_2O as an intermediate (Cohen and Gordon, 1978). N_2O may also be produced by coupled nitrification and denitrification at oxic/suboxic boundaries, due to the transfer of intermediates such as nitrate and nitrite (Yoshinari et al., 1997). Other possibilities are the production of N_2O during nitrifier-denitrification or aerobic denitrification (Wrage et al., 2001). Both processes enable nitrifiers to oxidize NH_4^+ to NO_2^-, followed by the reduction of NO_2^- to N_2O or N_2 (Robertson and Kuenen, 1984; Robertson et al., 1988; Richardson, 2000). In anoxic habitats N_2O is used, instead of oxygen, as an electron acceptor (Elkins et al., 1978; Cohen and Gordon, 1978).

The yield of N_2O during these processes strongly depends on the concentration of dissolved oxygen and nitrate (Brettar and Rheinheimer, 1991; Goreau et al., 1980; Vollack and Zumft, 2001; Wetzel, 1983), with maximal N_2O accumulation at the interface between oxic and suboxic layers and depletion in anoxic layers (Codispoti et al., 2005). Positive correlations between N_2O and oxygen or nitrate are commonly interpreted as an indication of N_2O production by nitrification (Yoshinari, 1976; Yoshida et al., 1989; Cohen and Gordon, 1978). In contrast, production by denitrification is inferred by missing correlations (Elkins et al., 1978; Cohen and Gordon, 1978). However, up to now the dominant production pathway for N_2O on the global scale remains unclear and is discussed controversially (Codispoti et al., 2001; Popp et al., 2002; Yamagishi et al., 2005).

Oceans emit more than 25 % of natural produced N_2O and contribute significantly to the global N_2O budget (Prather et al., 2001; Seitzinger et al. 2000). Particularly coastal regions, including estuarine and upwelling regions, play a major role for the formation and release of N_2O to the atmosphere (Bange et al., 1996; Naqvi et al., 2000; Seitzinger et al., 2000). In the

Baltic Sea, first investigations were made by Rönner (1983) who found the Baltic Sea to be a source of atmospheric N_2O. In contrast to open ocean areas coastal regions are expected to be more influenced by conversion processes in sediments or by riverine inputs. In the Bodden waters and Danish fjords of the Baltic Sea enhanced N_2O concentrations were correlated with seasonal riverine input (Jørgensen and Sørensen, 1985; Dahlke et al., 2000). Additionally, denitrification processes in sediments were shown to contribute to the release of N_2O in Danish fjords (Jørgensen and Sørensen, 1985).

1.2 Study area

Samples of dissolved N_2O were measured at 26 stations in the western, southern and central Baltic Sea. The cruise took place on board the German research vessel Gauss (expedition no. 11/03/04) from 13th October to 25th October 2003 as part of the Cooperative Monitoring in the Baltic Sea Environment (COMBINE) program of the Baltic Marine Environment Protection Commission (Helsinki Commission, HELCOM, see http://www.helcom.fi). The locations of sampled stations are shown in Fig. 1.

The Baltic Sea is an adjacent sea of the Atlantic Ocean and part of the European continental shelf. It consists of a series of basins (Arkona, Bornholm, and Gotland Basin; see Fig. 1), with restricted horizontal and vertical water exchange due to shallow sills and a clear salinity stratification of water masses.

In January 2003 a major inflow of cold, highly saline and oxygen-rich North Sea Water was observed. It was the most important inflow event since 1993 and terminated the ongoing stagnation period in the central Baltic Sea (Feistel et al., 2003; Nausch et al., 2003). This inflow event was preceded by a minor inflow of warmer and less oxygenated water in August 2002. Due to the inflow of North Sea Water oxygen conditions changed from anoxic to oxic in most parts of the Baltic Sea. From the inflow in January 2003 until our cruise in October 2003 water renewal was already detectable at the Farö Deep (# 286), however the western Gotland Basin was still unventilated (Feistel et al., 2003; Nausch et al., 2003).

Due to the fact that N_2O production highly depends on environmental conditions such as e.g. oxygen concentration (e.g., Naqvi et al., 2000) any natural or anthropogenic-induced shifts of coastal ecosystems will modulate the formation and subsequent release of N_2O to the atmosphere. In this context the inflow of North Sea Water into the Baltic Sea offered a good opportunity to investigate naturally changing environmental conditions with regard to the production of N_2O.

1.3 Definition of water masses

We refer to four different water masses, characterized by temperature, salinity and oxygen concentrations (Fig. 3). The definition of water masses follows the description of the 'Institut für Ostseeforschung' (IOW) cruise reports (Nausch, 2003a; Nagel, 2003; Feistel, 2003; Nausch, 2003b; Nausch, 2003c; Wasmund, 2003) and the hydrographic-chemical report of the Baltic Sea in 2003 (Nausch et al., 2004). These water masses were characteristic for the time period after the inflow event in summer and autumn 2003.

The Surface Water layer (sw) was characterized by uniform temperature and salinity, in combination with high oxygen concentrations. Below this layer, rapidly decreasing temperatures indicated Winter Water (ww), which is formed annually during convection in winter. Salinity and oxygen concentrations were still uniform. The 'old' Bottom Water (bw) was visible by increasing temperature and simultaneously increasing salinity. In this water mass, located below the Winter Water, oxygen concentrations decreased rapidly, to anoxic conditions at some stations. A permanent halocline between Winter Water and Bottom Water strongly restricts the vertical exchange and is the reason for the development of stagnant deep waters with oxygen depletion up to anoxia accompanied by accumulation of hydrogen sulphide (H_2S). Bottom Water, affected by the North Sea Water inflow in January 2003 (abw) was characterized by decreasing temperature and enhanced oxygen concentrations compared to previous Bottom Water (bw) values. Due to its higher density the affected Bottom Water lifts up the 'old' Bottom Water.

2. Methods

Water samples were taken using a combined Seabird SBE911 CTD and Hydrobios rosette sampler equipped with 13 free-flow bottles. Samples for N_2O analysis were collected in triplicate from various depths. The analytical method applied was a modification of the method described by (Bange et al., 2001). Bubble free samples were taken immediately following oxygen sampling from the rosette in 24 mL glass vials, sealed directly with butyl rubber stoppers and crimped with aluminium caps. To prevent microbial activity, samples were poisoned with 500 µL of a 2 mM mercury chloride solution.10 mL of the sample were then replaced with a helium headspace for each vial, and the samples were equilibrated for at least two hours at room temperature (temperature was recorded continuously). A 9 mL subsample from the headspace was used to flush a 2 mL sample loop after passing through a moisture trap (filled with Sicapent®, Merck Germany). Gaschromatographic separation was performed at 190 °C on a packed molecular sieve column (6 ft x 1/8" SS, 5 A, mesh 80/100,

Alltech GmbH, Germany). The N_2O was detected with an electron capture detector. A mixture of argon with 5 percent by volume methane was used as carrier gas with a flow of 21 mL min^{-1}. For the two-point calibration procedure we used standard gas mixtures with 311.8 ± 0.2 ppb and 346.5 ± 0.2 ppb N_2O in synthetic air (Deuste Steininger GmbH, Mühlhausen Germany). The standard mixtures have been calibrated against the NOAA (National Oceanic and Atmospheric Administration, Boulder, Co.) standard scale in the laboratories of the Air Chemistry Division of the Max Planck Institute for Chemistry, Mainz, Germany.

2.1 Calculations

N_2O water concentrations (C_{N2O}) were calculated as follows:

$$C_{N2O}\left[\text{nmol L}^{-1}\right] = \left(\beta \times P\, V_{wp} + \frac{x\,P}{R\,T} V_{hs}\right) / V_{wp} \qquad (1)$$

where β stands for the Bunsen solubility in nmol L^{-1} atm^{-1} (Weiss and Price, 1980), x is the dry gas mole fraction of N_2O in the headspace in ppb, P is the atmospheric pressure in atm, V_{wp} and V_{hs} stand for the volumes of the water and headspace phases, respectively. R is the gas constant (8.2054 10^{-2} L atm mol^{-1} K^{-1}) and T is the temperature during equilibration. The salinity was measured by the CTD-Sensor during water sample collection; the temperature was measured while subsampling the headspace of the sample vial (i.e. the equilibration temperature). The overall relative mean analytical error was estimated to be ± 1.8 %.

The excess N_2O (ΔN_2O) was calculated as the difference between the calculated N_2O equilibrium concentration and the measured concentration of N_2O as follows

$$\Delta N_2O \text{ (nmol L}^{-1}) = N_2O \text{ (observed)} - N_2O \text{ (equilibrium)}. \qquad (2)$$

Since the water masses in the Baltic Sea are comparably young (e.g. 11 years for the oldest bottom water at the Landsort Deep) (Meier, 2005) it is reasonable to calculate the equilibrium value with the actual atmospheric N_2O mole fraction. During the cruise we measured a mean of 318 ppb (± 3 ppb, n = 84) in the atmosphere, which is in good agreement with the monthly mean of 318.5 ±0.2 ppb in October 2003 measured at Mace Head, Ireland. This value was taken from the Advanced Global Atmospheric Gases Experiment (AGAGE) data set (updated version from May 2005, available at ftp://cdiac.esd.ornl.edu (subdirectory pub/ale_gage_Agage/Agage/gc-md/monthly) at the Carbon Dioxide Information Analysis Center in Oak Ridge, Tennessee).

The apparent oxygen utilization (AOU) was calculated as follows:

$$AOU\ (\mu mol\ L^{-1}) = O_2\ (equilibrium) - O_2\ (observed). \quad (3)$$

The equilibrium values of dissolved oxygen (O_2) were calculated with the equation given by (*Weiss*, 1970). The concentration of H_2S is expressed as the negative oxygen equivalent (1 µmol L^{-1} H_2S = -2.00 µmol L^{-1} O_2). Dissolved nutrients and CTD data were provided by the participating working groups.

The N_2O inventory of single basins m_{N2O} was calculated as follows:

$$m_{N2O}\,[tons] = \overline{C}_{N2O} * n_{N2O} * V * 10^{-3} \quad (4)$$

where $\overline{C}_{N2O}$ is the mean measured N_2O concentration in the single basins from the upper part of the halocline to the bottom (nmol L^{-1}), n_{N2O} is the mole weight of N_2O (44 g mol^{-1}) and V is the water volume of the single basins (km^3).

The water volumes are based on data published in chapter 4.4.1 (*HELCOM*, 1996), available at: www.vtt.fi/inf/baltic/balticinfo/index.html.

The N_2O content of basins was calculated with data of the following stations: Bornholm Basin: station 140, 200, 213, 222, eastern Gotland Basin: station 250, 259, 260, 272, western Gotland Basin: station 240, 245, 284. Station 286 is located in the northern part of the Gotland Basin and thus has not been taken into account.

Nitrification rates (N) were estimated for the Bornholm Basin and the eastern Gotland Basin.

$$N\left[nmol\ L^{-1}\ d^{-1}\right] = \frac{\Delta m_{N2O}}{d_{basin} * V_{basin} * n * 10^{-9}} * r_{N2O} \quad (5)$$

where Δm_{N2O} is the difference of calculated N_2O content of the basins before and after the inflow event in tons, d_{basin} is the number of days from the first observation of the intrusion of North Sea Water untill our measurements (assumed by data of the cruise reports of Nausch, 2003a; Nagel, 2003; Feistel, 2003; Nausch, 2003b; Wasmund, 2003; Nausch, 2003c).

V_{basin} is the calculated volume of the basins (km^3) (based on data published in chapter 4.4.1 (HELCOM, 1996), available at: www.vtt.fi/inf/baltic/balticinfo/index.html), n is the mole weight of N_2O (44 g mol^{-1}), and r_{N2O} is the assumed N_2O release of 0.3 % in continental shelves during nitrification (Seitzinger and Kroeze, 1998).

3. Results

In order to account for the hydrographic characteristics of the Baltic Sea and the direction of the inflow of North Sea Water, we present the results according to the following classifications: I) well-mixed basins such as the Kiel, Lübeck and Pomeranian Bights and II) clearly stratified basins such as the Arkona, the Bornholm, the western and the eastern Gotland Basin (see Fig. 2). For each basin selected profiles are shown.

3.1 Well-mixed basins

At shallow stations, with depths < 30 m (station 10, 12, 22, 30, 41, 46, 121, 130, 133, 360, OB Boje, OB 4, Fig. 1), water masses were well mixed, and profiles showed nearly uniform vertical distributions of all parameters (Fig. 3a). Concentrations of N_2O were near equilibrium; however the Pomeranian Bight (station 130, 133, OB Boje, OB 4) showed enhanced saturation values (104.6 ± 7.9 %) in comparison with the Kiel Bight (station 360) and the Lübeck (station 22) and Mecklenburg Bight (station 10, 12, 41, 46; 79.3 ± 10.7 %). No correlations were found between ΔN_2O and other parameters like O_2 and NO_3^- (Fig. 3b-c).

3.2 Stratified basins

Basins with water depths > 30 m (Fig. 4-7) were clearly stratified into layers of well mixed Surface Water (sw), Winter (ww) and Bottom Water (bw) as described above. At several stations Bottom Water was affected by North Sea Water (abw), up to the Farö Deep in the northern part of the central Baltic Sea (Fig. 1, station 286) (Feistel et al., 2003). However, below 110 m the deep water of the Farö Deep was still anoxic, though with decreasing H_2S concentrations from 125 m to the bottom (Fig. 6a, lower profiles). Stations in the western Gotland Basin such as the Landsort Deep (station 284, Fig. 7a) or the Karlsö Deep (station 245, not shown) were still unaffected by the inflow event, thus below 80 m H_2S concentrations were uniform.

3.2.1 Arkona Basin

In the Arkona Basin (stations 109 and 113 (Fig. 4a)), N_2O concentrations were constant and near equilibrium (10.9 ± 0.7 nmol L^{-1}) throughout the water column. In the Winter Water below the thermocline at 15 m O_2 concentrations decreased, associated with increasing NO_2^-, NO_3^- and NH_4^+. ΔN_2O was slightly negatively correlated with O_2 (Fig. 4b), and positively correlated with NO_3^- (Fig. 4c). At the bottom below 40 m inflowing North Sea (arrow in Fig.

4a) water formed a 5 to 10 m thick oxygen enriched layer, however with no clear influence on the N_2O concentration.

3.2.2 Bornholm Basin

In the Bornholm Basin (Fig. 5, stations 140, 200, 213 and 222), N_2O profiles in the central basin (stations 200 (not shown) and 213 (Fig. 5a)) can be clearly distinguished from stations where water flows into and out of the basin. At station 140 (inflow, not shown) concentrations and distribution of N_2O and ΔN_2O were comparable to the Arkona Basin. At station 222 (outflow, not shown) N_2O concentrations in the surface layer were uniform near equilibrium at approximately 10 nmol L^{-1}, below the surface layer concentrations were uniform around 15.4 nmol L^{-1}. In the central Bornholm Basin, at station 200 (not shown) and 213 (Fig. 5a) N_2O concentrations increased rapidly within the layer affected by North Sea Water (abw, below 60 m), with N_2O values up to 31.3 nmol L^{-1} (station 200). These were the highest values measured during the entire cruise. In water masses above, N_2O was near equilibrium, with slightly enhanced ΔN_2O values in the 'old' Bottom Water (bw, 40 – 60 m). In the Bornholm Basin ΔN_2O was clearly negatively correlated with oxygen and positively with NO_3^- (Fig. 5b-c), however, both correlations were nonlinear and were fitted best by polynomials.

3.2.3 Eastern Gotland Basin

The situation became more complex in the eastern Gotland basin (stations 259, 250, 260, 271 and 286). Profiles were not as homogeneous as in the Arkona or Bornholm Basin. Again, N_2O concentrations were near equilibrium in the surface layer (sw, 0 - 20/30 m) and the Winter Water (ww, 20/30 – 60 m). At station 271 (Fig. 6a, upper profiles) the Bottom Water (bw) was completely oxygenated, with N_2O values at approximately 20 nmol L^{-1} and positive ΔN_2O. At station 286 (Fig. 6a, lower profiles) the Bottom Water (bw) was affected by the North Sea Water too, but was still anoxic. Inflow of North Sea Water was detectable by decreasing H_2S concentrations down to the bottom. Throughout the Bottom Water N_2O concentrations remained near zero. At station 250 (not shown), 271 (Fig. 6a, upper profiles) and 286 (Fig. 6a, lower profiles) a sharp local minimum of N_2O concentrations was observed at depths between 90 and 110 m (see arrows in Fig. 6a), combined with a local minimum in NO_3^- values. Except for the anoxic water masses, ΔN_2O was linearly correlated with O_2 and NO_3^- (Fig. 6b-c).

3.2.4 Western Gotland Basin

The western Gotland Basin with stations 284 (Fig. 7a), 245 and 240 revealed the "old" conditions, showing characteristics as yet unaffected by the latest intrusion of oxic North Sea Water. N_2O in the surface layer (sw, 0 - 20/40 m) and Winter Water (ww, 20/40 – 60 m) was near equilibrium. Below 50 m, oxygen concentrations decreased rapidly and N_2O concentrations dropped sharply within the oxic/anoxic interface and remained near zero in the anoxic deep waters. ΔN_2O values were negative and were not correlated with NO_3^- (Fig. 7c). ΔN_2O was logarithmically correlated with oxygen (Fig. 7b).

3.3 Estimated contribution of the North Sea Water inflow to the production of N_2O

The North Sea Water inflow consisted of a water volume of 200 km^3 (Feistel and Nausch, 2003). With an assumed N_2O concentration of 10 ± 2 nmol L^{-1} (Law and Owens, 1990), the North Sea Water transported approximately 88 ± 18 tons N_2O into the Baltic Sea.

Before the North Sea Water inflow, the deep waters below the halocline were anoxic, not only in the western but also in the eastern Gotland Basin and the Bornholm Basin (Schmidt, 2002). Thus, N_2O concentrations near zero similar to measured profiles in the western Gotland Basin in October 2003 (Fig. 7a) can be assumed. This is supported by the drop in concentration at station 286 (Fig. 7a, lower profile), which is assumed to be related to the previously anoxic bottom water. The mean N_2O concentration in the western Gotland Basin was 0.97 ± 0.34 nmol L^{-1}, on the basis of these values the calculated N_2O content of the Bornholm Basin and the eastern Gotland Basin was approximately 64 ± 23 tons before the inflow (Table 1).

After the inflow event the Bornholm Basin and the eastern Gotland Basin are clearly influenced by the North Sea Water, whereas the western Gotland Basin was still unaffected (Nausch, 2003a; Nagel, 2003; Feistel, 2003; Nausch, 2003b; Wasmund, 2003; Nausch, 2003c). The N_2O content of the Bornholm Basin and the eastern Gotland Basin, calculated with the mean of measured N_2O concentrations below the halocline in these basins, was about 1194 ± 256 tons (Table 1).

4. Discussion

Over the past two decades the previously frequent inflows of North Sea Water became rather rare (Feistel and Nausch, 2003), and oxygen levels in deep waters decreased. Thus, oxygen conditions in the Baltic Sea deep water cover a continuum from almost permanently oxic (i.e.

Arkona Basin) to almost permanently anoxic conditions (i.e. western Gotland Basin), with changes at non-regular intervals between anoxic and oxic (i.e. Bornholm Basin, eastern Gotland Basin) (Feistel, 2003; Nausch, 2003a; Nausch, 2003b; Nausch, 2003c; Nagel, 2003; Wasmund, 2003).

The inflow event in January 2003 rapidly changed the environmental conditions of the deep basins. With respect to the oxygen dependent production of N_2O, our measured N_2O concentrations reflect the continuum of unaffected and changing oxygen conditions quite well. In oxic and well mixed waters, vertical N_2O profiles were homogenous, with concentrations near equilibrium (Fig. 3a). Anoxic deep water layers, unaffected by North Sea Water (i.e. in the western Gotland Basin), had N_2O concentrations near zero (Fig. 7a). Therefore, in both cases no correlations between N_2O and either oxygen or nitrate were found (Fig. 3b-c, Fig. 7b-c). In contrast, stratified and recently ventilated water bodies in the Bornholm and eastern Gotland Basin revealed N_2O distributions that were clearly correlated with oxygen and nitrate (Fig.5b-c, Fig. 6b-c).

These vertical N_2O distributions are in general agreement with the few previously published N_2O profiles from the central Baltic Sea (Rönner, 1983; Rönner and Sörensson, 1985; Brettar and Rheinheimer, 1992). However, the past environmental settings of the deep central Baltic Sea basins were different: N_2O profiles from the central Baltic Sea reported by (Rönner, 1983) were measured when oxic conditions prevailed during August-September 1977 after a strong inflow event in 1976/1977 (Schinke and Matthäus, 1998). Their N_2O profiles are comparable to our profiles, measured in the completely oxygenated Bornholm Basin during October 2003 (Fig. 5a). Anoxic conditions were re-established in July 1979 and May-June 1980. The shape of the N_2O profiles from the then anoxic Gotland Deep, measured by Rönner and Sörensson (1985) is comparable to the N_2O profiles measured in the western Gotland Basin (e.g., the Landsort Deep, Fig. 7a). This is the same for profiles measured by Brettar and Rheinheimer (1991) in August 1986 and July 1987 during the 1983-1993 stagnation periods (Schinke and Matthäus, 1998).

In the following sections we discuss the processes that may cause the observed distributions of N_2O in the different basins.

4.1 Non-biological aspects

In surface layers and well-mixed water bodies of shallow stations, observed N_2O concentrations were near the equilibrium due to exchange with the atmosphere. In the Winter Water N_2O concentrations were also near equilibrium, however with higher absolute values than in the surface layer (see Fig. 5a-7a). Mainly hydrographic aspects were here responsible

for the observed N_2O distribution. This water mass is formed during winter convection, when N_2O concentrations were in equilibrium with the atmosphere and this signal is conserved during stratification of the upper layer in summer. The lower temperature and hence higher N_2O solubility during formation of the Winter Water are the reason for the enhanced N_2O concentrations in this layer.

A non-biological factor affecting N_2O in the deep water of the Baltic Sea might be advection with inflowing North Sea Water. Intrusion of N_2O by North Sea Water should be detectable at stratified stations, where the inflow of North Sea Water was clearly identified. In the Arkona Basin (station 109 and 113) this inflow was detectable at the bottom by lower temperature and higher oxygen concentrations; however, N_2O concentrations did not increase and remained close to equilibrium (Fig. 4a-b). These results point to only low advection of N_2O by North Sea Water, and are supported by measurements of (Law and Owens, 1990). They found N_2O concentrations close to equilibrium up to approximately 10 nmol L^{-1} in the North Sea. Thus, the enhanced N_2O values detected in layers affected by North Sea Water, for example in the Bornholm Basin (station 200 and 213), must originate from biological *in situ* production since the inflow, rather than advection.

4.2 Biological aspects

Previous studies demonstrated the existence of N_2O producing bacteria and investigated the biological pathways, namely nitrification and denitrification in the Baltic Sea (Bauer, 2003; Brettar and Höfle, 1993; Brettar et al., 2001). Both processes are commonly inferred by correlations between N_2O and oxygen or nitrate (Yoshinari, 1976; Yoshida et al., 1989; Cohen and Gordon, 1978; Butler et al., 1989).

4.2.1 Anoxic waters

In general, in anoxic and H_2S containing bottom waters N_2O concentrations were constantly near zero, and therefore no correlation with either O_2 or NO_3^- was found. The N_2O production by nitrification and denitrification might probably be inhibited by the presence of H_2S (Joye and Hollibaugh, 1995; Knowles, 1982, Sørensen et al., 1980), and while changing to anoxic conditions, N_2O can be consumed during denitrification as an electron acceptor instead of oxygen (Elkins et al., 1978; Cohen and Gordon, 1978). However, in contrast to other authors (Rönner et al., 1983; Brettar and Rheinheimer, 1992) we found low and uniformly distributed concentrations of N_2O (up to 1.7 nmol L^{-1}) in the anoxic water masses, which may have been residuals of a previous production process during oxic conditions.

4.2.2 Suboxic waters

In suboxic waters and at the boundary to anoxic water masses N_2O is expected to be mainly produced by denitrification processes (Codispoti et al., 2001), usually indicated by decreasing NO_3^- concentrations and a secondary NO_2^- peak (Wrage et al., 2001; Kristiansen and Schaanning, 2002). These indicators for denitrification were found only at the Farö Deep (station 286, 90m). However, no accumulation of N_2O was observed, rather a local minimum of N_2O was found (Fig. 6a, indicated by arrows). Hannig et al. (2005) investigated denitrification associated microorganisms in the Gotland Basin (station 271 and 286) in October 2003. They did not find denitrification activities in suboxic water masses, but a high denitrifying potential restricted to a narrow depth range at the oxic-anoxic interface and the sulfidic zone. However, in these depths an accumulation of N_2O was not found either.

The local minimum of N_2O was observed not only at the Farö Deep, but also at the Gotland Deep (Fig. 6a, indicated by arrows) and station 250 (profile not shown). A residual signal of the small inflow event in August 2002 could be observed at these depths between 90 and 110 m (Feistel et al., 2003). We assume that this minimum of N_2O is a previous signal of former anoxic bottom water, pushed up by the small inflow event in August 2002. The restriction of denitrification activity to a narrow depth range at anoxic-oxic boundaries was not only reported by Hannig et al. (2005) but also by Brettar et al. (2001). Therefore, the lack of denitrification signals leads to the question, which processes might cause the measured N_2O concentrations.

4.2.3 Correlation between N_2O and O_2

In general, in oxic waters N_2O is positively correlated with nitrate, negatively with oxygen, indicating a production by nitrification. However, below a distinct threshold of oxygen concentration a clear inversion of relationship was found. Figure 8 shows the correlation between ΔN_2O and O_2 in the Baltic Sea. At O_2 concentrations > 50 µmol L^{-1} ΔN_2O is clearly negatively correlated with O_2, indicating production by nitrification (see Fig. 8, green data points). At O_2 concentrations < 20 µmol L^{-1} ΔN_2O and O_2 were significantly positively correlated (see Fig. 8, red data points), data between 20 µmol L^{-1} and 50 µmol L^{-1} were extremely scattered (see Fig. 8, black data points).

These findings suggest a change in N_2O converting processes. Particularly in environments with rapidly changing conditions it is advantageous for microorganisms to be able to switch between different metabolic pathways. The change between aerobic and anaerobic

metabolism and thus the yield of N_2O during these processes is probably controlled particularly by the O_2 concentration, although little is known about the detailed mechanisms (Baumann et al., 1996; John, 1977; Sørensen, 1987). Our results suggest a production of N_2O during nitrification until an oxygen threshold of around 20 - 50 µmol L^{-1}, whereas the exact concentration is not to be determined due to the scattered data. Below this threshold N_2O seemed to be degraded; probably used as an electron acceptor instead of oxygen and thereby reduced to N_2 (Elkins et al., 1978; Cohen and Gordon, 1978). In the literature, threshold values of 2 µmol L^{-1} for nitrification are reported (Carlucci and McNally, 1969; Gundersen et al., 1966). For several nitrifiers the ability to switch between 'classical' nitrification, nitrifier-denitrification and aerobic denitrification was shown (Wrage et al., 2001, Whittaker et al., 2000, Zart et al., 2000, Zehr and Ward, 2002). The oxygen sensitivity is species-specific and also enzyme-specific; therefore the scatter of data might reflect the variety of involved species and enzymes (Jiang and Bakken, 2000; Goreau et al., 1980; Wetzel, 1983; Robertson et al., 1988; Richardson, 2000). Bauer (2003) investigated NH_4^+ oxidizing bacteria in the eastern Gotland Basin, and found similar bacterial communities at different depths; their nitrification activities however depended on O_2 concentrations.

Therefore, the ability of nitrifiers to perform denitrifying processes and the lack of 'classical' denitrifying signals, a switch of N_2O producing processes by nitrifiers can be assumed. These findings are in agreement with the assumptions of Rönner (1983), who also assumed, that nitrification is the main N_2O production pathway in the Baltic Sea.

Alternatively, it is also possible to interpret the data from the hydrographical or temporal point of view. Figure 9 shows the same data set as shown in Fig. 8. This time the data set is grouped not according to the oxygen concentrations but to the affiliation to different basins. Station 286 was excluded due to its transitional character. At this station anoxic conditions in the deep waters were found similar to other stations in the western Gotland Basin, but H_2S concentrations were decreasing towards the bottom. This indicates beginning ventilation, however still too weak to lead to oxic conditions.

In the stratified basins such as the Bornholm Basin, and the eastern and western Gotland Basin correlations of ΔN_2O and O_2 were regionally different and not always linear (Fig. 5b-c, 6b-c, 7a, 9). Particularly in the Bornholm Basin, N_2O and oxygen as well as N_2O and nitrate showed significant non-linear relationships (Fig. 5b-c, 9). The Bornholm Basin, which was anoxic before the inflow (Schmidt, 2002), was ventilated by North Sea Water in January 2003, months before the northern part of the eastern Gotland Basin was affected by the inflow (Nausch, 2003a, Nausch et al., 2004). In October 2003 the oxygen conditions were already

switching back to suboxic conditions (Nausch, 2003c; Wasmund, 2003), visible by decreasing oxygen concentrations compared to the beginning of the year. Accordingly the duration of elevated oxygen concentration in the respective basins may contribute to the observed accumulation of N_2O. In the eastern Gotland Basin (Fig. 6b-c, 9) the anoxic conditions changed a few months after the Bornholm Basin: the Gotland Deep was ventilated by North Sea Water in May 2003 (Nausch, 2003b). Thus, there was less time for N_2O accumulation. For various communities of NH_4^+ oxidizing bacteria different lag times after switching from anoxic to oxic incubations were shown and the production of N_2O might not have started directly after the ventilation by North Sea Water (Bodelier et al., 1996). In the western Gotland Basin (Fig. 7b-c, 9) no ventilation by North Sea Water had occurred by October 2003, therefore degradation of N_2O at the oxic-anoxic interface was found. We suspect that the correlation between ΔN_2O and O_2 in the Bornholm Basin and the eastern Gotland Basin will become similar to those of the western Gotland Basin with time, when the conditions change to anoxic.

Summarizing, we assume a conversion of N_2O mainly by nitrifiers, depending on oxygen concentration and with significant spatial and temporal characteristics.

4.3 Estimated contribution of the North Sea Water inflow to the production of N_2O

The estimated N_2O content in the stratified basins showed distinctly higher values after the inflow of the North Sea Water than before. The N_2O concentration in the North Sea Water was assumed to be near equilibrium, so there was no significant advection of N_2O from the North Sea. Thus, the observed elevated N_2O concentrations in the Baltic Sea basins result from a stimulation of N_2O production by the inflow, most likely by advection of oxygen (see Table 1).

Although more than 1000 tons of N_2O were produced, it is questionable whether the North Sea Water inflow makes the Baltic Sea a source of atmospheric N_2O. Due to the strong salinity stratification, it can be assumed that the formed N_2O stays below the permanent halocline, and therefore it will not reach the atmosphere. Commonly N_2O budgets were modelled as a function of nitrification and denitrification. Seitzinger and Kroeze (1998) modelled the distribution of N_2O production, amongst others based on the input of nitrogen compounds into estuaries by rivers. However, estimations of global N_2O emissions do not or only to a small extent take into account the hydrographic aspects. The stratification of the

water column probably lead to a reduced release of calculated amounts, and accordingly to an overestimation of N_2O emissions.

The assumption of remaining N_2O below the halocline leads to the question, whether and to what extent the nitrogen cycle might be influenced.

Based on the calculated N_2O content of the basins and the assumption of nitrification as the main production pathway N_2O production rates and nitrification rates were estimated (Table 2). These nitrification rates are in good agreement with previously published rates for the Baltic Sea (Enoksson, 1986; Bauer 2003). Bauer (2003) calculated for the eastern Gotland Basin mean nitrification rates of 21.6 ± 11.1 nmol L^{-1} at 60 m depth, respectively 44.3 ±33.1 nmol L^{-1} at 100 m depth.

These rates are comparably low (e.g. Bianchi et al., 1999); therefore the influence on the nitrogen cycle in the Baltic Sea might be small, too. N_2O might play a minor role as a reserve- or buffer-molecule during the change to anoxic conditions, preserving nitrifying processes in exchange for oxygen for a short while.

5. Conclusions

In January 2003 a major inflow of cold, highly saline and oxygen-rich North Sea Water was observed, terminating the ongoing stagnation period in parts of the central Baltic Sea.

- In agreement with previous studies, we found N_2O production mainly in oxic water masses below the Winter Water layer.
- We found no indication for advection of N_2O by North Sea Water; however, the environmental conditions for N_2O production were clearly changed due to the North Sea Water inflow.
- The inflow leads to a stimulation of N_2O production below the permanent halocline, but due to the halocline, the Baltic Sea is not a significant source of N_2O to the atmosphere.
- There was no indication for an accumulation of N_2O during denitrification. In oxic and suboxic water masses nitrification seems to be the main production pathway. The occurrence of nitrifier-denitrification and aerobic denitrification is possible, but needs further investigations.

Acknowledgements

We thank the officers and crew of R/V Gauss for their excellent support. We especially thank R. Hoffmann (MPI for Chemistry, Mainz) for the calibration of the standard gas mixtures, and

the colleagues from the IOW for providing the CTD data and the nutrients. The investigations were financially supported by the Deutsche Forschungsgemeinschaft through grant WA1434/1. The German part of the HELCOM COMBINE program is conducted by the Leibniz Institut für Ostseeforschung Warnemünde on behalf of the Bundesamt für Seeschiffahrt und Hydrographie, Hamburg and is funded by the Bundesministerium für Verkehr, Bau und Stadtentwicklung, Berlin.

References

Bange, H.W., Rapsomanikis, S., and Andreae, M.O.: Nitrous oxide in coastal waters, Glob. Biogeochem. Cycles, 10(1), 197-207, 1996.

Bange, H.W., Rapsomanikis, S., and Andreae, M.O.: Nitrous oxide cycling in the Arabian Sea, J. Geophys. Res.-Oceans, 106(C1), 1053-1065, 2001.

Bauer, S.: Structure and function of nitrifying bacterial communities in the Eastern Gotland Basin (Central Baltic Sea), Rostock, Univ., Diss., 2003, H 2003 B 4373, 2003.

Baumann, B., Snozzi, M., Zehnder, A.J.B., and van der Meer, J.R.: Dynamics of denitrification activity of Paracoccus denitrificans in continuous culture during aerobic-anaerobic changes, J. Bacteriol., 178(15), 4367-4374, 1996.

Bianchi, M., Fosset, C., and Conan, P.: Nitrification rates in the NW Mediterranean Sea, Aquatic Microbial Ecology, 17(3), 267-278, 1999.

Bodelier, P.L.E., Libochant, J.A., Blom, C.W.P., and Laanbroek, H.J.: Dynamics of nitrification and denitrification in root-oxygenated sediments and adaptation of ammonia-oxidizing bacteria to low-oxygen or anoxic habitats, Appl. Environ. Microbiol., 62, 4100-4107, 1996.

Brettar, I., and Höfle, M.G.: Nitrous oxide producing heterotrophic bacteria from the water column of the central Baltic: abundance and molecular identification, Mar. Ecol. Prog. Ser., 94, 253-265, 1993.

Brettar, I., Moore, E.R.B., and Höfle, M.G.: Phylogeny and abundance of novel denitrifying bacteria isolated from the water column of the central Baltic Sea, Microb. Ecol., 42(3), 295-305, 2001.

Brettar, I., and Rheinheimer, G.: Denitrification in the central Baltic: evidence for hydrogen sulfide oxidation as motor of denitrification at the oxic-anoxic interface, Mar. Ecol. Prog. Ser. 77(2-3), 157-169, 1991.

Brettar, I., and Rheinheimer, G.: Influence of carbon availability on denitrification in the Central Baltic Sea, Limnol. Oceanogr., 37(6), 1146-1163, 1992.

Butler, J.H., Elkins, J.W., Thompson, T.M., and Egan, K.B.: Tropospheric and dissolved N2O of the West Pacific and East Indian Oceans during the El-Nino Southern Oscillation event of 1987, J. Geophys. Res.-Atmos., 94(D12), 14865-14877, 1989.

Carlucci, A.F. and McNally, P.M.: Nitrification by marine bacteria in low concentrations of substrate and oxygen, Limnol. Oceanogr., 14, 736-739, 1969.

Codispoti, L.A., Brandes, J.A., Christensen, J.P., Devol, A.H., Naqvi, S.W.A., Paerl, H.W., and Yoshinari, T.: The oceanic fixed nitrogen and nitrous oxide budgets: Moving targets as we enter the anthropocene?, Sci. Mar., 65, 85-105, 2001.

Codispoti, L.A., Yoshinari, T., and Devol, A.H.: Suboxic respiration in the oceanic water column, in Respiration in aquatic ecosystems, edited by Del Giorgio, P.A., and Williams, P.J.l.B., pp. 225-247, Oxford University Press, Oxford, 2005.

Cohen, Y., and Gordon, L.I.: Nitrous oxide in the oxygen minimum of the eastern tropical North Pacific: Evidence for its consumption during denitrification and possible mechanisms for its production, Deep-Sea Res., 25(6), 509-524, 1978.

Dahlke, S., Wolff, S., Meyer-Reil, L.-A., Bange, H.W., Ramesh, R., Rapsomanikis, S., and Andreae, M.O.: Bodden waters (southern Baltic Sea) as a source of methane and nitrous oxide, in Proceedings in Marine Sciences, Volume 2: Muddy Coast Dynamics and Resource Management, edited by Flemming, B.W., Delafontaine, M.T., and Liebezeit, G., pp. 137-148, Elsevier Science, Amsterdam, 2000.

Elkins, J.W., Wofsy, S.C., McElroy, M.B., Kolb, C.E., and Kaplan, W.A.: Aquatic sources and sinks for nitrous oxide, Nature, 275(5681), 602-606, 1978.

Enoksson, V.: Nitrification rates in the Baltic Sea: Comparison of three isotope techniques, Appl. Environ. Microbiol., 51(2), 244-250, 1986.

Feistel, R.: IOW Cruise report 11/03/02, March 2003, 2003. http://www.io-warnemuende.de/projects/monitoring/documents/cr110302.pdf

Feistel, R., Nausch, G., Matthäus, W., and Hagen, E.: Temporal and spatial evolution of the Baltic deep water renewal in spring 2003, Oceanol., 45(4), 623-642, 2003.

Feistel, R. and Nausch, G.: Water exchange between the Baltic Sea and the North Sea and conditions in the deep basins, HELCOM indicator fact sheets / Baltic Marine Environment Protection Commission – Helsinki Commission, 2003. http://www.helcom.fi/environment/indicators2003/inflow.html

Goreau, T.J., Kaplan, W.A., Wofsy, S.C., McElroy, M.B., Valois, F.W., and Watson, S.W.: Production of nitrite and nitrous oxide by nitrifying bacteria at reduced concentrations of oxygen, Appl. Environ. Microbiol., 40(3), 526-532, 1980.

Gundersen, K., Carlucci, A.F., and Boström, K.: Growth of some chemoautotrophic bacteria at different oxygen tensions, Experientia, 22, 229-230, 1966.

Hannig, M., Braker, G., Lavik, G., Kuypers, M., Dippner, J. W., and Jürgens, K.: Structure and activity of denitrifying bacteria in the water column of the Gotland Basin (Baltic Sea), Abstract presented at the SPOT-ON conference 2005, Warnemünde, June 26 – July 1, 2005.

HELCOM, Third periodic assessment of the state of the marine environment of the Baltic Sea 1989-1993, Balt. Sea Environ. Proc. no. 64b, p75, 1996. http://www.baltic.vtt.fi/balticinfo/index.html

Jiang, Q.Q., and Bakken, L.R.: Nitrous oxide production and methane oxidation by different ammonia-oxidizing bacteria, Appl. Environ. Microbiol., 65, 2679-2684, 2000.

Jørgensen, B.B, and Sørensen, J.: Seasonal cycles of O_2, NO_3^- and SO_4^{2-} reduction in estuarine sediments: The significance of a NO_3^- reduction maximum in spring, Mar. Ecol. Prog. Ser., 24, 65-74, 1985.

John, P.: Aerobic and anaerobic bacterial respiration monitored by electrodes, J. Gen. Microbiol., 98, 231-238, 1977.

Joye, S.B., and Hollibaugh, J.T.: Influence of sulfide inhibition of nitrification on nitrogen regeneration in sediments, Science, 270, 623-625, 1995.

Knowles, R.: Denitrification, Microbiological Reviews, 46, 43-70, 1982.

Kristiansen, S., and Schaanning, M.T.: Denitrification in the water column of an intermittently anoxic fjord, Hydrobiologia, 469, 77-86, 2002.

Law, C.S., and Owens, N.J.P.: Denitrification and nitrous oxide in the North Sea, Neth. J. Sea Res., 25(1-2), 65-74, 1990.

Meier, M.H.E.: Modelling the age of Baltic seawater masses: Quantification and steady state sensitivity experiments, J. Geophys. Res., 110(C02006), doi:10.1029/2004JC002607, 2005.

Nagel, K.: IOW Cruise report 11/03/01, February 2003, 2003. http://www.io-warnemuende.de/projects/monitoring/documents/cr110301.pdf

Naqvi, S.W.A., Jayakumar, D.A., Narvekar, P.V., Naik, H., Sarma, V., D'Souza, W., Joseph, S., and George, M.D.: Increased marine production of N2O due to intensifying anoxia on the Indian continental shelf, Nature, 408(6810), 346-349, 2000.

Nausch G.: IOW Cruise Report 40/03/22, January 2003, 2003a. http://www.io-warnemuende.de/projects/monitoring/documents/cr400322.pdf

Nausch G.: IOW Cruise Report 44/03/03, May 2003, 2003b. http://www.io-warnemuende.de/projects/monitoring/documents/cr440303.pdf

Nausch, G.: Cruise report 11/03/04, October 2003, 2003c. ttp://www.io-warnemuende.de/projects/monitoring/documents/cr110304.pdf

Nausch, G., Feistel, R., Lass, H.-U., Nagel, K., and Siegel, H.: Hydrographisch-chemische Zustandseinschätzung der Ostsee 2003, Meereswissenschaftliche Berichte, 59(1), 1-80, 2004.

Nausch, G., Matthäus, W., and Feistel, R.: Hydrographic and hydrochemical conditions in the Gotland Deep area between 1992 and 2003, Oceanologia, 45(4), 557-569, 2003.

Ostrom, N.E., Russ, M.E., Popp, B., Rust, T.M., and Karl, D.M.: Mechanisms of nitrous oxide production in the subtropical North Pacific based on determinations of the isotopic abundances of nitrous oxide and di-nitrogen, Chemosphere: Global Change Science, 2(3-4), 281-290, 2000.

Popp, B.N., Westley, M.B., Toyoda, S., Miwa, T., Dore, J.E., Yoshida, N., Rust, T.M., Sansone, F.J., Russ, M.E., Ostrom, N.E., and Ostrom, P.H.: Nitrogen and oxygen isotopomeric constraints on the origins and sea-to-air flux of N2O in the oligotrophic subtropical North Pacific gyre, Glob. Biogeochem. Cycles, 16(4), doi: 10.1029/2001GB001806, 2002.

Prather, M., Ehhalt, D., Dentener, F., Derwent, R., Dlugokencky, E., Holland, E., Isaksen, I., Katima, J., Kirchhoff, V., Matson, P., Midgley, P., and Wang, M.: Atmospheric chemistry and greenhouse gases, in Climate Change 2001: The Scientific Basis. Contribution of Working Group I to the Third Assessment Report of the Intergovernmental Panel on Climate Change, edited by Houghton, J.T., Ding, Y., Griggs, D.J., Noguer, M., Van der Linden, P.J., Dai, X., Maskell, K., and Johnson, C.A., pp. 239-287, Cambridge University Press, Cambridge, UK, 2001.

Richardson, D.J.: Bacterial respiration: A flexible process for a changing environment, Microbiology, 146, 551-571, 2000.

Robertson, L.A., and Kuenen, J.G.: Aerobic denitrification - Old wine in new bottles, Anton Leeuwenhoek J. Microbiol., 50(5-6), 525-544, 1984.

Robertson, L.A., Vanniel, E.W.J., Torremans, R.A.M., and Kuenen, J.G.: Simultaneous nitrification and denitrification in aerobic chemostat cultures of Thiosphaera pantotropha, Appl. Environ. Microbiol., 54(11), 2812-2818, 1988.

Rönner, U.: Distribution, production and consumption of nitrous oxide in the Baltic Sea, Geochim. Cosmochim. Acta, 47, 2179-2188, 1983.

Rönner, U., Sörensson, F., and Holmhansen, O.: Nitrogen assimilation by phytoplankton in the Scotia Sea, Polar Biol., 2(3), 137-147, 1983.

Rönner, U., and Sörensson, F.: Denitrification rates in the low-oxygen waters of the stratified Baltic Proper, Appl. Environ. Microbiol., 50, 801-806, 1985.

Schinke, H., and Matthäus, W.: On the causes of major Baltic inflows - an analysis of long time series, Continental Shelf Research, 18, 67-97, 1998.

Schmidt, M.: IOW Cruise Report 11/02/03, October 2002, 2002. http://www.io-warnemuende.de/projects/monitoring/documents/cr110203.pdf

Seitzinger, S.P., and Kroeze, C.: Global distribution of nitrous oxide production and N inputs in freshwater and coastal marine ecosystems, Glob. Biogeochem. Cycles, 12(1), 93-113, 1998.

Seitzinger, S.P., Kroeze, C., and Styles, R.V.: Global distribution of N_2O emissions from aquatic systems: Natural emissions and anthropogenic effects, Chemosphere: Global Science Change, 2, 267-279, 2000.

Sørensen, J.: Nitrate reduction in marine sediment: Pathways and interactions with iron and sulfur cycling, Geomicrobiology Journal, 5(3-4), 401-422, 1987.

Sørensen, J., Tiedje, J.M., and Firestone, R.B.: Inhibition by sulfide of nitric and nitrous oxide reduction by denitrifying Pseudomonas fluorescens, Appl. Environ. Microbiol., 39(1), 105-108, 1980.

Vollack, K.U., and Zumft, W.G.: Nitric oxide signaling and transcriptional control of denitrification genes in Pseudomonas stutzeri, J. Bacteriol., 183(8), 2516-2526, 2001.

Wasmund, N.: IOW Cruise Report 44/03/07, July-August 2003, 2003 http://www.io-warnemuende.de/projects/monitoring/documents/cr440307.pdf

Weiss, R.F.: The solubility of nitrogen, oxygen and argon in water and seawater, Deep-Sea Res., 17, 721-735, 1970.

Weiss, R.F., and Price, B.A.: Nitrous oxide solubility in water and seawater, Mar. Chem., 8, 347-359, 1980.

Wetzel, R.G.: Limnology, Saunders College Publishing, Philadelphia, Pa., 1983.

Whittaker, M., Bergnamm, D., Arciero, D. and Hooper, A.B.: Electron transfer during the oxidation of ammonia by the chemolithotrophic bacterium Nitrosomonas europaea, Biochim. Biophys. Acta, 1459, 346-355, 2000.

WMO, Scientific assessment of ozone depletion: 2002, pp. 498, WMO (World Meteorological Organization), Geneva, 2003.

Wrage, N., Velthof, G.L., van Beusichem, M.L., and Oenema, O.: Role of nitrifier denitrification in the production of nitrous oxide, Soil Biol. Biochem., 33(12-13), 1723-1732, 2001.

Yamagishi, H., Yoshida, N., Toyoda, S., Popp, B.N., Westley, M.B., and Watanabe, S.: Contributions of denitrification and mixing on the distribution of nitrous oxide in the North Pacific, Geophys. Res. Lett., 32(4), 2005.

Yoshida, N., Morimoto, H., Hirano, M., Koike, I., Matsuo, S., Wada, E., Saino, T., and Hattori, A.: Nitrification rates and ^{15}N abundances of N_2O and NO_3^- in the western North Pacific, Nature, 342, 895-897, 1989.

Yoshinari, T.: Nitrous oxide in the sea, Mar. Chem., 4, 189-202, 1976.

Yoshinari, T., Altabet, M.A., Naqvi, S.W.A., Codispoti, L., Jayakumar, A., Kuhland, M., and Devol, A.: Nitrogen and oxygen isotopic composition of N_2O from suboxic waters of the eastern tropical North Pacific and the Arabian Sea - Measurement by continuous-flow isotope-ratio monitoring, Mar. Chem., 56(3-4), 253-264, 1997.

Zart, D., Schmidt, I., and Bock, E.: Significance of gaseous NO for ammonia oxidation by Nitrosomonas eutropha, Antonie van Leeuwenhoek, 77, 49-55, 2000.

Zehr, J.P., and Ward, B.B.: Nitrogen cycling in the ocean: New perspectives on processes and paradigms, Appl. Environ. Microbiol., 68(3), 1015-1024, 2002.

Figure captions

Fig. 1: Map of the western, southern and central Baltic Sea with locations of the stations. The stations were grouped as follows: well-mixed stations are number 10, 12, 22, 30, 41, 46, 121, 130, 133, 360, OB Boje and OB 4; the Arkona Basin is represented by station 109 and 113; the Bornholm Basin is represented by station 140, 200, 213 and 222; in the eastern Gotland Basin station 250, 259, 260, 271 and 286 were grouped; and the western Gotland Basin is represented by station 240, 245 and 284. The arrow indicates the main flow direction of North Sea Water.

Fig. 2: Characterization of different water masses in the Baltic Sea, for example at station 271 in the Eastern Gotland Basin (triangles: temperature (°C), circles: salinity, squares: oxygen (µmol 10^1 L^{-1}).

Fig. 3: well mixed basins; a) left plot with profiles of N_2O, calculated N_2O equilibrium concentration, NO_3^-, NO_2^- at station 41 in the Mecklenburg Bight and right plot with profiles of temperature, salinity and oxygen at station 41 in the Mecklenburg Bight; b) ΔN_2O plotted against oxygen at all stations < 30 m; c) ΔN_2O plotted against NO_3^- at all stations < 30 m

Fig. 4: Arkona Basin; a) station 113 (Arkona Deep): left plot with profiles of N_2O, N_2O equilibrium concentration, NO_3^-, NO_2^-, right plot with profiles of temperature, salinity and oxygen, the arrow indicate the influence of North Sea Water; abbreviations see Fig. 2.; b) ΔN_2O plotted against oxygen (at all stations in the Arkona Basin, $y = -0.011\ x + 3.132$, $R^2 = 0.67$); c) ΔN_2O plotted against NO_3^- (at all stations in the Arkona Basin, $y = 0.546\ x - 0.807$, $R^2 = 0.66$)

Fig. 5: central Bornholm Basin; a) station 213 (Bornholm Deep): left plot with profiles of N_2O, N_2O equilibrium concentration, NO_3^-, NO_2^-, right plot with profiles of temperature, salinity and oxygen, abbreviations see Fig. 2; b) ΔN_2O plotted against oxygen (at all stations in the Bornholm Basin, $y = 0.0003\ x^2 - 0.1531\ x + 19.517$, $R^2 = 0.88$); c) ΔN_2O plotted against NO_3^- (at all stations in the Bornholm Basin, $y = 0.0585\ x^2 + 0.1438\ x - 0.6155$, $R^2 = 0.90$)

Fig. 6: Eastern Gotland Basin; a) station 271 (Gotland Deep, upper plots) and 286 (Farö Deep, lower plots): left plots with profiles of N_2O, N_2O equilibrium concentration, NO_3^-, NO_2^-; right plots with profiles of temperature, salinity and oxygen, abbreviations see Fig. 2; b) ΔN_2O plotted against oxygen (at all stations in the Eastern Gotland Basin, $y = -0.019\ x + 5.625$, $R^2 = 0.67$ (except for $O_2 < 3$ µmol L^{-1})); c) ΔN_2O plotted against NO_3^- (at all stations in the Eastern Gotland Basin, $y = 0.639\ x - 0.459$, $R^2 = 0.62$ (except for $O_2 < 3$ µmol L^{-1}))

Fig. 7: Western Gotland Basin; a) station 284 (Landsort Deep): left plot with profiles of N_2O, N_2O equilibrium concentration, NO_3^-, NO_2^-, right plot with profiles of temperature, salinity and oxygen, abbreviations see Fig. 2; b) ΔN_2O plotted against oxygen (at all stations in the Western Gotland Basin; $y = 2.2467\ Ln(x) - 13.322$, $R^2 = 0.86$, (with exception of $O_2 < 0$ µmol L^{-1})); c) ΔN_2O plotted against NO_3^- (at all stations in the Western Gotland Basin)

Fig. 8. Correlation between ΔN_2O and O_2 in the Baltic Sea. Correlations were calculated for oxic waters with O_2 concentrations > 50 µmol L^{-1} (green coloured, $y = -0.019\ x + 5.41$, $R^2 = -0.70$) and < 20 µmol L^{-1} (red coloured, $y = 1.038\ x - 11.36$, $R^2 = 0.81$). These concentrations were empirically tested and gave the best fittings for both correlations.

Fig. 9. Correlation between ΔN_2O and O_2 in the Baltic Sea; Correlations were calculated for the Bornholm Basin (station 140, 200, 213, 222, green coloured, $y = -6.83\ Ln(x) + 37.88$, $R^2 = 0.86$), the eastern Gotland Basin (station 259, 250, 260, 271, blue coloured, $y = -0.02\ x + 5.88$, $R^2 = 0.70$) and the western Gotland Basin (station 284, 240, 245, red coloured, $y = 2.25\ Ln(x) - 13.32$, $R^2 = 0.86$). Anoxic data and station 286 were excluded.

Tables

Table 1: Estimated N_2O content of single basins in the Baltic Sea below the halocline, before and after the inflow of North Sea Water in January 2003

	mean N_2O conc. below the halocline (nmol L^{-1})	Water volume (km^3)	N_2O content before the inflow event (tons)	N_2O content after the inflow event (tons)
Bornholm Basin	> 50 m 16.59 ± 5.61	306	13 ± 5	223 ± 76
eastern Gotland Basin	> 70 m 18.46 ± 3.43	1195	51 ± 18	971 ± 180
Σ		1501	**64 ± 23**	**1194 ± 256**
western Gotland Basin	> 70 m 0.97 ± 0.34	657	28 ± 10	28 ± 10

Table 2: Estimated nitrification rates in the Bornholm Basin and the eastern Gotland Basin, based on the assumption of 0.3 % N_2O release during nitrification (Seitzinger and Kroeze, 1998)

	Δm_{N2O} (tons)	d_{basin} (day)	Water volume (km^3)	N_2O production rate (nmol L^{-1} d^{-1})	nitrification rate (nmol L^{-1} d^{-1})
Bornholm Basin	220 ± 81	265	306	0.059 ± 0.023	19.62 ± 7.57
eastern Gotland Basin	920 ± 198	167	1195	0.105 ± 0.021	34.92 ± 6.87

Figures

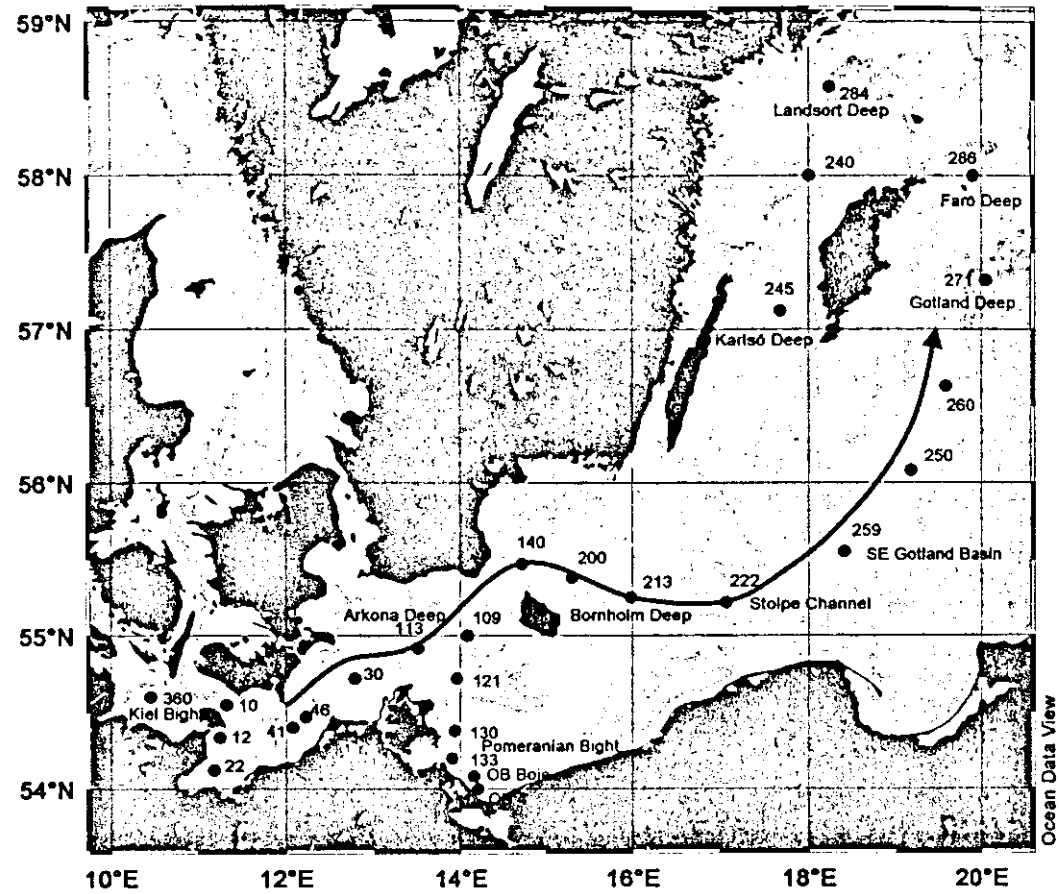

f01 (jpg)

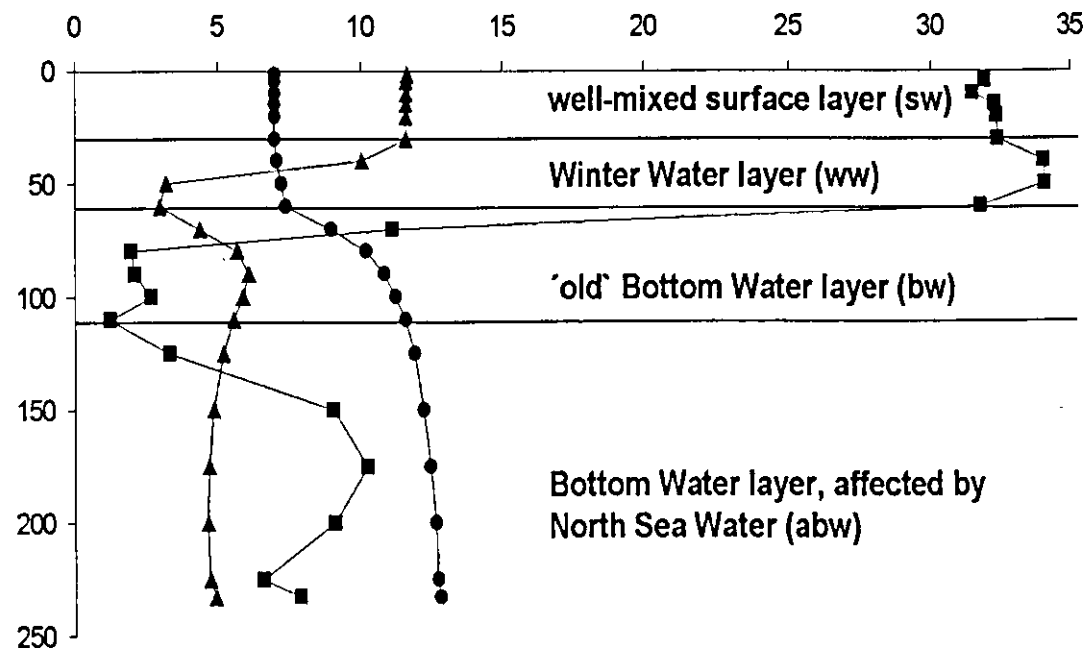

f02 (jpg)

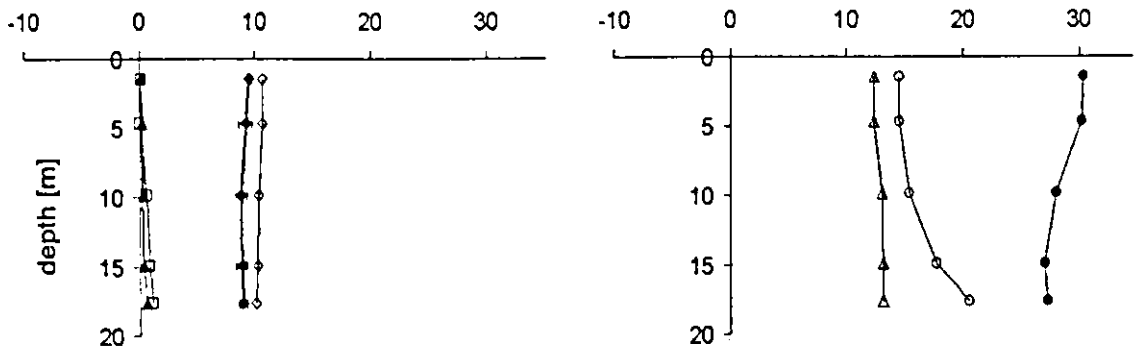

f03a (jpg)

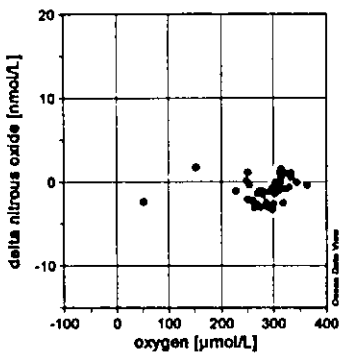

f03b (jpg)

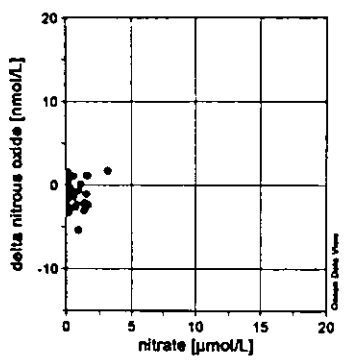

f03c (jpg)

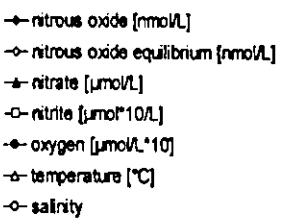

legend of f03a-c (jpg)

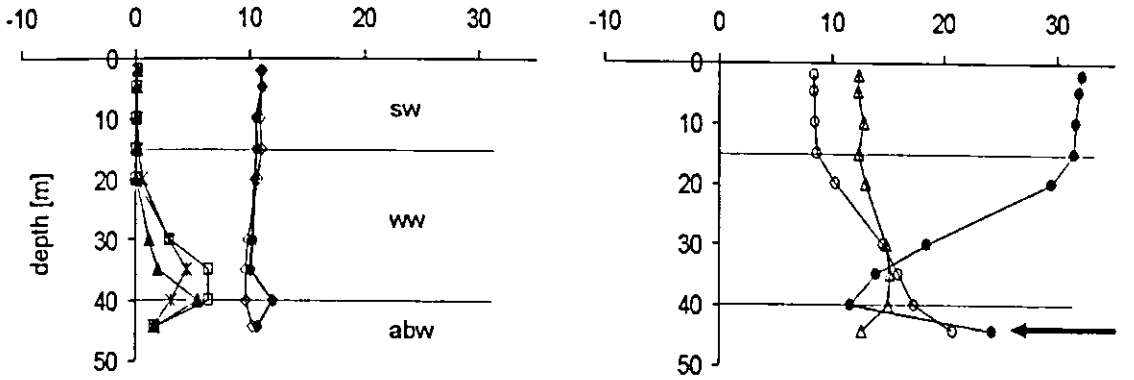

f04a (jpg)

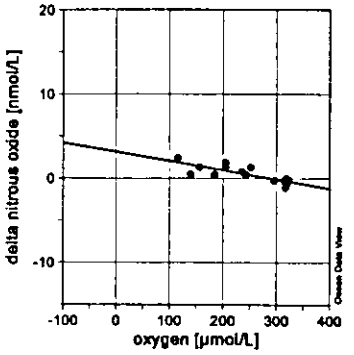

f04b (jpg)

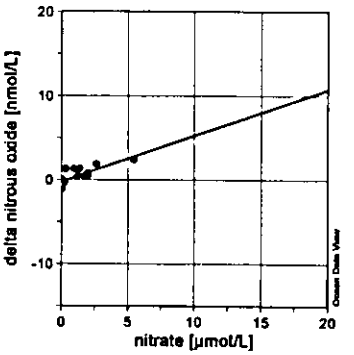

f04c (jpg)

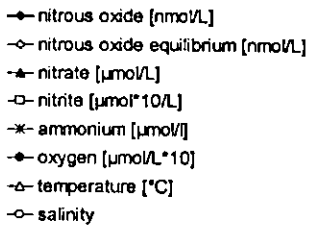

legend of f04a-c (jpg)

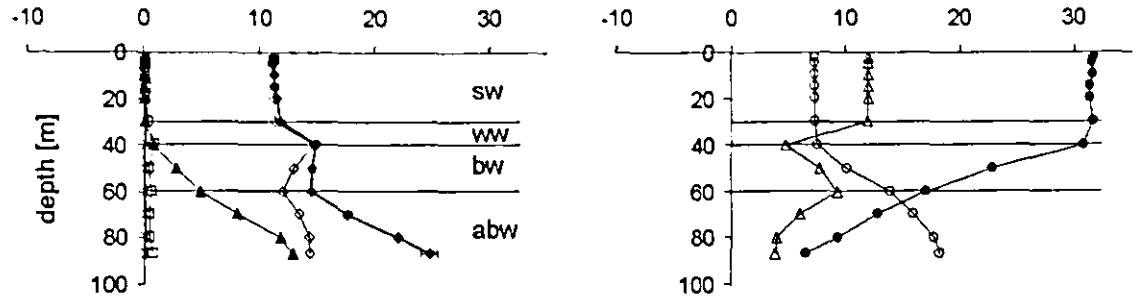

f05a (jpg)

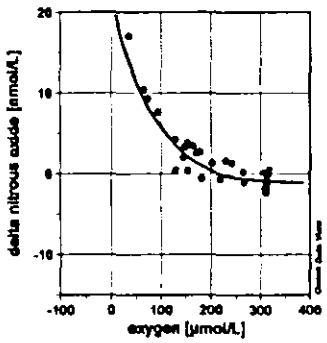

f05b (jpg)

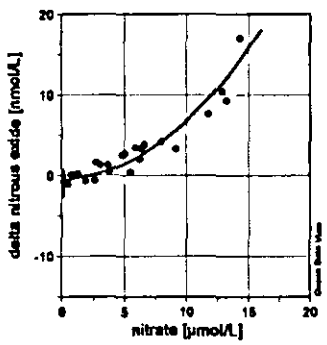

f05c (jpg)

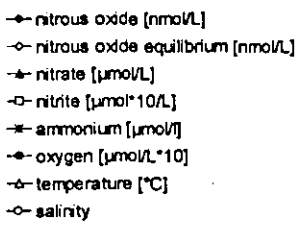

legend of f05a-c (jpg)

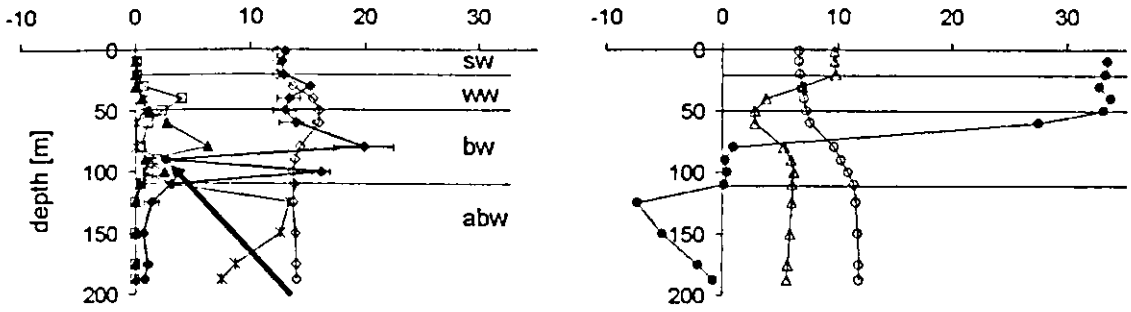

f06a station 271 (Gotland Deep) (jpg)

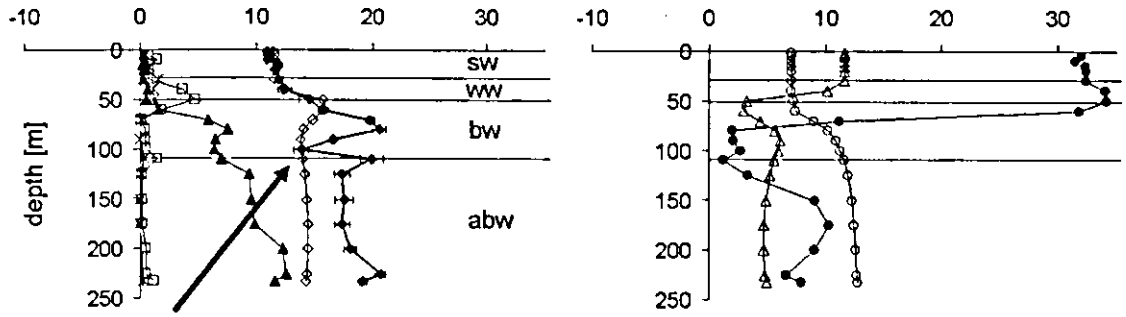

f06a station 286 (Farö Deep) (jpg)

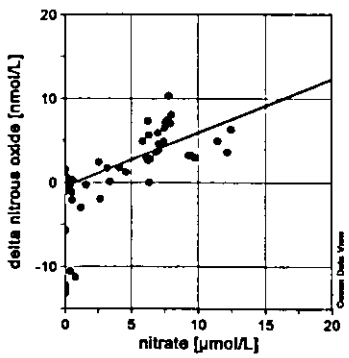

f06b

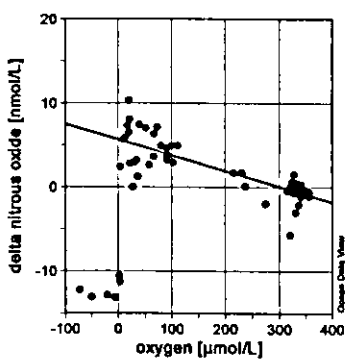

f06c (jpg)

- nitrous oxide [nmol/L]
- nitrous oxide equilibrium [nmol/L]
- nitrate [µmol/L]
- nitrite [µmol*10/L]
- ammonium [µmol/l]
- oxygen [µmol/L*10]
- temperature [°C]
- salinity

legend of f06a-c (jpg)

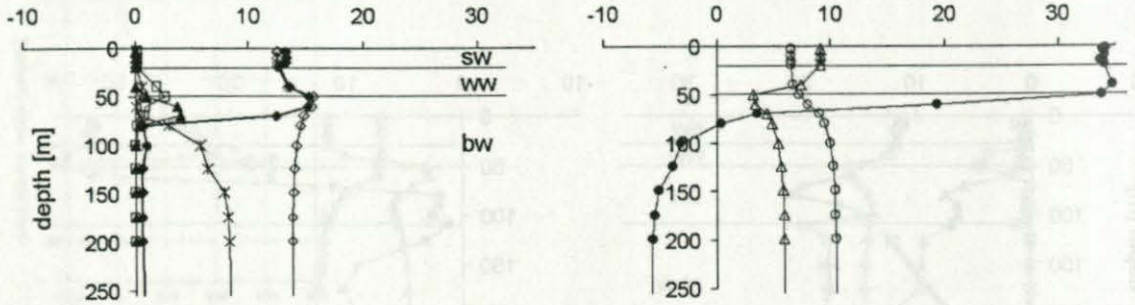

f07a (jpg)

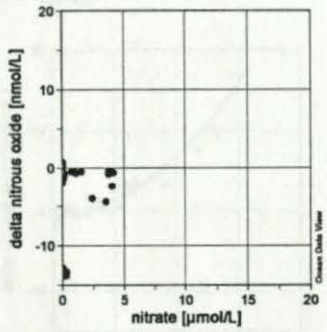

f07b (jpg)

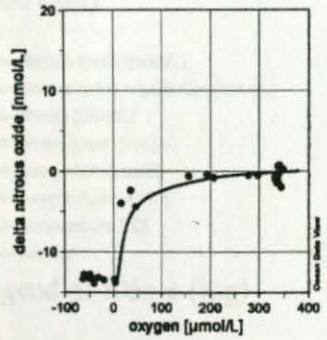

f07c (jpg)

- nitrous oxide [nmol/L]
- nitrous oxide equilibrium [nmol/L]
- nitrate [µmol/L]
- nitrite [µmol*10/L]
- ammonium [µmol/l]
- oxygen [µmol/L*10]
- temperature [°C]
- salinity

legend of f07a-c (jpg)

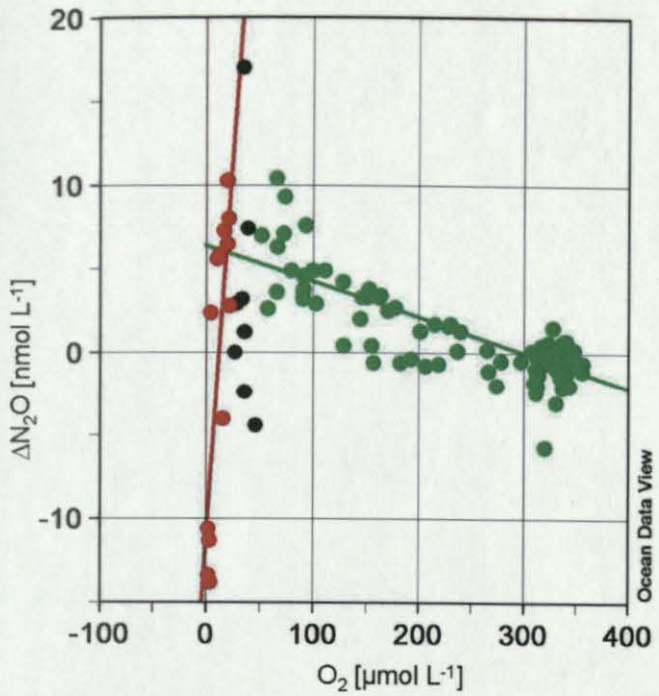

f08 (jpg)

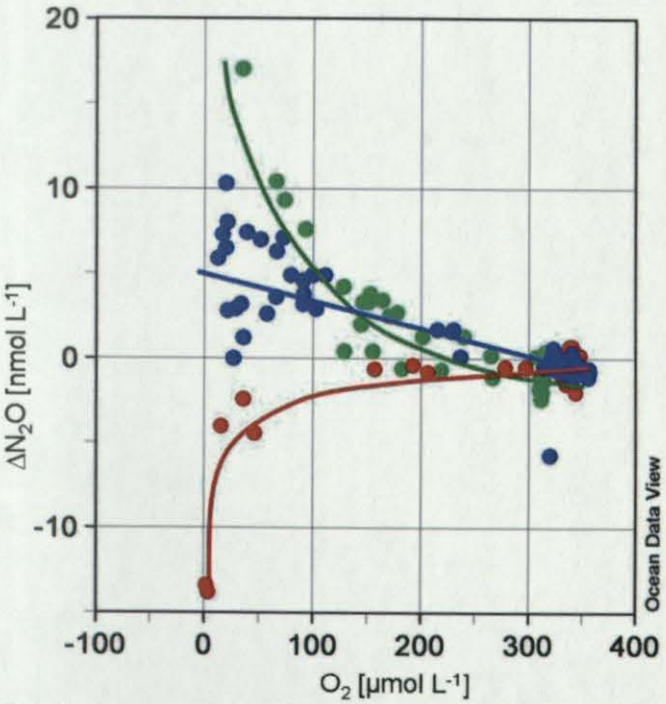

f09 (jpg)

Atmos. Chem. Phys., 1, 61–71, 2001
www.atmos-chem-phys.org/acp/1/61/

Atmospheric Chemistry and Physics

Nitrous oxide emissions from the Arabian Sea: A synthesis

H. W. Bange[1,7], M. O. Andreae[1], S. Lal[2], C. S. Law[3], S. W. A. Naqvi[4], P. K. Patra[2,8], T. Rixen[5,9], and R. C. Upstill-Goddard[6]

[1]Max Planck Institute for Chemistry, Mainz, Germany
[2]Physical Research Laboratory, Ahmedabad, India
[3]Plymouth Marine Laboratory, Plymouth, United Kingdom
[4]National Institute of Oceanography, Dona Paula, Goa, India
[5]University of Hamburg, Hamburg, Germany
[6]University of Newcastle, Newcastle upon Tyne, United Kingdom
[7]now at Institute for Marine Research, Kiel, Germany
[8]now at Frontier Research System for Global Change, Yokohama, Japan
[9]now at Center for Tropical Marine Ecology, Bremen, Germany

Received: 7 August 2001 – Published in Atmos. Chem. Phys. Discuss.: 3 September 2001
Revised: 22 November 2001 – Accepted: 3 December 2001 – Published: 28 December 2001

Abstract. We computed high-resolution (1° latitude × 1° longitude) seasonal and annual nitrous oxide (N_2O) concentration fields for the Arabian Sea surface layer using a database containing more than 2400 values measured between December 1977 and July 1997. N_2O concentrations are highest during the southwest (SW) monsoon along the southern Indian continental shelf. Annual emissions range from 0.33 to 0.70 Tg N_2O and are dominated by fluxes from coastal regions during the SW and northeast monsoons. Our revised estimate for the annual N_2O flux from the Arabian Sea is much more tightly constrained than the previous consensus derived using averaged in-situ data from a smaller number of studies. However, the tendency to focus on measurements in locally restricted features in combination with insufficient seasonal data coverage leads to considerable uncertainties of the concentration fields and thus in the flux estimates, especially in the coastal zones of the northern and eastern Arabian Sea. The overall mean relative error of the annual N_2O emissions from the Arabian Sea was estimated to be at least 65%.

1 Introduction

Nitrous oxide (N_2O) is an atmospheric trace gas that influences, directly and indirectly, the Earth's climate (Prather et al., 2001). Source estimates indicate that the world's oceans play a major role in the global budget of atmospheric N_2O (Seitzinger et al., 2000). Upwelling regions, such as the eastern tropical Pacific and the Arabian Sea, are sites of high N_2O production via denitrification and/or nitrification processes that occur at the boundaries of the oxygen depleted water masses (Codispoti et al., 1992). Following the studies of Law and Owens (1990) and Naqvi and Noronha (1991), it has been speculated that the Arabian Sea, especially its upwelling-dominated northwestern part, represents a hot spot for N_2O emissions and makes a substantial contribution to the global budget of atmospheric N_2O. However, the situation is apparently somewhat more complicated, because recent data show seasonal N_2O emissions from the continental shelf area of India also to be important (Naqvi et al., 2000). Previous N_2O flux estimates are compromised by significant temporal and spatial biases. Moreover, we recognize that in efforts to model global oceanic N_2O emissions, the Arabian Sea appears to be under-represented mainly owing to the relatively low spatial resolution of the applied models and/or missing data from this region (Nevison et al., 1995; Seitzinger et al., 2000; Suntharalingam and Sarmiento, 2000). Here we present a comprehensive compilation of N_2O measurements from the Arabian Sea surface layer from 1977 to 1997. These data were used to calculate mean seasonal and annual climatological N_2O fields with a 1° latitude × 1° longitude resolution. On the basis of the N_2O surface concentration fields, N_2O emissions from the Arabian Sea were reassessed.

Correspondence to: H. W. Bange (hbange@ifm.uni-kiel.de)

Table 1. Overview of the N_2O Source Data

Arabian Sea Region	Cruise Dates	Method	N	References
West, Central	Dec 1977–Jan 1978	Con	668	Weiss et al. (1992)[a]
Northwest, Central	Sep 1986	Dis	19	Law and Owens (1990)
East, Central	Dec 1988	Dis	15	Naqvi and Noronha (1991)
East, Central	Apr–May 1994, Feb–Mar, Jul–Aug 1995, Aug 1996, Feb 1997	Dis	125	Lal and Patra (1998)[b]
Northwest, Central	Sep, Nov–Dec 1994	Dis	47	Upstill-Goddard et al. (1999)
Northwest, Central	May, Jul–Aug 1995, Mar, May–Jul 1997	Con	1569	Bange et al. (1996a)[c] Bange et al. (2000)[c]
East	Jul 1995	Dis	20	Naqvi et al. (1998)

Con stands for continuous measurements.
Dis stands for measurements of discrete samples. N stands for number of data points.
[a] Data are available from the anonymous ftp site cdiac.esd.ornl.edu (subdirectory /pub/ndp044) at the Carbon Dioxide Information Analysis Center in Oak Ridge, Tennessee.
[b] Data are included in the JGOFS-India data compilation on CD-ROM available from the Indian National Oceanographic Data Centre, Goa, India (ocean@csnio.ren.nic.in).
[c] Data are available from the German JGOFS data management (http://www.ifm.uni-kiel.de/jgofs/dm).

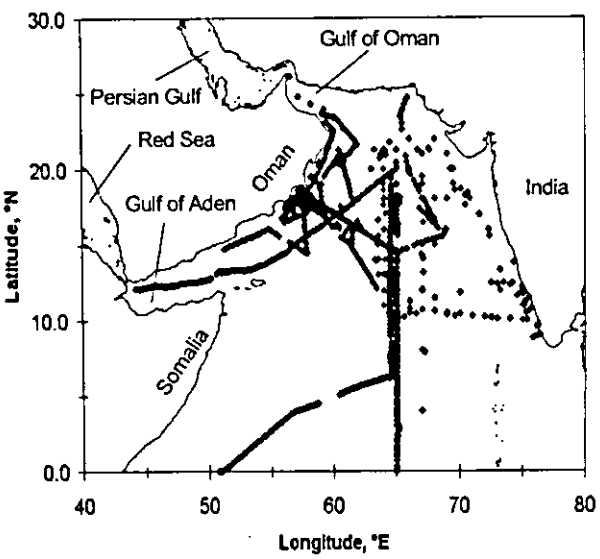

Fig. 1. Map of the Arabian Sea with locations of the N_2O measurements in the surface layer used in our study (see Table 1).

2 Data sources

For our study we compiled N_2O measurements from 0–10 m water depth within the study area (44°–80° E, 0°–27° N) excluding the Persian Gulf and the Red Sea (Fig. 1). The majority of the data were collected during individual national contributions to the international Joint Global Ocean Flux Study (JGOFS) – Arabian Sea Process Study between 1994 and 1997. Pre-JGOFS data were from cruises in 1977/1978, 1986, and 1988. An overview of the data sources is given in Table 1. (Unfortunately, data from the 1992 Netherlands Indian Ocean Program were unavailable for this reassessment.) N_2O concentrations are typically reported in nmol L^{-1}, however, the data listed in Weiss et al. (1992) are in dry mole fractions. We recalculated the Weiss et al. (1992) N_2O concentrations with the reported water temperature, a mean seasonal salinity of 35.75, as calculated from climatological salinity data (see below), and an atmospheric pressure of 1 atm (Weiss and Price, 1980). We are aware that this procedure introduces an additional error; however, the dependence of the N_2O solubility on salinity and pressure is small and the resulting uncertainty of about ± 1% is acceptable for our purposes.

Weekly averaged wind speeds for the period July 1987 to December 1995 were derived from satellite-based Special Sensor Microwave / Imager measurements by using an algorithm developed by Schlüssel (1995) (see Appendix A). Weekly composites of 18 km × 18 km gridded, day and night multichannel sea surface temperatures (SSTs) satellite data for the period 1986 to 1995 were provided by the Physical Oceanography Distributed Active Archive Center of the Jet Propulsion Laboratory, California Institute of Technology, Pasadena, California (http://podaac.jpl.nasa.gov:2031/DATASET_DOCS/avhrr_wkly_mcsst.html). Monthly climatological salinities with a resolution of 1° × 1° were obtained

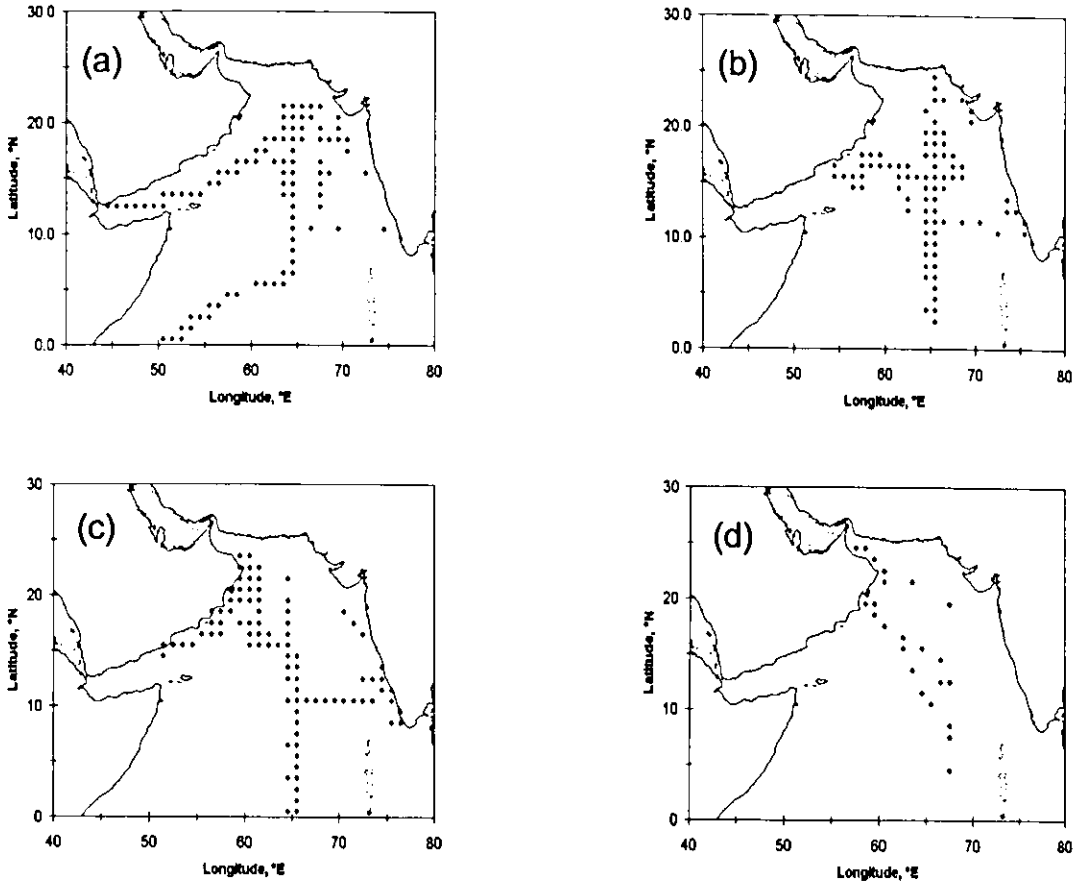

Fig. 2. Seasonal maps of N_2O pixels. **(a)** DJF, **(b)** MAM, **(c)** JJA, and **(d)** SON.

from the World Ocean Atlas 1998 (http://www.nodc.noaa.gov/OC5/data_woa.html).

3 N_2O fields

For the calculation of the N_2O fields we applied a modified procedure originally described by Conkright et al. (1994) and further developed by Kettle et al. (1999). The original data sets were combined to form a database with 2463 values. The database was then divided into 12 monthly databases. A statistical checking procedure was implemented, wherein the monthly database values were pooled into 5°× 5° squares. For each 5°× 5° square a mean and standard deviation (sd) were calculated and individual data were compared with the mean. Values falling outside 3 times the sd of the mean were omitted and the procedure was repeated until no further values were eliminated. In squares with 3 values or fewer, the checking procedure was omitted and the remaining values accepted. This procedure removed 49 data points. The modified monthly databases were then subdivided into 1° × 1° squares. Mean N_2O values (so-called N_2O pixels) were calculated from the data in each square. If there was only one value within the square, it was accepted as a pixel. Monthly N_2O pixel data sets were then combined into four seasonal sets: northeast (NE) monsoon (December to February, DJF), intermonsoon (March to May, MAM), southwest (SW) monsoon (June to August, JJA), and intermonsoon (September to November, SON) (Figs. 2a-d). Finally, the four seasonal sets were combined to form an annual N_2O pixel set. For the annual and for each of the four seasonal and pixel sets, we calculated means for Arabian Sea biogeographic provinces, i.e. the Northwestern Arabian Upwelling, Indian Monsoon Gyres, and Western India Coastal provinces (INDW) (Longhurst, 1998). The biogeographic means were used to create a 1°× 1° first-guess field which was smoothed with a 9-point 2-dimensional operator (Shuman, 1957). A 1°× 1° correction field was computed for each of the seasonal and annual N_2O pixel data by applying the distance-weighted interpolation scheme of Conkright et al. (1994) (see Appendix A). In order to preclude any smoothing of small-scale features, we reduced the influence radius from 555 km to 222 km. The correction field was then added to the first-guess field and smoothed (Shu-

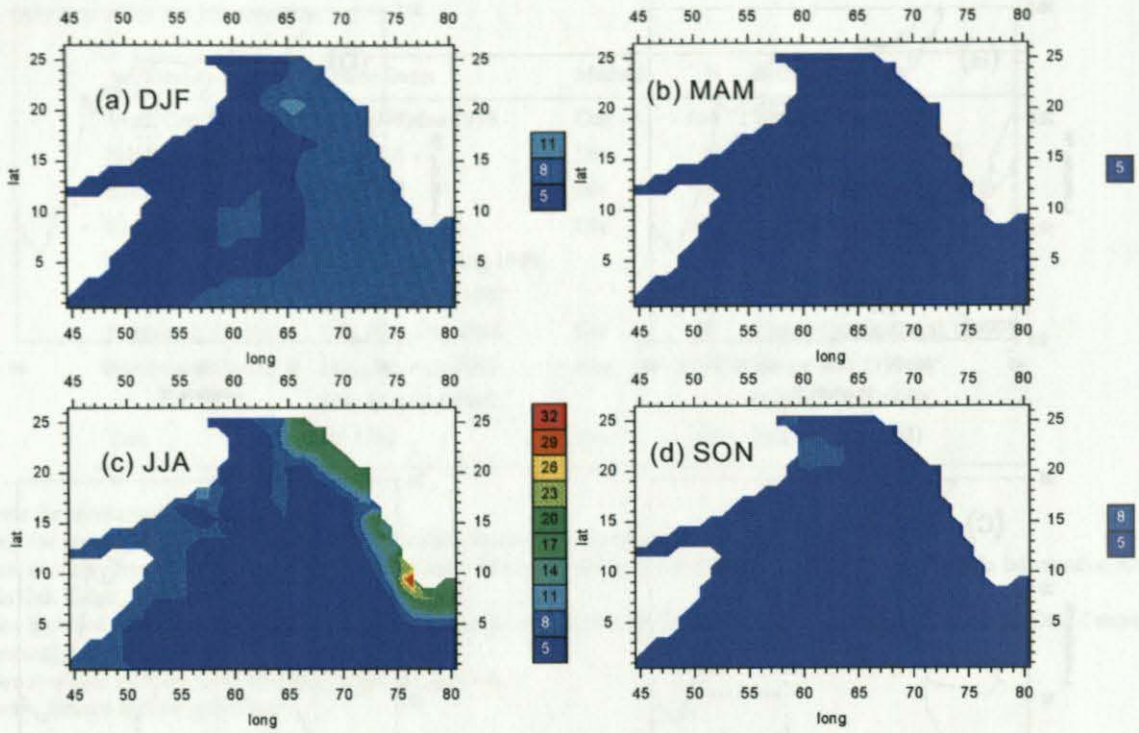

Fig. 3. Seasonal maps of the final N_2O 1°× 1° fields (in nmol L^{-1}). **(a)** DJF, **(b)** MAM, **(c)** JJA, and **(d)** SON. Contour labelling starts with 5 nmol L^{-1}; minimum concentration range is shown in dark blue (5–8 nmol L^{-1}), maximum concentration range is shown in red (> 32 nmol L^{-1}).

man, 1957), yielding the final 1°× 1° annual and seasonal N_2O fields. The final seasonal and annual N_2O concentration fields are available from the German JGOFS data management (http://www.ifm.uni-kiel.de/jgofs/dm).

4 Air-sea exchange

The air-sea exchange flux density (F) was parameterized as

$$F = k_w(u)(C_w - C_a),$$

where k_w is the gas transfer coefficient as a function of wind speed (u in 10 m height), C_w is the N_2O seawater concentration, and C_a is the equilibrium N_2O concentration in seawater. C_a was calculated using

$$C_a = \beta(T, S)x'P,$$

where x' is the atmospheric N_2O dry mole fraction, P is the atmospheric pressure, and β is the Bunsen solubility, which is a function of the water temperature (T) and salinity (S) (Weiss and Price, 1980). To calculate k_w, we used the tri-linear $k_w - u$ relationship of Liss and Merlivat (1986) (LM86), the quadratic $k_w - u$ relationship for climatological wind data of Wanninkhof (1992) (W92), and the combined linear and quadratic $k_w - u$ relationship from Nightingale et al. (2000) (N00) (Equations of the LM86, W92, and N00 approaches are given in Appendix B). k_w was adjusted by multiplying with $(Sc/600)^{-n}$ ($n = 2/3$ for wind speeds <3.6 m s^{-1} and $n = 1/2$ for wind speeds >3.6 m s^{-1}) for LM86, $(Sc/660)^{-0.5}$ for W92, and $(Sc/600)^{-0.5}$ for N00, where Sc is the Schmidt number for N_2O. Sc was calculated using empirical equations for the kinematic viscosity of seawater (Siedler and Peters, 1986) and the diffusion coefficient of N_2O in water. The N_2O diffusion coefficients (D_{N2O} in m^2 s^{-1}) were calculated with Eq. (1) derived from the data given in Broecker and Peng (1974) and, alternatively, with the new Eq. (2) derived from a compilation of actual measurements (Rhee, 2000):

$$\log_{10} D_{N2O} = -1008.28/RT - 5.245 \quad (1)$$

$$D_{N2O} = 3.16 \times 10^{-6} \exp(-18370/RT), \quad (2)$$

where T is the water temperature in K and R is the universal gas constant. Equation (1) ist based on 5 measurements of N_2O diffusion coefficients in water in a temperature range from 14° to 25°C (see compilation by Himmelblau, 1964). Unfortunately, these rather old values (two of them were already published in 1898, the rest was published in 1957) show a considerable scattering, indicating an uncertainty of up to 20% for values calculated with Eq. (1) (Broecker and Peng, 1974). Equation (2) is based on 49 measurements of

Table 2. N_2O fluxes from the Arabian Sea calculated with the N_2O diffusion coefficient of Broecker and Peng (1974)

N_2O Fields	Flux,[a] Tg N_2O	Percentage,[a] %
DJF	0.08 / 0.13 / 0.19	22 / 25 / 24
MAM	0.01 / 0.01 / 0.02	3 / 2 / 3
JJA	0.25 / 0.33 / 0.51	68 / 65 / 65
SON	0.03 / 0.04 / 0.06	8 / 8 / 8
Sum	0.37 / 0.51 / 0.78	

[a] First value calculated according to LM86; second value calculated according to N00, and third value calculated according to W92.

Table 3. N_2O Fluxes from the Arabian Sea calculated with the N_2O diffusion coefficient of Rhee (2000)

N_2O Fields	Flux,[a] Tg N_2O	Percentage,[a] %
DJF	0.07 / 0.12 / 0.17	21 / 26 / 24
MAM	0.01 / 0.01 / 0.02	3 / 2 / 3
JJA	0.23 / 0.30 / 0.45	70 / 64 / 64
SON	0.02 / 0.04 / 0.06	6 / 9 / 9
Sum	0.33 / 0.47 / 0.70	

[a] First value calculated according to LM86; second value calculated according to N00, and third value calculated according to W92.

N_2O diffusion coefficients in water in the temperature range from 14° to 95°C (see compilation by Rhee, 2000), thus providing a more reasonable fit for the N_2O diffusion with a considerable reduced uncertainty of less then 10% (Rhee, 2000). We did not apply a correction for seawater since the effect of seawater on the diffusion of dissolved gases is variable (King et al., 1995) and, to our knowledge, no measurements of the N_2O diffusion in seawater have been published.

C_w was taken from the 1° × 1° seasonal N_2O fields (DJF, MAM, JJA, SON). For the calculation of β, Sc, and k_w, seasonal 1° × 1° fields of wind speed, SST, and salinity were computed from the data sources given above. Atmospheric pressure was set to 1 atm. A mean x' of 307 ppb for the period July 1978–July 1997 was calculated from the monthly mean values observed at the Cape Grim (Tasmania) and Adrigole/Mace Head (Ireland) monitoring stations of the ALE/GAGE/AGAGE program (updated version July 2000). The data are available from the anonymous ftp site cdiac.esd.ornl.edu (subdirectory /pub/ale_gage_Agage/Agage/monthly) at the Carbon Dioxide Information Analysis Center in Oak Ridge, Tennessee. N_2O fluxes were calculated by multiplying the area of a 1° × 1° square with its flux density calculated as described above. The sum of the N_2O fluxes of the 1° × 1° squares yields the total N_2O emissions from the Arabian Sea (surface area: 6.8 × 10^{12} m^2). The length of one degree of the meridian and the parallel (based on the international ellipsoid) were taken from the tables in Smith (1974).

5 Results and discussion

Derived seasonal N_2O concentration fields are shown in Fig. 3. Elevated N_2O concentrations occur in coastal areas of the Arabian Sea during JJA (Fig. 3c). During DJF, N_2O is higher in the eastern than in the western Arabian Sea, whereas during MAM and SON these N_2O distributions are rather similar (Figs. 3b and 3c). However, the SON database is comparatively small, lending a note of caution to such a conclusion (Fig. 2d). The seasonal variability in N_2O concentrations is clearly dominated by coastal upwelling in the Arabian Sea. During the SW monsoon, N_2O-rich subsurface waters are brought to the surface layer (see e.g., Bange et al., 2000; Patra et al., 1999). Interestingly, maximum N_2O concentrations are found on the eastern Indian continental shelf, consistent with the observations by Patra et al. (1999). However, the calculated N_2O values in the eastern Arabian Sea (>70° E) during JJA and SON, 5.8 to 36.3 nmol L^{-1} (Figs. 3c and 3d), are considerably lower than the 5.3–436 nmol L^{-1} range recently reported by Naqvi et al. (2000). It is possible that the enormous N_2O accumulation observed along the Indian coast during the late summer and autumn is in part due to an (anthropogenic?) intensification of the natural coastal hypoxic system as a shift to anoxic conditions in the subsurface layers appears to have occurred in recent years (Naqvi et al., 2000). But if the N_2O concentrations were high even before this intensification, then our analysis would underestimate the N_2O concentrations and the associated fluxes from this region, especially during SON (see below).

Annual N_2O emissions computed as the sum of the seasonal N_2O emissions range from 0.37 to 0.78 Tg N_2O yr^{-1}, depending on which air-sea transfer parameterization is used (Table 2). The use of the N_2O diffusion coefficient of Rhee (2000) yielded about 10% lower N_2O emissions ranging from 0.33 to 0.70 Tg (Table 3). Thus, we conclude that previous estimates using the N_2O diffusion coefficient of Broecker and Peng (1974) may be overestimated. However, we emphasize that the annual flux estimates presented here are associated with a mean relative error of at least 65% (for further details of the error discussion see Appendices C and D).

N_2O emissions during the SW monsoon (JJA) dominate the annual emissions, accounting for about 64–70% of the total. The second largest contribution occurs during the NE monsoon (DJF) (21–26%), whereas emissions from the intermonsoon period MAM seems to be of minor importance (2–3%). Our revised estimate for the annual N_2O flux from the Arabian Sea is much more tightly constrained than the previous consensus of 0.16–1.5 Tg N_2O yr^{-1} derived using aver-

Table 4. Summary of various N_2O flux estimates for the Arabian Sea

Source region	Area, 10^6 km^2	Flux, Tg N_2O yr^{-1}	References
Central, west (>15° N)	1.6	0.22–0.39	Law and Owens (1990)
Central, east	6.2	0.44	Naqvi and Noronha (1991)
Central, west	6.2	0.8–1.5	Bange et al. (1996a)
Central, east	6.2	0.56–1.00	Lal and Patra (1998)
Central, west	8.0	(0.41–0.75)[a]	Upstill-Goddard et al. (1999)
Central, west (> 6° N)	4.9	0.16–0.31	Bange et al. (2000)
>15° N	1.6	0.10–0.21	This study[b]
> 6° N	4.4	0.28–0.60	
> Equator	6.8	0.37[c]–0.78[c]	

[a] Fluxes are calculated according to LM86 (first value) and W92 (second value) unless stated otherwise (see footnotes b and c).
[b] Fluxes are calculated according to LM86 (first value) and the stagnant-film model of Broecker and Peng (1974) (second value).
[c] Flux calculated according to LM86.
[d] Semi-annual flux.
[e] Data calculated with the diffusion coefficient of Broecker and Peng (1974).
[f] Taken from Table 2.

aged in-situ data from a smaller number of studies (Table 4) (Bange et al., 1996a; Bange et al., 2000; Lal and Patra, 1998; Law and Owens, 1990; Naqvi and Noronha, 1991; Upstill-Goddard et al., 1999). The data listed in Table 4 depict the "historical" development of published N_2O flux estimates for the Arabian Sea and show a considerable divergence. However, the fluxes listed are difficult to compare since they were extrapolated to different Arabian Sea surface areas and partly biased by the use of non-seasonal data sets and limited spatial data coverage.

6 Conclusions

Our calculated seasonal N_2O concentration fields and associated air-sea fluxes for the Arabian Sea yield an annual N_2O flux of 0.33 (±0.21) – 0.70 (±0.46) Tg N_2O. This flux represents approximately 2–35% of the currently estimated global oceanic N_2O source of 2–17 Tg N_2O yr^{-1} (Bange et al., 1996b; Nevison et al., 1995; Suntharalingam and Sarmiento, 2000). The Arabian Sea is the most intensely studied region for N_2O emissions in the world ocean. Given its disproportionately large contribution to this total and the lack of adequate coverage in other potentially important oceanographic regimes, the potential marine contribution to atmospheric N_2O could be somewhat higher than these estimates suggest. Future N_2O flux estimates could be improved by using N_2O concentration data from time series measurements at selected stations in the key regions of the Arabian Sea such as the coastal upwelling areas and the central Arabian Sea.

Appendix A: Some useful equations

Weekly averaged wind speeds in 10 meter height (u_{10} in m s^{-1}) for the period July 1987 to December 1995 were derived from satellite-based Special Sensor Microwave / Imager (SSM/I) measurements by using an algorithm developed by Schlüssel (1995):

$$u_{10} = c_0 + c_1 T_{19v} + c_2 (T_{19v} - T_{19h}) + c_3 T_{22v} + c_4 T_{37v} + c_5 (T_{37v} - T_{37h})$$

T is the brightness temperature in K; v and h depict vertical and horizontal polarisations; 19, 22, and 37 depict radiometer channels at 19.35, 22.24, and 37.0 GHz, respectively. Values for $c_i (i = 0, ..., 5)$ are listed in Table 5.

The used 9-point 2-dimensional smoothing procedure (Shuman, 1957) is given as:

$$z_{ij} = z_0 + 0.5v(l - v)(z_2 + z_4 + z_6 + z_8 + 4z_0) + 0.25\, v^2 (z_1 + z_3 + z_5 + z_7 - 4z_0).$$

$z_0, ..., z_8$ stand for the elements in a 9-point grid with z_0 in the centre. Numbering starts with z_1 in the upper left corner of the grid and continues counter clockwise. z_{ij} is the resulting value at the grid point coordinates i and j; and v is called the smoothing element index of the two smoothing elements, one applied in each dimension. In this study v was set to 0.5.

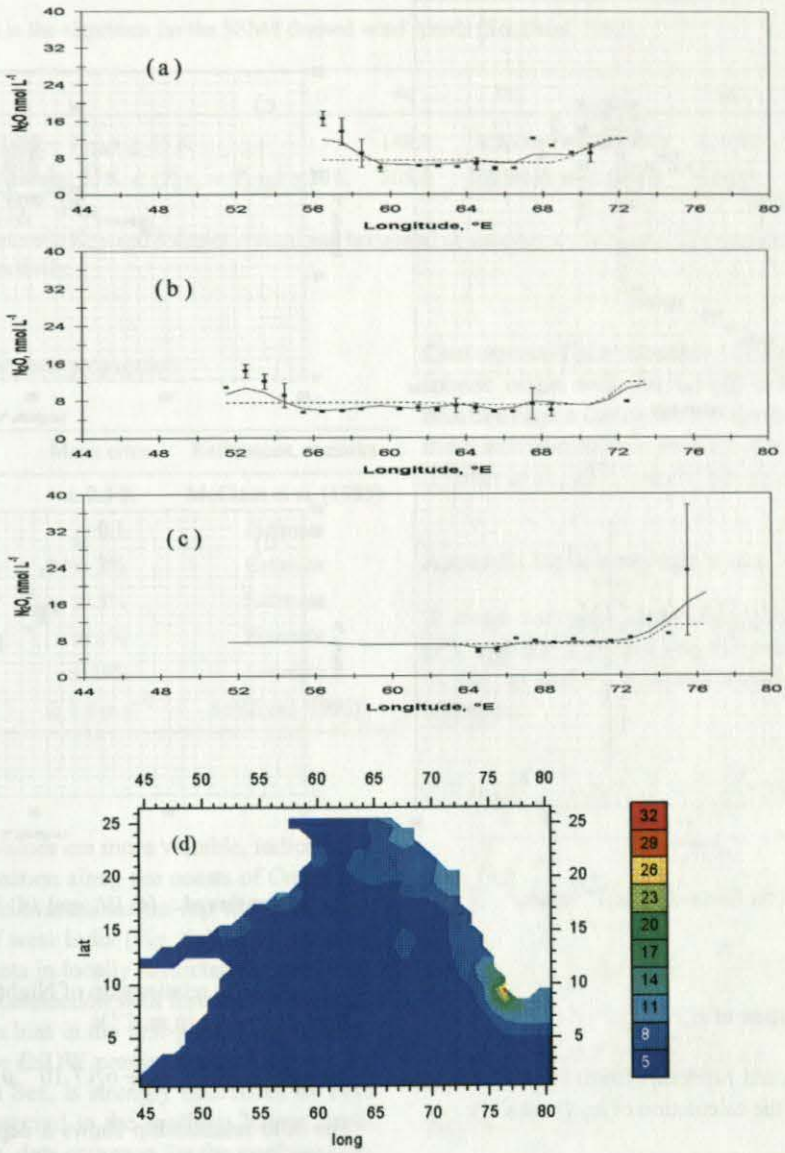

Fig. 4. Annual mean N_2O concentrations (in nmol L^{-1}) along selected latitudes. The solid line is the predicted N_2O from the final $1° \times 1°$ field, the dashed line stands for the smoothed first-guess field, and the solid squares represent the annual mean N_2O with standard deviation of all measurements within the $1° \times 1°$ squares along the given latitude. (When less than 3 values were available no standard deviation is given.) **(a)** 18.5° N, **(b)** 15.5° N, and **(c)** 10.5° N. In **(d)** the corresponding annual mean N_2O field (in nmol L^{-1}) is shown.

The $1° \times 1°$ N_2O correction field was computed by applying the distance-weighted interpolation scheme used by Conkright et al. (1994)

$$C_{ij} = \frac{\sum_{s=1}^{n} W_s Q_s}{\sum_{s=1}^{n} W_s}$$

where C_{ij} is the correction factor at the grid point coordinates (i, j); i and j are the coordinates of a grid point in the east-west and north-south directions, respectively; n is the number of observations that fall within the area around the point i, j defined by the influence radius (R); Q_s is the difference between the observed mean and the first-guess at the S^{th} point in the influence area; W_s is the weight function:

$$W_s = \exp\left(\frac{-4r^2}{R^2}\right).$$

r is the distance of the oberservation from the grid pont i, j. When $r > R$, then $W_s = 0$. In this study the influence radius R was set to 222 km.

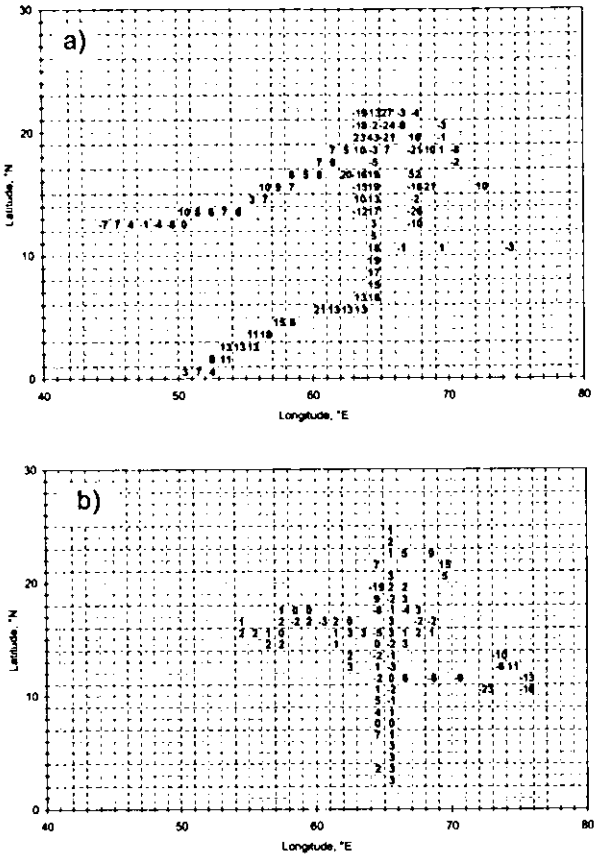

Fig. 5. Relative errors of the final field 1° × 1° values.
(a) DJF, (b) MAM.

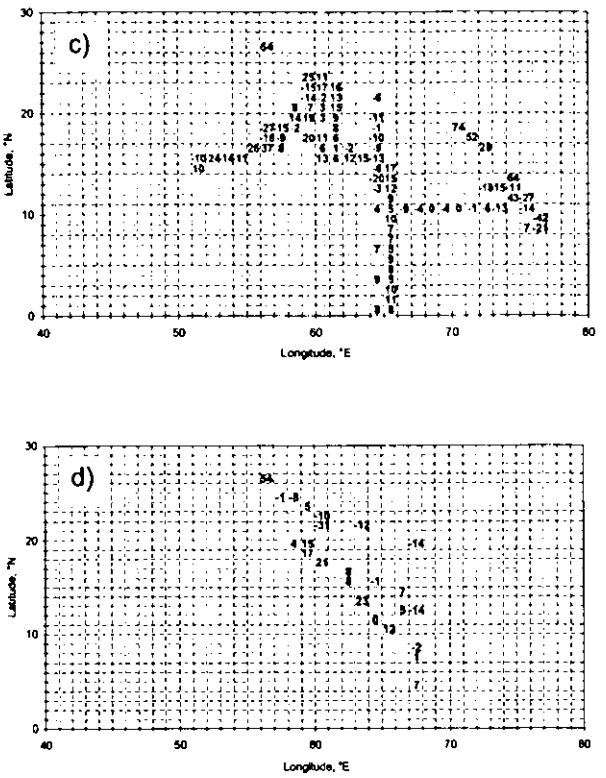

Fig. 5. Continued.: (c) JJA, and (d) SON.

Appendix B: Calculation of k_w

The approach of Liss and Merlivat (1986) (LM86) consists of three equations for the calculation of k_w (in m s^{-1}):

$$k_w = 4.72\ 10^{-7} u_{10} \quad (u_{10} \leq 3.6\,\mathrm{m\,s^{-1}})$$
$$k_w = 7.92\ 10^{-6} u_{10} - 2.68\ 10^{-5} \quad (3.6\,\mathrm{m\,s^{-1}} < u_{10} \leq 13\,\mathrm{m\,s^{-1}})$$
$$k_w = 1.64\ 10^{-5} u_{10} - 1.40\ 10^{-4} \quad (u_{10} > 13\,\mathrm{m\,s^{-1}}).$$

The LM86 relationship is based on datea obtained from a lake study and a laboratory study at high wind speeds. The approach of Liss and Merlivat (1986) is usually applied with both short-term and long-term wind speeds.

Wanninkhof (1992) (W92) proposed the following relationship for the calculation of k_w (in m s^{-1}) with climatological wind speed data:

$$k_w = 1.08\ 10^{-6} u_{10}^2 .$$

This approach is only valid when using long-term averaged (climatological) wind speeds.

the $k_w - u$ relationship of Nightingale et al. (2000)(N00) is given by (k_w in m s^{-1}):

$$k_w = 9.25\ 10^{-7} u_{10} + 6.17\ 10^{-7} u_{10}^2 .$$

The N00 relationship shows a dependence on wind speeds intermediate between those of Liss and Merlivat (1986) and Wanninkhof (1992). Moreover, the N00 relationship is in reasonable agreement with estimates of k_w based on globally averaged wind speeds.

Appendix C: Error estimate

In order to evaluate the fit of the computed final N_2O concentrations to the observations, we compared mean annual 1° × 1° data with the smoothed first-guess field and the final field along selected latitudes (Fig. 4). Figure 5 shows the relative error of the predicted seasonal final fields (the so-called interpolation error), estimated as the difference between the final value in each 1° × 1° square and the 1° × 1° pixel data (see Fig. 2). There is a good agreement between predicted values and the observations in the central Arabian Sea during MAM (Fig. 5b). For the monsoon seasons DJF and JJA the relative

Table 5. Coefficients used in the algorithm for the SSM/I derived wind speeds (Schlüssel, 1995)

	c_0	c_1	c_2	c_3	c_4	c_5
$T_{19h} \leq 165$ K and $(T_{37v} - T_{37h}) \geq 55$ K	149.0	0.8800	-0.4887	-0.4642	-0.7131	-0.4668
165 K $< T_{19h} \leq 190$ K and 55 K $< (T_{37v} - T_{37h}) \leq 20$ K	205.6	-0.083449	-0.07933	0.1066	-0.7346	-0.9132

T is the brightness temperature in K; v and h depict vertical and horizontal polarisations; 19, 22, and 37 depict radiometer channels at 19.35, 22.24, and 37.0 GHz, respectively.

Table 6. Errors used for the error propagation

Observable quantity	Mean error	References, remarks
Water temperature, T	$\pm$ 0.5 K	McClain et al. (1985)
Salinity, S	$\pm$ 0.1	Estimate
N_2O dry mole fraction, x'	$\pm$ 2%	Estimate
Atmospheric pressure, P	$\pm$ 5%	Estimate
Kinematic viscosity, ν	$\pm$ 1%	Estimate
Diffusion of N_2O, D	$\pm$ 10%	Estimate
Wind speed, u	$\pm$ 1.4 m s^{-1}	Schlüssel (1995)

errors of the predicted values are more variable, indicating a considerable underestimation along the coasts of Oman and southwest India, and an overestimation (up to 74%) along the continental shelf of west India (Fig. 5c). The tendency to focus on measurements in locally restricted features such as coastal upwelling in connection with insufficient seasonal data coverage leads to a bias in the first-guess field. For example, the mean for the INDW province, which covers the eastern coastal Arabian Sea, is strongly influenced by high N_2O concentrations observed in the southern Indian continental shelf. In contrast, data coverage for the northern continental shelf is poor, and consequently the first-guess field determines the final N_2O concentration, leading to high uncertainties in this area as indicated by Figs. 5a–5d.

A further uncertainty is introduced by the fact that the N_2O surface concentrations are depending on SST, salinity, atmospheric pressure and the atmospheric N_2O mixing ratio which are, at least partly, subject of long term trends due to global change (Barnett et al., 2001; Levitus et al., 2000). For example, the mean tropospheric N_2O dry mole fractions (see data from the ALE/GAGE/AGAGE program available from the anonymous ftp site cdiac.esd.ornl.edu, subdirectory is given above) increased from about 300 ppb in the late 1970s to about 315 ppb in 1999 suggesting a trend of increasing N_2O surface concentrations. However, a quantification of such trends in sea surface N_2O concentrations is not possible due to the lack of time series measurements in the Arabian Sea. The seasonal northward shift of the Intertropical Convergence Zone introduces air masses of southern hemispheric origin with lower N_2O mole fractions to the Arabian Sea region during the SW monsoon. However, since the mean interhemispheric gradient of N_2O is only about 0.8 ppb (Prather et al., 2001) we did not account for this effect.

Appendix D: Error propagation

A rough estimate of the mean error of the flux density (F), introduced by the uncertainties of the observables (i.e. T, S, u, P, and x'), was calculated according to the following equations:

$$\Delta F = \sqrt{\left(\frac{\partial F}{\partial C_w}\Delta C_w\right)^2 + \left(\frac{\partial F}{\partial C_a}\Delta C_a\right)^2 + \left(\frac{\partial F}{\partial k_w}\Delta k_w\right)^2 + \left(\frac{\partial F}{\partial Sc}\Delta Sc\right)^2}$$

$$\Delta C_a = \sqrt{\left(\frac{\partial C_a}{\partial x'}\Delta x'\right)^2 + \left(\frac{\partial C_a}{\partial \beta}\Delta \beta\right)^2 + \left(\frac{\partial C_a}{\partial P}\Delta P\right)^2}$$

$$\Delta \beta = \sqrt{\left(\frac{\partial \beta}{\partial T}\Delta T\right)^2 + \left(\frac{\partial \beta}{\partial S}\Delta S\right)^2}$$

$$\Delta k_w = \frac{\partial k_w}{\partial u}\Delta u$$

$$\Delta Sc = \sqrt{\left(\frac{\partial Sc}{\partial D_{N2O}}\Delta D_{N2O}\right)^2 + \left(\frac{\partial Sc}{\partial \nu}\Delta \nu\right)^2}$$

where ν stands for the kinematic viscosity of seawater and the operator ∂/∂ depicts the partial differential. For a strict treatment of the error propagation, the standard deviation of each parameter should be known. Since this was not the case, we replaced the standard deviation partly with best estimates of the mean error (depicted by the Δ symbol, data listed in Table 6). For ΔC_w we used the mean relative error (i.e. the interpolation error) calculated from the seasonal data shown in Fig. 5 (see also the Appendix A: Error estimate). We calculated the relative error $\Delta F/F$ for each 1° × 1° square of the four seasonal N_2O fields. Table 7 gives an overview of the resulting mean relative errors of the seasonal flux densities. Not surprisingly, the lowest mean relative error of C_w is associated with highest relative error of resulting flux

Table 7. Overview of the mean relative errors of N_2O surface concentrations and N_2O flux densities

	Mean $\Delta C_w/C_w$, ± %	Mean $\Delta F/F$, ± %
DJF	11	75
MAM	4	330
JJA	14	79
SON	12	442

densities. During MAM the dissolved N_2O concentrations are low and resulting in only small concentration differences ($C_w - C_a$) across the ocean-atmosphere interface which in turn lead to high mean relative errors of the flux densities. During the monsoon season JJA, N_2O concentrations in the coastal upwelling zones are considerable higher causing a higher mean relative error of C_w and comparable low mean relative errors of the resulting flux density. The mean relative errors for the seasonal flux densities yield the overall mean relative error of the annual N_2O emissions from the Arabian Sea of at least 65%. Systematic errors caused by uncertainties in parameterizations such as N_2O diffusion in seawater (determination of the N_2O diffusion have not been made in seawater-like systems (see literature compilation in Rhee, 2000)) and air-sea exchange approaches are not accounted for in this estimate (see Results and discussion). Moreover, it is important to keep in mind that the calculation of any climatological data fields are biased by the chosen smoothing and averaging routines (see e.g. Sterl, 2001).

A detailed analysis of errors introduced by different filling routines, averaging procedures etc. is beyond the scope of this study. Generally, gas exchange estimates suffer from the fact that a direct (i.e. at sea) determination of the processes responsible for the gas exchange across the ocean-atmosphere interface is still a technological challenge (Frost and Upstill-Goddard, 1999; Jähne and Haußecker, 1998).

Acknowledgements. We acknowledge the invaluable help of the officers and crews of the various research vessels involved. HWB thanks S. van Dijk, J. Kettle, and A. Suthhof for inspiring discussions and C. Strametz for help with the manuscript. The investigations were supported by the U.K. Natural Environment Research Council (NERC) Arabesque initiative, the German Bundesministerium für Bildung, Wissenschaft, Forschung und Technologie (grants 03F0137A, 03F0183G, 03F0241C), and the Max Planck Society, and the Institute for Marine Research, Kiel.

References

Bange, H. W., Rapsomanikis, S., and Andreae, M. O.: Nitrous oxide emissions from the Arabian Sea, Geophys. Res. Lett., 23, 3175–3178, 1996a.

Bange, H. W., Rapsomanikis, S., and Andreae, M. O.: Nitrous oxide in coastal waters, Global Biogeochem. Cycles, 10, 197–207, 1996b.

Bange, H. W., Rixen, T., Johansen, A. M., Siefert, R. L., Ramesh, R., Ittekkot, V., Hoffmann, M. R., and Andreae, M. O.: A revised nitrogen budget for the Arabian Sea, Global Biogeochem. Cycles, 14, 1283–1298, 2000.

Barnett, T. P., Pierce, D. W., and Schnur, R.: Detection of anthropogenic climate change in the world's oceans, Science, 292, 270–274, 2001.

Broecker, W. S. and Peng, T.-S.: Gas exchange rates between air and sea, Tellus, 26, 21–35, 1974.

Codispoti, L. A., Elkins, J. W., Yoshinari, T., Friederich, G. E., Sakamoto, C. M., and Packard, T. T.: On the nitrous oxide flux from productive regions that contain low oxygen waters, in Oceanography of the Indian Ocean, edited by B. N. Desai, 271–284, Oxford Publishing, New Delhi, 1992.

Conkright, M., Levitus, S., and Boyer, T. P.: NOAA Atlas NESDIS 1, World Ocean Atlas 1994, Volume 1: Nutrients, National Environmental Satellite, Data, and Information Service, National Oceanic and Atmospheric Administration, US Department of Commerce, Washington DC, 1994.

Frost, T. and Upstill-Goddard, R. C.: Air-sea exchange into the millennium: Progress and uncertainties, Oceanogr. Mar. Biol. Ann. Rev., 37, 1–45, 1999.

Jähne, B., and Haußecker, H.: Air-water gas exchange, Annual Rev. Fluid Mech., 30, 69–91, 1998.

Kettle, A. J., Andreae, M. O., Amouroux, D., Andreae, T. W., Bates, T. S., Berresheim, H., Bingemer, H., Boniforti, R., Curran, M. A. J., DiTullio, G. R., Helas, G., Jones, G. B., Keller, M. D., Kiene, R. P., Leck, C., Levasseur, L., Malin, G., Maspero, M., Matrai, P., McTaggart, A. R., Mihalopoulos, N., Nguyen, B. C., Novo, A., Putaud, J. P., Rapsomanikis, S., Roberts, G., Schebeske, G., Sharma, S., Simo, R., Staubes, R., Turner, S., and Uher G.: A global database of sea surface dimethylsulfide (DMS) measurements and a procedure to predict sea surface DMS as a function of latitude, longitude, and month, Global Biogeochem. Cycles, 13, 399–444, 1999.

King, D. B., De Bryun, W. J., Zheng, M., and Saltzman, E. S.: Uncertainties in the molecular diffusion coefficient of gases in water for the estimation of air-sea exchange, in Air-water gas transfer, edited by B. Jähne and E. C. Monahan, pp. 13–22, AEON Verlag & Studio, Hanau, Germany, 1995

Lal, S. and Patra, P. K.: Variabilities in the fluxes and annual emissions of nitrous oxide from the Arabian Sea, Global Biogeochem. Cycles, 12, 321–327, 1998.

Law, C. S. and Owens, N. J. P.: Significant flux of atmospheric nitrous oxide from the northwest Indian Ocean, Nature, 346, 826–828, 1990.

Levitus, S., Antonov, J. I., Boyer, T. P., and Stephens, C.: Warming of the Ocean, Science, 287, 2225–2229, 2000.

Liss, P. S. and Merlivat, L.: Air-sea exchange rates: Introduction and synthesis, in The Role of Air-Sea Exchange in Geochemical Cycling, edited by P. Buat-Ménard, 113–127, D. Reidel Publishing Company, Dordrecht, 1986.

Longhurst, A.: Ecological geography of the sea, 398 pp., Academic Press, San Diego, 1998.

McClain, E. P., Pichel, W. G., and Walton, C. C.: Comparative performance of AVHRR-based multichannel sea surface tempera-

tures, J. Geophys. Res., 90, 11, 587–11, 601, 1985.
Naqvi, S. W. A., Jayakumar, D. A., Narvekа, P. V., Naik, H., Sarma, V. V. S. S., D'Souza, W., Joseph, S., and George, M. D.: Increased marine production of N_2O due to intensifying anoxia on the Indian continental shelf, Nature, 408, 346–349, 2000.
Naqvi, S. W. A. and Noronha, R. J.: Nitrous oxide in the Arabian Sea, Deep-Sea Res., 38, 871–890, 1991.
Naqvi, S. W. A., Yoshinari, T., Jayakumar, D. A., Altabet, M. A., Narvekar, P. V., Devol, A. H., Brandes, J. A., and Codispoti, L. A.: Budgetary and biogeochemical implications of N_2O isotope signatures in the Arabian Sea, Nature, 394, 462–464, 1998.
Nevison, C. D., Weiss, R. F., and Erickson III, D. J.: Global oceanic emissions of nitrous oxide, J. Geophys. Res., 100, 15, 809–15, 820, 1995.
Nightingale, P., Malin, G., Law, C. S., Watson, A. J., Liss, P. S., Liddicoat, M. I., Boutin, J., and Upstill-Goddard, R. C.: In-situ evaluation of air-sea gas exchange parameterizations using novel conservative and volatile tracers, Global Biogeochem. Cycles, 14, 373–387, 2000.
Patra, P. K., Lal, S., Venkataramani, S., De Sousa, S. N., Sarma, V. V. S. S., and Sardesai, S.: Seasonal and spatial variability in N_2O distribution in the Arabian Sea, Deep-Sea Res. I, 46, 529–543, 1999.
Prather, M., Ehhalt, D., Dentener, F., Derwent, R., Dlugokencky, E., Holland, E., Isaksen, I., Katima, J., Kirchhoff, V., Matson, P., Midgley, P., and Wang, M.: Atmospheric chemistry and greenhouse gases, in Climate Change 2001: The Scientific Basis. Contribution of Working Group I to the Third Assessment Report of the Intergovernmental Panel on Climate Change, edited by Houghton, J. T., Ding, Y., Griggs, D. J., Noguer, M., Van der Linden, P. J., Dai, X., Maskell, K., and Johnson, C. A., 239–287, Cambridge University Press, Cambridge, UK, 2001.
Rhee, T. S.: The process of air-water gas exchange and its application, PhD thesis, Texas A & M University, College Station, 2000.
Schlüssel, P.: Passive Fernerkundung der unteren Atmosphäre und der Meeresoberfläche aus demWeltraum, Habilitationsschrift Ber. A20, 175 pp., Zentrum für Meeres- und Klimaforschung der Universität Hamburg, Germany, 1995.
Seitzinger, S. P., Kroeze, C., and Styles, R. V.: Global distribution of N_2O emissions from aquatic systems: Natural emissions and anthropogenic effects, Chemosphere: Global Change Sci., 2, 267–279, 2000.
Shuman, F. G.: Numerical methods in weather prediction: II. Smoothing and filtering, Mon. Weath. Rev., 85, 357–361, 1957.
Siedler, G. and Peters, H.: Properties of sea water, in Oceanography, Landolt-Börnstein New Ser., Group V, vol. 3a, edited by Sündermann, J., 233–264, Springer Verlag, New York, 1986.
Smith, F. G. W. (Ed.): CRC Handbook of Marine Science, vol. I, 627 pp., CRC Press Inc., Boca Raton, 1974
Sterl, A.: On the impact of gap-filling algorithms on variability patters of reconstructed oceanic surface fields, Geophys. Res. Lett., 28, 2473–2476, 2001.
Suntharalingam, P. and Sarmiento, J. L.: Factors governing the oceanic nitrous oxide distribution: Simulations with an ocean general circulation model, Global Biogeochem. Cycles, 14, 429–454, 2000.
Upstill-Goddard, R. C., Barnes, J., and Owens, N. J. P.: Nitrous oxide and methane during the 1994 SW monsoon in the Arabian Sea/northwestern Indian Ocean, J. Geophys. Res., 104, 30, 067–30, 084, 1999.
Wanninkhof, R.: Relationship between wind speed and gas exchange over the ocean, J. Geophys. Res., 97, 7373–7382, 1992.
Weiss, R. F. and Price, B. A.: Nitrous oxide solubility in water and seawater, Mar. Chem., 8, 347–359, 1980.
Weiss, R. F., Van Woy, F. A., and Salameh, P. K.: Surface water and atmospheric carbon dioxide and nitrous oxide observations by shipboard automated gas chromatography: Results from expeditions between 1977 and 1990, Carbon Dioxide Information Analysis Center, Oak Ridge National Laboratory, Oak Ridge, Tennessee, USA, 1992.

Indian Journal of Marine Sciences
Vol. 33(1), March 2004, pp 77-83

Air-sea exchange of nitrous oxide and methane in the Arabian Sea: A simple model of the seasonal variability

Hermann W. Bange
Marine Biogeochemistry Division,Institute for Marine Research,Düsternbrooker Weg 20,24105 Kiel, Germany
[E-mail: hbange@ifm.uni-kiel.de]

Received 29 August 2003

With a simple box model the seasonal variability of N_2O and CH_4 were simulated in surface layers in the central and western Arabian Sea. The model was able to reproduce the N_2O measurements except for times when cold water filaments occur (i.e., during the SW monsoon). Based on the comparison of model results and measurements, it is concluded that the saturation of N_2O in the surface layer of the Arabian Sea is mainly controlled by (i) the wind-driven air-sea exchange during the SW monsoon, (ii) entrainment of N_2O from the subsurface layer, and (iii) sea surface temperature variability. However, the contribution of the factors listed above to the seasonality of the N_2O saturations is different in the selected areas. The overall good agreement of model results and the majority of N_2O measurements suggest that N_2O formation in the surface layer of the Arabian Sea is negligible. The comparison of model's results and CH_4 measurements revealed a more complex situation, partly due to considerable inconsistencies in the available CH_4 data. Thus, the situation for CH_4 remains unresolved and inconclusive.

[Key words: Nitrous oxide, methane, Arabian Sea, air-sea exchange, box model]
[IPC Code: Int. Cl.[7] C09K 3/30]

Both nitrous oxide (N_2O) and methane (CH_4) are atmospheric trace gases, which directly and indirectly, influence the present-day climate of the Earth[1]. N_2O and CH_4 are naturally produced during microbial processes such as nitrification/denitrification (N_2O) and methanogenesis (CH_4) in considerable amounts in terrestrial and oceanic environments[2,3]. Measurements of atmospheric and dissolved N_2O and CH_4 in oceanic areas are still sparse and the derived emission estimates are associated with large uncertainties mainly due to the fact that an adequate seasonal data coverage is mostly lacking[4-9]. However, due to the activities during the Arabian Sea Process Study [as part of the international Joint Global Ocean Flux Study (JGOFS) program] and other investigations, an increasing number of N_2O and CH_4 data sets for the Arabian Sea are now available[10,11]. In order to reveal the major mechanism for the observed seasonality of N_2O and CH_4 in the Arabian Sea surface layer[10,11], a model approach was chosen in which the seasonal variability of the dissolved gases is estimated from basic meteorological and hydrographical parameters. A successful modelling would allow developing tools for future monitoring of N_2O and CH_4 surface distributions and their emissions to the atmosphere in the Arabian Sea area. Using a simple box model which includes the temporal variability of air-sea exchange, the mixed surface layer depth and seawater temperature, I computed the theoretical seasonal pattern of the N_2O and CH_4 saturation in the surface layer of three selected areas in the central and western Arabian Sea and compared the model results with measurements.

Model Description

A simple box model was developed to simulate the temporal variability ($\delta C_w/\delta t$) of N_2O and CH_4 concentrations in the mixed layer (Fig. 1):

$$\delta C_w/\delta t = (\delta C_w/\delta t)_{ase} + (\delta C_w/\delta t)_{mix} \quad \ldots (1)$$

where $(\delta C_w/\delta t)_{ase}$ stands for the air-sea gas exchange across the ocean-atmosphere interface, $(\delta C_w/\delta t)_{mix}$ stands for the vertical mixing of N_2O or CH_4 into or out of the mixed layer. The present model consists of one box, the mixed surface layer, where temperature and gas concentration are homogeneously distributed. Time series of monthly seawater temperature[12], mixed layer depth[13], and wind speed[14] were used to simulate the seasonal variability of N_2O and CH_4 at three stations in the central and western Arabian Sea (Figs. 2 and 3, Table 1).

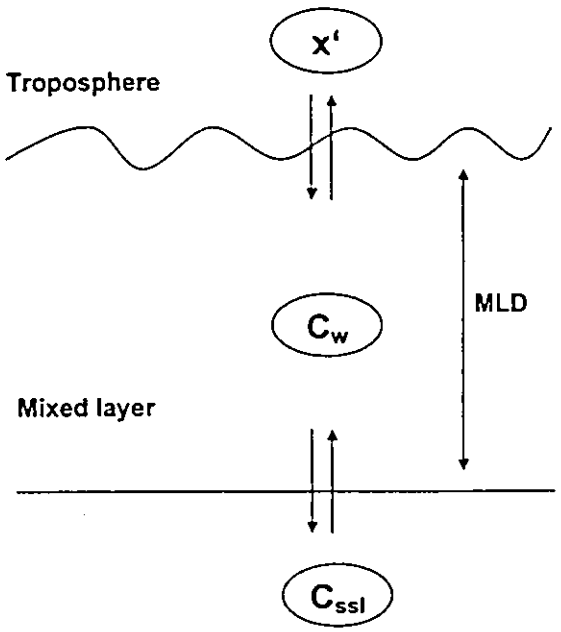

Fig. 1—Outline of the box model; C_w stands for concentration of N_2O or CH_4 in the mixed layer, C_{ssl} stands for concentration of N_2O or CH_4 in the subsurface layer, x' stands for the mole fraction of N_2O or CH_4 in the atmosphere, and MLD stands for mixed layer depth.

Table 1—Model parameters

Target areas	
SAST	09.5°–10.5° N, 64.5°–65.5° E
CAST	13.5°–15.5° N, 64.5°–65.5° E
WAST	15.5°–16.5° N, 59.5°–61.5° E
Input parameters	
Water temperature	Monthly means[a] (see Fig. 3)
Mixed layer depth	Monthly means[b] (see Fig. 3)
Wind speed	Monthly means[c] (see Fig. 3)
N_2O atmospheric mole fraction	311 ppb; 309 ppb (SW monsoon)[d]
CH_4 atmospheric mole fraction	1.8 ppm; 1.7 ppm (SW monsoon)[d]

[a] World Ocean Atlas[12].

[b] Data Set Atlas for Oceanographic Modelling Samuels & Cox[13]

[c] ECMWF Re-Analysis Project[14]

[d] During the SW monsoon the atmospheric mole fraction is lower due to fact that air masses from the southern hemisphere enter the Arabian Sea region as a consequence of the northward shift of the Intertropical Convergence Zone (ITCZ).

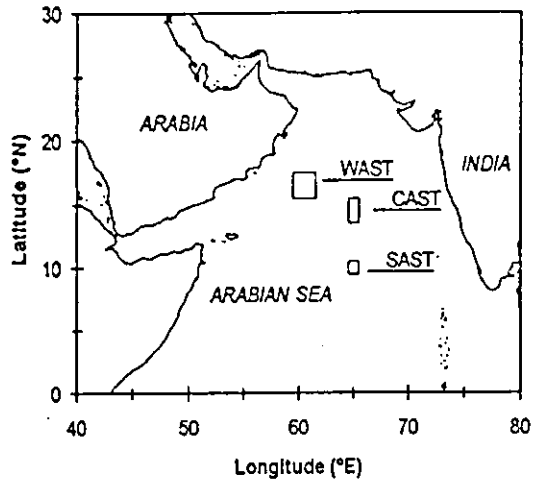

Fig. 2—Map of the Arabian Sea showing the areas WAST (Western Arabian Sea Station), CAST (Central Arabian Sea Station) and SAST (Southern Arabian Sea Station) selected for this study.

In this model, the temporal variability of gas exchange depends on the air–sea exchange flux density (F) and the mixed layer depth (MLD)[15]:

$$(\delta C_w/\delta t)_{ase} = F / MLD \quad \ldots (2)$$

F was parameterised as :

$$F = k_w(u)\,(C_w - C_a), \quad \ldots (3)$$

where k_w is the gas transfer coefficient as a function of wind speed (u), C_w is the N_2O seawater concentration, and C_a is the equilibrium gas concentration in seawater. C_a was calculated as :

$$C_a = \beta(SST, S)\,x', \quad \ldots (4)$$

where x' is the atmospheric dry mole fraction and β is the Bunsen solubility, which is a function of the water temperature (SST) and salinity (S)[16,17]. To calculate k_w, the tri-linear k_w–u relationship of Liss & Merlivat[18] (LM86), the quadratic k_w–u relationship for climatological wind data of Wanninkhof[19] (W92), and the combined linear and cubic k_w–u relationship from Wanninkhof & McGillis[20] (WM99) were used. k_w was adjusted by multiplying with $(Sc/600)^{-n}$ (n = 2/3 for wind speeds <3.6 m s^{-1} and n = 1/2 for wind speeds >3.6 m s^{-1}) for LM86[18], $(Sc/660)^{-0.5}$ for W92[19] and WM99[20], where Sc is the Schmidt number for N_2O. Sc at a salinity of 35 ‰ was calculated using empirical equations for the kinematic viscosity of seawater[21] and the diffusion coefficients of N_2O and CH_4 in water[22,23].

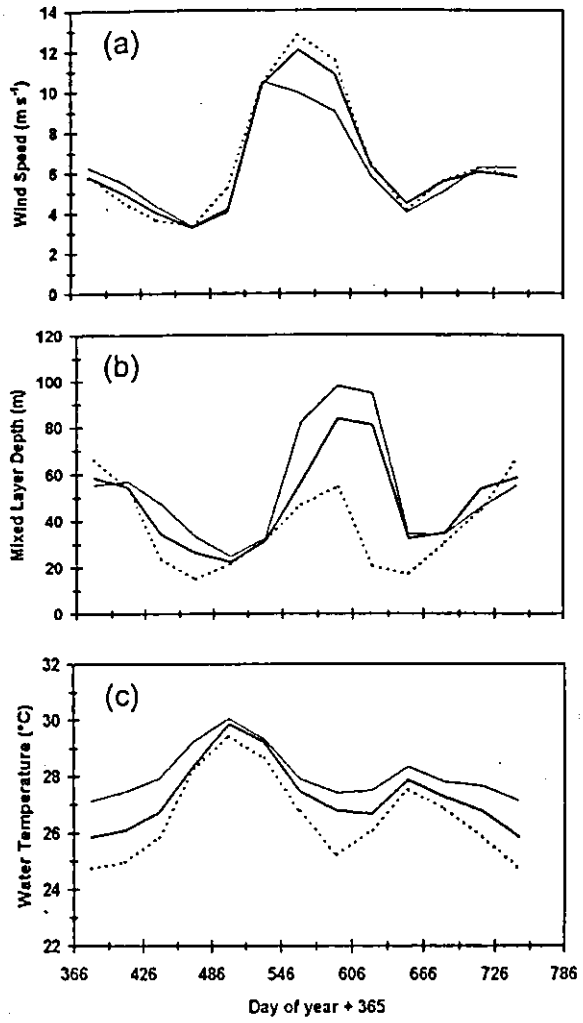

Fig. 3—Model input parameters; (a) monthly wind speeds; (b) monthly mixed layer depth; and (c) monthly water temperature for the areas WAST (dashed line), CAST (bold line) and SAST (thin line).

The gas concentration mixed into the surface layer by entrainment (ΔC_{mix}) at a given time step was computed with the approach of Peng *et al.*[24]:

$$\Delta C_{mix} = (C_{ssl} - C_w(t))\ \Delta MLD / (MLD(t) + \Delta MLD) \quad \ldots (5)$$

where C_{ssl} stands for the gas concentration in the subsurface layer (i.e., below the lower boundary of the mixed layer) and ΔMLD represents the change of the MLD at the given time step. The general shapes of N_2O and CH_4 depth profiles in the Arabian Sea suggest that surface production is not dominating their vertical distributions[25,27]. Thus, it seems reasonable to assume downward mixing to be negligible (in this case $\Delta C_w = 0$). The reported values of 8 nmol L^{-1} and 3 nmol L^{-1} were adopted for the C_{ssl} of N_2O and CH_4, respectively[25,26]. There are indications that significant spatial and seasonal variations of C_{ssl} for both N_2O and CH_4 exist[27,28]. However, seasonal and spatial variations of C_{ssl} were not introduced since appropriate time series measurements are not available. The concentration of the dissolved gases C_w at time t was calculated as follows:

$$C_w(t + \Delta t) = C_a(t + \Delta t) + \Delta C_w \quad \ldots (6)$$

$$\Delta C_w = (F / MLD)\ \Delta t + \Delta C_{mix} \quad \ldots (7)$$

where $C_a(t)$ is the equilibrium concentration computed with the atmospheric mixing ratio depending on the seawater temperature and salinity at the time t. The time step Δt was set to 12 hours, a value that is lower than the system's typical relaxation time, which is of the order of days or weeks depending on the wind speed and the mixed layer depth. At time $t = 0$, C_w was calculated using a prescribed saturation (Sat in %, i.e., 100% = equilibrium):

$$C_w(0) = C_a(0)\ Sat / 100 \quad \ldots (8)$$

The results of the model computations are presented as saturation $Sat(t)$ of at time t in the mixed surface layer:

$$Sat(t) = 100 C_w(t) / C_a(t)\ [\%] \quad \ldots (9)$$

The model results become stable within the first model year, thus results from the second model year are shown (days 366–745).

Model input parameters are listed in Table 1. Model results were compared to saturation data from the data sets for N_2O[29-32] as well as for CH_4[26,32,33].

Results and Discussion

Nitrous oxide (N_2O)

Figure 4 shows the results of the N_2O model runs for the SAST (Southern Arabian Sea Station at 10°N 65°E), CAST (Central Arabian Sea Station at 14.5°N 65°E) and WAST (Western Arabian Sea Station at 16.3°N 60.5°E) areas. Generally, the model results show enhanced N_2O saturations during the first intermonsoon period from March to late May with maximum values at the end of April (around model day 486). This is caused by the seasonal increase of the SST, which causes higher N_2O saturation because of lower solubility and the fact that the variation in SST is faster than the equilibration time of the air-sea

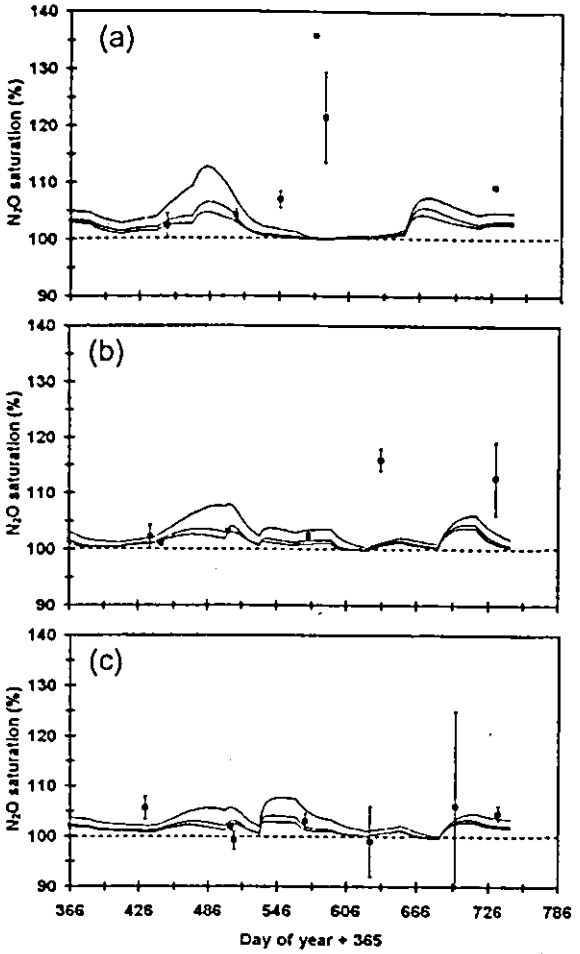

Fig. 4—Results of the N_2O model; (a) WAST, (b) CAST and (c) SAST. Measurements are given as mean values with standard deviation (when available). Three different air-sea exchange models were applied (see text for details). The air-sea exchange models of Liss & Merlivat[18] and Wanninkhof[19] envelop the range of model results.

exchange. During the southwest (SW) monsoon (late May–September, model days 510–638), N_2O saturations are driven by both the high monsoonal wind speeds and the seasonal deepening of the *MLD*. However the effects are counteracting. High wind speeds lead to high emissions and subsequent depletion of N_2O in the mixed layer, whereas deepening of the mixed layer leads to an entrainment of N_2O from the subsurface layer. Since the mixed layer deepening is most pronounced at SAST (Fig. 2), the effect of entrainment is most pronounced at SAST, but almost not visible at station WAST. The winter deepening of the *MLD* during the end of the second intermonsoon and the northeast (NE) monsoon from mid of October to January (model days 653–745) leads to a third period of enhanced saturations

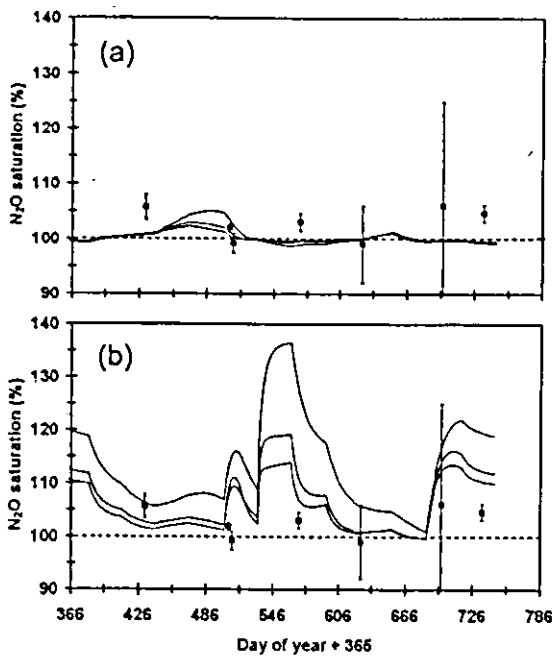

Fig. 5—N_2O model results for station SAST; (a) without entrainment (C_{ssl} = 0 nmol L^{-1}), (b) with entrainment (C_{ssl} = 16 nmol L^{-1}). Three different air-sea exchange models were applied (see text for details). The air-sea exchange models of Liss & Merlivat[18] and Wanninkhof[19] envelop the range of model results.

because of the entrainment of N_2O from the subsurface layer.

In order to check the model sensitivity for the choice of C_{ssl}, we performed model runs for station SAST with extreme values for C_{ssl} (0 and 16 nmol L^{-1}) (Fig. 5). The incorporation of moderate entrainment (C_{ssl} = 8 nmol L^{-1}, Fig. 4c) brings the model results at station SAST (and at station CAST, sensitivity runs not shown) into a good agreement with the measurements, indicating that the basic assumption of C_{ssl} = 8 nmol L^{-1} is reasonable.

For comparison, N_2O saturations based on measurements are shown in Fig. 4. There is a good agreement between the measurements and model results for SAST and partly for stations CAST and WAST as well. At station WAST, maximum N_2O saturations of up to 135% have been reported for the SW monsoon period, however, these values are not matched by the model results. This discrepancy is due to the fact that the WAST area is influenced by cold water filaments which originate from upwelling centres at the coast of the Arabian peninsula[34]. Arabian Sea filaments typically show enhanced N_2O concentrations[30,35]. Filaments might cause the mismatch of model results and measurements at CAST during the late SW monsoon as well. However,

this result is not surprising, since advective processes are not parameterised in the model. Lal & Patra[36] reported surface N_2O saturations for the NE and SW monsoons and for the intermonsoon (April–May) at stations in the proximity of SAST and CAST. Their values lie in the range from 110% to 152% with highest values during the NE monsoon in February/March (136% at stations close to SAST and 152% at stations close to CAST). It appears that the present model when extended to their stations would not represent the monsoon data by Lal & Patra[36]. The reason for the apparent discrepancy might be due to strong advective processes during the SW monsoon together with an unusual deepening of the mixed layer during the NE monsoon.

Methane (CH_4)

Figure 6 shows the modelled CH_4 saturations for the stations SAST, CAST and WAST. The general shape of the model results is similar to the N_2O model results (see previous section). In contrast to the N_2O model, a comparison of CH_4 model results and measurements reveal significant discrepancies. At SAST the model generally underestimates the observed CH_4 saturations, whereas at CAST and WAST some of the measurements are in very good agreement with the model results. Therefore, a general conclusion is difficult to draw. On the one hand, one might argue that a missing CH_4 formation in the surface layer might be the reason for a general underestimation of the model. On the other hand, the very good agreement of some measurements and model results at CAST and WAST does not imply a missing CH_4 source. Additionally, some of the discrepancies arise because there is considerable inconsistency in the CH_4 measurements. For example, at CAST a difference in the CH_4 observations of up to 40% CH_4 saturation was noted, based on two independent observations on the same day and the same year. Similar inconsistencies also occur in the data set of the WAST area.

Conclusion

With a simple box model the seasonal variability of the saturations of N_2O and CH_4 in surface layers of three areas in the central and western Arabian Sea have been simulated. The model was able to reproduce the N_2O measurements except for times when cold water filaments occur (i.e., at WAST and CAST during the SW monsoon). Based on the

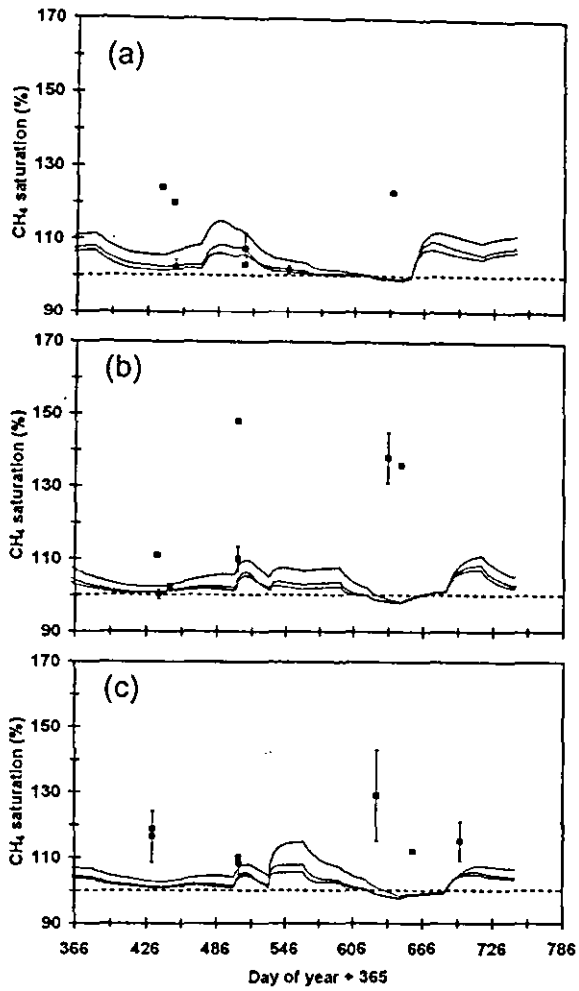

Fig. 6—Results of the CH_4 model; (a) WAST, (b) CAST and (c) SAST. Measurements are given as mean values with standard deviation (when available). Three different air-sea exchange models were applied (see text for details). The air-sea exchange models of Liss & Merlivat[18] and Wanninkhof[19] envelop the range of model results.

comparison of model results and measurements, it is concluded that the saturation of N_2O in the surface layer of the Arabian Sea is mainly controlled by (i) the wind-driven air-sea exchange during the SW monsoon, (ii) entrainment of N_2O from the subsurface layer, and (iii) SST variability. However, the contribution by the factors listed above to the seasonality of the N_2O saturations is different. For example, N_2O saturations at CAST during the non-monsoon season are mainly determined by the seasonal variability of the SST, whereas at the southernmost area (SAST), the entrainment of N_2O results in maximum N_2O saturations during the SW monsoon season. It has been suggested that N_2O might be produced in the ocean surface layer of the

subtropical Pacific Ocean[37] and the Caribbean Sea[38]. However, the overall good agreement of model results and measurements suggests that N_2O formation in the surface layer of the Arabian Sea is negligible. This is in agreement with the results by Naqvi & Noronha[39].

The situation for CH_4 appears to be more complex. The comparison of model results and CH_4 measurements at SAST revealed a considerable underestimation by the model, possibly indicating an *in-situ* source of CH_4 in the surface layer as suggested by various authors[40-42]. However, the results for stations CAST and WAST are not in line with this result, partly due to the considerable inconsistency of the available CH_4 measurements. Thus, the situation for CH_4 remains unresolved and no final conclusion can be drawn for CH_4.

Acknowledgement

Thanks are due to A.J. Kettle for extracting the climatological data sets. The investigation was supported by the Max Planck Society, the Institute for Marine Research, Kiel, and the German *Bundesministerium für Bildung, Wissenschaft, Forschung und Technologie* through grants 03F0137A, 03F0183G and 03F0241C.

References

1 Prather M, Ehhalt D, Dentener F, Derwent R, Dlugokencky E, Holland E, Isaksen I, Katima J, Kirchhoff V, Matson P, Midgley P & Wang M, Atmospheric chemistry and greenhouse gases, in: *Climate Change 2001: The Scientific Basis Contribution of Working Group I to the Third Assessment Report of the Intergovernmental Panel on Climate Change*, edited by JT Houghton, Ding, Y, Griggs, DJ, Noguer, M, Van der Linden, P J, Dai, X, Maskell, K & Johnson, C A, (Cambridge University Press, Cambridge), 2001, pp. 239–287.

2 Cicerone R J & Oremland R S, Biogeochemical aspects of atmospheric methane, *Global Biogeochem Cycles*, 2 (1988) 299–327.

3 Codispoti L A, Brandes J A, Christensen J P, Devol A H, Naqvi S W A, Paerl H W & Yoshinari T, The oceanic fixed nitrogen and nitrous oxide budgets: Moving targets as we enter the anthropocene? *Scientia Marina*, 65 (2001) 85–105.

4 Bange H W, Rapsomanikis S & Andreae M O, Nitrous oxide in coastal waters, *Global Biogeochem Cycles*, 10 (1996) 197–207.

5 Nevison C D, Weiss R F & Erickson III D J, Global oceanic emissions of nitrous oxide, *J Geophys Res*, 100 (1995) 15,809–15,820.

6 Suntharalingam P & Sarmiento J L, Factors governing the oceanic nitrous oxide distribution: Simulations with an ocean general circulation model, *Global Biogeochem Cycles*, 14 (2000) 429–454.

7 Seitzinger S P, Kroeze C & Styles R V, Global distribution of N_2O emissions from aquatic systems: Natural emissions and anthropogenic effects, *Chemosphere: Global Change Sci*, 2 (2000) 267–279.

8 Bange H W, Bartell U H, Rapsomanikis S & Andreae M O, Methane in the Baltic and North Seas and a reassessment of the marine emissions of methane, *Global Biogeochem Cycles*, 8 (1994) 465–480.

9 Bates T S, Kelly K C, Johnson J E & Gammon R H, A reevaluation of the open ocean source of methane to the atmosphere, *J Geophys Res*, 101 (1996) 6953–6961.

10 Bange H W, Andreae M O, Lal S, Law C S, Naqvi S W A, Patra P K, Rixen T & Upstill-Goddard R C, Nitrous oxide emissions from the Arabian Sea: A synthesis, *Atmos Chem Phys*, 1 (2001) 61–71.

11 Naqvi S W A, Bange H W, Gibb S W, Goyet C, Hatton A D & Upstill-Goddard R C, Biogeochemical ocean-atmosphere transfers in the Arabian Sea, *Progr Oceanogr*, 2004 (submitted).

12 Conkright M, Levitus S & Boyer T P, NOAA Atlas NESDIS 1, World Ocean Atlas 1994 (National Environmental Satellite, Data, and Information Service, National Oceanic and Atmospheric Administration, US Department of Commerce, Washington DC) 1994.

13 Samuels B L, & Cox M, Data set atlas for oceanographic modeling, *Ocean Modeling*, 75 (1987) 1–3.

14 Gibson J K, Kållberg P, Uppala S, Hernandez A, Nomura A & Serrano E, ECMWF Re-Analysis Project Report Series 1 ERA description, (European Centre for Medium-Range Weather Forecasts, Reading, UK), 1997, pp. 72.

15 Louanchi F, Metzl N & Poisson A, Modelling the monthly sea surface-CO_2 fields in the Indian Ocean, *Mar Chem*, 55 (1996) 265–279.

16 Weiss R F & Price B A Nitrous oxide solubility in water and seawater, *Mar Chem*, 8 (1980) 347–359.

17 Wiesenburg D A & Guinasso Jr N L, Equilibrium solubilities of methane, carbon monoxide, hydrogen in water and seawater, *J Chem Eng Data*, 24 (1979) 356–360.

18 Liss P S & Merlivat L, "Air-sea exchange rates: Introduction and synthesis", in: *The role of air-sea exchange in geochemical cycling*, edited by P Buat-Ménard, (D Reidel Publishing Company, Dordrecht) 1986, pp.113–127.

19 Wanninkhof R, Relationship between wind speed and gas exchange over the ocean, *J Geophys Res*, 97 (1992) 7373–7382.

20 Wanninkhof R & McGillis W R A cubic relationship between air-sea gas CO_2 exchange and wind speed, *Geophys Res Lett*, 26 (1999) 1889–1892.

21 Siedler G & Peters H, Properties of sea water, in: *Oceanography, Landolt-Börnstein New Series Vol V/3a*, edited by J Sündermann, (Springer Verlag, Berlin) 1986, pp. 233–264.

22 Broecker W S & Peng T H, Gas exchange rates between air and sea, *Tellus*, 26 (1974) 21–35.

23 Jähne B, Heinz G & Dietrich W, Measurements of the diffusion coefficients of sparingly soluble gases in water, *J Geophys Res*, 92 (1987) 10,767–10,776.

24 Peng T H, Takahashi T, Broecker W S & Olafsson J, Seasonal variability of carbon dioxide, nutrients and oxygen

in the North Atlantic surface water: Observations and a model, *Tellus*, 39B (1987) 439–458.

25 Bange H W, Rapsomanikis S & Andreae M O, Nitrous oxide cycling in the Arabian Sea, *J Geophys Res*, 106 (2001) 1053–1065.

26 Delling N, *Volatile hydrocarbons in the Arabian Sea – Distribution, formation and budgeting* [*Leichtflüchtige Kohlenwasserstoffe im Arabischen Meer – Verteilung, Genese und Bilanzierung*], Ph.D. thesis, University of Hamburg, Germany, 2002.

27 Patra P K, Lal S, Venkataramani S, Gauns M & Sarma V V S S, Seasonal variability in distribution and fluxes of methane in the Arabian Sea, *J Geophys Res*, 103 (1998) 1167–1176.

28 Patra P K, Lal S, Venkataramani S, De Sousa S N, Sarma V V S S & Sardesai S, Seasonal and spatial variability in N_2O distribution in the Arabian Sea, *Deep-Sea Res I*, 46 (1999) 529–543.

29 Bange H W, Rixen T, Johansen A M, Siefert R L, Ramesh R, Ittekkot V, Hoffmann, M R & Andreae, M O, A revised nitrogen budget for the Arabian Sea, *Global Biogeochem Cycles*, 14 (2000) 1283–1297.

30 Bange H W, Rapsomanikis S & Andreae M O, Nitrous oxide emissions from the Arabian Sea, *Geophys Res Lett*, 23 (1996) 3175–3178.

31 Weiss R F, Van Woy F A & Salameh P K, *Surface water and atmospheric carbon dioxide and nitrous oxide observations by shipboard automated gas chromatography: Results from expeditions between 1977 and 1990*, Report no SIO 92-11, ORNL/CDIAC-59, NDP-044 (Carbon Dioxide Information Analysis Center, Oak Ridge National Laboratory, Oak Ridge, Tennessee, USA) 1992.

32 Upstill-Goddard R C, Barnes J & Owens N J P, Nitrous oxide and methane during the 1994 SW monsoon in the Arabian Sea/northwestern Indian Ocean, *J Geophys Res*, 104 (1999) 30,067–30,084.

33 Bange H W, Ramesh R, Rapsomanikis S & Andreae M O, Methane in the surface waters of the Arabian Sea, *Geophys Res Lett*, 25 (1998) 3547–3550.

34 Lee C M, Jones B H, Brink K H & Fischer A S, The upper-ocean response to monsoonal forcing in the Arabian Sea: Seasonal and spatial variability, *Deep-Sea Res II*, 47 (2000) 1177–1226.

35 Lendt R, Hupe A, Ittekkot V, Bange H W, Andreae M O, Thomas H, Al Habsi S & Rapsomanikis S, Greenhouse gases in cold water filaments in the Arabian Sea during the southwest monsoon, *Naturwissenschaften*, 86 (1999) 489–491.

36 Lal S & Patra P K, Variabilities in the fluxes and annual emissions of nitrous oxide from the Arabian Sea, *Global Biogeochem Cycles*, 12 (1998) 321–327.

37 Dore J E & Karl D M, Nitrification in the euphotic zone as a source for nitrite, nitrate, and nitrous oxide at station ALOHA, *Limnol Oceanogr*, 41 (1996) 1619–1628.

38 Morell J M, Capella J, Mercado A, Bauzá J & Corredor J E, Nitrous oxide fluxes in Caribbean and tropical Atlantic waters: Evidence for near surface production, *Mar Chem*, 74 (2001) 131–143.

39 Naqvi S W A & Noronha R J, Nitrous oxide in the Arabian Sea, *Deep-Sea Res*, 38 (1991) 871–890.

40 Karl D M & Tilbrook B D, Production and transport of methane in oceanic particulate organic matter, *Nature*, 368 (1994) 732–734.

41 De Angelis M A & Lee C, Methane production during zooplankton grazing on marine phytoplankton, *Limnol Oceanogr*, 39 (1994) 1298–1308.

42 Holmes E, Sansone F J, Rust T M & Popp. B N, Methane production, consumption, and air-sea exchange in the open ocean: An evaluation based on carbon isotopic ratios, *Global Biogeochem Cycles*, 14 (2000) 1–10.

Nitrous oxide in the surface layer of the tropical North Atlantic Ocean along a west to east transect

Sylvia Walter, Hermann W. Bange, and Douglas W. R. Wallace

Forschungsbereich Marine Biogeochemie, Leibniz-Institut für Meereswissenschaften (IFM-GEOMAR), Kiel, Germany

Received 10 March 2004; accepted 16 July 2004; published 5 October 2004.

[1] Nitrous oxide (N_2O) was measured during the first German SOLAS (Surface Ocean – Lower Atmosphere Study) cruise in the tropical North Atlantic Ocean on board R/V *Meteor* during October/November 2002. About 900 atmospheric and dissolved N_2O measurements were performed with a semi-continuous GC-ECD system equipped with a seawater-gas equilibrator. Surface waters along the main transect at 10°N showed no distinct longitudinal gradient. Instead, N_2O saturations were highly variable ranging from 97% to 118% (in the Guinea Dome Area, 11°N, 24°W). When approaching the continental shelf of West Africa, N_2O surface saturations went up to 113%. N_2O saturations in the region of the equatorial upwelling (at 0–1.5°N, 23.5–26°W) were correlated with decreasing sea surface temperatures and showed saturations up to 109%. The overall mean N_2O saturation was 104 ± 4% indicating that the tropical North Atlantic Ocean is a net source of atmospheric N_2O. *INDEX TERMS:* 4820 Oceanography: Biological and Chemical: Gases; 0312 Atmospheric Composition and Structure: Air/sea constituent fluxes (3339, 4504); 0322 Atmospheric Composition and Structure: Constituent sources and sinks. **Citation:** Walter, S., H. W. Bange, and D. W. R. Wallace (2004), Nitrous oxide in the surface layer of the tropical North Atlantic Ocean along a west to east transect, *Geophys. Res. Lett.*, *31*, L23S07, doi:10.1029/2004GL019937.

1. Introduction

[2] Nitrous oxide (N_2O) is an important atmospheric trace gas because it influences, directly and indirectly, the Earth's climate to a significant degree: In the troposphere, it acts as a greenhouse gas with a relatively long atmospheric lifetime [*Intergovernmental Panel on Climate Change (IPCC)*, 2001] whereas in the stratosphere it is the major source for nitric oxide radicals, which are involved in one of the main ozone reaction cycles [*World Meteorological Organization*, 2003]. Published source estimates indicate that the world's oceans play a major role in the global budget of atmospheric nitrous oxide [*IPCC*, 2001]. Generally, oligotrophic areas seem to be near equilibrium with the atmosphere, whereas coastal and equatorial upwelling areas show enhanced N_2O concentrations [*Nevison et al.*, 1995; *Suntharalingam and Sarmiento*, 2000]. Here we present about 900 measurements of dissolved and atmospheric N_2O during the first German SOLAS (Surface Ocean – Lower Atmosphere Study) cruise. It is the first high-resolution data set of N_2O in the tropical North Atlantic Ocean along a West to East transect and it is complementary to previous N_2O measurements of *Oudot et al.* [1990, 2002] and *Weiss et al.* [1992].

[3] The cruise took place on board R/V *Meteor* (expedition no. M55) from Willemstad (Curaçao, Netherl. Antilles) to Douala (Cameroon) from 12 October to 17 November 2002. The cruise track consisted of two main transects: (i) The West to East transect along 10–12°N covering the oligotrophic tropical North Atlantic Ocean and the continental shelf area of the West African coast off Guinea Bissau and (ii) a shorter West to East transect along the equatorial upwelling (Figure 1).

2. Method

[4] N_2O was determined with a gas chromatograph equipped with an electron capture detector. Further details of the analysis system are described in *Bange et al.* [1996]. A series of measurements of atmospheric N_2O and N_2O in seawater-equilibrated air followed by two standards was repeated every 50 min. Mixtures of N_2O in synthetic air were used to obtain two-point calibration curves. The mixtures used contained 311.7 ± 0.1 and 346.5 ± 0.2 ppb N_2O, respectively. These are gravimetrically prepared gas mixtures (Deuste Steininger GmbH, Mühlhausen Germany) and have been calibrated against the NOAA (National Oceanic and Atmospheric Administration, Boulder, Co.) standard scale in the laboratories of the Air Chemistry Division of Max Planck Institute for Chemistry Mainz, Germany. The precision, calculated as the ratio of the standard deviation of the atmospheric measurements and the mean atmospheric mixing ratio, was 0.8%.

[5] Seawater was pumped continuously from a depth of 4 m into a shower-type equilibrator developed by R. F. Weiss (Scripps Institution of Oceanography, La Jolla, Ca.). N_2O concentrations (C, in nmol L^{-1}) were calculated by applying the solubility equation of *Weiss and Price* [1980]:

$$C = \beta(T,S)x' P,$$

where x' is the measured N_2O dry mole fraction, P is the atmospheric pressure, and β is the solubility coefficient, which is a function of the water temperature (T) and salinity (S). Time series of seawater temperature (SST), salinity, wind speed, and atmospheric pressure were obtained from the ship's records. Differences between the seawater temperature at the seawater intake and the continuously recorded water temperature in the equilibrator were corrected:

$$C_w = C\beta(T_{eq})/\beta(SST)$$

with $\beta(SST)$ and $\beta(T_{eq})$ representing the N_2O solubility at seawater temperature and water temperature inside the

0094-8276/04/2004GL019937$05.00

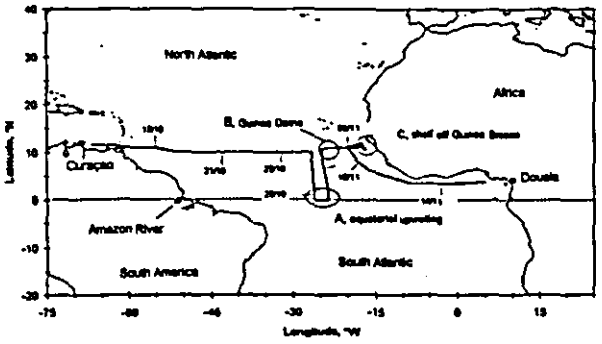

Figure 1. Cruise track of M55 in October–November 2002. N_2O measurements were started 17 October and were finished 14 November. Areas of special interest discussed in the text are marked.

equilibrator at the time of the measurement, respectively. N_2O saturations (*Sat*) in % (i.e., 100% = equilibrium) were calculated as follows:

$$Sat = 100\, C_w / C_a$$

where C_a is the equilibrium concentration of dissolved N_2O based on the actual measurement of ambient air (see above). The mean relative errors of the N_2O concentrations and saturations were calculated to be 1.2% and 1.6%, respectively (details of the error propagation computation are given by *Bange et al.* [2001]).

3. Results and Discussion

[6] The mean atmospheric N_2O dry mole fraction was 318 ± 3 ppb. Due to the seasonal northward shift of the Intertropical Convergence Zone to about 10°N, the origin of the air masses sampled during the cruise were from both the northern and the southern hemisphere. 4-days air mass back trajectories (provided by the German Weather Service, Offenbach, Germany) indicated that air masses sampled at latitudes south of 7°N originated from the southern hemisphere. Based on this classification we computed mean N_2O values for northern and southern hemisphere air masses of 319 ± 3 ppb and 317 ± 2 ppb, respectively. The observed atmospheric values are in agreement with N_2O measurements at the baseline monitoring stations Ragged Point, Barbados and Cape Grim, Tasmania. Monthly mean values were 317 ppb (Cape Grim) and 318 ppb (Ragged Point) for October/November 2002. These values were taken from the Advanced Global Atmospheric Gases Experiment (AGAGE) data set (updated version from November 2003) [*Prinn et al.*, 2000]. AGAGE data are available from the anonymous ftp site ftp://cdiac.esd.ornl.edu (subdirectory pub/ale_gage_Agage/Agage/gc-md/monthly) at the Carbon Dioxide Information Analysis Center in Oak Ridge, Tennessee.

[7] N_2O saturations along the main cruise track ranged from 97% to 118% and the SST was generally between 27 and 30°C (Figure 2). Since the main cruise track was located between the eastward flowing North Equatorial Countercurrent (NECC) and the westward flowing North Equatorial Current (NEC) [*Stramma and Schott*, 1999], we crossed several times meandering waters of different origins causing a high variability of the N_2O saturation: Low N_2O saturations of about 100% observed around 24 Oct., 27–28 Oct., and 2 Nov. were generally associated with decreases in salinity (Figure 2). This results from the retroflection of the North Brazil Current, which advects Amazon plume waters (with low N_2O, see below) eastward into the NECC [*Fratantoni and Glickson*, 2002]. Freshwater influences were observed twice: First, at around 50°E (19 Oct., Figure 2) when we crossed the northern boundary of the Amazon river plume (minimum salinity 32.14) and second, on the continental shelf off West Africa where we measured a drop in salinity down to 31.30 (5–6 Nov., Figure 2). N_2O saturations were not enhanced in the Amazon River plume, whereas an increase in N_2O saturations up to 113% were observed on the West African shelf. The low N_2O saturations in the Amazon River plume were attributed to the fact that N_2O-rich waters from the Amazon River are N_2O-depleted because of outgasing to the atmosphere and mixing with near-equilibrium oceanic waters while distributed to the North [*Oudot et al.*, 2002]. The high N_2O saturations on the continental African shelf might result from N_2O-rich riverine waters or groundwater seepage, but not from coastal upwelling as indicated by the uniform SSTs. N_2O saturations up to 118% were observed in the area of the Guinea Dome at 11°N, 24°E (3–4 Nov., Figure 2) which is well-known for pronounced Ekman upwelling [*Siedler et al.*, 1992; *Signorini et al.*, 1999]. In the equatorial region (0–1.5°N, 28–30 Oct., Figure 2) SSTs dropped well below 27°C and were associated with enhanced N_2O saturations (up to 109%). We found a good

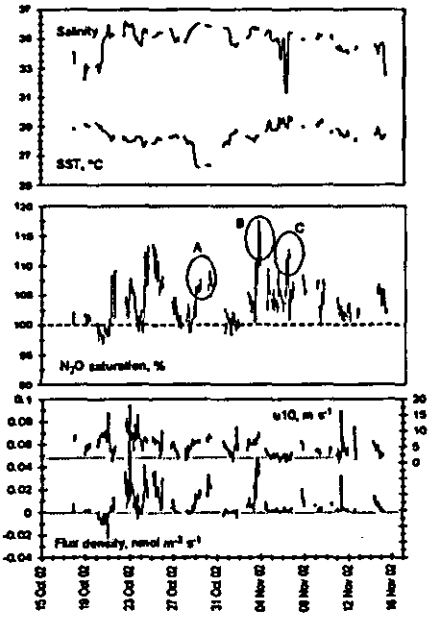

Figure 2. Salinity, seasurface temperature (SST), N_2O saturation, wind speed in 10 m height (u10), and N_2O flux density during M55. Area of special interest discussed in the text are marked (see Figure 1): A, equatorial upwelling; B, Guinea Dome; C, shelf off West Africa (water depths <200 m).

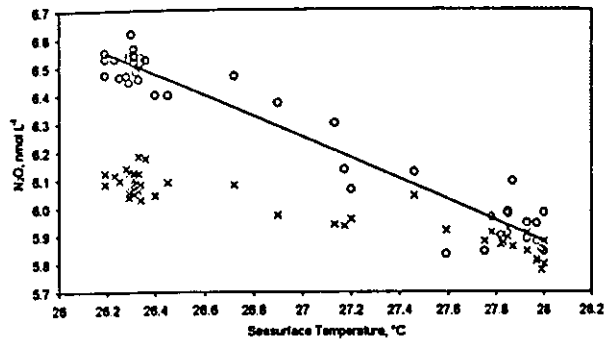

Figure 3. Correlation ($r^2 = 0.94$, n = 46) of SST and N_2O concentration in the equatorial upwelling area (0–2°N, 23.5–26°W). Open circles stand for in-situ measurements and crosses stand for the corresponding equilibrium concentrations calculated as a function of the actual SST, Salinity, atmospheric dry mole fraction, and ambient pressure.

correlation between N_2O concentrations and SST in the equatorial upwelling region (Figure 3) indicating that the enhanced surface N_2O saturations were resulting from upwelling of N_2O-enriched subsurface waters.

[8] In order to account for the NECC/NEC system and the observed N_2O features we defined two latitudinal aligned open ocean regions and a shelf region: 1) the tropical North Atlantic ranging from 1.5–12°N with SST >27°C, 2) the equatorial upwelling from 0–1.5°N with SST <27°C, and 3) the shelf area off the West African coast (water depth <200 m). An overview of the regional mean concentrations and saturations is given in Table 1. The mean N_2O concentrations and saturations of the shelf and equatorial regions are significantly enhanced compared to the 1.5–12°N region. The high variability calculated for the tropical North Atlantic region is biased by the complex hydrography, which is influenced by the Amazon plume, the NECC/NEC system and the Guinea Dome upwelling with highly variable N_2O concentrations. However, a more detailed regional analysis is hampered by the limited data set.

[9] Our data from the tropical North Atlantic are in agreement with previously published data. Recently, *Oudot et al.* [2002] reported a mean N_2O saturation of 108 ± 3%, mainly measured along two transects at 7.5°N and 4.5°S during January–March 1993. They also observed a trend towards enhanced values when approaching the West African coast (up to 118%). In a previous study in the Guinea Dome area during June–August 1986, *Oudot et al.* [1990] observed mean N_2O saturations in the range from 126 ± 5 to 132 ± 6% which are considerably higher than our results (Table 1). In the period from 1979 to 1989, *Weiss et al.* [1992] took part in several measurement campaigns with cruise tracks across the tropical North Atlantic Ocean. Their N_2O measurements are in good agreement with the results presented here. For example, the mean N_2O saturation during the first part of the TTO/TAS leg 3 in February 1983, which covered two transects along 9.5°N (from 20.25 to 28°W) and 28°W (from 9.5 to the equator), was about 105%. Enhanced values during TTO/TAS leg 3 were observed on the coast off Guinea-Bissau (up to 179%) and in the equatorial upwelling (up to 111%). In contrast to our measurements, the high N_2O values observed off Guinea Bissau were caused by coastal upwelling (SST <27°) [*Weiss et al.*, 1992]. Summarizing the results from various N_2O measurements in the open tropical North Atlantic, we found only slight differences (with the exception of the data from the Guinea Dome area by *Oudot et al.* [1990]). Significant differences as found for the Guinea Dome might be caused by seasonal variability of the circulation patterns [*Stramma and Schott*, 1999] in connection with different spatial data coverage. Since coastal upwelling was absent during our cruise, N_2O saturations on the shelf off West Africa were comparably low.

4. N_2O Air-Sea Exchange

[10] The air–sea exchange flux density (F) was parameterized as

$$F = k_w(u)(C_w - C_a),$$

where k_w (in m s^{-1}) is the gas transfer coefficient as a function of wind speed (u in 10 m height), C_w is the measured N_2O seawater concentration, and C_a is the equilibrium N_2O concentration in seawater based on the measured atmospheric value (for calculation of C_w and C_a see Methods section). To calculate k_w, we used the combined linear and quadratic $k_w - u$ relationship from *Nightingale et al.* [2000] (N00):

$$k_w = 9.25\ 10^{-7}\,u + 6.17\ 10^{-7}\,u^2.$$

The N00 relationship shows a dependence on wind speeds intermediate between the commonly used relationships of *Liss and Merlivat* [1986] and *Wanninkhof* [1992]. The measured wind speeds were normalized to 10 m height by using the relationship of *Garratt* [1977]. k_w was adjusted by multiplying with $(Sc/600)^{-0.5}$, where Sc is the *Schmidt* number for N_2O. Sc was calculated using empirical

Table 1. Mean N_2O Concentrations, Saturations, and Flux Densities During M55[a]

	Overall Mean (n = 451)	0–1.5°N (n = 27)	1.5–12°N (n = 416)	Shelf (n = 8)
Concentration, nmol L^{-1}	6.00 ± 0.24	6.49 ± 0.07	5.27 ± 0.20	6.31 ± 0.11
Saturation, %	104 ± 4	107 ± 1	103 ± 3	110 ± 2
Flux density, nmol m^{-2} s^{-1}	0.007 ± 0.011	0.018 ± 0.006	0.006 ± 0.011	0.002 ± 0.002

[a]Values are given as mean ± 1sd. Number of measurements is given in parenthesis.

equations for the kinematic viscosity of seawater [*Siedler and Peters*, 1986] and the diffusion coefficient of N_2O in water. N_2O diffusion coefficients (D_{N2O} in $m^2\ s^{-1}$) were calculated with the equation derived from a compilation of actual measurements [*Rhee*, 2000]:

$$D_{N2O} = 3.16 \times 10^{-6} \exp(-18370/RT),$$

where T is the water temperature in K and R is the universal gas constant. The commonly used equation for D_{N2O} by *Broecker and Peng* [1974] was replaced since *Rhee*'s [2000] equation provides a more reasonable fit with a considerably reduced uncertainty of less than 10% [*Rhee*, 2000]. Flux densities calculated with the above equation are lower by about 10% when compared to computations with *Broecker and Peng*'s [1974] equation [*Bange et al.*, 2001]. We did not apply a correction of D_{N2O} for seawater since the effect of seawater on the diffusion of dissolved gases is not uniform [*King et al.*, 1995] and, to our knowledge, no measurements of the N_2O diffusion in seawater have been published.

[11] The regional mean flux densities clearly reflect the interplay of saturation and wind speeds (Figure 2 and Table 1). In the equatorial region enhanced N_2O saturations and comparably high wind speeds result in high flux densities, whereas over the shelf enhanced N_2O saturations were associated with very low wind speed resulting in low flux densities (Figure 2). The mean flux density of the tropical North Atlantic region is biased by the high variability of both N_2O saturations and wind speeds. The overall mean N_2O flux density was 0.007 ± 0.011 nmol $m^{-2}\ s^{-1}$ which is at the lower end of previously published flux densities: *Oudot et al.* [1990, 2002] computed overall mean flux densities of 0.013–0.021 nmol $m^{-2}\ s^{-1}$ and 0.026 ± 0.032 nmol $m^{-2}\ s^{-1}$ for the tropical North and South Atlantic and the Guinea Dome area, respectively. The obvious discrepancy might be caused by different spatial data coverage, seasonal variability of the N_2O concentrations and wind speeds, and the use of different approaches for the transfer coefficient k_w.

5. Summary

[12] N_2O saturations in the tropical North Atlantic Ocean during October–November 2002 were highly variable and range from 97 to 118%. The mean overall saturation was 104 ± 4%. Enhanced saturations were observed in the Guinea Dome area (up to 118%), in the equatorial upwelling (up to 109%), and the shallow continental shelf area off the West African Coast (up to 113%). Our results are in agreement with previously published data sets. We found a good correlation of seawater temperature with N_2O concentrations in the equatorial upwelling area. We conclude that the tropical North Atlantic Ocean is a net source of N_2O to the atmosphere with a pronounced regional variability.

[13] **Acknowledgments.** We thank A. Körtzinger and M. O. Andreae for technical support and acknowledge the help of the other M55 participants and the officers and crew of R/V *Meteor*. We especially thank R. Hoffmann for the calibration of our standards and two anonymous reviewers for their valuable comments. We are indebted to the authorities of Guinea-Bissau for permission to work in their territorial waters. The investigations were financially supported by the *Deutsche Forschungsgemeinschaft* through grants WA1434/1 and WA1434/3.

References

Bange, H. W., S. Rapsomanikis, and M. O. Andreae (1996), The Aegean Sea as a source of atmospheric nitrous oxide and methane, *Mar. Chem.*, *53*, 41–49.

Bange, H. W., M. O. Andreae, S. Lal, C. S. Law, S. W. A. Naqvi, P. K. Patra, T. Rixen, and R. C. Upstill-Goddard (2001), Nitrous oxide emissions from the Arabian Sea: A synthesis, *Atmos. Chem. Phys.*, *1*, 61–71.

Broecker, W. S., and T.-H. Peng (1974), Gas exchange rates between air and sea, *Tellus*, *26*, 21–35.

Fratantoni, D. M., and D. A. Glickson (2002), North Brazil Current ring generation and evolution observed with SeaWiFS, *J. Phys. Oceanogr.*, *32*, 1058–1074.

Garratt, J. R. (1977), Review of the drag coefficients over oceans and continents, *Mon. Weather Rev.*, *105*, 915–929.

Intergovernmental Panel on Climate Change (2001), *Climate Change 2001: The Scientific Basis: Contribution of Working Group I to the Third Assessment Report of the Intergovernmental Panel on Climate Change (IPCC)*, 881 pp., Cambridge Univ. Press, New York.

King, D. B., W. J. De Bryun, M. Zheng, and E. S. Saltzman (1995), Uncertainties in the molecular diffusion coefficient of gases in water for the estimation of air-sea exchange, in *Air-Water Gas Transfer*, edited by B. Jähne and E. C. Monahan, pp. 13–22, Aeon Verlag, Hanau, Germany.

Liss, P. S., and L. Merlivat (1986), Air-sea exchange rates: Introduction and synthesis, in *The Role of Air-Sea Exchange in Geochemical Cycling*, edited by P. Buat-Ménard, pp. 113–127, D. Reidel, Norwell, Mass.

Nevison, C. D., R. F. Weiss, and D. J. Erickson III (1995), Global oceanic emissions of nitrous oxide, *J. Geophys. Res.*, *100*, 15,809–15,820.

Nightingale, P., G. Malin, C. S. Law, A. J. Watson, P. S. Liss, M. I. Liddicoat, J. Boutin, and R. C. Upstill-Goddard (2000), In situ evaluation of air-sea gas exchange parameterizations using novel conservative and volatile tracers, *Global Biogeochem. Cycles*, *14*, 373–387.

Oudot, C., C. Andrie, and Y. Montel (1990), Nitrous oxide production in the tropical Atlantic Ocean, *Deep Sea Res.*, *37*, 183–202.

Oudot, C., P. Jean-Baptiste, E. Fourré, C. Mormiche, M. Guevel, J.-F. Ternon, and P. Le Corre (2002), Transatlantic equatorial distribution of nitrous oxide and methane, *Deep Sea Res., Part I*, *49*, 1175–1193.

Prinn, R. G., et al. (2000), A history of chemically and radiatively important gases in air deduced from ALE/GAGE/AGAGE, *J. Geophys. Res.*, *105*, 17,751–17,792.

Rhee, T. S. (2000), The process of air-water gas exchange and its application, Ph.D. thesis, Texas A&M Univ., College Station.

Siedler, G., and H. Peters (1986), Properties of sea water, in *Oceanography, Landolt-Börnstein New Ser.*, vol. 3a, edited by J. Sündermann, pp. 233–264, Springer-Verlag, New York.

Siedler, G., N. Zangenberg, R. Onken, and A. Morlière (1992), Seasonal changes in the tropical Atlantic circulation: Observation and simulation of the Guinea Dome, *J. Geophys. Res.*, *97*, 703–715.

Signorini, S. R., R. G. Murtugudde, C. R. McClain, J. R. Christian, J. Picaut, and A. J. Busalachhi (1999), Biological and physical signatures in the tropical and equatorial Atlantic, *J. Geophys. Res.*, *104*, 18,367–18,382.

Stramma, L., and F. Schott (1999), The mean flow field of the tropical Atlantic Ocean, *Deep Sea Res., Part II*, *46*, 279–303.

Suntharalingam, P., and J. L. Sarmiento (2000), Factors governing the oceanic nitrous oxide distribution: Simulations with an ocean general circulation model, *Global Biogeochem. Cycles*, *14*, 429–454.

Wanninkhof, R. (1992), Relationship between wind speed and gas exchange over the ocean, *J. Geophys. Res.*, *97*, 7373–7382.

Weiss, R. F., and B. A. Price (1980), Nitrous oxide solubility in water and seawater, *Mar. Chem.*, *8*, 347–359.

Weiss, R. F., F. A. Van Woy, and P. K. Salameh (1992), Surface water and atmospheric carbon dioxide and nitrous oxide observations by shipboard automated gas chromatography: Results from expeditions between 1977 and 1990, *Rep. NDP-044*, Carbon Dioxide Info. Anal. Cent., Oak Ridge Natl. Lab., Oak Ridge, Tenn.

World Meteorological Organization (2003), *Scientific Assessment of Ozone Depletion: 2002*, 498 pp., World. Metereol. Organ., Geneva.

H. W. Bange, D. W. R. Wallace, and S. Walter, Forschungsbereich Marine Biogeochemie, Leibniz-Institut für Meereswissenschaften (IFM-GEOMAR), Düsternbrooker Weg 20, D-24105 Kiel, Germany. (hbange@ifm-geomar.de)

Version 08 Jan 2006

Nitrous oxide and methane in European coastal waters

submitted to *Estuarine, Coastal and Shelf Science*

Special section EU CarboEurope - GHG project specific study "Coastal ecosystems greenhouse gas budget"

Hermann W. Bange

Forschungsbereich Marine Biogeochemie
IFM-GEOMAR
Leibniz-Institut für Meereswissenschaften
Düsternbrooker Weg 20
24105 Kiel
Germany

ph.: +49-431-600 4204
fax: +49-431-600 4202
e-mail: hbange@ifm-geomar.de

Abstract

Coastal areas such as continental shelves, estuaries, deltas, fjords and lagoons can release high amounts of nitrous oxide (N_2O) and methane (CH_4) to the atmosphere. However, estimates of trace gas emissions are often biased by incomplete spatial and temporal coverages. Based on a compilation of literature data, the distributions of N_2O and CH_4 in European coastal areas (i.e. Arctic Ocean, Baltic Sea, North Sea, northeastern Atlantic Ocean, Mediterranean Sea, Black Sea) were reviewed and their emissions to the atmosphere reassessed. Maximum N_2O saturations were found in estuarine systems, whereas the shelf waters which are not influenced by freshwater plumes are close to equilibrium with the atmosphere. This implies that N_2O is exclusively formed in estuarine systems. European coastal waters are a net source of N_2O to the atmosphere (0.21 – 0.40 Tg N yr^{-1}) with the major contribution coming from estuarine/river systems and not from open shelf areas. European shelf areas contribute significantly (up to 16 %) to the global oceanic N_2O emissions. CH_4 saturations show a high temporal and spatial variability with maximum values in estuarine/fjord systems. European coastal areas are a source of atmospheric CH_4 (0.25 – 0.48 Tg C yr^{-1}) and contribute significantly to the overall global CH_4 oceanic emissions. However, this estimate still seems to be a severe underestimation since CH_4 fluxes from estuaries and shallow seeps are not adequately represented. Future N_2O and CH_4 emissions from coastal areas strongly depend on the degree of eutrophication of coastal waters and might increase in the future.

Keywords:

nitrous oxide, methane, continental shelves, estuaries, air-water exchange

1. Introduction

Nitrous oxide (N_2O) and methane (CH_4) are atmospheric trace gases, which, directly and indirectly, influence the present-day climate of the Earth (IPCC, 2001; WMO, 2003). Thus, an assessment of the natural and anthropogenic sources and sinks as well as the formation pathways of N_2O and CH_4 is essential both to understand past Earth's climate variability and to estimate the future development of Earth's climate. The world's oceans including its coastal zones, as natural sources of N_2O and CH_4, play a major role in the global budget of atmospheric N_2O, but only a minor role in the global budget of atmospheric CH_4 (IPCC, 2001). However, measurements of oceanic N_2O and CH_4 are still sparse and the derived emission estimates are associated with large uncertainties (Bange et al., 1994; Bange et al., 1996b; Bates et al., 1996; Nevison et al., 1995; Seitzinger et al., 2000; Suntharalingam and Sarmiento, 2000).

N_2O in oceanic environments is mainly formed as a byproduct during nitrification ($NH_4^+ \rightarrow NH_2OH \rightarrow NO_2^- \rightarrow NO_3^-$) and as an intermediate during denitrification ($NO_3^- \rightarrow NO_2^- \rightarrow N_2O \rightarrow N_2$). In both processes, the yield of N_2O strongly depends on the concentration of dissolved oxygen (O_2) (e.g. Codispoti et al. 2005; Goreau et al., 1980). Both, nitrification and denitrification are microbial processes and can occur in the water column, in the sediments and in the interior of suspended particles (e.g. Codispoti et al., 2005; Nevison et al. 2003; Schropp et al. 1983). CH_4 is formed during the decomposition of organic material by microbial methanogenesis (e.g. Cicerone and Oremland 1988). Since CH_4 formation requires strictly anaerobic conditions, CH_4 is produced in anoxic environments such as sediments, in the interior of suspended particles or in zooplankton guts during grazing (e.g. De Angelis and Lee, 1994; Holmes et al., 2000; Karl and Tilbrook, 1994). Additionally, CH_4 is oxidized under aerobic as well as anaerobic conditions in

the water column and in the sediments (e.g. Boetius et al., 2002; King, 1992). On the continental shelf so-called geological CH_4 can be released directly to the water column through mud volcanoes, via groundwater input or seeping at pockmark structures (e.g. Etiope and Klusman, 2002; Judd et al. 2002a).

The objective of the present study is to give an overview of the distributions of N_2O and CH_4 in European coastal areas and to reassess their emissions to the atmosphere. Moreover, the major formation pathways of N_2O and CH_4 in coastal areas are described. Future research activities to improve our understanding of N_2O and CH_4 cycling in coastal areas are outlined at the end.

1.1 Methodological remarks

For the purpose of this study, European coastal areas are defined as the European continental shelf with water depths <200m. For details of the area classification see Uher (2005). European coastal areas consist of the complete Baltic and the North Seas as well as parts of the Mediterranean Sea (i.e. the Adriatic and Aegean Seas) and the Black Sea, parts of the Northeast (NE) Atlantic Ocean (i.e. the English Channel, the Celtic (Irish) Sea and the Bay of Biscay) and parts of the Arctic Ocean (i.e. the Norwegian and Barents Seas) (Figure 1). Also included in the studies are estuaries, fjords and other systems at the interface between the continental shelf and the terrestrial environment (Figure 2). An overview of the locations of the studies discussed in the text is given in Figures 3 and 4. For details of the environmental settings (i.e. hydrography, biogeochemical conditions etc.) of the marginal seas, estuaries etc. mentioned in the text the reader is referred to appropriate publications and textbooks.

In the literature dissolved N_2O and CH_4 are generally either expressed as a concentration (in nmol L^{-1}, nmol kg^{-1} or mL L^{-1} as for CH_4 in some cases) or

saturation (in %), which is the ratio of the measured gas concentration to the expected equilibrium concentration. The equilibrium concentration in turn depends on the water temperature, salinity, ambient air pressure and the atmospheric N_2O or CH_4 mixing ratio (Weiss and Price, 1980; Wiesenburg and Guinasso Jr., 1979). Thus, a saturation of 100% indicates that the water phase is in equilibrium with the overlying atmosphere. Saturation values <100% indicate undersaturation (i.e. uptake of N_2O or CH_4 into the water phase) whereas saturation values >100% stand for supersaturation (i.e. N_2O or CH_4 release from the water phase to the atmosphere).

In order to have a high degree of transparency, I predominately used publications in international journals or books. "Grey" literature such as PhD thesis etc. is only cited when unavoidable.

2. Overview: Nitrous oxide (N_2O)

2.1 Arctic Ocean

There seem to be no N_2O data available from the coastal areas of the Arctic Ocean.

2.2 Baltic Sea

First measurements (during August–September 1977, July 1979 and May–June 1980) of N_2O in the surface layer (0-0.5m) of the central and northern Baltic Sea were in the range from 79% to 148% (with an average of 123% for the Baltic Proper) indicating that the Baltic Sea was source of N_2O to the atmosphere (Rönner, 1983). In the well-oxygenated water column below the mixed layer, increasing N_2O concentrations were generally associated with an increase of nitrate (NO_3^-) and a decrease of oxygen (O_2) (Rönner, 1983). However, N_2O concentrations sharply drop

down within the oxic/anoxic interface in the deep basins of the central Baltic Sea and remain constant at levels close to zero in anoxic deep waters (Brettar and Rheinheimer, 1991; Rönner, 1983). Based on the observed negative correlation between N_2O and O_2 and the positive correlation between N_2O and NO_3^-, Rönner (1983) concluded that in oxygen-rich waters N_2O is produced during nitrification. In contrast, the depletion of N_2O in the anoxic waters of the deep basins of the Baltic Sea is caused by N_2O consumption during denitrification (Brettar and Rheinheimer, 1991; Rönner, 1983).

A seasonal study (five campaigns between 1994 and 1997) in the shallow lagoons of the southern Baltic Sea / western Oder River estuary area (the so-called Bodden waters with water depths ranging from 0.5 to 8.5 m) revealed saturations in the range from 91% to 312%, with a pronounced maximum at the sampling station near the mouth of the Peene River in March (Bange et al., 1998a). Thus, Bange et al. (1998a) concluded that enhanced N_2O concentrations in the Bodden waters were linked to the seasonal peak of the Peene River run off. However, the prevailing cause for the N_2O concentrations in the Bodden waters remained unclear since the enhanced N_2O concentrations could either have been caused directly through input of high riverine N_2O concentrations or indirectly through a high input of NO_3^- which in turn might have fuelled sedimentary denitrification (Dahlke et al., 2000). Incubation of sediment cores from the Bodden waters showed both consumption and release of N_2O; however, no correlation was found between nitrification and denitrification activities in the cores and N_2O formation (Dahlke et al., 2000).

Two seasonal studies in the shallow estuarine waters of the Limfjorden and Norsminde Fjords at the east coast of Jutland, Denmark, revealed that considerably enhanced dissolved N_2O concentrations (up to 490 nmol L^{-1}) occurred during spring which were partly associated with high riverine NO_3^- input (Jensen et al., 1984;

Jørgensen and Sørensen, 1985). In the two Danish fjords N_2O flux to the atmosphere was mainly balanced by N_2O released from sedimentary denitrification (Jensen et al., 1984; Jørgensen and Sørensen, 1985).

2.3 North Sea

The first survey of dissolved N_2O in the North Sea was performed by Law and Owens (1990) in June 1986 and July 1987. They found a mean N_2O surface (0-1m) saturation of 102% in the northern and central North Sea and a mean surface saturation of 130% in the southeastern part of the North Sea (i.e. the German Bight) indicating that the North Sea acted a source of N_2O to the atmosphere. Nitrification was suggested as source for N_2O in the water column, whereas the contribution of N_2O produced by sedimentary denitrification was shown to be negligible (Law and Owens, 1990). Bange et al. (1996b) measured mean surface saturations of 104% and 100% for the central North Sea (September 1991) and the German Bight (September 1991 and 1992), respectively.

Estuaries located along the western North Sea are generally a source of N_2O to the atmosphere. However, considerable seasonal and spatial variability along the estuarine salinity gradient of the N_2O saturations have been observed. In the Colne River estuary, for example, N_2O saturations ranged from about 80% up to 5190% (Dong et al., 2002; Robinson et al., 1998). In the Humber estuary N_2O saturations during a study from March to December 1996 ranged from 100% to 4250% (avg. 425%) (Barnes and Owens, 1998). N_2O saturations in the Tweed estuary from September 1997 to March 1997 were in the range from 96%-110% (avg. 100%) (Barnes and Owens, 1998). Comparable to the estuaries located along the English coast, N_2O saturations in the Scheldt estuary at the Dutch North Sea coast were in the range from 100% to 3100% (seasonal study from October 1993 to July 1996 by

de Wilde and de Bie (2000)). Additionally, de Bie et al. (2002) calculated a median N_2O saturation of 710% for the Scheldt estuary during 13 monthly surveys along the salinity gradient from April 1997 to April 1998.

Two different dominating pathways for N_2O formation in estuaries along the North Sea coast have been identified: (i) water column nitrification in the maximum turbidity zone (MTZ) in the low salinity regions of the Scheldt and Humber Estuaries (Barnes and Owens, 1998; De Bie et al., 2002; De Wilde and De Bie, 2000) and (ii) sedimentary denitrification in the Colne Estuary (Dong et al., 2002; Robinson et al., 1998). It seems that the evolved estuarine N_2O formation pathway strongly depends on local settings such as the water column distributions of O_2 and nutrients (NH_4^+ and NO_2^-) as well as the microbial community (De Bie et al., 2002; Dong et al., 2002).

Investigation of the N_2O emission rates from intertidal sediments along the Scheldt Estuary from September 1990 to December 1991 and in the western Wadden Sea from April 1989 to March 1990) revealed a high degree of spatial and seasonal variability (Kieskamp et al., 1991; Middelburg et al., 1995). Interestingly, intertidal sediments can even act as a temporary sink for atmospheric N_2O (Kieskamp et al., 1991; Middelburg et al., 1995). No clear relationship of N_2O emission rates either with nitrification nor denitrification rates were detected (Middelburg et al., 1995). However, Middelburg et al. (1995) were able to establish a linear relation between the annual integrated N_2O emission rates from the intertidal sediments and the nitrogen loading.

2.4 English Channel, Bay of Biscay

A comprehensive study on N_2O cycling has been performed in the Tamar Estuary (southwest England) during August 1988 and June 1990 by Law et al. (1992). N_2O saturations were in the range from about 100% to 330% and were

attributed to sedimentary denitrification and to a minor degree to water column nitrification in the MTZ, terrestrial runoff and sewage input (Law et al., 1991; Law et al., 1992). Additionally, denitrifying bacteria in epiphytic communities on the surface of the macroalgae Enteromorpha sp. from the Tamar estuary showed a high potential of N_2O production during spring-summer (Law et al., 1993).

N_2O saturations in the Gironde Estuary (southwest France) measured during a campaign in November 1991 ranged from 106% to 165% (average 132%) (Bange et al., 1996b). A further study of the N_2O distribution in the Gironde estuary in June 1997 indicated that the highest N_2O surface concentrations are found in the maximum turbidity zone (MTZ) in the low salinity region of the estuary (Abril et al., 2000). Abril et al. (2000) found a good correlation between suspended particulate matter and dissolved N_2O and concluded that N_2O is produced in the MTZ; however, the processes responsible for N_2O formation (water column nitrification or sedimentary denitrification) have not been deciphered (Abril et al., 2000).

2.5 Mediterranean Sea, Adriatic Sea, Aegean Sea

N_2O saturations along five transects in the Gulf of Lions (northwestern Mediterranean Sea) and the adjacent Rhone River Plume in June 1998 and March-November 1997 ranged from 0% to appr. 200% (i.e. 15 nmol L^{-1}) and up to 41 nmol L^{-1}, respectively (Marty et al., 2001). N_2O saturations in the inner Gulf of Thermaikos (northwestern Aegean Sea) during April 1998 were found to be in the range from 84% to 309% (Marty et al., 2001). Associated measurements of the bacterial production showed nitrifying and denitrifying activities in suspended particulate matter, however, a direct relationship between the measured N_2O concentrations and N_2O formation rates was not found (Marty et al., 2001).

Measurements during a study from May 1996 to January 1998 in the shallow Sacca di Goro, a coastal lagoon in the Po River delta in the northern Adriatic Sea, revealed N_2O saturations in the range from 0% – 6635% with highest N_2O fluxes to the atmosphere in autumn and winter (Leip, 1999). N_2O saturations at one station in the open Adriatic Sea in August 1996 were found to be slightly undersaturated (85% – 100%) in the surface (0-20m) and supersaturated (up to 140%) down to the bottom at 70m (Leip, 1999). Leip (1999) attributed the high N_2O saturation in the lagoon to input of N_2O by the Po River. Additionally, the spatial N_2O distribution in the lagoon seemed to be influenced by the incoming Adriatic Sea water and sedimentary N_2O production (Leip, 1999).

A survey of N_2O surface concentrations during a cruise in the coastal waters of the eastern Ionian Sea and the northern Aegean Sea in July 1993 showed a mean N_2O saturation of about 107% (Bange et al., 1996a). During the same cruise a mean N_2O saturation of 103% was found in the Amvrakikos Bay (at the west coast of Greece). Interestingly, N_2O concentrations along the salinity gradient in the Amvrakikos Bay showed a positive correlation with the salinity indicating that N_2O was not produced in the Amvrakikos Bay (Bange et al., 1996a).

2.6 Black Sea

In July 1995 the mean N_2O saturations on the Black Sea's northwestern shelf / Danube River plume and in the open Black Sea were 112% (Amouroux et al., 2002). No correlation between N_2O concentrations and salinity was found and the formation pathways remained unidentified (Amouroux et al., 2002).

3. Overview: Methane (CH_4)

3.1 Arctic Ocean: Norwegian Sea, Barents Sea

In the Barents Sea considerably enhanced CH_4 concentrations (up to 56.7 nmol L^{-1}) were found over a pockmark field east of Bear Island (Lammers et al., 1995). However, surface CH_4 concentrations were near equilibrium or slightly supersaturated (up to 3.8 nmol L^{-1}, i.e. 125 %) because the high CH_4 plume concentrations are rapidly oxidized or diluted by mixing with ambient waters with lower CH_4 concentrations (Lammers et al., 1995). This is in line with the study of the fate of CH_4 in the plume of the Håkon Mosby mud volcano in the deep Norwegian Sea by Damm and Budéus (2003). In a recently published study, Damm et al. (2005) presented their CH_4 measurements in the shelf waters and two fjords on the continental shelf of Southwest Spitsbergen. CH_4 concentrations were in the range from 1.8 to 240.8 nmol L^{-1} (maximum saturation was about 7200%). Obviously, CH_4 was released to the water column from several inter-granual seepages or micro-seepages along the shelf in about 100-200 m depth. The Spitsbergen shelf is known to be sites of gas hydrates deposits, natural seabed gas seeps and buried active petroleum source rocks (Damm et al., 2005). Once released to the water column, CH_4 concentrations were lowered due to oxidation and mixing processes.

3.2 Baltic Sea

Surface CH_4 saturations in the Baltic Sea generally show a great spatial and seasonal variability in the open Baltic Sea (Bange et al., 1994) as well as in the shallow coastal regions (Abril and Iversen, 2002; Bange et al., 1998a; Bussmann and Suess, 1998; Heyer and Berger, 2000; Schmaljohann, 1996). Mean area-weighted CH_4 surface saturations in the southern and central basins of the Baltic Sea were 113% and 395% in February and July/August 1992, respectively (Bange et al., 1994).

CH_4 saturations in the shallow, well ventilated coastal fjords of the southwestern Baltic Sea such as the Randers Fjord, Eckernförde Bay and the shallow lagoons of Bodden waters in the southern Baltic Sea / western Oder River estuary area range from slightly below equilibrium (62%) to values up to appr. 25,700,000% (642,000 nmol L^{-1}) (Abril and Iversen, 2002; Bange et al., 1998a; Bussmann and Suess, 1998; Heyer and Berger, 2000).

Measurements of CH_4 concentrations in the anoxic deep waters of the central basin of the Baltic Sea (Gotland Basin) during January/February 1990 revealed values of up to 400 nmol L^{-1}, whereas in the oxygenated water column CH_4 concentrations were considerably lower (4.5 – 120 nmol L^{-1}) (Dzyuban et al., 1999). Fenchel et al. (1995) reported CH_4 concentrations exceeding 30,000 nmol L^{-1} in the bottom water of the anoxic basin of the Marianger Fjord (east coast of Denmark) in August 1994. Accumulation of CH_4 (up 2700 nmol L^{-1}) in the Kiel Harbour has been observed during stagnation periods when the water column became anoxic during the end of the summers of 1992 and 1993 (Schmaljohann, 1996).

In the Baltic Sea, the interplay of the various CH_4 formation and consumption processes seems to be complex. There are several factors which have been identified to cause the observed high seasonal and spatial variability of dissolved CH_4. Rivers entering the estuarine systems of the Baltic Sea seems to be enriched in CH_4 thus riverine CH_4 can be responsible for enhanced CH_4 concentrations in the upper estuaries / fjords or near coastal areas (Abril and Iversen, 2002; Bange et al., 1994; Bange et al., 1998a). The main CH_4 formation process is methanogenesis in the sediments. However, sedimentary aerobic CH_4 oxidation provides an effective barrier for sedimentary CH_4 to reach the water column (Abril and Iversen, 2002; Dahlke et al., 2000; Schmaljohann, 1996). Nevertheless, CH_4 release (e.g., via diffusion) from the sediments still provides the significant source for dissolved CH_4 in

the water column (Fenchel et al., 1995; Schmaljohann, 1996). In the water column itself, considerable rates of aerobic as well as anaerobic CH_4 oxidation have been observed in a few studies (Abril and Iversen, 2002; Fenchel et al., 1995). Shifts from oxic to anoxic conditions significantly enhance CH_4 formation in the sediments (Schmaljohann, 1996) and water column (Dzyuban et al., 1999). Moreover, seasonal variations of water temperature, wind speeds and availability of organic matter have been identified to regulate, directly or indirectly, estuarine CH_4 emissions to the atmosphere (Abril and Iversen, 2002; Bange et al., 1998a; Heyer and Berger, 2000).

Apart from methanogenesis, natural seepage of CH_4, as observed in the CH_4-rich pockmark structures of the Eckernförde Bay (Bussmann et al., 1999), in the Kattegat (Dando et al., 1994; Laier et al., 1992) and in the Stockholm Archipelago (Söderberg and Flodén, 1992) are significant sources of dissolved CH_4 in the water column, but poorly quantified in terms of their significance for CH_4 emissions to the atmosphere.

3.3 North Sea, English Channel, Bay of Biscay, coastal NE Atlantic

CH_4 surface measurements during a transect from the southern North Sea to the NE Atlantic in November 1980 by Conrad and Seiler (1988) showed a clear trend of mean saturations from about 140% in the southern North Sea to 100% in the Bay of Biscay. Comparable CH_4 saturations (95% – 130%) were observed in the open southern North Sea by Bange et al. (1994) and Scranton and McShane (1991). A strong CH_4 concentration gradient towards the Dutch coast (up to 12,000%) associated with the Rhine River plume were observed by Scranton and McShane (1991) and De Wilde and Duyzer (1995) during two measurement campaigns in March 1989 and October 1993, respectively. During a cruise from east to west along 58°N in the central North Sea which was followed by a transect to the German Bight

in May 1994, Rehder et al. (1998) observed a remarkably high spatial variability of CH_4 surface saturations in the range from 103% to 50,000% (i.e., 1453 nmol L^{-1}) (Rehder et al., 1998). The extraordinary high values were resulting from CH_4 released from an abandoned borehole (Rehder et al., 1998). During the same cruise, enhanced CH_4 saturations (from 130% up to >1000%) were observed in the Skagerrak (eastern North Sea), the Dogger Bank (central North Sea) and the German Bight / Elbe River estuary (Rehder et al., 1998). Werneke et al. (1994) observed significantly enhanced CH_4 concentrations (up to 625,000 nmol kg^{-1}) in 1 m height above the seafloor when passing a seepage area in the northeastern North Sea. However, the CH_4 concentrations in the plume decreased to about 6 nmol kg^{-1} in 25 m height above the seafloor (Werneke et al., 1994). At two stations at the Norwegian coast (Haugesund and Bømla Fjord), CH_4 concentrations ranged from about 6 nmol kg^{-1} (surface) to about 250 nmol kg^{-1} (bottom water in 130 m water depth at Haugesund) (Werneke et al., 1994). During a series of measurements along the English east coast and southern North Sea (Dutch coast), Upstill-Goddard et al. (2000) found CH_4 saturations from 74% to 2245%.

A series of CH_4 measurements have been performed in several estuaries along the North Sea (Elbe, Ems, Rhine, Scheldt, Thames, Humber, Tyne), the Bay of Biscay (Loire and Gironde) and the NE Atlantic (Douro and Sado) yielding CH_4 saturations from significantly undersaturated (70% in the Gironde) up to highly supersaturated (49,700% in the Rhine River) (De Wilde and Duyzer, 1995; Middelburg et al., 2002; Upstill-Goddard et al., 2000). The distribution of CH_4 saturations along the estuarine salinity gradients showed great seasonal and spatial variabilities. Generally, CH_4 saturations at the interface to the coastal waters were comparable to those measured in the open North Sea and the open Bay of Biscay. Maximum estuarine CH_4 saturations were observed in the upper parts of the

estuaries at low salinities. In the Framvaren Fjord (south coast of Norway) CH_4 concentrations from about 1000 nmol L^{-1} (surface) up 26,000 nmol L^{-1} (anoxic bottom water) were measured (Lidstrom, 1983).

In contrast to the various studies in the Baltic Sea (see above), it seems that less attention has been paid to identify the responsible CH_4 formation/consumption processes in the North Sea area. Scranton and McShane (1991) measured CH_4 oxidation rates in the water column and concluded that loss by oxidation is a minor sink in view of the high sea-to-air emissions. Anaerobic CH_4 oxidation in the anoxic water column of Framvaren Fjord was observed by Lidstrom (1983). Riverine input, sedimentary release and formation within the turbidity maximum zone have been suggested as possible sources for estuarine CH_4, however, the processes itself have not been identified (Middelburg et al., 2002; Rehder et al., 1998; Scranton and McShane, 1991; Upstill-Goddard et al., 2000).

There is increasing evidence that the release of so-called geological CH_4 from natural seepages and abandoned boreholes contribute significantly to the atmospheric CH_4 emissions especially from the North Sea (Judd et al., 1997; Rehder et al, 1998). In the Skagerrak, for example, large areas of CH_4-charged sediments and associated plumes of CH_4 gas bubbles in the water column have been identified (Hempel et al., 1994; Hovland, 1992; Zimmermann et al., 1997). Further areas where CH_4-rich sediments have been verified are the UK shelf (Judd et al., 1997; Judd et al., 2002b), the Belgian coast (Missiaen et al., 2002), the Spanish Atlantic coast (Garcia-Gil et al., 2002) and the western Irish Sea (Yuan et al., 1992). However, it is difficult to assess the atmospheric emissions solely based on seabed seepage rates and/or plumes of gas bubbles (Judd et al., 1997; Leifer and Kumar Patro, 2002).

3.4 Mediterranean Sea, Adriatic Sea, Aegean Sea

CH_4 concentrations along five transects in the Gulf of Lions (northwestern Mediterranean Sea) and the adjacent Rhone River Plume in June 1998 and March-November 1997 ranged from 0 nmol L^{-1} to 1263 nmol L^{-1} and up to 1363 nmol L^{-1}, respectively (Marty et al., 2001). There was a clear trend from maximum CH_4 concentrations at the Rhone River mouth to the open Mediterranean Sea. CH_4 concentrations in the inner Gulf of Thermaikos (northwestern Aegean Sea) during April 1998 were found to be in the range from 0 to 1378 nmol L^{-1} (Marty et al., 2001). Associated measurements of the bacterial production showed CH_4 production in suspended particulate matter, however, a direct relationship between the measured CH_4 concentrations and CH_4 formation rates was not found (Marty et al., 2001). CH_4 saturations at one station in the open Adriatic Sea in August 1996 were found to be supersaturated (appr. 400% – 450%) in the surface layer (0 – 10m) and supersaturated as high as 2750% below the surface layer down to 70m (Leip, 1999).

A survey of CH_4 surface concentrations during a cruise in the coastal waters of the eastern Ionian Sea and the northern Aegean Sea in July 1993 showed a mean CH_4 saturation from 148% (3.2 nmol L^{-1}) to 231% (4.8 nmol L^{-1}) (Bange et al., 1996a). During the same cruise a mean CH_4 saturation of 522% (11.1 nmol L^{-1}) was found in the Amvrakikos Bay (at the west coast of Greece).

CH_4 gas release from geological sources has been reported from the northern Adriatic Sea (Conti et al., 2002). In the central Aegean Sea, hydrothermal systems also release a considerable amount of gas to the water column, however, in the sampled gas bubble plumes, the fraction of CH_4 was generally less than 10% (Dando et al., 1995).

3.5 Black Sea

In July 1995 the mean CH_4 surface saturations on the Black Sea's northwestern shelf and in the Danube River plume were 567% (13 nmol L^{-1}) and 5340% (131 nmol L^{-1}), respectively (Amouroux et al., 2002). A comparable range of CH_4 concentrations (22 – 380 nmol L^{-1}) were observed by Ivanov et al. (2002) at 11 stations during a cruise on the northwestern shelf of the Black Sea in August 1995. CH_4 was formed during methanogenesis in the shallow shelf sediments with higher formation rates in summer than in spring (Ivanov et al., 2002). Despite the fact that considerable CH_4 oxidation rates occur in the sediments and in the water column, CH_4 release from the sediments seemed to maintain the high CH_4 concentrations in the water column (Ivanov et al., 2002).

In a recent study of the influence of CH_4 seeps on CH_4 surface saturation in the northwestern Black Sea, Schmale et al. (2005) found CH_4 surface saturations up to 143% for the open Black Sea, whereas CH_4 saturations above a seep on the shallow shelf (90 m) were up to 294%. They concluded that only seeps in shallow shelf waters have the potential to contribute to the surface CH_4 saturation in the Black Sea, whereas contributions from deep water (>100m) CH_4 seeps are negligible. This is in contrast to the study by Lein (2005) who showed that the CH_4 released from mud volcanoes in the deep Black Sea can reach the surface waters and, thus, contribute to the CH_4 emissions to the atmosphere as well.

Occurrence of shallow gas-charged sediments and CH_4 bubble plumes has been reported from many areas along the Black Sea coast (see e.g. Dimitrov (2002), Tkeshelashvili et al. (1997), Ergun et al. (2002), Kutas et al. (2002)). However, the contribution of gas seepages to the overall high CH_4 concentrations in water column

and the atmospheric emissions are largely unknown. CH_4 seeps along the shelf slope, which are already located within the zone of the permanent anoxic deep waters, were found to be associated with thick microbial mats with potentially high anaerobic CH_4 oxidation rates (Michaelis et al., 2002).

4. Emission estimates

4.1 N_2O

The majority of the N_2O surface saturation data presented above indicate that European coastal waters are generally supersaturated with N_2O (especially in estuarine systems), despite the fact that in some cases undersaturations (<100%) have been observed. Since saturations greater than 100% result in a N_2O flux from the ocean surface to the atmosphere, European coastal waters are a net source of N_2O to the atmosphere. N_2O saturations for various European shelf areas and estuaries are listed in Tables 1a and 1b. Studies, which either do not report N_2O saturations explicitly or do not allow reconstructing N_2O saturations, were not included. If there were multiple studies for the same location, only the study with the better seasonal coverage was listed. From the data listed in Tables 1a and 1b we calculated mean N_2O saturations of 113% and 465% for the European shelf and estuaries, respectively. Based on the mean N_2O saturations we calculated mean N_2O emissions of 0.12 Tg N yr^{-1} and 0.19 Tg N yr^{-1} for the European shelf and estuaries, respectively (for details see Table 2). The resulting overall N_2O emissions range from 0.15 to 0.4 Tg N yr^{-1} (with a mean of 0.31 Tg N yr^{-1}). Our estimate is in good agreement with the result (0.29 Tg N yr^{-1}) from a recent model study of Seitzinger and Kroeze (1998) in which the N_2O formation was quantified via denitrification and nitrification in European coastal waters (i.e. NE Atlantic between 45° and 66°N, Baltic

Sea, Mediterranean Sea and Black Sea). In their study, N_2O formation was linked to riverine nitrate inputs, which in turn were estimated as a function of the atmospheric deposition of nitrogen oxides (NO_y), fertilizer use and sewage inputs (Seitzinger and Kroeze, 1998). Their model calculations yielded annual N_2O productions of 0.06 Tg (=10^{12}g) N and 0.23 Tg N for the European estuaries/continental shelf and rivers, respectively. Global estimates of the N_2O emissions from coastal areas are in the range from 1.9 Tg N yr^{-1} (Seitzinger and Kroeze, 1998) to 6.7 Tg N yr^{-1}(Bange et al., 1996b). Thus, European coastal waters may contribute up to 16% of the today's global coastal N_2O emissions. Using current trends of the increase of the human population, fertilizer use and NO_y deposition, Kroeze and Seitzinger (1998) predicted the N_2O production in European coastal waters for the year 2050. The resulting N_2O estimates were 0.10 Tg N yr^{-1} and 0.33 Tg N yr^{-1} for the European estuaries/continental shelf and rivers, respectively, suggesting that future coastal N_2O production might increase by 67% and 43% respectively. However, the overall global coastal N_2O production in 2050 might increase to 4.9 Tg N yr^{-1} indicating that the future contribution by European coastal waters (9%) to the global production will be lower than today (Kroeze and Seitzinger, 1998).

4.2 CH_4

CH_4 in the surface layer is generally supersaturated, except for a few cases (see text above). Therefore, European coastal waters are a net source for atmospheric CH_4. CH_4 surface concentrations range from slightly undersaturated (= 1 – 4 nmol L^{-1}) to extremely supersaturated (= 642,000 nmol L^{-1}) indicating a high seasonal and spatial variability. CH_4 saturations for various European shelf areas and estuaries are listed in Tables 3a and 3b. Studies, which either do not report CH_4

saturations explicitly or do not allow reconstructing CH_4 saturations, were not included. If there were multiple studies for the same location, only the study with the better seasonal coverage was listed. From the data listed in Tables 3a and 3b we calculated mean CH_4 saturations of 224% and 3643% for the European shelf and estuaries, respectively. Based on the mean CH_4 saturations we calculated mean CH_4 emissions of 0.13 Tg C yr^{-1} and 0.24 Tg C yr^{-1} for the European shelf and estuaries, respectively (for details see Table 4). The resulting overall CH_4 emissions range from 0.25 to 0.48 Tg C yr^{-1} (with a mean of 0.37 Tg C yr^{-1}). The emission estimate for the European shelf (excl. estuaries) is in good agreement with a previous estimate by Bange et al. (1994). They estimated a total flux of 0.11 Tg C yr^{-1} for the European coastal shelf waters (North Sea, Baltic Sea, Mediterranean Sea, Black Sea; excl. estuaries) which represents about 1.5% of the overall global CH_4 emissions from the shelf (excl. estuaries) (Bange et al., 1994). I conclude that emissions from the European shelf and estuarine areas contribute significantly to the overall global CH_4 oceanic emissions (0.3 Tg C yr^{-1} for the open ocean, Bates et al. (1996)). However, the overall estimate presented here still seems to be an severe underestimation since estuarine CH_4 fluxes and CH_4 fluxes from geological sources are not adequately represented: For example, Upstill-Goddard et al. (2000) estimated an annual CH_4 emission of 0.09 Tg C from estuaries in the southern North Sea alone. Judd et al. (1997) estimated the CH_4 flux to the atmosphere by natural seepages on the UK shelf to be in the range from 0.09 to 2.6 Tg C yr^{-1}. Moreover, Dimitrov (2002) computed that annually between 0.02 Tg C and 0.11 Tg C are emitted from the Bulgarian shelf (Black Sea) to the atmosphere by natural CH_4 seepages. Adding the mean fluxes via natural CH_4 seepages from the North Sea and the Bulgarian shelf (Judd et al., 1997; Dimitrov, 2002) and the estimate by Upstill-Goddard et al. (2000) yields an atmospheric CH_4 flux of about 1.5 Tg C yr^{-1}. This value is certainly a severe

underestimation since natural seepages from gassy, CH_4-bearing sediments, which occur all over at the European shelf (for an overview see Fleischer et al. (2001)), as well as the major part of estuarine CH_4 emissions is not adequately represented. In view of the fact that open ocean emissions for CH_4 have been estimated to be as low as 0.3 Tg C yr^{-1} (Bates et al., 1996) it as obvious that the significance of coastal CH_4 emissions on a regional (European) and on a global scale is much higher then previously thought.

4.3 Uncertainties

The emission estimates discussed above are associated with large uncertainties:

(i) Data coverage. Despite an increasing number of studies dealing with the distribution of N_2O and CH_4 in coastal waters, their distributions in large parts of the coastal areas (in Europe as well as globally) are still unknown.

(ii) Seasonality. Since the formation of N_2O and CH_4 is mainly driven by biological processes, the observed variability is influenced by the pronounced seasonality of various parameters such as temperature, riverine nutrient inputs etc. Unfortunately, most studies are biased towards the summer months.

(iii) Air-sea exchange models. There are still considerably uncertainties associated with the applied air-sea exchange models, thus the choice of the model introduces an additional bias. Furthermore, the choice of the used wind speeds (i.e. in-situ wind speeds vs. climatological data) is resulting in an additional variability. These and other uncertainties associated with the air-sea exchange are discussed by Upstill-Goddard (2005).

5. Conclusions and outlook

5.1 N_2O

Based on the data presented, three main conclusions can be drawn:

(i) Highest N_2O saturations were observed in estuaries and fjords, whereas in open coastal waters (i.e. shelf waters not influenced by freshwater) N_2O saturations are close to the expected equilibrium saturation. This indicates that N_2O is exclusively formed in estuarine systems.

(ii) European coastal waters are a net source of N_2O to the atmosphere; however, the major contribution comes from the estuarine/river systems and not from the open shelf areas. European shelf areas contribute significantly (up to 16 %) to the global oceanic N_2O emissions.

(iii) It is obvious that sedimentary denitrification and water column nitrification seem to be the major N_2O formation processes. However, the yield of N_2O from both processes strongly depends on the local O_2 concentrations, thus O_2 is the key factor regulating N_2O production (and its subsequent emissions to the atmosphere). Additionally, N_2O distributions in estuaries show a pronounced seasonal variability. In anoxic waters, such as the deep basin of the central Baltic Sea or parts of the shallow Po River delta, N_2O is consumed by water column denitrification.

There might be two further, however, largely unknown N_2O sources in European coastal areas: First, coastal upwelling brings N_2O from subsurface layers to the surface, thus it can be an additional, physically driven, source of N_2O to the atmosphere (Nevison et al., 2004). Despite small local upwelling areas along the

European coasts, a large coastal upwelling site is found at the Atlantic coast of Portugal. However, studies on N_2O during the upwelling events along the coast of Portugal are not known yet. Second, organic matter release from fish farming activities could increase the dissimilatory nitrate reduction to ammonium (DNRA) in the sediments underlying the fish cages, whereas denitrification was found to be unaffected (Christensen et al., 2000). DNRA, however, might be an additional source of N_2O (Welsh et al., 2001).

Future N_2O emissions from coastal areas strongly depend on nitrogen inputs to coastal waters and will most probably increase in the future (Kroeze and Seitzinger, 1998). Eutrophication and/or increasing deposition of nitrogen-containing aerosols already increased the number of coastal areas with severe O_2 depletion on a global scale (UNEP, 2004). This, in turn, might result in conditions favourable for enhanced N_2O production as observed along the West Indian shelf where N_2O surface saturations up to 8250% (436 nmol L^{-1}) have been measured due to a dramatic depletion of O_2 concentrations (Naqvi et al., 2000).

5.2 CH_4

Based on the data presented, three main conclusions can be drawn:

(iv) CH_4 concentrations show a high temporal and spatial variability in European coastal waters. Maximum concentrations were observed in estuarine/fjord systems indicating that CH_4 is mainly formed in shallow coastal regions.

(v) European coastal areas are a net source of atmospheric CH_4. Natural CH_4 seepages and associated CH_4 bubble plumes as observed in the shallow North and Baltic Seas and in the Black Sea, are an additional source which has not

been quantified adequately for the European coastal waters. Thus, it seems that European coastal CH_4 emissions are considerably underestimated.

(vi) The main CH_4 formation process is methanogenesis in the sediments and its subsequent release to the water column. Shifts from oxic to anoxic conditions significantly enhance CH_4 formation in the sediments and water column. Sedimentary aerobic and anaerobic CH_4 oxidation processes reduce CH_4 concentrations, however, it seems that these processes cannot prevent CH_4 from accumulation.

CH_4 emissions from coastal upwelling areas are of regional importance as observed in the well-studied coastal upwelling centres in the Arabian Sea and the coast off Oregon (Bange et al., 1998b; Rehder et al., 2002). Thus, an additional CH_4 source might be CH_4 emissions from the upwelling region along the coast of Portugal; however, studies on CH_4 in this region are not known yet. CH_4 releases from mud volcanoes are of minor importance because they are usually located in the deeper parts of the continental shelf slope (Miles, 1995; Milkov, 2000) and the CH_4 plume concentrations are rapidly oxidized or diluted by mixing with ambient waters with lower CH_4 concentrations before reaching the atmosphere. This was shown in the studies of the Håkon Mosby mud volcano (Norwegian Sea) by Damm and Budéus (2003) and Lein (2005). This is in contrast to the study by Lein (2005) who suggested that the CH_4 release from mud volcanoes in the deep Black Sea can contribute to the atmospheric CH_4 emissions. Seeps located in shallow shelf waters (<100 m) seem to influenced surface CH_4 concentrations (Damm et al., 2005; Schmale et al., 2005). Future CH_4 emissions from coastal areas strongly depend on inputs of nutrients and organic matter to coastal waters and will most probably increase in the future. Eutrophication already increased the number of coastal areas with severe O_2

depletion on a global scale (UNEP, 2004). This, in turn, might result in conditions favourable for enhanced CH_4 production.

5.3 Outlook

Despite the fact that our knowledge on the distribution of N_2O and CH_4 in coastal areas is still associated with a high degree of uncertainty, a rough impact assessment of various parameters which might influence today's and future N_2O and CH_4 emissions from European coastal waters is given in Table 5. It is obvious that in order to quantify today's and future emissions of N_2O and CH_4 we need more measurements, new tools and approaches such as:

(i) Time series measurements of dissolved and atmospheric concentrations along the salinity gradients in selected coastal and estuarine systems (intertidal estuaries, fjords, lagoons, upwelling areas) in order to resolve the seasonality.

(ii) Time series measurements of N_2O and CH_4 formation processes along the salinity gradients in selected estuarine systems (intertidal estuaries, fjords, lagoons etc.) in order to reveal the major formation pathways.

(iii) Measurements of CH_4 emissions from shallow geological sources (natural seepages) in order to quantify the contribution by geological CH_4.

(iv) Development of obligatory standard protocols to measure N_2O and CH_4 in the water and in the atmosphere. N_2O and CH_4 measurements should be performed with standards which have to be intercalibrated against internationally accepted standard scales.

(v) Development of autonomously operating N_2O/CH_4 measurement systems to be used on ferry lines or ships of opportunity to gain a high temporal and spatial resolution of the distribution of N_2O and CH_4 in surface waters.

6. Acknowledgements

This review was initiated during a workshop in Gdansk in July 2003 on "Coastal Ecosystems Greenhouse Gas Budget" as part of the EU CarboEurope – Greenhouse Gases Project Specific Study. I especially thank the project coordinator Jozef Pacyna for his kind invitation to attend the workshop and Stein Manø for organisation of the workshop. Moreover, I acknowledge the support of the Leibniz-Institut für Meereswissenschaften (IFM-GEOMAR) Kiel. This work was funded by EU CarboEurope – Greenhouse Gases Project Specific Study grant no. EVK2-CT-2002-20014.

7. References

Abril, G., Iversen, N., 2002. Methane dynamics in a shallow non-tidal estuary (Randers Fjord, Denmark). Marine Ecology-Progress Series 230, 171–181.

Abril, G., Riou, S.A., Etcheber, H., Frankignoulle, M., De Wit, R. Middelburg, J.J., 2000. Transient, tidal time-scale, nitrogen transformations in an estuarine turbidity maximum - fluid mud system (the Gironde, south-west France). Estuarine and Coastal Shelf Science 50, 703–715.

Amouroux, D., Roberts, G., Rapsomanikis, S., Andreae, M.O., 2002. Biogenic gas (CH_4, N_2O, DMS) emission to the atmosphere from near-shore and shelf waters of the north-western Black Sea. Estuarine Coastal Shelf Science 54, 575–587.

Bange, H.W., Bartell, U.H., Rapsomanikis, S., Andreae, M.O., 1994. Methane in the Baltic and North Seas and a reassessment of the marine emissions of methane. Global Biogeochemical Cycles 8, 465–480.

Bange, H.W., Dahlke, S., Ramesh, R., Meyer-Reil, L.-A., Rapsomanikis, S., Andreae, M.O., 1998a. Seasonal study of methane and nitrous oxide in the coastal waters of the southern Baltic Sea. Estuarine Coastal Shelf Science 47, 807–817.

Bange, H.W., Ramesh, R., Rapsomanikis, S., Andreae, M.O., 1998b. Methane in the surface waters of the Arabian Sea. Geophys. Res. Lett. 25, 3547–3550.

Bange, H.W., Rapsomanikis, S., Andreae, M.O., 1996a. The Aegean Sea as a source of atmospheric nitrous oxide and methane. Marine Chemistry 53, 41–49.

Bange, H.W., Rapsomanikis, S., Andreae, M.O., 1996b. Nitrous oxide in coastal waters. Global Biogeochemical Cycles 10, 197–207.

Barnes, J., Owens, N.J.P., 1998. Denitrification and nitrous oxide concentrations in the Humber estuary, UK, and adjacent coastal zones. Marine Pollution Bulletin 37, 247–260.

Bates, T.S., Kelly, K.C., Johnson, J.E., Gammon, R.H., 1996. A reevaluation of the open ocean source of methane to the atmosphere. Journal of Geophysical Research 101, 6953–6961.

Boetius, A., Ravenschlag, K., Schubert, C.J., Rickert, D., Widdel, F., Giesecke, A., Amann, R., Jorgensen, B. B., Witte, U., Pfannkuche, O., 2000. A marine microbial consortium apparently mediating anaerobic oxidation of methane. Nature 407, 623–626.

Brettar, I., Rheinheimer, G., 1991. Denitrification in the central Baltic: Evidence for H_2S oxidation as motor of denitrification at the oxic-anoxic interface. Marine Ecology-Progress Series 77, 157–169.

Bussmann, I., Dando, P.R., Niven, S.J., Suess, E., 1999. Groundwater seepage in the marine environment: Role for mass flux and bacterial activity. Marine Ecology-Progress Series 178, 169–177.

Bussmann, I., Suess, E., 1998. Groundwater seepage in Eckernförde Bay (Western Baltic Sea): Effect on methane and salinity distribution of the water column. Continental Shelf Research 18, 1795–1806.

Christensen, P.B., Rysgaard, S., Sloth, N.P., Dalgaard, T., Schwaerter, S., 2000. Sediment mineralization, nutrient fluxes, denitrification and dissimilatory nitrate reduction to ammonium in an estaurine fjord with sea cage trout farm. Aquatic Microbial Ecology 21, 73–84.

Cicerone, R.J., Oremland, R.S., 1988. Biogeochemical aspects of atmospheric methane. Global Biogeochemical Cycles 2, 299–327.

Codispoti, L.A., Yoshinari, T., Devol, A.H., 2005. Suboxic respiration in the oceanic water column. In: Del Giorgio, P.A., Williams, P.J.le.B. (Eds.), Respiration in aquatic ecosystems. Oxford University Press, Oxford, pp. 225–247.

Conrad, R., Seiler, W., 1988. Methane and hydrogen in seawater (Atlantic Ocean). Deep-Sea Research 35, 1903–1917.

Conti, A., Stefano, A., Zuppi, G.M., 2002. Gas seeps and rock formation in the northern Adriatic Sea. Continental Shelf Research 22, 2333–2344.

Dahlke, S., Wolff, S., Meyer-Reil, L.-A., Bange, H.W., Ramesh, R., Rapsomanikis, S., Andreae, M.O., 2000. Bodden waters (southern Baltic Sea) as a source of methane and nitrous oxide. In: Flemming, B.W., Delafontaine, M.T., Liebezeit, G. (Eds.), Proceedings in Marine Sciences, Volume 2: Muddy Coast Dynamics and Resource Management. Elsevier Science, Amsterdam, pp. 137–148.

Damm, E., Budéus, G., 2003. Fate of vent-derived methane in seawater above the Håkon Mosby mud volcano (Norwegian Sea). Marine Chemistry 82, 1–11.

Damm, E., Mackensen, A., Budéus, G., Faber, E., Hanfland, C., 2005. Pathways of methane in seawater: Plume spreading in an Arctic shelf environment (SW-Spitsbergen). Continental Shelf Research 25, 1453–1472.

Dando, P.R., Hughes, J.A., Leahy, Y., Niven, S.J., Taylor, L.J., Smith, C., 1995. Gas venting rates from submarine hydrothermal areas around the island of Milos, Hellenic Volcanic Arc. Continental Shelf Research 15, 913–929.

Dando, P.R., Jensen, P., O'Hara, S.C.M., Niven, S.J., Schmaljohann, R., Schuster, U., Taylor, L.J., 1994. The effects of methane seepage at an intertidal/shallow subtidal site on the shore of the Kattegat, Vendsyssel, Denmark. Bulletin of the Geological Society of Denmark 41, 65–79.

De Angelis, M.A., Lee, C., 1994. Methane production during zooplankton grazing on marine phytoplankton. Limnology and Oceanography 39, 1298–1308.

De Bie, M.J.M., Middelburg, J.J., Starink, M., Laanbroek, H.J., 2002. Factors controlling nitrous oxide at the microbial community and estuarine scale. Marine Ecology-Progress Series 240, 1–9.

De Wilde, H.J.P., De Bie, M.J.M., 2000. Nitrous oxide in the Schelde estuary: Production by nitrification and emission to the atmosphere. Marine Chemistry 69, 203–216.

De Wilde, H.P.J., Duyzer, J., 1995. Methane emissions off the Dutch coast: Air-sea concentrations differences versus atmospheric gradients. In: Jähne, B., Monahan E.C. (Eds.), Air-water gas transfer. AEON Verlag & Studio, Hanau, pp. 763–773.

Dimitrov, L., 2002. Contribution to atmospheric methane by natural seepages on the Bulgarian continental shelf. Continental Shelf Research 22, 2429–2442.

Dong, L.F., Nedwell, D.B., Underwood, G.J.C., Thornton, D.C.O., Rusmana, I., 2002. Nitrous oxide formation in the Colne estuary, England: The central role of nitrite. Applied and Environmental Microbiology 68, 1240–1249.

Dzyuban, A.N., Krylova, I.N., Kuznetsova, I.A., 1999. Propperties of bacteria distribution and gas regime within the water column of the Baltic Sea in winter. Oceanology 39, 348–351.

Ergun, M., Dondurur, D., Cifci, G., 2002. Acoustic evidence for shallow gas accumulations in the sediments of the eastern Black Sea. Terra Nova 14, 313–320.

Etiope, G., Klusman, R.W., 2002. Geological emissions of methane to the atmosphere. Chemosphere 49, 777–789.

Fenchel, T., Bernard, C., Esteban, G., Finlay, B.J., Hansen, P.J., Iversen, N., 1995. Microbial diversity and activity in a Danish fjord with anoxic deep water. Ophelia 43, 45–100.

Fleischer, P., Orsi, T.H., Richardson, M.D., Anderson, A.L., 2001. Distribution of free gas in marine sediments: A global overview. Geo-Marine Letters 21, 103–122.

Garcia-Gil, S., Vilas, F., Garcia-Garcia, A., 2002. Shallow gas features in incised-valley fills (Ría de Vigo, NW Spain): A case study. Continental Shelf Research 22, 2303–2315.

Goreau, T.J., Kaplan, W.A., Wofsy, S.C., McElroy, M.B., Valois, F.W., Watson, S.W., 1980. Production of NO_2^- and N_2O by nitrifying bacteria at reduced concentrations of oxygen. Applied and Environmental Microbiology 40, 526–532.

Hempel, P., Spieß, V., Schreiber, R., 1994. Expulsion of shallow gas in the Skagerrak - Evidence from sub-bottom profiling, seismic, hydroacoustical and geochemical data. Estuarine, Coastal and Shelf Science 38, 583–601.

Heyer, J., Berger, U., 2000. Methane emission from the coastal area in the southern Baltic Sea. Estuarine, Coastal and Shelf Science 51, 13–30.

Holmes, E., Sansone, F.J., Rust, T.M., Popp, B.N., 2000. Methane production, consumption, and air-sea exchange in the open ocean: An evaluation based on carbon isotopic ratios. Global Biogeochemical Cycles 14. 1–10.

Hovland, M., 1992. Pockmarks and gas-charged sediments in the eastern Skagerrak. Continental Shelf Research 12, 1111–1119.

IPCC, 2001. Climate change 2001: The scientific basis. Contribution of working group I to the third assessment report of the Intergovernmental Panel on Climate

Change. Cambridge University Press, Cambridge (UK) and New York (USA), 881 pp.

Ivanov, M.V., Pimenov, N.V., Rusanov, I.I., Lein, A.Y., 2002. Microbial processes of the methane cycle at the north-western shelf of the Black Sea. Marine Ecology-Progress Series. 54, 589–599.

Jensen, H.B., Jørgensen, K.S., Sørensen, J., 1984. Diurnal variation of nitrogen cycling in coastal, marine sediments II. Nitrous oxide emission. Marine Biology 83, 177–183.

Jørgensen, B.B., Sørensen, J., 1985. Seasonal cycles of O_2, NO_3^- and SO_4^{2-} reduction in estuarine sediments: The significance of an NO_3^- reduction maximum in spring. Marine Ecology-Progress Series 24, 65–74.

Judd, A., Davies, G., Wilson, J., Holmes, R., Baron, G., Bryden, I., 1997. Contributions of atmospheric methane by natural seepage on UK continental shelf. Marine Geology 137, 165–189.

Judd, A.G., Hovland, M., Dimitrov, L.I., García Gil, S., Jukes, V., 2002a. The geological methane budget at continental margins and its influence on climate change. Geofluids 2, 109–126.

Judd, A.G., Sim, R., Kingston, P., McNally, J., 2002b. Gas seepage on an intertidal side: Torrey Bay, Firth of Forth, Scotland. Continental Shelf Research 22, 2317–2331.

Karl, D.M., Tilbrook, B.D., 1994. Production and transport of methane in oceanic particulate organic matter. Nature 368, 732–734.

Kieskamp, W.M., Lohse, L., Epping, E., Helder, W., 1991. Seasonal variation in the denitrification rates and nitrous oxide fluxes in intertidal sediments of the western Wadden Sea. Marine Ecology-Progress Series 72, 145–151.

King, G.M., 1992. Ecological aspects of methane oxidation, a key determinant of global methane dynamics. Advances in Microbial Ecology 12, 431–468.

Kroeze, C., Seitzinger, S.P., 1998. Nitrogen inputs to rivers, estuaries, and continental shelves and related nitrous oxide emissions in 1990 and 2050: A global model. Nutrient Cycling in Agroecosystems 52, 152–212.

Kutas, R.I., Rusakov, O.M., Kobolev, V.P., 2002. Gas seeps in the northwestern Black Sea: Geological and geophysical studies. Russian Geology and Geophysics 43, 664–670.

Laier, T., Jørgensen, N.O., Buchardt, B., Cederberg, T., Kuijpers, A., 1992. Accumulation and seepages of biogenic gas in northern Denmark. Continental Shelf Research 12, 1173–1186.

Lammers, S., Suess, E., Hovland, M., 1995. A large methane plume east of Bear Island (Barents Sea): Implications for the marine methane cycle. Geologische Rundschau 84, 59–66.

Law, C.S., Owens, N.J.P., 1990. Denitrification and nitrous oxide in the North Sea. Netherlands Journal of Sea Research 25, 65–74.

Law, C.S., Rees, A.P., Owens, N.J.P., 1991. Temporal variability of denitrification in estuarine sediments. Estuarine, Coastal and Shelf Science 33, 37–56.

Law, C.S., Rees, A.P., Owens, N.J.P., 1992. Nitrous oxide: Estuarine sources and atmospheric flux. Estuarine, Coastal and Shelf Science 35, 301–314.

Law, C.S., Rees, A.P., Owens, N.J.P., 1993. Nitrous oxide production by estuarine epiphyton. Limnology and Oceanography 38, 435–441.

Leifer, I., Kumar Patro, R., 2002. The bubble mechanism for methane transport from shallow sea bed to the surface: A review and sensitivity study. Continental Shelf Research 22, 2409–2428.

Lein, A.Y., 2005. Methane flows from cold methane seeps in the Black Sea and Norwegian Seas: Quantitative estimates. Geochemistry International 43, 395–409.

Leip, A., 1999. Nitrous oxide (N_2O) emissions from a coastal catchment in the delta of the Po river: Measurements and modeling of fluxes from a Mediterranean lagoon and agricultural soils. Ph.D. Thesis, University of Bayreuth, Bayreuth, Germany, unpublished.

Lidstrom, M.E., 1983. Methane consumption in Franvaren, an anoxic fjord. Limnology and Oceanography 28, 1247–1251.

Liss, P.S., Merlivat, L., 1986. Air-sea exchange rates: Introduction and synthesis. In: Buat-Ménard, P. (Ed.), The role of air-sea exchange in geochemical cycling. D. Reidel Publishing Company, Dordrecht, pp. 113–127.

Marty, D., Bonin, P., Michotey, V., Bianchi, M., 2001. Bacterial biogas production in coastal systems affected by freshwater inputs. Continental Shelf Research 21, 2105–2115.

Michaelis, W., Seifert, R., Nauhaus, K., Treude, T., Thiel, V., Blumenberg, M., Knittel, K., Gieseke, A., Peterknecht, K., Pape, T., Boetius, A., Amann, R., Jørgensen, B.B., Widdel, F., Peckmann, J. R., Pimenov, N. V., Gulin, M. B., 2002. Microbial

reefs in the Black Sea fueled by anaerobic oxidation of methane. Science 297, 1013–1015.

Middelburg, J.J., Klaver, G., Nieuwenhuize, J., Markusse, R.M., Vlug, T., Van der Nat, F.J.W.A., 1995. Nitrous oxide emissions from estuarine intertidal sediments. Hydrobiologia 311, 43–55.

Middelburg, J.J., Nieuwenhuize, J., Iversen, N., Høgh, N., De Wilde, H., Helder, W., Seifert, R., Christof, O., 2002. Methane distribution in European tidal estuaries. Biogeochemistry 59, 95–119.

Miles, P.R., 1995. Potential distribution of methane hydrate beneath the European continental margins. Geophysical Research Letters 22, 3179–3182.

Milkov, A.V., 2000. Worldwide distribution of submarine mud volcanoes and associated gas hydrates. Marine Geology 167, 29–42.

Missiaen, T., Murphy, S., Loncke, L., Henriet, J.-P., 2002. Very high-resolution seismic mapping of shallow gas in the Belgian coastal zone. Continental Shelf Research 22, 2291–2301.

Naqvi, S.W.A., Jayakumar, D.A., Narveka, P.V., Naik, H., Sarma, V.V.S.S., D'Souza, W., Joseph, S., George, M.D., 2000. Increased marine production of N_2O due to intensifying anoxia on the Indian continental shelf. Nature 408, 346–349.

Nevison, C., Butler, J.H., Elkins, J.W., 2003. Global distribution of N_2O and □N_2O-AOU yield in the subsurface ocean. Global Biogeochemical Cycles 17, 1119, doi:10.1029/2003GB002068.

Nevison, C., Lueker, T., Weiss, R.F., 2004. Quantifying the nitrous oxide source from coastal upwelling. Global Biogeochemical Cycles 18, GB1018, doi:10.1029/2003GB002110.

Nevison, C.D., Weiss, R.F., Erickson III, D.J., 1995. Global oceanic emissions of nitrous oxide. Journal of Geophysical Research 100, 15,809–15,820.

Rehder, G., Collier, R.W., Heeschen, K., Kosro, P.M., Barth, J. Suess, E., 2002. Enhanced marine CH_4 emissions to the atmosphere off Oregon caused by coastal upwelling. Global Biogeochemical Cycles 16, doi 10.1029/2000GB001391.

Rehder, G., Keir, R.S., Suess, E., Pohlmann, T., 1998. The multiple sources and patterns of methane in North Sea waters. Aquatic Geochem.istry 4, 403–427.

Robinson, A.D., Nedwell, D.B., Harrison, R.M., Ogilvie, B.G., Hypernutrified estuaries as a source of N_2O emission to the atmosphere: The estuary of the River Colne, Essex, UK. Marine Ecology-Progress Series 164, 59–71.

Rönner, U., 1983. Distribution, production and consumption of nitrous oxide in the Baltic Sea. Geochimica et Cosmochimica Acta 47, 2179–2188.

Schmale, O., Greinert, J., Rehder, G., 2005. Methane emission from high-intensity marine gas-seeps in the Black Sea into the atmosphere. Geophysical Research Letters 32, L07609, doi:10.1029/2004GL021138.

Schmaljohann, R., 1996. Methane dynamics in the sediment and water column of Kiel Harbour (Baltic Sea). Marine Ecology-Progress Series 131, 262–273.

Schropp, S.J., Schwarz, J.R., 1983. Nitrous oxide production by denitrifying microorganisms from the eastern tropical Pacific and the Caribbean Sea. Geomicrobiology Journal 3, 17–31.

Scranton, M.I., McShane, K., 1991. Methane fluxes in the southern North Sea: The role of European rivers. Continental Shelf Research 11, 37–52.

Seitzinger, S.P., Kroeze, C., Global distribution of nitrous oxide production and N inputs in freshwater and coastal marine ecosystems. Global Biogeochemical Cycles 12, 93–113.

Seitzinger, S.P., Kroeze, C., Styles, R.V., 2000. Global distribution of N_2O emissions from aquatic systems: Natural emissions and anthropogenic effects. Chemosphere: Global Change Science 2, 267–279.

Söderberg, P., Flodén, T., 1992. Gas seepages, gas eruptions and degassing structures in the seafloor along the Strömma tectonic lineament in the crystalline Stockholm Archipelago, east Sweden. Continental Shelf Research 12, 1157–1171.

Suntharalingam, P., Sarmiento, J.L., 2000. Factors governing the oceanic nitrous oxide distribution: Simulations with an ocean general circulation model. Global Biogeochemical Cycles 14, 429–454.

Tkeshelashvili, G.I., Egorov, V.N., Mestvirishivili, S.A., Parkhaladze, G. S., Gulin, M. B., Gulin, S.B., Artemov, Y.G., 1997. Methane emissions from the Black Sea bottom in the mouth zone of the Suspa river at the Coast of Georgia. Geochemistry International 35, 284–288.

Uher, G., 2005. Distribution and air-sea exchange of reduced sulphur gases in European coastal waters. Estuarine, Coastal and Shelf Science THIS VOLUME, XX–XX.

UNEP, 2004. United Nations Envrionment Programme, Global Environment Outlook Year Book 2003, UNEP, Nairobi, Kenya, pp. 76.

Upstill-Goddard, R.C., 2005. TITLE. Estuarine, Coastal and Shelf Science THIS VOLUME, XX–XX.

Upstill-Goddard, R.C., Barnes, J., Frost, T., Punshon, S., Owens, N.J.P., 2000. Methane in the southern North Sea: Low-salinity inputs, estuarine removal, and atmospheric flux. Global Biogeochemical Cycles 14, 1205–1217.

Wanninkhof, R., 1992. Relationship between wind speed and gas exchange over the ocean. Journal of Geophysical Research 97, 7373–7382.

Weiss, R.F., Price, B. A., 1980. Nitrous oxide solubility in water and seawater. Marine Chemistry 8, 347–359.

Welsh, D.T., Castadelli, G., Bartolli, M., Poli, D., Careri, M., De Wit, R., Viaroli, P., 2001. Denitrification in an intertidal seagrass meadow, a comparison of ^{15}N-isotope and acetylene-block techniques: Dissimilatory nitrate reduction to ammonia as a source of N_2O?. Marine Biology 139, 1029–1036.

Wernecke, G., Flöser, G., Korn, S., Weitkamp, C., Michaelis, W., 1994. First measurements of the methane concentration in the North Sea with a new in-situ device. Bulletin of the Geological Society of Denmark 41, 5–11.

Wiesenburg, D.A., Guinasso Jr., N.L., 1979. Equilibrium solubilities of methane, carbon monoxide, hydrogen in water and seawater. Journal of Chemical and Engineering Data 24, 356–360.

WMO, 2003. World Meteorological Organization, Scientific assessment of ozone depletion: 2002. WMO, Geneva, pp. 498.

Yuan, F., Bennell, J.D. Davis, A.M., 1992. Acoustic and physical characteristics of gassy sediments in the western Irish Sea. Continental Shelf Research 12, 1121–1134.

Zimmermann, S., Hughes, R.G., Flügel, H.J., 1997. The effect of methane seepage on the spatial distribution of oxygen and dissolved sulphide within a muddy sediment. Marine Geology 137, 149–157.

Table 1a: Compilation of average N_2O surface saturations in European shelf waters (excluding estuarine systems and river plumes, see Table 1b).

Region	Date	Avg. N_2O (range or sd), nmol L^{-1}	Reference
		Baltic Sea	
Baltic Proper	1977-1980*	127** (111 – 138)	Rönner (1983)
Bothnian Sea	Jun 1980	119** (101 – 130)	Rönner (1983)
Bothnian Bay	Jun 1980	116** (109 – 120)	Rönner (1983)
Gotland Deep	1986-1987*	112**	Brettar and Rheinheimer (1991)
		North Sea	
German Bight	1991-1992*	100 (99 – 101)	Bange et al. (1996b)
German Bight	Jul 1987	130	Law and Owens (1990)
Central North Sea	Sep 1991	104 ± 1	Bange et al. (1996b)
Central North Sea	Jul 1987	102	Law and Owens (1990)
		Mediterranean Sea	
Northern Aegean Sea	Jul 1993	106 ± 2	Bange et al. (1996a)
Eastern Ionian Sea	Jul 1993	107 ± 3	Bange et al. (1996a)
Gulf of Lions	Jun 1998	86** (0 – 197)	Marty et al. (2001)
Gulf of Thermaikos	Apr 1998	171** (84 – 309)	Marty et al. (2001)
Adriatic Sea	Aug 1996	93** (85 – 100)	Leip (1999)
		Black Sea	
Northwestern shelf	Jul 1995	112	Amouroux et al. (2002)
Average		113 ± 21	

sd stands for standard deviation.
* study with a seasonal/interannual coverage, for details see reference.
** values estimated based on the information given in the reference.

Table 1b: Compilation of average N_2O surface saturations in European estuarine systems and river plumes.

Region	Date	Avg. N_2O (range or sd), nmol L^{-1}	Reference
		Baltic Sea	
Bodden waters	1994-1997*	108** (100 – 120)	Bange et al. (1998a)
		North Sea	
Colne	1993-1994*	2645** (100 – 5190)	Robinson etal. (1998)
Scheldt	1997-1998*	710	De Bie et al. (2002)
Humber	1995-1996*	452 (100 – 4250)	Barnes and Owens (1998)
Tweed	1996-1997*	100 (96 – 110)	Barnes and Owens (1998)
Humber Wash plume	May 1995	113* (100 – 125)	Barnes and Owens (1998)
		NE Atlantic	
Gironde	Nov 1992	132 (106 – 165)	Bange et al. (1996b)
Tamar	1988-1990*	215** (100 – 330)	Law et al. (1992)
		Mediterranean Sea	
Amvrakikos Bay	Jul 1993	103 ± 2	Bange et al. (1996a)
Sacca di Goro	1996-1997*	490 (0 – 6635)	Leip (1999)
Rhone plume	1997*	398** (226 – 555)	Marty et al. (2001)
		Black Sea	
Danube plume	Jul 1995	112	Amouroux et al. (2002)
Average		465 ± 716	

sd stands for standard deviation.
* study with a seasonal/interannual coverage, for details see reference.
** values estimated based on the information given in the reference.

Table 2: Estimate of the annual N_2O emissions from European shelf and estuarine areas.

	Area[1], 10^{12} m^2	Avg. saturation[2], %	ΔC[3], nmol L^{-1}	Emissions[4] (LM86), Tg N yr^{-1}	Emissions[4] (W92), Tg N yr^{-1}
Shelf	3.18	113	1.1	0.08	0.15
Estuaries	0.17	465	34	0.13	0.25

[1] According to Uher (2005).
[2] see Tables 1a and 1b.
[3] ΔC stands for the concentration difference across the ocean/atmosphere interface and was calculated as $\Delta C = (\text{saturation}/100^*C_{air}) - C_{air}$. C_{air} was calculated with the Bunsen coefficient of Weiss and Price (1980) for a water temperature of 15°C and salinities of 35 and 15 for shelf and estuaries, respectively. We applied a mean atmospheric N_2O dry mole fraction of 308 ppb (i.e. the mean for the period 1980-1998 corresponding to the dates of the listed measurements)
[4] LM86 stands for the model approach of Liss and Merlivat (1986). W92 stands for the model approach of Wanninkhof (1992) for climatological wind speeds. We applied a mean wind speed of 7 m s^{-1}. N_2O Schmidt numbers were calculated with the mean water temperature and salinities as given in footnote 3.

Table 3a: Compilation of average CH_4 surface saturations in European shelf waters (excluding estuarine systems and river plumes, see Table 3b).

Region	Date	Avg. CH_4 (range or sd), satuation, %	Reference
		Arctic Sea	
Barents Sea	Aug 1991	120 (115 – 125)	Lammers et al. (1995)
		Baltic Sea	
Baltic Proper	1992*	254 (113 – 395)	Bange et al. (1994)
		North Sea	
Southern North Sea	Nov 1980	140	Conrad and Seiler (1988)
German Bight	Sep 1991	126 ± 8	Bange et al. (1994)
Southern Bight	Mar 1989	113 (95 – 130)	Scranton and McShane (1991)
Central North Sea	May 1994	215 (120 – 332)	Rehder et al. (1998)
Southern North Sea	Aug 1993	338 (118 – 701)	Upstill-Goddard et al. (2000)
Off UK east coast	1995-1999	129 (112 –136)	Upstill-Goddard et al. (2000)
		NE Atlantic	
Bay of Biscay	Nov 1980	100	Conrad and Seiler (1988)
		Mediterranean Sea	
Adriatic Sea	Aug 1996	425* (420 – 450)	Leip (1999)
Eastern Ionian Sea	Jul 1993	148 ± 22	Bange et al. (1996a)
Northern Aegean Sea	Jul 1993	231 ± 32	Bange et al. (1996a)
		Black Sea	
Northwestern shelf	Jul 1995	567	Amouroux et al. (2002)
Average		224 ± 142	

sd stands for standard deviation.
* study with a seasonal/interannual coverage, for details see reference.
** values estimated based on the information given in the reference.

Table 3b: Compilation of average CH_4 surface saturations in European estuarine systems and river plumes.

Region	Date	Avg. CH_4 (range or sd), saturation, %	Reference
		Baltic Sea	
Randers Fjord	2000*	6840** (1640 – 13,380)	Abril and Iversen (2002)
Bodden waters	1994-1997*	7802** (105 – 15,500)	Bange et al. (1998a)
Eckernförde Bay	1993-1994*	838** (793 – 7803)	Bussmann and Suess (1998)
		North Sea	
Humber	1995-1996*	4436 (238 – 21,048)	Upstill-Goddard et al. (2000)
Tyne	Jan 1996	5843 (450 – 20,000)	Upstill-Goddard et al. (2000)
Elbe	Apr 1997	580 (130 – 29,800)	Middelburg et al. (2002)
Ems	Jul 1997	3150 (9200 – 13,100)	Middelburg et al. (2002)
Thames	Feb 1999	570 (150 – 6700)	Middelburg et al. (2002)
Rhine	1996-1998*	8400 (140 – 49,700)	Middelburg et al. (2002)
Scheldt	1996-1998*	3210 (380 – 3210)	Middelburg et al. (2002)
		NE Atlantic	
Loire	Sep 1998	660 (340 – 23,100)	Middelburg et al. (2002)
Gironde	1996-1998*	580 (70 – 13,400)	Middelburg et al. (2002)
Douro	Sep 1998	3610 620 – 5720)	Middelburg et al. (2002)
Sado	Sep 1998	5900 (940 – 158,000)	Middelburg et al. (2002)
		Mediterranean Sea	
Amvrakikos Bay	Jul 1993	522 ± 177	Bange et al. (1996a)
		Black Sea	
Danube plume	Jul 1995	5340	Amouroux et al. (2002)
Average		3643 ± 2814	

sd stands for standard deviation.
* study with a seasonal/interannual coverage, for details see reference.
** values estimated based on the information given in the reference.

Table 4: Estimate of the annual CH_4 emissions from European shelf and estuarine areas.

	Area[1], 10^{12} m^2	Avg. saturation[2], %	ΔC[3], nmol L^{-1}	Emissions[4] (LM86), Tg C yr^{-1}	Emissions[4] (W92), Tg C yr^{-1}
Shelf	3.18	224	3.1	0.09	0.17
Estuaries	0.17	3643	99.5	0.16	0.31

[1] According to Uher (2005).
[2] see Tables 3a and 3b.
[3] ΔC stands for the concentration difference across the ocean/atmosphere interface and was calculated as $\Delta C = (\text{saturation}/100^{*}C_{air}) - C_{air}$. C_{air} was calculated with the Bunsen coefficient of Wiesenburg and Guinasso (1979) for a water temperature of 15°C and salinities of 35 and 15 for shelf and estuaries, respectively. We applied a mean atmospheric CH_4 dry mole fraction of 1.83 ppm (i.e. the mean for the period 1980-2000 corresponding to the dates of the listed measurements)
[4] LM86 stands for the model approach of Liss and Merlivat (1986). W92 stands for the model approach of Wanninkhof (1992) for climatological wind speeds. We applied a mean wind speed of 7 m s^{-1}. CH_4 Schmidt numbers were calculated with the mean water temperature and salinities as given in footnote 3.

Table 5: Impact assessment of various parameters which might influence today's and future N_2O and CH_4 emissions from European coastal waters. Classification scheme: – = minor; + = moderate; ++ = high; ? = unknown.

	N_2O	CH_4
Eutrophication	++	++
Coastal upwelling	+	–
Release from natural seepages	n.a.	++
Fish farming	–	?
Ecosystem shifts due to climate change	?	?

n.a. stands for not applicable.

Figure captions

Figure 1: Map with European marginal seas indicated: 1 – Barents Sea; 2 – Norwegian Sea; 3 – Baltic Sea; 3a – Kattegat; 4 – North Sea; 4a – Skagerrak; 4b – German Bight; 5 – English Channel; 6 – Bay of Biscay; 7 – Celtic (Irish) Sea; 8 – NE Atlantic; 9 – Mediterranean Sea; 9a – Adriatic Sea; 9b – Aegean Sea; 10 – Black Sea.

Figure 2: Locations of prominent coastal areas, estuaries, fjords and other features mentioned in the text. 1 – pockmark field; 2 – Bodden waters/Oder River estuary; 3 – Fjords along the east coast of Jutland, Denmark (Norsminde Fjord, Limfjorden, Randers Fjord, Marianger Fjord) and northern Germany (Eckernförde Bay, Kiel Harbour); 4 – Framvaren Fjord; 5 – Elbe River; 6 – Ems River; 7 – western Wadden Sea; 8 – Scheldt River, Rhine River; 9 – Estuaries along the English east coast (Tyne River, Colne River, Humber Estuary, Thames River); 10 – Tamar River; 11 – Loire River; 12 – Gironde estuary; 13 – Douro River; 14 – Sado River; 15 – Rhone River, Golf of Lions; 16 – Po River delta, Sacca di Goro; 17 – Amvrakikos Bay; 18 – Golf of Thermaikos; 19 – Danube River Delta.

Figure 3: Locations of studies of N_2O in European coastal waters.

Figure 4: Locations of studies of CH_4 (incl. observations of CH_4 bubble plumes and CH_4 enriched sediments) in European coastal waters.

Figure 1:

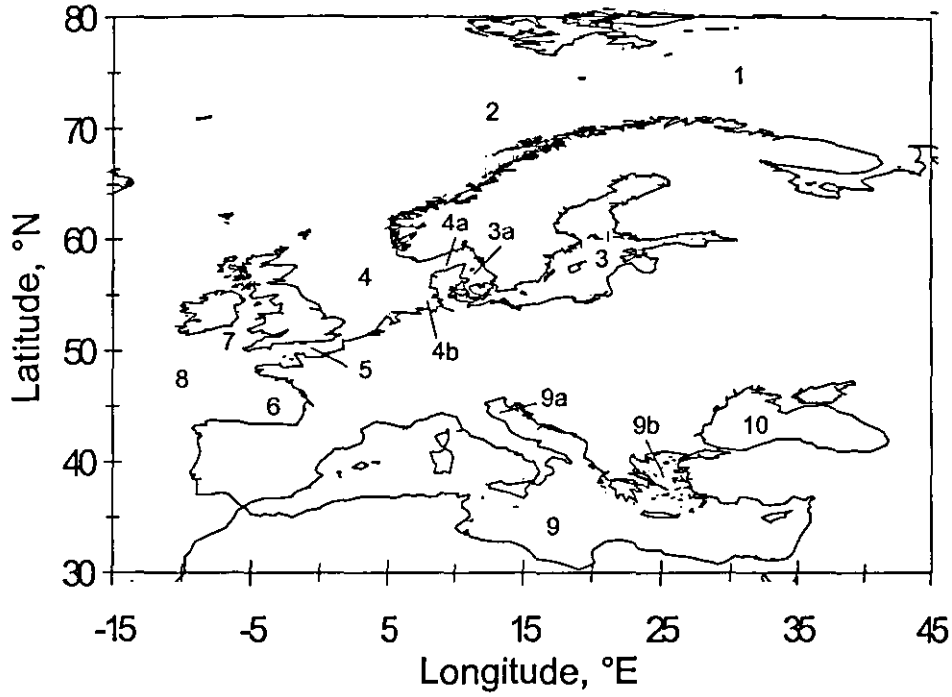

Figure 2:

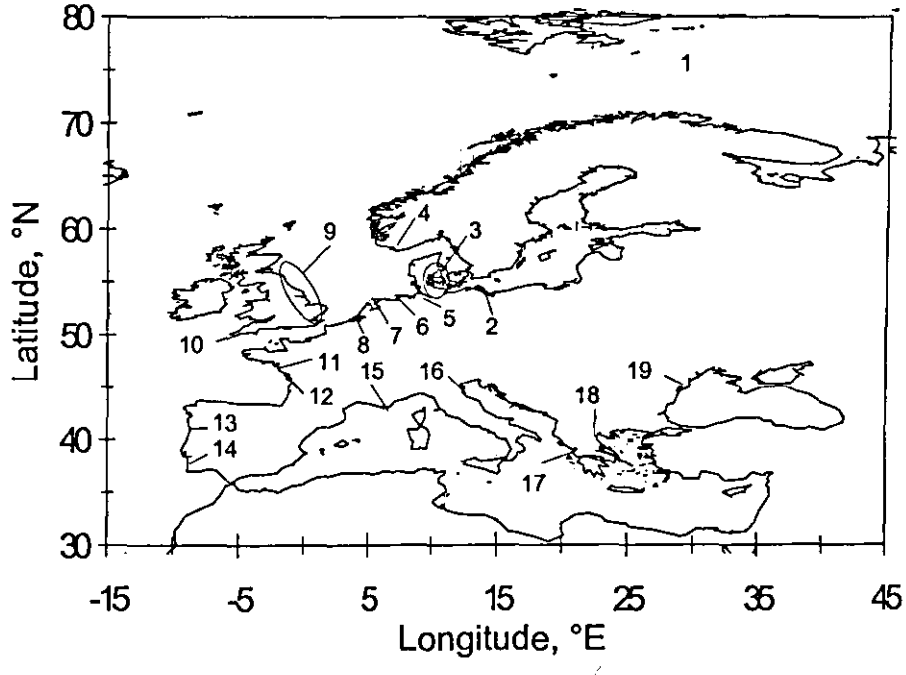

Figure 3:

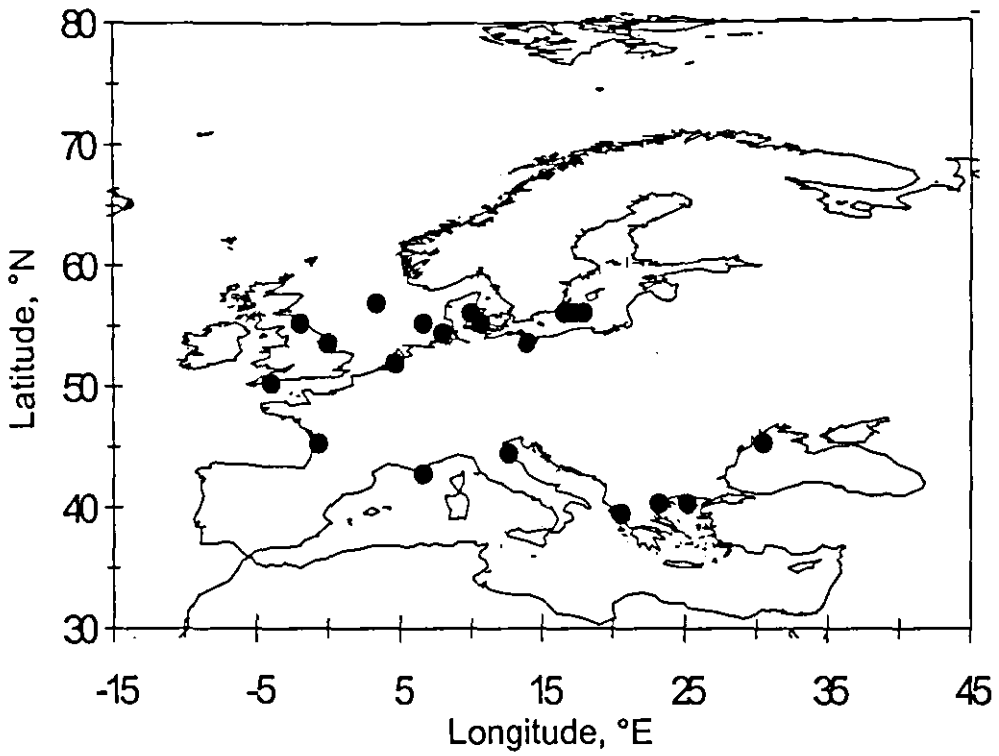

Figure 4: